REGULATION OF OSTEOGENIC DIFFERENTIATION OF MESENCHYMAL STEM CELLS DERIVED FROM BONE MARROW, AMNION, CHORION, PLACENTA, AND UMBILICAL CORD

BY

MISS KULISARA MARUPANTHORN

A DISSERTATION SUBMITTED IN PARTIAL FULFILLMENT
OF THE REQUIREMENTS FOR THE DEGREE OF DOCTOR OF
PHILOSOPHY IN MEDICAL SCIENCE
FACULTY OF MEDICINE
THAMMASAT UNIVERSITY
ACADEMIC YEAR 2015

REGULATION OF OSTEOGENIC DIFFERENTIATION OF MESENCHYMAL STEM CELLS DERIVED FROM BONE MARROW, AMNION, CHORION, PLACENTA, AND UMBILICAL CORD

BY

MISS KULISARA MARUPANTHORN

A DISSERTATION SUBMITTED IN PARTIAL FULFILLMENT
OF THE REQUIREMENTS FOR THE DEGREE OF DOCTOR OF
PHILOSOPHY IN MEDICAL SCIENCE
FACULTY OF MEDICINE
THAMMASAT UNIVERSITY
ACADEMIC YEAR 2015

THAMMASAT UNIVERSITY
FACULTY OF MEDICINE

DISSERTATION

BY

MISS KULISARA MARUPANTHORN

ENTITLED

REGULATION OF OSTEOGENIC DIFFERENTIATION OF MESENCHYMAL
STEM CELLS DERIVED FROM BONE MARROW, AMNION, CHORION,
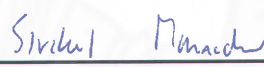PLACENTA, AND UMBILICAL CORD

was approved as partial fulfillment of the requirements for
the degree of Doctor of Philosophy in Medical Sciences

on June 30, 2016

Chairman

_____
(Asst. Prof. Anongnad Ngamjariyawat, Ph.D.)

Member and Advisor

_____
(Assoc. Prof. Sirikul Manochantr, Ph.D.)

Member and Co-advisor

_____
(Asst. Prof. Pakpoom Kheolamai, M.D., Ph.D.)

Member and Co-advisor

_____
(Asst. Prof. Chairat Tantrawatpan, Ph.D.)

Member

_____
(Methichit Wattanapanitch, Ph.D.)

Dean

_____
(Assoc. Prof. Preecha Wanichsetakul, M.D.)

Thesis Title	REGULATION OF OSTEOGENIC DIFFERENTIATION OF MESENCHYMAL STEM CELLS DERIVED FROM BONE MARROW, AMNION, CHORION, PLACENTA, AND UMBILICAL CORD
Author	Miss Kulisara Marupanthorn
Degree	Degree of Doctor of Philosophy (Medical Sciences)
Major Field/Faculty/University	Cellular and Molecular Biology Faculty of Medicine Thammasat University
Thesis Advisor	Assoc. Prof. Sirikul Manochantr, Ph.D.
Thesis Co-Advisor	Asst. Prof. Pakpoom Kheolamai, M.D., Ph.D.
Thesis Co-Advisor	Asst. Prof. Chairat Tantrawatpan, Ph.D.
Academic Years	2015
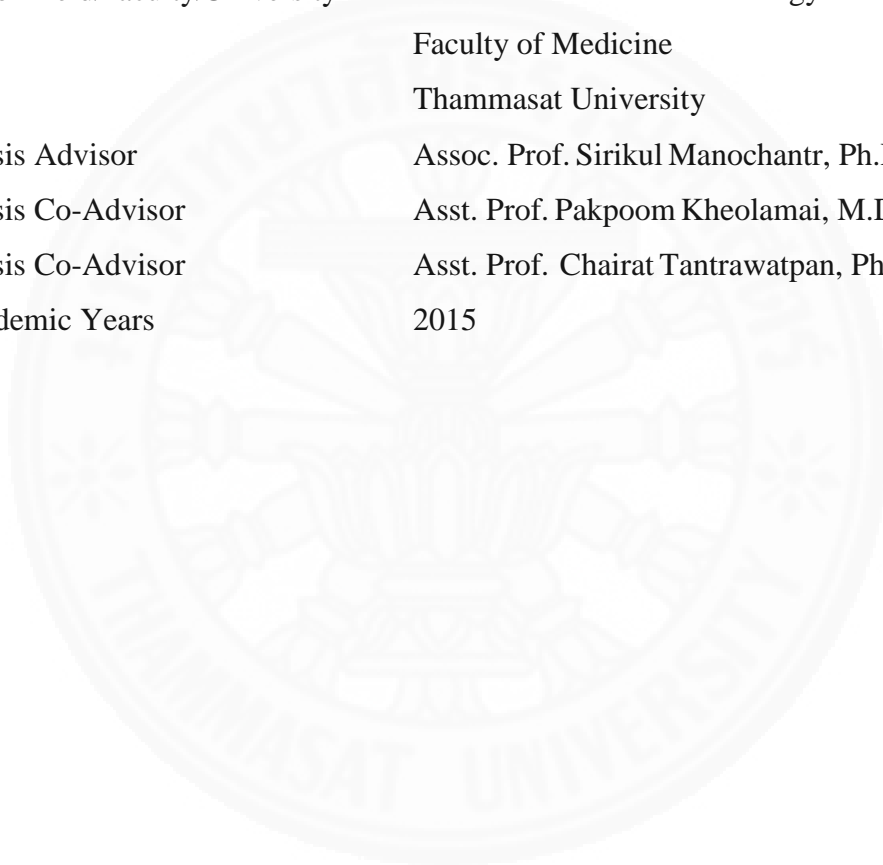
ABSTRACT

Mesenchymal stem cells (MSCs) are multipotent cells that can give rise to various cell types of the mesodermal lineage. They are promising source for cell therapy in regenerative medicine. Recently, MSCs derived from postnatal tissues; amnion, chorion, placenta and umbilical cord, have been suggested as the alternative sources of MSCs for clinical applications. Although MSCs derived from these tissues can differentiate into osteoblast with a phenotypic similarity to that of bone marrow-derived MSCs, the differentiation ability is not efficient. MSCs from postnatal tissues take a longer period of time for differentiation into osteoblasts. Previous studies have shown the benefits of bone morphogenetic protein 2 (BMP-2) in bone tissue regeneration. Therefore, this study aims to examine the effect of BMP-2 on osteogenic differentiation of MSCs derived from postnatal tissues and compare to that of MSCs derived from bone marrow. The degree of osteogenic differentiation after BMP-2 treatment was assessed by alkaline phosphatase expression, alkaline phosphatase (ALP) activity, and the expression profiles of osteogenic differentiation marker genes, Runt-related transcription factor 2 (*RUNX-2*), *Osterix* (*OSX*), and *Osteocalcin* (*OCN*). The expression level and function of microRNAs (miRNAs) related to osteogenic differentiation (miR-31, miR-106a and miR-148a) were also studied. The results showed that BMP-2 enhanced the osteogenic differentiation capacity of MSCs derived from both postnatal tissues and bone marrow. MiR-31, miR-106a and miR-148a were down-regulated during the process of osteogenic differentiation of these MSCs. After transfection with anti-miRNAs, ALP activity and osteogenic differentiation marker genes were increased over the time of differentiation. The data obtained from this study lead to the potential for using these MSCs as the alternative sources for bone regeneration. Moreover, the information of miRNAs expression and function during osteogenic differentiation may be useful for the development of new therapeutics or enhanced an *in vitro* culture technique required for stem cell-based therapies in the regenerative medicine.

Keywords: mesenchymal stem cells, bone morphogenetic protein-2, microRNA, osteoblast, alkaline phosphatase

ACKNOWLEDGEMENTS

TABLE OF CONTENTS

LIST OF TABLES

LIST OF FIGURES

LIST OF ABBREVIATIONS

Symbols/Abbreviations	Term
%	Percent
/	Per
<	Less than
AECs	Amniotic epithelial cells
AF-MSCs	Amniotic fluid-derived multipotent mesenchymal stromal cells
ALP	Alkaline phosphatase
AM	Amnion
AM-MSCs	Amnion-derived mesenchymal stem cells
APC	Adenomatous polyposis coli
BM	Bone marrow
BM-MSCs	Bone marrow-derived mesenchymal stem cells
C/EBPα	*CCAAT/enhancer‑binding protein α*
CFU-F	Colony-forming units – fibroblast
CH	Chorion
CH-MSCs	Chorion-derived mesenchymal stem cells
°C	Degree of Celsius
CD	Cluster of differentiation
cm	Centimeter
CO_2	Carbondioxide
Co-smad	Common-partner Smad
CSD	Critical-sized defect
DGCR8	DiGeorge syndrome critical region gene 8
dH_2O	Distilled water
Dkk	Dickkopf
DMEM	Dulbecco's Modified Eagle's Medium
DMSO	Dimethylsulfoxide
ECM	Extracellular matrix
et al.	Et alii, and colleagues

FBS	Fetal bovine serum
Fgf18	Fibroblast growth factor 18
FHL2	Four and a half LIM domains protein 2
FITC	Fluorescein isothiocyanate
FOXO1A	Forkhead box protein O1
FZD	Membrane receptor complex composed of Frizzled
g	Gram
GAPDH	*Glyceraldehyde 3-phosphate dehydrogenase*
GPCRs	G protein-coupled receptors
GSK	Glycogen synthase kinase
h	Hour
HCV	Hepatitis C virus
FGF	Fibroblast growth factor
IgG1	Immunoglobulin G1
IgG2a	Immunoglobulin G2a
I-smad	Inhibitory Smad
ITGA5	Integrin alpha-5
LDL	Low-density lipoprotein
LEF	*Lymphoid-enhancer-binding factor*
LNA	Locked nucleic acid
LRPs	Low-density lipoprotein receptor-related proteins
M	Molar or mole per liter (concentration)
mg	Milligram
mg/L	Milligram per liter
mg/mL	Milligram per milliliter
min	Minute
miRNA	MicroRNA
mL	Milliliter
mM	Millimolar
mRNA	Messenger RNA

Nfatc1	*Nuclear factor of activated T cells, cytoplasmic 1*
Oct-4	*Octamerbinding transcription factors*
OD	Optical density
OCN	*Osteocalcin*
OSX	*Osterix*
PBS	Phosphate buffered saline
pH	Log concentration of (H^+)-1
PL	Placenta
PL-MSCs	Placenta- derived mesenchymal stem cells
pNPP	*p*-nitrophenyl phosphate
Pre-miRNA	Precursor-miRNA
Pri-miRNA	Primary miRNA
qRT-PCR	Quantitative real time polymerase chain reaction
RISC	RNA induced silencing complex
rpm	Round per minute
R-smad	Receptor-regulated Smad
RUNX2	Runt-related transcription factor 2
SEM	Standard error of mean
Smad	Mothers against decapentaplegic homolog
TCFs	*T-cell-specific transcription factors*
TLDA	TaqMan Low Density Arrays
TRACP	*Tartrate resistant acid phosphatase*
UC	Umbilical cord
UC-MSCs	Umbilical cord-derived mesenchymal stem cells
UTRs	Untranslated regions
VEGF	Vascular endothelial growth factor
µg	Microgram
µL	Microlitre
µg/mL	Microgram per milliliter
α	Alpha

β	Beta
β-TCP	β-tricalcium phosphate
γ	Gamma

CHAPTER 1

INTRODUCTION

1.1 Introduction

Nowadays, an evidence of degenerative bone diseases are increasing because of ageing population. In addition, the number of patients suffering from bone defects caused by physical trauma represent significant morbidity which affect the patient's quality of life and cost for the public healthcare system. To address this issue, several interventions including bone autografts have been exploited to improve the capability of bone tissue regeneration, leading to reduction of both total costs and hospitalization period. However, autografts have some major problems, including donor site morbidity and limited availability. Over the past 10 years, tissue engineering using mesenchymal stem cells (MSCs) gained an important issue in regenerative medicine, due to their ability to differentiate not only into mesodermal lineage but also endodermal and ectodermal lineages (1, 2). The characteristics of differentiation to tissue-specific manner endow a great promise to the use of MSCs in the fields of regenerative medicine.

The use of MSCs in orthopedics has been shown great clinical potential as therapeutic agent in regenerative medicine for many years (3, 4). Currently, MSCs those are used in clinical field are mainly isolated from bone marrow. However, the use of MSCs from bone marrow has several limitations including the invasive procedure for harvesting bone marrow and the limited amout of MSCs in bone marrow especially in aging population (5). During the individual's lifetime, both the availability and the differentiation ability of these cells are diminished, leading to incomplete or total absence of tissue regeneration. In many instances, the amount of MSCs that can be obtained from bone marrow is less than the critical quantity of cells that are needed for tissue repair (3). In addition, many studies demonstrated that there is an accumulation of senescent MSCs and their progeny in aging bone marrow (5-7). Recently, several groups reported the success of the isolation of

mesenchymal stem cells from postnatal tissues including, amnion, chorion, placenta, umbilical cord and Wharton's jelly (8 - 12). These tissues are generally discarded after delivery; therefore, they are available in large supply and the cell isolation does not involve any invasive procedures for the donor (10, 13, 14).

Although MSCs derived from these sources have been assumed to exhibit similar characteristics to MSCs derived from bone marrow, some differences at least in term of osteogenic differentiation ability were also reported. MSCs derived from postnatal tissues can be differentiated into osteoblast with a phenotypic similarity to that of bone marrow derived MSCs (BM-MSCs). However, the differentiation ability is not consistent. In addition, MSCs from postnatal tissues took a longer period of time for induced differentiation into osteoblasts. Previous study reported that bone morphogenetic proteins (BMPs) 2, 4, and 7 can stimulate the entire process of osteogenic differentiation of BM-MSCs *in vitro* (15). Clinical orthopedic studies have shown the benefits of bone morphogenetic protein 2 (BMP-2) in bone tissue regeneration. In addition, several studies have supported the use of BMP-2 in periodontal regeneration, sinus lift bone-grafting, and non-unions in oral surgery (16, 17). Although the use of BMP-2 for bone tissue regeneration has been extensively studied, the BMP-2 induced osteogenic differentiation of MSCs from postnatal tissues are not fully examined especially the underlying molecular events governing the osteogenic differentiation of these MSCs.

Over the last few years, some new important players including microRNAs (miRNAs) have emerged in translational regulation with implications in stem cell fate and behavior. They are a large family of non-coding single-strand RNAs with 18 – 25 nucleotides which modulate gene expression at post-transcriptional level. They bind to the 3'-untranslated region (3'-UTR) of target mRNAs to mediate gene suppression by promoting degradation of target genes or inhibiting those translations (18, 19). There is increasing information addressing the involvement of miRNAs in osteogenic differentiation of MSCs (20). Various miRNAs have been demonstrated to influence the fate of bone precursors including miR-31, miR-106a, and miR-148a (21). In addition, previous studies have demonstrated that many miRNAs; such as miR-204,and miR-211 participate in the regulation of Runt-related transcription factor 2 (*RUNX-2*) expressions that drive the commitment and differentiation of MSCs towards osteogenic lineage (22). During osteogenic differentiation, miR-31,

miR-106a, and miR-148a are under expressed in differentiated human bone marrow-derived mesenchymal stem cells (hBM-MSCs) (21). These miRNAs target to *RUNX-2* but their target verification and functional analysis are needed to provide more conclusive evidence to explain the regulatory mechanisms of these miRNAs (21).

Taken together, this study aims to examine the effect of BMP-2 on osteogenic differentiation of MSCs derived from postnatal tissues and compare to that of BM-MSCs. The underlining molecular mechanism such as the expression of transcription factor, signaling cascade pathways and the change in the expression of miRNAs which involved in osteogenic differentiation of these MSCs were also investigated. The data obtained will provide new insights into the underlying molecular mechanisms involved in the regulation of osteogenic differentiation of MSCs derived from both bone marrow and postnatal tissues, leading to the advance procedure for bone tissue regeneration in the future. Moreover, this data will add the potential for using MSCs derived from postnatal tissues as alternative sources for tissue engineering or cell therapy in regenerative medicine.

1.2 Objective

1.2.1 Overall objective

To study the regulation of osteogenic differentiation of mesenchymal stem cells derived from bone marrow, amnion, chorion, placenta, and umbilical cord.

1.2.2 Specific objectives

1. To characterize MSCs derived from amnion, chorion, placenta, and umbilical cord and compare to MSCs derived from bone marrow in the aspect of morphology, immunophenotype and differentiation capacity.

2. To study the osteogenic differentiation potential of MSCs derived from amnion, chorion, placenta, and umbilical cord and compare to that of bone marrow-derived MSCs.

3. To study the effects of BMP-2 on osteogenic differentiation of MSCs derived from amnion, chorion, placenta, and umbilical cord and compare to that of bone marrow-derived MSCs.

4. To study the genes expression profiling of MSCs derived from amnion, chorion, placenta, and umbilical cord during osteogenic differentiation and compare to that of bone marrow-derived MSCs.

5. To study the miRNAs expression profiling of MSCs derived from amnion, chorion, placenta, and umbilical cord during osteogenic differentiation and compare to that of bone marrow-derived MSCs.

6. To study the underlying mechanism of miRNAs in regulating osteogenic differentiation of MSCs derived from amnion, chorion, placenta, and umbilical cord and compare to that of bone marrow-derived MSCs.

CHAPTER 2

REVIEW OF LITERATURE

2.1. Bone structure

Bone is a dynamic mineralized constituent which provides structural support, mineral and stem cell reserves for the body. The functions range from structural support for the body to roles in maintaining homeostasis. Structure and support for the body are the most obvious role, with the skeletal system as a whole providing a normal force for other tissues and organs to resist gravity. Protection is also inferred for tissues and organs from impacting forces, especially with axial bones covering vital organs in the thoracic cavity. Another function of bone includes the ability to store and release minerals when needed to maintain appropriate levels in circulation. Specifically the resident mineral of bone tissue, hydroxyapatite, is composed mostly of calcium and phosphorus. Calcium and phosphorus are vital in essentially every system in the body, from neurotransmitter release, to muscle contractions, to various biochemical processes, and so on. Lastly, bone provides a location for the storage of stem cells, residing in bone marrow. These cells are vital to supplying new cells for the repair of tissue damage, resupplying the immunological system, generating erythrocytes for the circulatory system, and other functions requiring new cells.

A mixture of inorganic and organic matter provides essential properties to the tissue that allows for these functions to occur. Inorganic calcium and phosphate minerals combine with organic collagen fibers to form crystalline structures. The secretion, bonding, and breakdown of the mineral and fiber interactions are all controlled by cellular processes. The combination of solid, tensile, matter with living cells creates a solid material that constantly adapts to present needs of both the local environment and the body as a whole. This is accomplished by osteoblasts, osteoclasts, and osteocytes which either secretes, absorb, or control extracellular matrix around them. The interaction between cells and abundant, tensile extracellular matrix create one of the most versatile, functional tissues in the body.

Bones can be divided into long bones, such as tibia and femur, and flat bones, such as skull bones, scapula, and mandible. Furthermore, two types of bone can be distinguished according to the pattern of extracellular matrix: cortical bone and trabecular bone (Fig. 2.1). Cortical bone comprises about 80% of the skeleton and is predominantly located at the external part of the bone and in the diaphysis of long bones. It is structured as parallel osteons composed of dense layers (lamellae) of calcified tissue with Haversian canals in the middle (Fig. 2.2) (23). Trabecular bone is predominantly located in the inner parts of small bones and in the epiphyses of long bones. In addition, it makes up the majority of the vertebral bodies. It is composed of a network of thin calcified trabeculae. Cortical bone provides the skeleton with mechanical and structural supports whereas trabecular bone is responsible for the metabolic functions of bone. The spaces between the trabeculae are occupied by bone marrow consisting of highly branched vascular sinuses and a number of different cell types, including hematopoietic stem cells (HSCs), MSCs, and their progeny. The main function of bone marrow is to produce and maintain an appropriate amount of blood cells through a process called hematopoiesis. In addition, bone marrow plays a central role in the immune system, being the site of B-cell maturation.

The outer surface of cortical bone, except at joints where bone is lined by articular cartilage, is surrounded by a layer of connective tissue called periosteum which is attached to bone by strong collagenous fibers called Sharpey's fibers (Fig. 2.1). In addition, periosteum provides an attachment for muscles and tendons. Periosteum consists of fibroblasts and osteo-chondroprecursor cells embedded in fibrous extracellular matrix. These progenitors and their differentiation into osteoblasts or chondrocytes are responsible for appositional bone growth and fracture healing (24). The inner surface of cortical and trabecular bone is covered by a membranous structure called endosteum, which contains blood vessels, osteoblasts and osteoclasts as well as their progenitor cells. Bone resorption typically exceeds bone formation on the endosteal surface with aging, leading to enlarged marrow space (25).
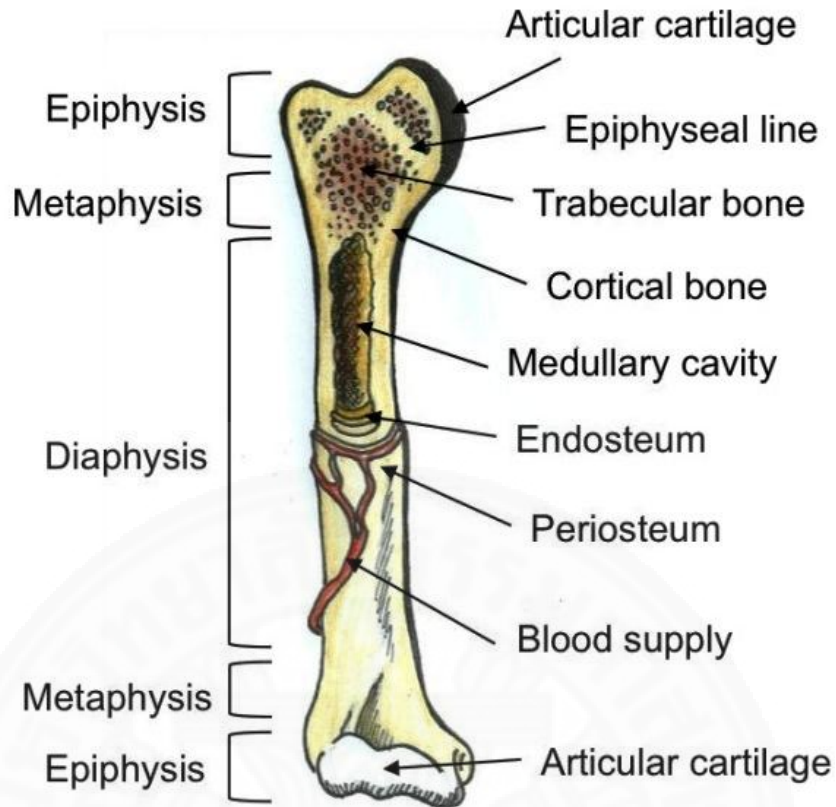
Figure 2.1: A schematic presentation of the structure of a long bone (26).
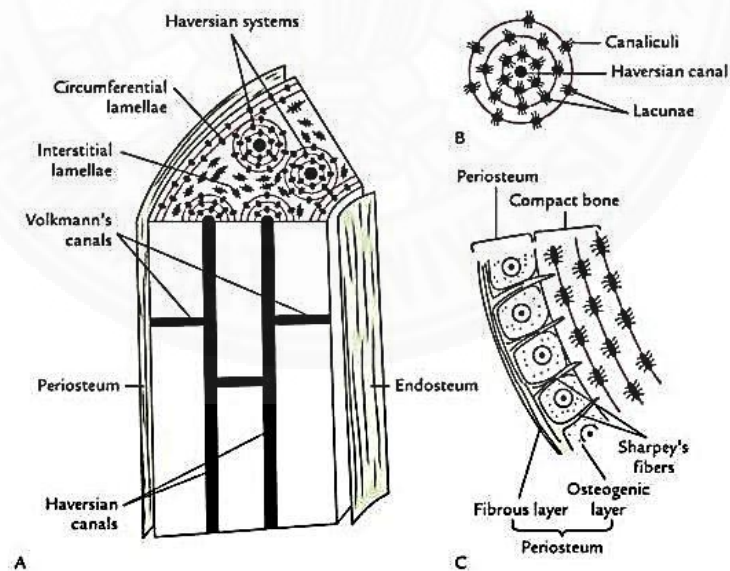
Figure 2.2: The structure of a compact bone: A, harvarsian systems and lamellae: B, an osteon; C, periosteum and outer circumferential lamellae of a compact bone (23) .

2.2. Bone formation

Bone develops through 2 distinct mechanisms: intramembranous and endochondral ossifications. Intramembranous ossification, which predominates in cranial bones and parts of the mandible and clavicle, takes place in mesenchymal condensations through differentiation of embryonic mesenchymal progenitors into bone-forming osteoblasts. The ossification center increases in size by appositional growth as more osteoblasts are formed from the mesenchymal cells of the surrounding periosteum (Fig. 2.3). The collagen-proteoglycan-rich matrix produced by osteoblasts becomes calcified, resulting in woven bone with irregular orientation of type I collagen fibrils. The woven bone is later remodeled and replaced by mature lamellar bone.

In contrast, the majority of the bone is developed through endochondral ossification which is characterized by the formation of a cartilaginous anlage and subsequent replacement of the cartilage with bone (Fig. 2.3). The cartilaginous anlage is formed as embryonic mesenchymal cells condense and differentiate into chondroblasts, which secrete various components of the extracellular matrix (ECM), including type II collagen and the proteoglycan aggrecan. Cartilage increases in size through two different mechanisms. Appositional growth occurs at the external parts of the anlage in the perichondrium, where mesenchymal cells continue to differentiate into chondroblasts, and secrete the cartilaginous matrix. In contrast, interstitial growth occurs within the cartilaginous anlage through chondrocyte division and enlargement.

As the endochondral bone formation proceeds, chondroblast mature into chondrocytes, which, in turn, become hypertrophic (enlarged) and change their genetic program to synthesize type X collagen. Consequently, capillaries invade the perichondrium, and mesenchymal cells are differentiating into osteoblasts, which start to produce bone matrix. This results in formation of a bone collar underneath the periosteal layer, which is now referred to as the periosteum. Matrix mineralization is followed by the vascular invasion and the migration of osteoblast precursor cells into the cartilaginous model, triggering the formation of the primary ossification center inside the bone. The primary spongiosa formed on the cartilaginous remnants is later remodeled by osteoclasts, and woven bone as well as cartilage remnants are replaced with lamellar bone. In late fetal life and early childhood, secondary ossification centers appear in the epiphyses of long bones by a mechanism very

similar to that seen in the formation of the primary center. The diaphysis will be separated from the epiphyses by cartilaginous growth plate that will ensure the longitudinal growth of the skeleton. In humans, growth plates close by fusion of epiphyses and metaphyses when growth ceases at puberty. However, in small rodents, such as the mouse and rat, growth plates are active throughout life (27).

The bone comprises several functionally different cell types including osteoblasts, osteocytes and osteoclasts. Osteoblasts originate from non-hematopoietic compartment of bone marrow stem cells that have been variously termed including mesenchymal stromal cells, skeletal stem cells, and most frequently, mesenchymal stem cells or MSCs.
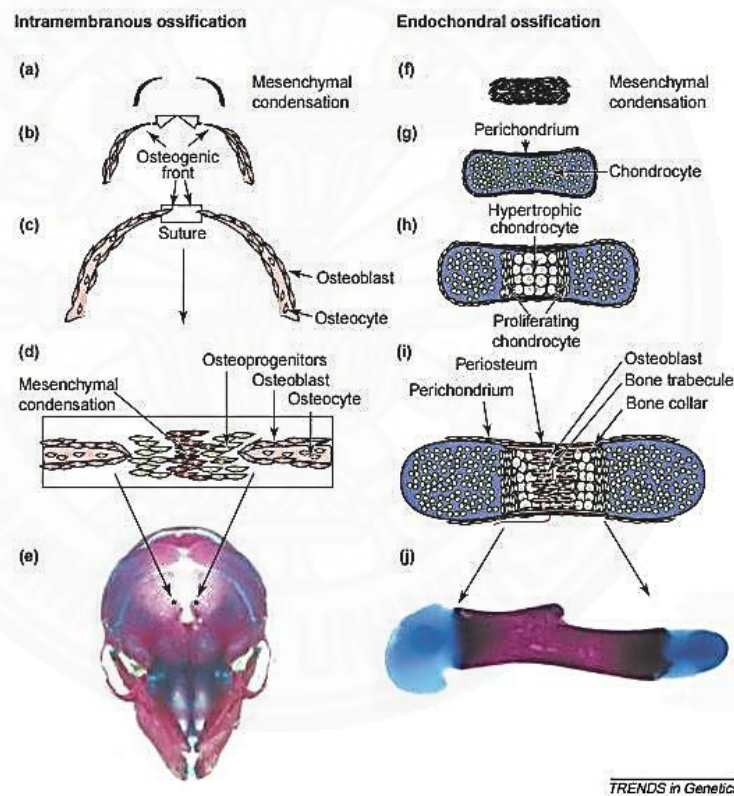
Figure 2.3: Intramembranous ossification and endochondral ossification (a–d). Craniofacial bones are formed directly from condensations of mesenchymal cells without the formation of a cartilage intermediate, a process described as intramembranous ossification. (e) A schematic frontal view of a mouse skull (E18.5) stained with alizarin red and alcian blue. (f – j) In contrast, long bones are formed by endochondral ossification (28).

2.3. Roles of osteoblast and osteoclast in the bone formation of bone

Bone remodeling, or turnover, is mediated by the delicate balance of osteoblast and osteoclast numbers and activities (29). Osteoblasts are polarized bone-forming cells located on the surface of bone matrix. They are characterized by a round nucleus, a large circular Golgi complex, a well-developed endoplasmic reticulum, and a cuboidal morphology. In addition, osteoblasts are distinguished by the production of *type I collagen*, *alkaline phosphatase* and *Osteocalcin* (*OCN*). Besides matrix synthesis, osteoblasts are known to regulate the mineralization process. Bone-lining cells of osteoblast lineage are observed as single layers of flattened cells on quiescent bone surfaces undergoing neither bone formation nor resorption (30). Although identified already years ago, very little is known about the differentiation or function of these cells. Another subtype of osteoblastic cells is constituted by osteocytes located within the bone matrix. They are thought to originate as osteoblasts become trapped in the synthesized matrix and are thereby considered as the terminal differentiation stage of osteoblast lineage. Osteocytes are connected with each other via long cytoplasmic processes which pass through the bone matrix. Through this network of thin canaliculi, osteocytes are suggested to account for the biomechanical regulation of bone mass and structure.

Osteoclasts are large multinucleated cells specialized in bone resorption. They are required during skeletal development to shape the forming bones and throughout life in the process of bone remodeling. Due to their special function, osteoclasts are provided with several unique features including the capacity to polarize on bone, the formation of specific membrane domains upon matrix degradation, an exceptionally high number of mitochondria and Golgi complexes, and the cytoplasm filled with lysosomes. In addition, osteoclasts are characterized by the formation of actin ring upon attachment to bone (31) and by the expression of a number of osteoclast-specific genes such as *tartrate resistant acid phosphatase (TRACP)*, *cathepsin K*, calcitonin receptor, and αvβ3 integrin. Osteoclasts resorb bone via the ruffled border membrane domain facing the bone surface. The resorption lacuna becomes acidic by protons secreted from osteoclasts. The low pH ensures rapid dissolution of hydroxyapatite and the residual organic matrix are digested by lysosomal enzymes derived from osteoclasts. The digested matrix is internalized,

transported across the cell, and finally released to the surroundings through the functional secretory domain of the basal membrane (32).
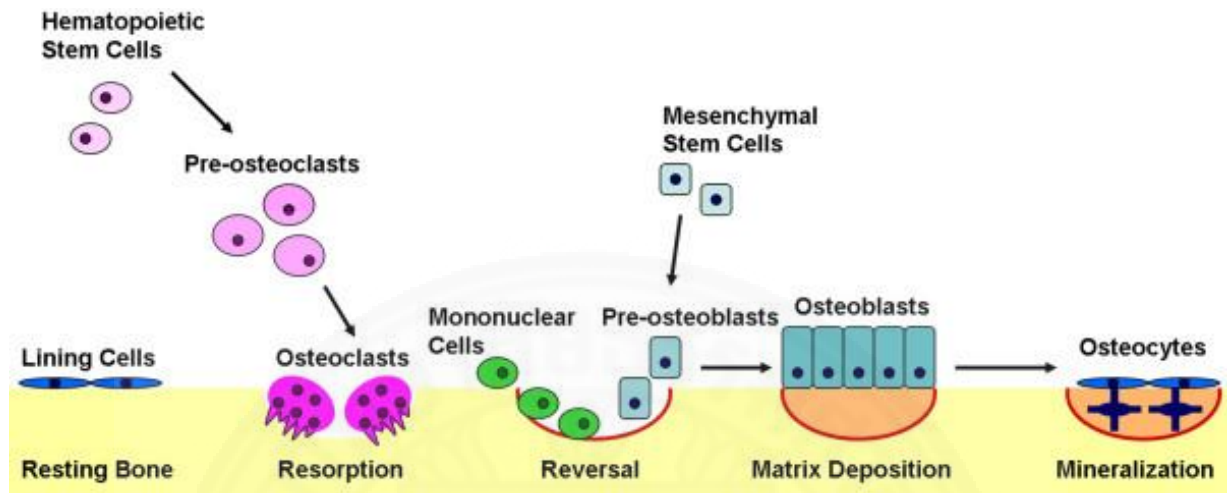
Figure 2.4: Bone remodeling begins when osteoclasts resorb bone mineral and matrix. Mononuclear cells prepare the resorbed surface for osteoblasts, which generate newly synthesized matrix as they differentiate. Matrix mineralization and the differentiation of some osteoblasts into osteocytes complete the remodeling cycle (29).

2.4. Gene expression during osteoblastogenesis

Bone development is controlled by a complex network of signaling pathways comprising of transcription factors, growth factors, hormones, vitamins, and other signaling molecules. These factors contribute to skeletal development mainly through modulation of bone cell proliferation and/or differentiation (33).

Differentiation of bone marrow mesenchymal stem cells into osteoprogenitors, preosteoblasts and finally into mature osteoblasts involves multiple transcription factors and signaling pathways. Runt related transcription factor 2 (*RUNX-2*), formerly called *Cbfa1* is recognized as the master regulator and the earliest marker of osteogenesis (Fig. 2.5). Deletion of *RUNX-2* in mice results in complete lack of bone tissue and death just after birth (34, 35). Due to the maturational arrest of osteoblasts, the skeleton in these mice comprises only chondrocytes and cartilage with no evidence of vascular or mesenchymal invasion. Besides its function in osteogenesis, *RUNX-2* regulates chondrocyte hypertrophy thereby acting as a molecular switch

between osteogenesis and chondrogenesis. *RUNX-2* expression increases in cells of the osteoblast lineage during development, but decreases and disappears in the pre-hypertrophic chondrocytes (36). The activation of osteogenesis by *RUNX-2* is mediated through several target genes, including *Osteocalcin* (*OCN*), *Osteopontin* and *Bone sialoprotein* (37). A number of different molecules have been identified to interact with and modify *RUNX-2* activity during skeletogenesis, such as transcription factors *Twist1* and *Twist2* (38), and the signal transducers of TGF-β superfamily receptors, Smads (mothers against decapentaplegic homolog) (39, 40).
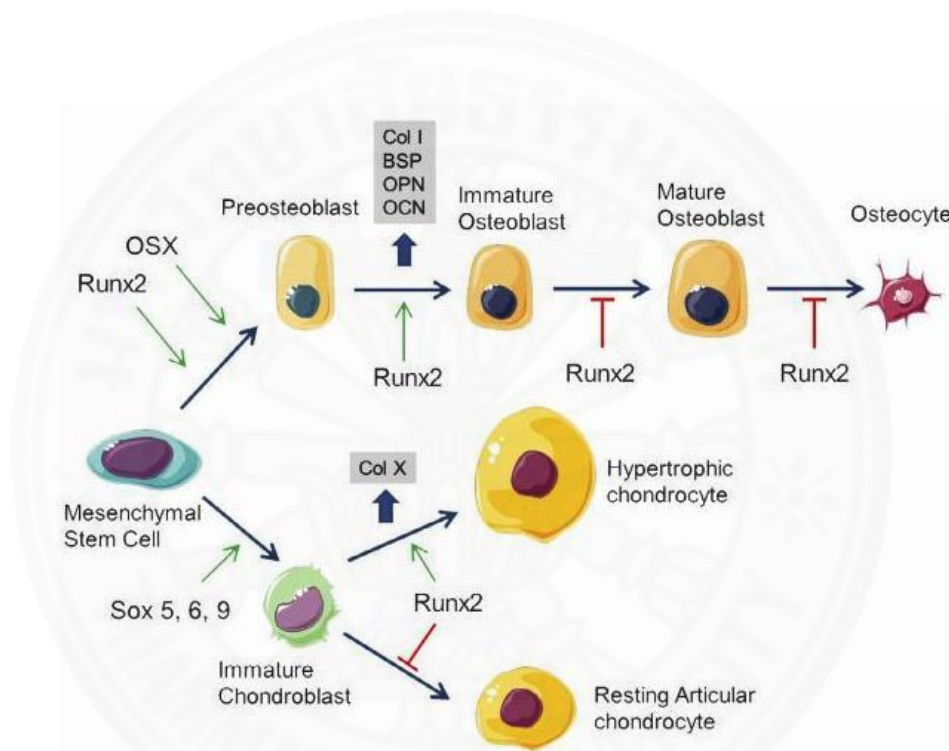
Figure 2.5: The osteoblast-differentiation pathway. Multipotential mesenchymal progenitor cells differentiate first into preosteoblasts in a process that requires *RUNX-2*. Preosteoblasts express low levels of type I collagen (*Col1a1*), which is typical of mesenchymal cells. (41).

Osterix (*OSX/Sp7*) is another transcription factor which is crucial for osteoblast development, both during embryonic development and in postnatal life. It acts downstream of *RUNX-2* and in its absence no bone formation occurs leading to perinatal lethality (42). *OSX* is specifically expressed in osteoblasts of all skeletal elements. Its transcription is known to be regulated positively by *RUNX-2* (43) and *Nfatc1* (*Nuclear factor of activated T cells, cytoplasmic 1*) (44, 45), and negatively by

the tumor suppressor p53 (46). However, other mechanisms that regulate *OSX* expression as well as the detailed information on its function remain poorly understood.
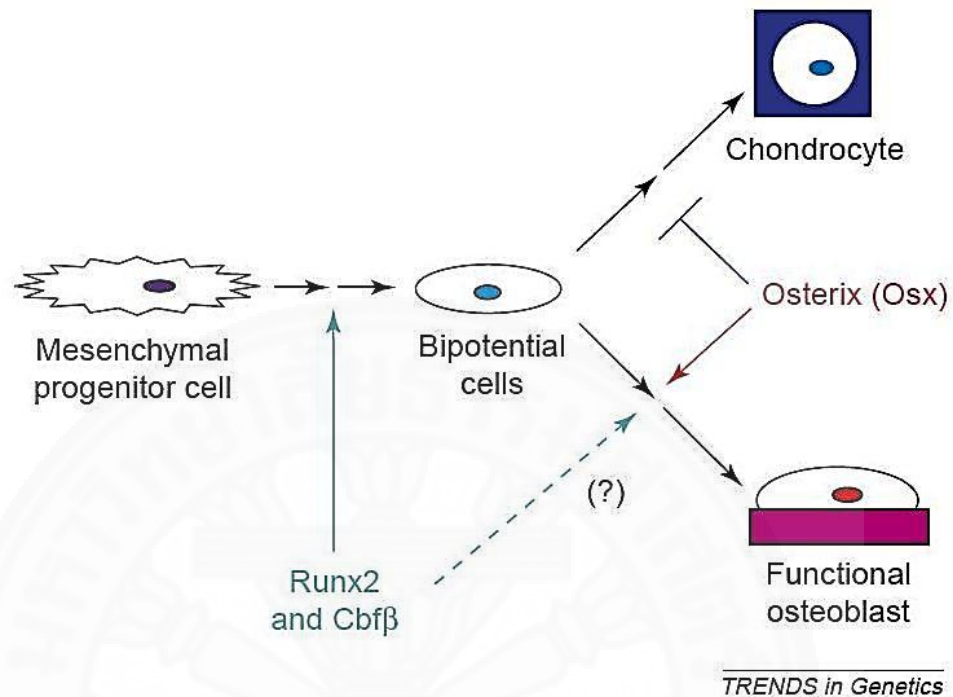
Figure 2.6: A hypothetical role of *OSX* in segregating osteoblast and chondrocyte lineages from a common osteochondroprogenitor (28).

Wnt/β-catenin signaling has emerged to play an important role in osteoblast differentiation and skeletal development. *Wnts* comprise a family of 19 secreted proteins that activate intracellular signaling pathways by binding to a membrane receptor complex composed of Frizzled (FZD), G protein-coupled receptors (GPCRs), and low-density lipoprotein (LDL) receptor-related proteins (LRPs). *Wnts* can function through canonical and noncanonical pathways, of which the canonical *Wnt/β-catenin* pathway is better characterized. In a canonical pathway, the binding of a *Wnt* ligand to LRP5 or LRP6 leads to inhibition of a protein complex consisting of axin, glycogen synthase kinase (GSK)-3β and adenomatous polyposis coli (APC) protein. This leads to the stabilization of β-catenin, since the axin/GSK-3β/APC complex normally promotes the proteolytic degradation of the β-catenin. The activation of *Wnt* target gene expression occurs as β-catenin translocates to

the nucleus and activates *lymphoid‑enhancer‑binding factor (LEF)/T‑cell‑specific transcription factors (TCFs)* (47) (Fig. 2.7).
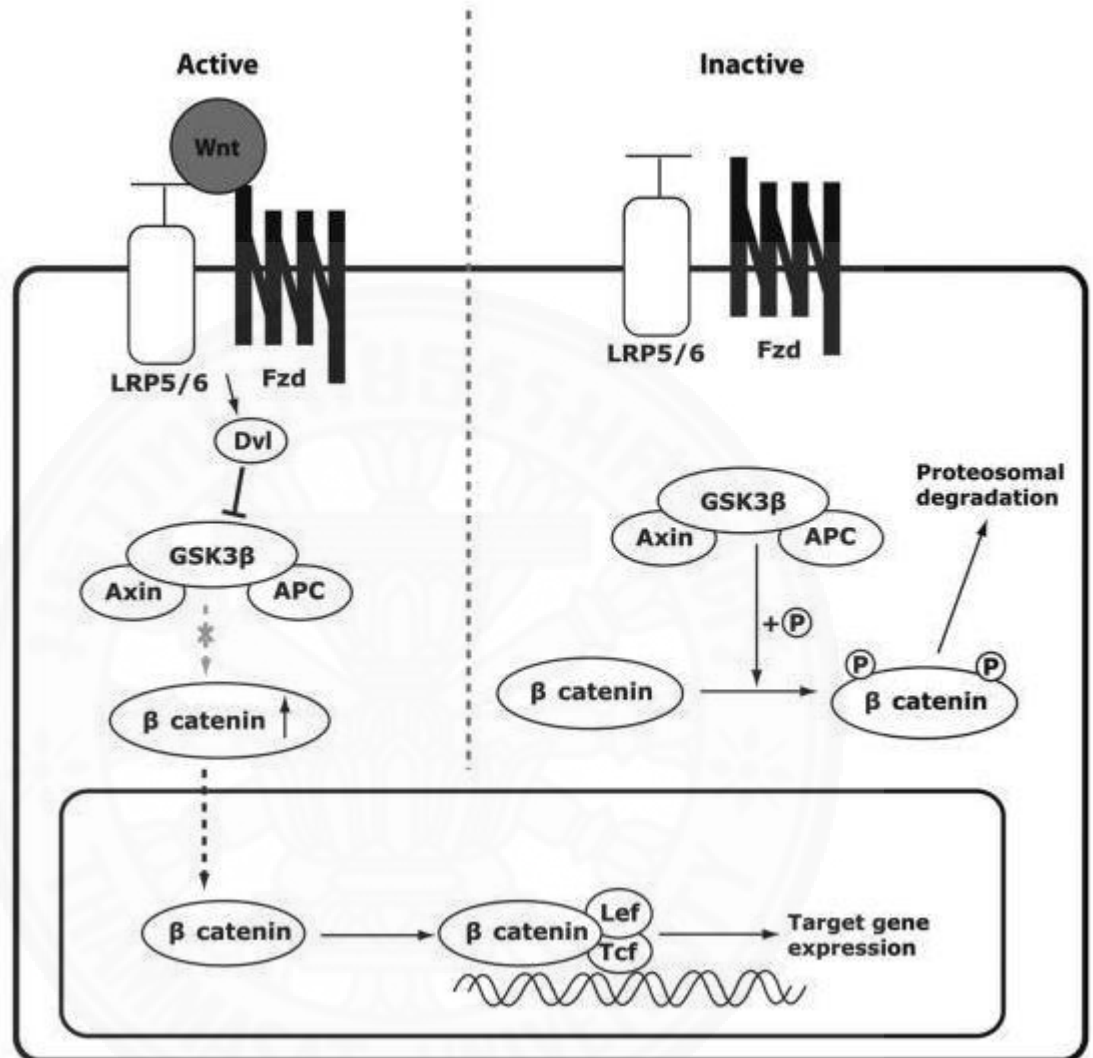
Figure 2.7: Diagrammatic representation of the canonical *Wnt* signaling pathway (47).

Wnt/β‑catenin signaling has been shown to regulate osteogenesis through multiple mechanisms. Activation of *Wnt/β‑catenin* signaling appears to be required for osteoblast lineage commitment as conditional deletion of β-catenin gene in mesenchymal progenitors results in increased chondrocyte formation at the expense of osteoblast differentiation both in vitro and in vivo (48, 49). On the other hand, *Wnt* seems to favor osteogenesis at the expense of adipogenesis by inhibiting the adipogenic transcription factors *CCAAT/enhancer‑ binding protein α* (*C/EBPα*) and peroxisome proliferator-activated receptor γ (*PPARγ*) in bipotential mesenchymal precursors (50, 51). The positive effect of Wnt/ β-catenin on osteogenesis has been

shown to involve a direct stimulation of *RUNX-2* gene expression (52). Wnt/β-catenin signaling also promotes the proliferation and mineralization activity of mature osteoblasts and reduces osteoblast apoptosis, as evidenced by *Lrp5* and *Lrp6* knockout mice (53, 54). Mice lacking *Lrp5*, similarly as patients with inactivating *Lrp5* mutations, exhibit low bone mass due to impaired bone formation. In contrast, a single point mutation G171V in *LRP5* is associated with increased bone mass in at least two human kindred (56, 57). The same mutation in HBM (high bone mass) transgenic mice displays a similar phenotype, characterized by high bone mass and enhanced bone strength (58). Currently, a large number of additional *LRP5* mutations associated with increased or decreased bone mass have been reported, indicating the importance of Wnt/β- catenin signaling in the control of bone mass. The phenotype of *Lrp6*-deficient mice with delayed ossification at birth and a low bone mass phenotype in adults correspond to those observed in mice carrying mutations in different *Wnt* genes (54). The Wnt/β-catenin signaling pathway is controlled by a number of regulatory proteins which, as a consequence, contribute to the regulation of osteoblast differentiation and function. For instance, the members of the Dickkopf (Dkk) family of proteins, together with their receptors Kremen1/2, inhibit Wnt/β-catenin signaling through internalization of Lrp5/6 from the cell surface. As a consequence, the Dkk/Kremen complex prevents the binding of Wnt proteins to the Lrp5/6 co-receptor. Ectopic expression of Dkk1 results in impaired osteoblast differentiation and maturation *in vitro* while mice that are deficient in a single Dkk1 allele exhibit a high-bone-mass phenotype (59). Dkk2 appears to play a role in late stages of osteoblast differentiation and mineralization of bone matrix. Mice lacking Dkk2 are osteopenia and osteoblasts from these mice exhibit impaired mineralization in response to osteogenic induction (60).

In the process of bone formation, some osteoblasts become embedded in their own synthesized osteoid, and subsequently differentiate into the terminal stage of the osteoblastic cell lineage, becoming an osteocyte. Simultaneously, other cells undergo apoptosis or remain on the bone surface, becoming flattened lining cells (Fig. 2.8). The expression of *alkaline phosphatase* (*ALP*) in the mature osteoblast disappears when the cell differentiates into an osteocyte.
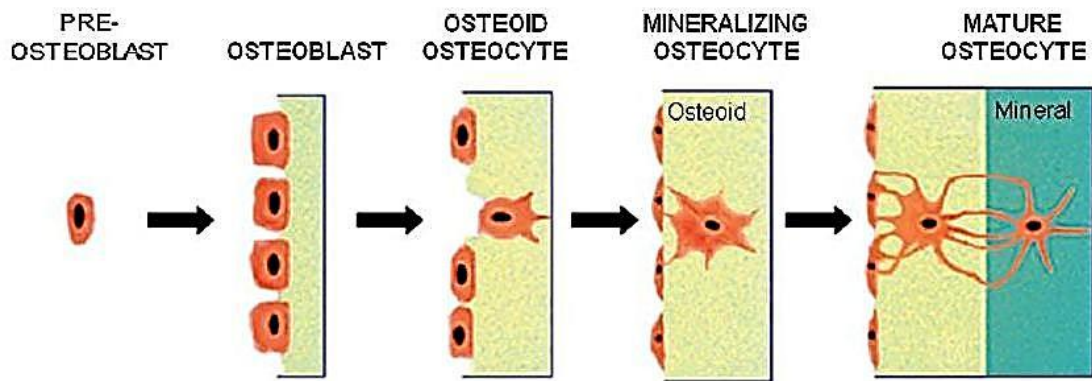
Figure 2.8: Pre-osteoblast differentiates into an osteocyte. The osteocyte appears to be the descendant of the matrix-producing osteoblast. Simultaneously, other cells undergo apoptosis or remain on the bone surface, becoming flattened lining cells (61)**.**

2.5. BMP signaling in bone development

Bone morphogenetic proteins (BMPs) are polypeptides. They are members of the transforming growth factor-β (TGF-β) superfamily of proteins that affects on mesenchymal stem cells. Several BMPs have been shown to promote chondrogenic and osteogenic differentiation of mesenchymal stem cells *in vitro*, and bone formation and repair *in vivo* (16).

Since its discovery in the 1960s by Urist, so far, approximately 20 BMPs have been identified and characterized. Of these twenty BMPs, BMPs 2-9 belong to the transforming growth factor-β (TGF–β) superfamily. Within this TGF–β superfamily, two members in particular, BMP-2 and BMP-7, have become the subject of extensive research. Exhibiting great osteogenic capacity, BMP-2 and BMP-7 have the ability to radically induce osteoblast differentiation in a variety of cell types and their significance in bone development is supported in various experimental studies (62, 63).

Although most BMPs are expressed in a variety of tissues during embryogenesis, some are detected in only a restricted set of tissues after birth. In adult mice, BMP-3, BMP-4, BMP-5 and BMP-6 are highly expressed in lung, whereas BMP-7 is highly expressed in kidney. The expression levels of BMP-4 and BMP-6 are much higher in adults than in young mice. Osteoblasts are an important source of

BMPs in bone matrix, and expression of some BMP mRNAs is induced during bone formation. BMP-4 is transiently induced in callus-forming cells in the early phase of fracture healing. BMP-6 is highly expressed in hypertrophic chondrocytes, which are intermediate between cartilage and bone during endochondral ossification (64).

BMPs are translated as large preproproteins containing signal peptides. Proproteins undergo dimerization, after which specific proteolytic enzymes cleave the dimerized proprotein to generate biologically active dimeric mature proteins. It has been shown that some BMP heterodimers are more potent in inducing ectopic bone formation than their respective homodimers (65).

Signaling by TGF-β superfamily members, including BMPs, is generally initiated upon their binding to transmembrane receptors. BMPs bind to two major types of membrane-bound serine/threonine kinase receptors, type I and type II receptors. BMP receptor oligomerization appears to be different from activin and TGF-β receptor oligomerization. For activin and TGF-β receptors, the ligands first bind to type II receptors, which in turn leads to the recruitment of type I receptors (Fig. 2.9). However, it has been demonstrated that BMPR-II and type I receptors form both homomeric and heteromeric complexes, even before ligand stimulation (64, 66).
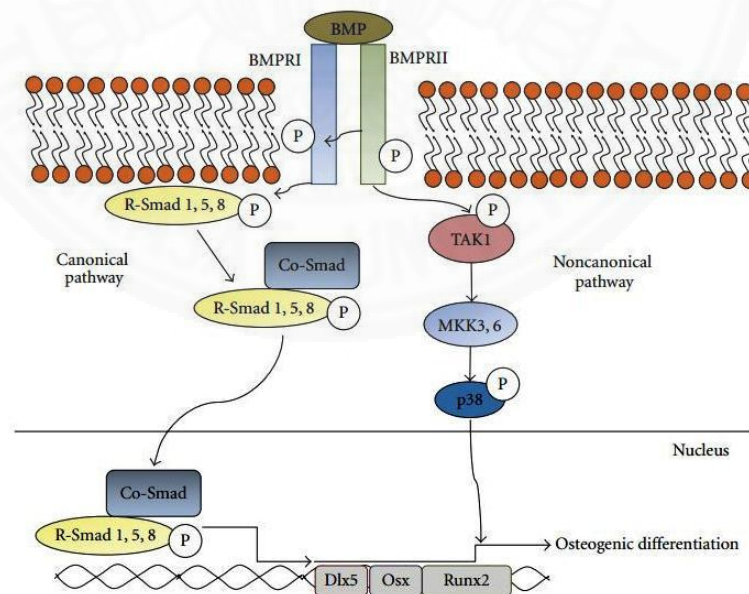
Figure 2.9: Schematic diagram of the canonical Smad-mediated and Smad-independent p38 MAPK pathways for BMP signal transduction (67).

Smad proteins play central roles in intracellular signaling by members of the TGF-β superfamily. Upon binding of a BMP ligand, the type II receptor transphosphorylates the type I receptor at an intracellular juxtamembrane site termed the GS domain. The phosphorylated type I receptor, in turn, phosphorylates a set of intracellular substrate signaling proteins collectively known as Smads. Smad proteins are classified into three subgroups, i.e., receptor-regulated Smads (R-Smads), a common-partner Smad (Co-Smad) and inhibitory Smads (I-Smads). The BMP-specific R-Smads, Smad1, Smad5, and Smad8 are phosphorylated by the BMP type I receptors at their carboxy-terminal Ser-Ser-X-Ser motifs. The phosphorylated Smad proteins form complexes with the Co-Smad, Smad4, translocate into the nucleus, bind to the regulatory elements of target genes, and regulate their transcription (65, 66). Smads are critically involved in osteoblast differentiation. Smad1 and Smad5 have been shown to be the major signaling molecules for inducing differentiation of myoblastic C2C12 cells into osteoblasts. Smad1 and Smad5, but not Smad8, synergize with Smad4 to promote chondrocyte differentiation from chondroprogenitor cells. By contrast, Smad8 and Smad4 exhibit modest effects in mesenchymal cells (64, 66).

Smad transcription factors are substrates of activated type I receptor kinases in the cytoplasm. The phosphorylated Smad proteins translocate into the nucleus, bind to the regulatory regions of target genes and regulate their transcription (64, 66). Thus, Smad proteins are key molecules in the transduction of signals from the cell membrane to the nucleus. Overexpression of Smad1, Smad5 or Smad8 induces ALP activity and *OCN* production in C2C12 and 10T1/2 cells (68). Smad4 is a Co-Smad that cooperates with all R-Smads. By contrast, both Smad6 and Smad7 inhibit signal transduction of the all TGF-β superfamily members. Smad signals are regulated positively and negatively not only by other Smads but also by transcriptional activators and/or repressors (64). Although BMP is known to be one of the most powerful cytokines to induce ectopic bone formation and strongly promotes differentiation of mesenchymal cells into osteoblasts and chondrocytes (64, 66, 69), until recently, it was still unknown whether BMP was really important for bone formation in physiological and pathological conditions, because mice lacking BMP-2 or BMP-4 die at early embryonic stages.

BMP induces *RUNX-2* expression in mesenchymal progenitors in a Smad-dependent fashion. *RUNX-2* interacts with Smad1 and Smad5, and regulates the expression of target genes which are involved in osteoblast differentiation (69, 70). However, several molecules inhibit this signaling cascade, thereby suppressing osteoblast differentiation. For example, Smad6 negatively controls osteoblast differentiation as an inhibitory Smad (69). Yoshida *et al*. showed that Tob, a member of the emerging family of anti-proliferative proteins, inhibits Smad1, Smad5 and Smad8, and consequently suppresses osteoblast differentiation. Furthermore, Tob-deficient mice showed greater bone mass resulting from increased numbers of osteoblasts (70). Therefore, these inhibitory network systems also contribute to the differentiation of MSCs into osteoblasts.

2.6. Bone engineering and bone grafting

Bone grafting is a surgical procedure where missing or damaged bone is repaired or replaced using natural or synthetic materials; from the patient's own body, from a donor, or using synthetic or natural substitutes such as hydroxyapatite, collagen or coral. Bone grafts can be used to repair fractures that fail to heal properly or voids that are extremely complex. The use of mesenchymal stem cells in bone graft application has been postulated for many years, with experimental animal data showing efficacy in intervertebral disc treatment (71).

Autografts are considered the gold standard for bone grafting, due to their osteogenic potential, osteoconductivity, and osteoinductivity. Furthermore, there are minimal immunological issues associated as a result of complete histo-compatibility (72). Moreover, autologous stem cells obviously do not have the same communicable disease transmission risk as allogeneic cells. While for most patients, autologous stem cell therapy may be suitable many studies have shown a lower differentiation potential in older patients (5). As result, some have postulated that allogeneic cells may be better suited for those patients.

Allografts from a different patient are most frequently used for spinal fusion surgery. In recent years the use of allograft has increased, due to improvements in the methods of procurement, preparation and storage, and also through the desire to avoid donor site morbidity associated with autogenously bone. In addition, allogeneic cells are proving a ready supply of cells for therapy (3).

Bone tissue engineering is a rapidly evolving technology, which aims at generating bone substitutes for the reconstruction of skeletal defects. Beyond the use and implantation of a cellular scaffolding biomaterials, bone engineers envision the possibility to interface stem cells to biomaterials for the *ex vivo* construction of bone-engineered constructs that functionally resemble the native tissue and/or promote a stable and enduring integration of the implanted construct. After *in vivo* implantation, the bone-engineered constructs ought to i) establish an appropriate connection with the surrounding tissue, ii) preserve cell viability and promote the regeneration of a functional tissue, iii) be immune tolerated and/or not elicit any adverse reaction (73). Stem cell-based bone engineering dates back to 1995, when de Bruyn et al. reported the ability of bone marrow cells to form bone after ectopic implantation in rabbits (74). Since then, many of experiments have been reported, both *in vitro* (75, 76) and *in vivo* in animal models (77 - 79) assessing the potential of stem cells for bone regeneration and engineering applications, although few examples of clinical applications have been reported so far (80). The intramembranous ossification pathway, with stem cells directly primed toward the osteogenic lineage, is adopted as an optimal strategy when engineering bone substitutes, especially due to the inferior time required to achieve bone formation (81). However, some authors have recently revisited the idea to engineer bone substitutes via the endochondral ossification pathway (82, 83), principally because a cartilaginous template may allow circumventing the limitations associated with low oxygen tension experienced for large engineered constructs. The proper combination of scaffolding materials, cells and pattern of biochemical and biophysical conditions represent today a great challenge for developing clinically relevant bone substitutes for the repair of large skeletal defects.

2.7. Mesenchymal stem cells

2.7.1 Characteristics of mesenchymal stem cells

Mesenchymal stromal cells or mesenchymal stem cells (MSCs) refers to a population of adherent adult stem cells defined by their ability to give rise to differentiated mesenchymal cell types including osteoblasts, adipocytes, and chondrocytes (84). Originally identified as fibroblast precursors within the bone

marrow (85). This population was later defined as originating from the stromal framework (86), hence the term mesenchymal stromal cell. Then, this population has been considered an adult stem cell population within the bone marrow, and called mesenchymal stem cell (87).

MSCs exhibit a fibroblast-liked morphology, form colonies when grown at clonal densities that referred to as colony-forming units – fibroblast or CFU-F (85). They can differentiate into osteoblasts, chondrocytes, and adipocytes under standard *in vitro* differentiating conditions. Human MSCs have been defined by the positive expression of the cell surface antigens, CD73, CD90, CD105, and a lack of expression of hematopoietic antigens including CD11b or CD14, CD34, CD45, CD79 or CD19, and HLA-DR (88). A comprehensive list of surface antigen expression on MSC was recently published (89). Despite the exhaustive number of studies conducted to define MSCs by their surface antigen expression profile, variability still exists within MSC populations due to differences in the species, tissue sources, and the *in vitro* culture conditions used. While this effort provides a necessary first step in standardization of the human MSC field, future efforts are necessary to better characterize these cells and identify markers capable of teasing apart this seemingly heterogeneous population and relating cellular phenotypes to biological function (84).

2.7.2 Sources of mesenchymal stem cells

Over the last decade, gestational tissue from human including the umbilical cord (UC), amnion (AM) (89), placenta (PL) and chorion (CH) (90) have been found to be a rich and valuable sources of MSCs. MSCs isolated from these tissues are bio-equivalent to BM-MSCs. Since these tissues are discarded after birth, the cells are easily accessible without ethical concerns.

It has recently been shown that amniotic tissues are a rich source of adherent cells that meet the criteria for human mesenchymal stem cells proposed by the Mesenchymal and Tissue Stem Cell Committee of the International Society for Cellular Therapy (88), and in agreement with the recommendation, the cells, isolated from the membrane and the fluid, were named amniotic membrane mesenchymal stromal cells (AM-MSCs) and amniotic fluid-derived multipotent mesenchymal stromal cells (AF-MSCs), respectively (91). Both AM-MSC and AF-MSC cells are free from ethical concerns and have the capacity for multi-lineage differentiation.

In addition, amniotic membrane may also provide another cell type, i.e. amniotic epithelial cells (AECs), derived from the embryonic ectoderm. Human AECs are unique cells exhibiting the characteristics of stem cells, i.e. *in vitro* the ability to produce cells of three germ layers (92).

The transplantation of human amniotic membrane has been performed in ophthalmology since the 1950s in the treatment of ocular disorders. Amniotic membrane was used as not only a substitute, but also as a scaffold upon which cells may migrate and regenerate, forming healthy tissues. The existence of a high number of mesenchymal stem cells with osteogenic and adipogenic potential within the amniotic membrane was reported for the first time in 2004 (10). AM-MSCs are easily isolated through mechanical and sequential trypsin and collagenase digestion, in a significant number, approximately 2×10^6 cells per gram of the amnion (93). They exhibit a fibroblast-like morphology and have a capacity to differentiate towards not only adipogenic and osteogenic, but also chondrogenic, myogenic and endothelial lineages (94). AM-MSCs have the capacity to support the hematopoiesis of CD34+ cells in co-cultures, even in the absence of exogenous cytokines. There is a possibility that the co-transplantation of the umbilical cord blood-derived hematopoietic stem cells with AM-MSCs might induce earlier and more complete recovery of hematopoiesis. This was observed in a mouse model (95) and if this observation is also confirmed in humans, this method would provide new insights for cord blood stem cell transplants. Of note, the amniotic membrane is avascular tissue, which does not contain endothelial cells; nevertheless, AM-MSCs have angiogenic abilities. Alviano and co-workers showed that AM-MSCs spontaneously form capillary-like structures when they are cultured in semisolid medium. Supplementing the culture medium with vascular endothelial growth factor (VEGF) strengthens the AM-MSCs angiogenic behavior (94). AM-MSCs are capable of secreting several growth factors that support angiogenesis and tissue remodeling, and decrease inflammation, such as: transforming growth factor-β (TGF-β), basic fibroblast growth factor (FGF), epidermal growth factor (EGF), keratinocyte growth factor, and hepatocyte growth factor (HGF) (96). The AM-MSCs retained a stable morphology for more than 20 passages. The phenotype of AM-MSCs (CD29, CD73, CD44 positive and CD14, CD34, CD45 negative) is similar to MSCs derived from adult bone marrow and umbilical cord blood (97). The genetic profiles of the AM-MSCs were compared with

the umbilical cord blood and bone marrow derived mesenchymal stem cells (BM-MSCs). The AM-MSCs express *octamer binding transcription factors* (*Oct-4*) – molecular markers typical for embryonic stem cells – at higher levels than BM-MSCs, which may suggest a higher position of these cells within the stem cell hierarchy compared with bone marrow derived-mesenchymal stem cells. The primitiveness of AM-MSCs also confirmed their anti-inflammatory and low immunogenic characteristics. It has been shown that AM-MSCs have the highest proliferation rates *in vitro* compared to fetal or adult stem cells (98).

Potential mesenchymal stem cells have been isolated from chorion. The morphological features of the cells isolated from the chorion are similar to those described for BM-MSCs and other type of mesenchymal stem cells. The effectiveness of the procedures of chorion derived mesenchymal stem cells isolation was confirmed by the presence of surface marker characteristic for BM-MSCs and the lack of hematopoietic and endothelial markers (99).

Mesenchymal stem cells derived from the chorion (CH-MSCs) have a significantly better chondrogenic, osteogenic, myogenic, and neurogenic differentiation potential than AM-MSCs (12). It may be related to the different origins of these two membranes, the chorion is derived from the trophoblast, the amnion is derived from the embryoblast (the inner cell mass of the blastocyst). There are a few reports stating that CH-MSCs could not be cultured *in vitro* beyond 5 passages (12). Many reports have shown that CH-MSCs are able to persist in culture for a maximum of 10 passages (99). Perhaps these cells have specific, unknown culture requirements. Despite this, the chorion, as a fetomaternal organ discarded following birth, represent important, valuable and promising sources of mesenchymal and hematopoietic stem cells.

The advantages of mesenchymal stem cells derived from placenta (PL-MSCs) are the lack of ethical controversies and the easily accessible source without invasive procedures. The number of potential donors of tissue for isolating PL-MSCs is also high. PL-MSCs are readily isolated from placenta using a variety of methods. The most popular one involves mechanical mincing, hemolysis for removing red blood cells, and trypsin digestion.

It was shown that PL-MSCs are able to differentiate into adipocytes, osteoblasts, myofibroblasts, hepatic cells, and neural-like cells under appropriate

conditions (100). An important aspect for clinical application of MSCs is the immunomodulatory capacity of PL-MSCs. Preliminary observation provides additional evidence concerning the potential immunomodulatory properties of MSCs, which may play a role in the induction of tolerance to allografts. Li and colleagues demonstrated that PL-MSCs do not induce allogenic lymphocyte proliferation and may inhibit a mixed lymphocyte reaction (MLR) (101). However, the mechanisms underlying these processes remain unknown.

Cells isolated from the umbilical cord, referred to as umbilical cord-derived mesenchymal stem cells (UC-MSCs), exhibit fibroblast like morphology and adhere to plastic culture flask. There are a few methods for the isolation of UC-MSCs, e.g. density gradient centrifugation and two-step enzymatic digestion. The most efficient method is via enzymatic degradation of the extracellular matrix to release the cells from the cord. These cells can be isolated in large numbers, approximately 1.5×10^6 cells per centimeter of the umbilical cord (102). Proliferation analysis revealed that human UC-MSCs have a faster population doubling time than BM-MSCs (103). UC-MSCs meet the basic criteria for MSCs established by the Mesenchymal and Tissue Stem Cell Committee of the International Society for Cellular Therapy in 2006. They (i) are plastic-adherent when maintained under standard culture conditions, (ii) have the capacity for osteogenic, adipogenic, and chondrogenic differentiation, and (iii) express CD73, CD90, and CD105, but do not express the hematopoietic lineage markers CD14, CD11b, CD34, CD45, CD19, and CD79 (88).

MSCs isolated from umbilical cord (UC-MSCs) are a highly homogeneous population of cells; it has been shown that UC-MSCs can differentiate into several lineages, including adipocytes, chondrocytes, osteoblasts, neuronal cells, endothelial cells, cardiomyocytes (16), hepatocyte-like cells, and pancreatic beta cells (102-105).

2.7.3 Proliferation potential of MSCs

Human MSCs expanded in a culture dish gradually change their appearance from spherical to spindle in shape as they transition from suspension to adherent culture condition under standard growth conditions i.e., 10% FBS-containing medium (106). Expanding MSCs undergo changes in their growth pattern from an initial lag phase to a rapid expansion phase. As adherent cultures are propagated, only

a fraction of cells remains clonogenic (able to generate CFU-F under standard growth conditions), suggesting the presence of an *in vitro* niche for true MSCs within the cultures (106). Unlike other stem cell populations such as human embryonic stem cells, most human MSCs in culture display a limited expansion potential *in vitro* about 5 – 10 passages and decreased differentiation potential with increased culture. Whether this lack of unlimited self-renewal is a result of insufficient or sub-optimal isolation techniques, growth in cell culture conditions or is a true indicator of the stemness associated with this population is yet to be determined. Although some studies have indicated no significant differences in regard to the morphology, phenotype, and immunosuppressive properties of MSC-liked cells, differences have been observed in regard to the success rate of isolating MSCs from tissue sources such as 100% for BM and AT-MSCs and 63% for umbilical cord blood derived MSCs (UCB-MSCs). Also, while the MSC colony frequency was lowest in UCB and highest in AT, it was found that UCB-MSCs could be cultured longer and showed higher proliferative capacity while BM-MSCs displayed reduced culture longevity. Most strikingly, UCB-MSCs showed limited adipogenic differentiation capacity, while BM- and AT-MSCs displayed a standard tri-lineage differentiation potential (107). By contrast, another report showed that applying identical culture conditions to MSCs from diverse sources resulted in major differences in MSC frequency and expansion potential, but the basic biological features of the expanded cells were comparable (108).

2.7.4 Differentiation potential of mesenchymal stem cells

Many accumulated reports since the discovery of human MSCs has convincingly shown that MSCs from diverse sources retain the ability to differentiate into various mesodermal lineages including osteoblasts, chondrocytes, and adipocytes (109). In addition, differentiation into additional cell types of mesodermal origin (skeletal muscle, smooth muscle, cardiac muscle, endothelial cells, etc.) and cells derived from other germ layers (neurons, hepatocytes, beta cells, etc.) have been reported, but thus far there is a lack of definitive evidence as to the functionality of these differentiated cells (91, 110). To elucidate the phenotype of differentiated MSCs, several classical assays have been employed including alkaline phosphatase and alizarin red S staining for osteoblasts, oil red O staining for adipocytes, and

alcian blue staining for chondrocytes. But these methods are limited in terms of defining the multipotential differentiation nature of MSCs (110, 111). There is a need for new additional assays to define the multipotential nature of MSCs as well as to identify early stage precursors of differentiating lineages, such as pre-osteoblast, pre-adipocyte, and pre-chondrocyte populations.

Establishing stem cell identity and function is defined by the prospective isolation of a single stem cell in order to prove (a) self-renewal, (b) multipotential differentiation, and (c) repopulating capacity. These considerations are difficult to demonstrate with a single MSC. For human MSCs, intrinsic tissue turnover poses a barrier to assess the self-renewal rate of undifferentiated stem cells. Similarly, it is not clear whether the greater differentiation potential is acquired during cell culture of MSCs. Extensive transcription profiling and *in vitro* and *in vivo* assays have identified specific genes implicated in osteogenesis (*FHL2*, *ITGA5*, *Fgf18*), chondrogenesis (*FOXO1A*), and tenogenesis (*Smad8*) (112). Further data is required to develop effective directed differentiation techniques to isolate a specific lineage. A decline in the frequency of potent MSCs has been implicated in aging and degenerative diseases. Thus, identifying the ideal cells for *ex vivo* expansion will form a major pursuit for an efficacious clinical application. Similarly, though it is difficult to demonstrate the efficiency of repopulation of MSCs, studies have confirmed the co-transplantation of MSCs and CD34+ cells can promote hematopoietic stem cell transplantation and hematopoietic recovery *in vivo* (113). Following transplantation, MSCs are expected to reduce the damage and activate the endogenous regenerative potential in recipient tissue (114). The challenges in MSC field can be addressed by developing clearly defined conditions of MSC isolation, expansion in cell culture, low or high seeding density, different culture media used such as, serum-free and xeno-free culture medium or with serum supplementation, extent of *ex vivo* expansion, that will significantly improve the understanding of basic properties of MSC and their utility in immune and therapeutically benefit (84).

Regenerative medicine is a rapidly growing specialty. Recently, regenerative medicine was defined as the field of research focused on the repair, replacement or regeneration of cells, tissues, and organs (115). The primary goal is to augment the body's natural ability to replace tissue damaged or destroyed by injury or disease. Stromal cell research has proven invaluable in the development of cellular therapy

because of enormous contributions to knowledge of the mechanisms of cellular proliferation and differentiation (116). Many current treatments may be augmented or replaced by regenerative medicine, and a number of therapies are currently under investigation. In addition to orthopedics, they have been used mainly for bone grafting of skeletal defects, in the management of delayed unions and non-unions, to obtain spinal arthrodesis (117), in the treatment of osteonecrosis (118), and, more recently, for tissue engineering purposes. Continued research is underway to incorporate stromal cells into standard treatments.

2.8. Osteogenic differentiation of MSCs

Mesenchymal stem cells are the key stem cells involved in bone regeneration and can be readily isolated from bone marrow (13). Once purified these cells can be expanded, differentiated and delivered together with a bone graft to enhance repair. The process of MSCs differentiation into osteoblasts and ultimately osteocytes, also known as osteogenesis, is activated and regulated by a variety of soluble factors and physical environment *in vivo*. Mesenchymal stem cells can be induced to differentiate into osteoblasts *in vitro* through the addition of soluble factors such as; glucocorticoids, growth factors, hormones, and vitamins (13). The most commonly used combination of soluble factors to promote osteogenic differentiation *in vitro* is dexamethasone, ascorbic acid and β- glycerophosphate. Each constituent stimulates or supports osteogenic differentiation of mesenchymal stem cells *in vitro*.

Dexamethasone is a synthetic corticosteroid, although not found naturally in the body, imitates the actions of various glucocorticoids such as cortisol, oestradiol, testosterone, vitamin D3. Glucocorticoids influence the expression of many genes, through binding to specific activator proteins. In the absence of a glucocorticoid, activator proteins are kept in the cytosol and cannot bind DNA. *In vitro* dexamethasone can stimulate osteogenic differentiation of MSC and acts at multiple points in the differentiation process to stimulate osteoblastic maturation; transforming MSCs morphology from spindle-shaped to cuboidal, increasing alkaline phosphatase (ALP) activity and enhancing mineralization (119). It was previously thought that dexamethasone was required for MSCs differentiation *in vitro* however; multiple studies have demonstrated it enhances osteogenic differentiation but is not essential

(120, 121). Long-term intake of dexamethasone *in vivo* can result in osteoporosis, through decreased osteoblast activity (122).

Ascorbic acid is an essential component in the synthesis of hydroxyproline and hydroxylysine, two key components required to stabilize the collagen triple helix and to form intermolecular crosslinks within collagen (123). Several studies have shown that ascorbic acid concentration is correlated with collagen production by osteoblasts and also linked to enhanced ALP activity (124).

β-glycerophosphate provides a source of organic phosphate ions that promote mineralization *in vitro* (125). Despite several studies, the exact mechanism behind this mineralization remains unclear, but may be related to the ability of ALP to hydrolyze organic phosphate and release inorganic phosphate (126).

2.9. Postnatal tissues

2.9.1 Amnion

The amniotic membrane is a tissue of fetal origin and is composed of three major layers: a single epithelial layer, a thick basement membrane, and an avascular mesenchyme (127) (Fig. 2.10). The amniotic membrane has no nerves, muscles or lymphatic vessels in the amnion. The amniotic membrane is derived from the inner cell mass in the blastocyst and is adjacent to the trophoblast cells and lines the amniotic cavity. It can be easily separated from the underlying chorion, with which it never truly fuses at the cellular level. The amnion is embryologically continuous with the epithelium of the umbilical cord, where it firmly fuses during development and cannot be dislodged (128) (Fig. 2.11). The important function of the amniotic membrane is to provide the developing embryo with protection against desiccation and an environment for suspension in which the embryo can grow without distortion by pressure from surrounding structures.
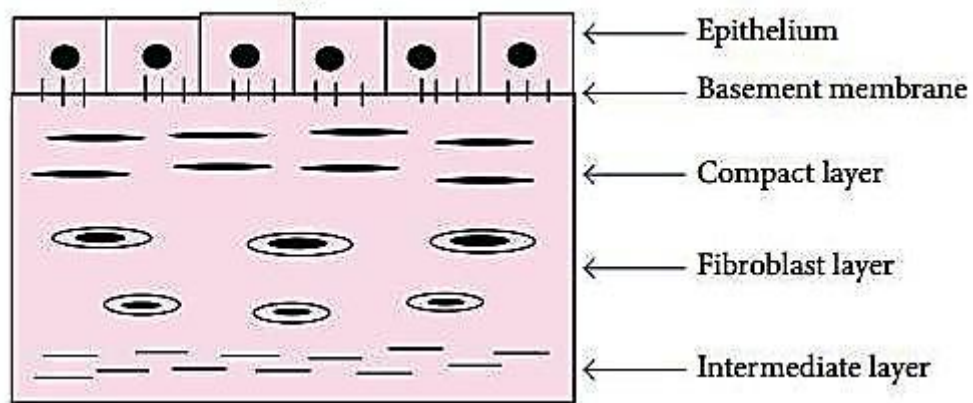
Figure 2.10: Line diagrammatic representation of histological architecture of amnion (129).
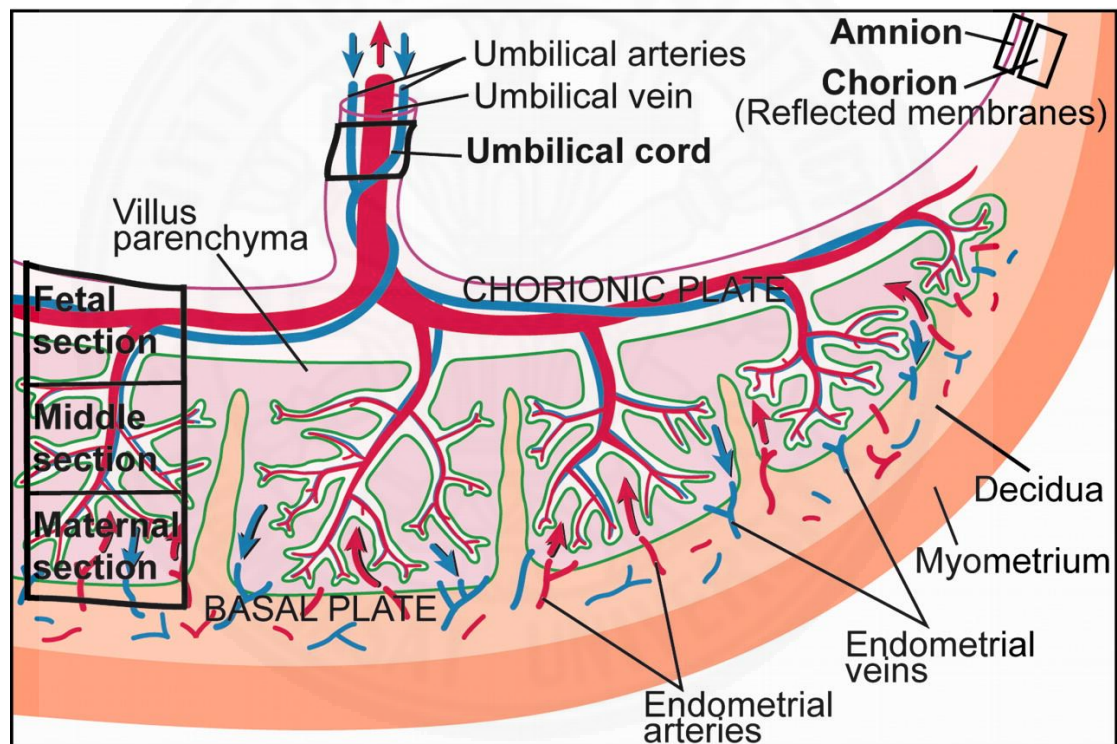
Figure 2.11: Schematic representation of a human term placenta (128).

2.9.2 Chorion

The chorion is the most outer membrane that is formed between the developing fetus and the mother's organism during pregnancy. Once the primitive chorionic villi are formed and throughout the pregnancy, distinct subtypes of the trophoblast can be recognized. Chorionic villi are composed of mesenchymal and trophoblastic components. The mesenchyme of chorionic villi contains stromal cells

and blood vessels that are directly connected to the fetal circulation via the umbilical cord. The surface of chorionic villi is covered by two layers of trophoblast, an inner mononuclear cytotrophoblast and an outer multinucleated syncytiotrophoblast (130). Chorion is composed of reticular layer, basement membrane, and trophoblasts (129) (Fig. 2.12).
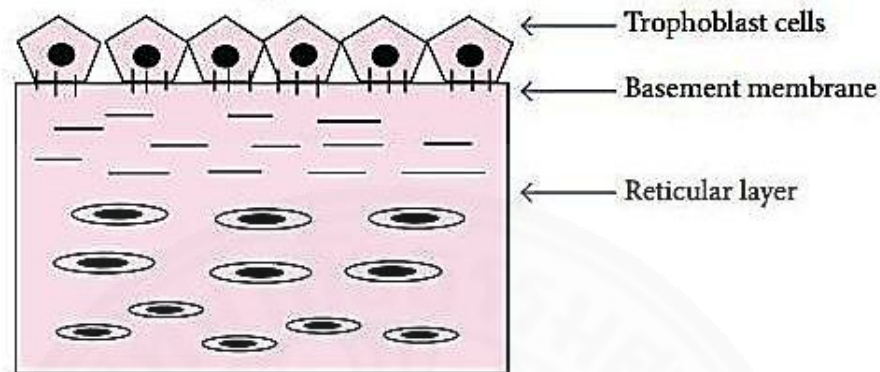
Figure 2.12: Line diagrammatic representation of histological architecture of chorion (129).

2.9.3 Placenta

The utero-placental unit is composed of both fetal tissue derived from the chorionic sac and maternal tissue derived from the endometrium. In the mature placenta, the fetal aspect is called the chorionic plate. This region carries the fetal chorionic blood vessels, which are branching radials from the umbilical vessels. The maternal aspect of the placenta is called the basal plate. In between these two regions is the intervillous space, which contains the main functional units of the placenta, extensively branched and closely packed villous structures containing fetal blood vessels. It is at the terminal regions of these chorionic villi that the large majority of maternal-fetal exchange occurs (131) (Fig. 2.11).

2.9.4 Umbilical cord

The umbilical cord is the connecting cord from the developing embryo to the placenta. It develops from the yolk sac and allantois. It forms by the fifth week of fetal development, replacing the yolk sac as the source of nutrients for the fetus. The cord is not directly connected to the mother's circulatory system, but instead joins the placenta, which transfers materials to and from the mother's blood without allowing direct mixing. The umbilical cord in a full term neonate is usually about

50 centimeters long and about 2 centimeters diameter. In the umbilical cord two arteries and one vein are surrounded by a mucoid connective tissue, called Wharton's jelly (Fig. 2.11). Wharton's jelly is composed of myofibroblast-like stromal cells, collagen fibers, and proteoglycans (132).

2.10. The regulation of gene expression by microRNA

MicroRNAs (miRNAs) are a class of short non-coding RNA molecules that regulate gene expression at post-transcriptional level by binding to specific sequences within a target mRNA (19, 133). MiRNAs have been reported to be involved in almost every biological process, including development timing, cell differentiation, cell proliferation, cell death, metabolic control, transposon silencing, and antiviral defense (134). Hundreds of miRNAs, which are evolutionarily conserved, have been identified in humans. To date, more than 3% of the genes in humans have been found to encode for miRNAs. About 40 % to 90 % of the human proteins encoding genes are under miRNA-mediated gene regulation (135). MiRNA genes are found as single or clustered transcription units (136, 137), short (approximately 21-nucleotide) non-coding RNAs that regulate transcript localization, polyadenylation, and translation. MiRNAs are direct negative regulators of gene expression that bind to specific sequences within a target mRNA (133). They are expressed from the intron regions of protein-coding or non-protein-coding genes; in some cases, they are expressed as independent transcription units (138). They mediate post transcriptional gene silencing by binding to sites of antisense complementarity in 3′ untranslated regions (UTRs) of target mRNAs (139).

MiRNAs are synthesized through multiple steps (Fig. 2.13). Initially, a miRNA is transcribed into a primary miRNA (pri-miRNA) in the nucleus by RNA polymerase II. The pri-miRNA is processed by the double-stranded RNA binding protein coded by DiGeorge syndrome critical region gene 8 (DGCR8) and the nuclear RNase III enzyme Drosha into stem-loop structured pre-miRNAs (140). The pre-miRNA is further transported to the cytoplasm by the Ras-related nuclear protein-guanosine-5′-triphosphate-dependent export receptor Exportin-5 and then cleaved by a second RNase III endonuclease Dicer. This process forms a transient, double stranded miRNA of 22 nucleotides. The miRNA duplex is incorporated into a multicomponent protein complex known as RNA induced

silencing complex (RISC), which contains the Argonuate 2 protein (141). During the functional process, one strand of the miRNA duplex is rapidly removed and degraded, while the other strand is selected as a mature miRNA. The mature miRNA negatively regulates gene expression through translational repression or mRNA cleavage, which depends on the extent of complementarity between the miRNA and its target. If the target mRNA has perfect complementarity to the miRNA-armed RISC, the mRNA will be cleaved and degraded (Fig. 2.13) (142, 143). However, same to the most common finding in mammalian cells, miRNAs target mRNAs with imperfect complementarity and suppress their translation, resulting in the reduced expression of the corresponding proteins (144, 145).
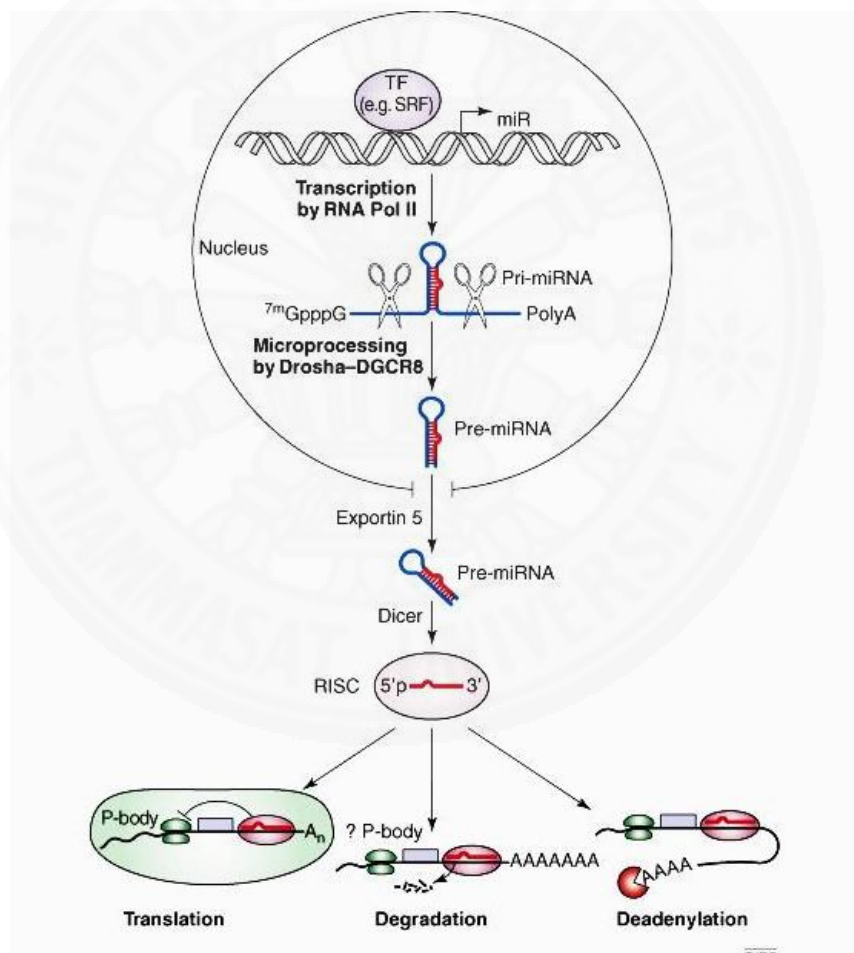
Figure 2.13: The model of miRNAs biogenesis and function (146).

Microarray technology has been widely and successfully used in genomic and biologic research (147). The application of locked nucleic acid (LNA), one of many

successful examples of microarray technology adopted into miRNA studies, modifies oligonucleotide probes by modifying the LNA contents in the probe and eliminating the diversity of melting temperature (Tm) values in individuals. Thus, microarray technology enhances binding affinity and leads to the improvement of miRNA detection specificity and sensitivity (148).

Bead-based arrays, which carry uniquely colored (up to 100 colors), five-micron polystyrene beads and are covered with oligonucleotide capture probes specific to a single miRNA, are hybridized to biotinylated miRNA and then stained with streptavidin-phycoerythrin. Bead-based arrays allow for the inclusion of many combinations of miRNA capturing beads into a single pool, which are adjusted based on the interaction of bead-coupled probes and provide greater flexibility over time as more miRNAs are discovered and their corresponding beads are created (149).

Quantitative real-time reverse transcription polymerase chain reaction (qRT-PCR) assay is a rapid and reproducible method that has been widely applied in miRNA research over the years; the procedure is recognized as a gold standard for miRNA determination (150). TaqMan technology, a relatively mature technology for the qRT-PCR application, has been adopted into miRNA research; it utilizes a stem-loop structure specific for binding mature miRNA. An innovative design of TaqMan Low Density Arrays (TLDA), developed from TaqMan technology, has become a medium-throughput method for real-time RT-PCR that uses 384-well microfluidics cards. A single TLDA card may assay up to 384 miRNAs (151).

Prediction and validation of the miRNAs target, the 5′ proximal end of a mature miRNA (nucleotide positions 2nd to 7th, or 2nd to 8th) is referred to as the seed region. This region is important for target recognition by binding to the seed (nucleus) complementary sequence in the 3′ UTR of target mRNAs. Computational and experimental techniques for predicting miRNA targets are mainly based on programming alignment to identify conserved complementary motifs in the 3′ UTR with the seed sequence of the miRNA (152). These sophisticated bioinformatic approaches reveal that a miRNA is estimated to target, on average, hundreds of mRNAs (153). In the last few years, many distinct computational methods and algorithms have been developed to predict miRNA targets. Among them, TargetScanS (154), PicTar (155) and miRanda (156) are the most common target prediction programs, whereas miRBase (157), Argonaute, and

miRGen (158) are databases that combine a compilation of miRNAs with target prediction modules. Prediction of miRNA targets by computational approaches is based mainly on the following steps. The first step is the identification of potential miRNA binding sites in the mRNA 3′ UTR according to specific base-pairing rules, especially strong Watson-Crick base-pairing of the seed region (6 or 7 nucleotides at the 5′ end) of the miRNA to a complementary site in the 3′ UTR of the mRNA. The second step involves the implementation of cross-species conservation requirements. The third step requires local miRNA-mRNA interactions with a positive balance of minimum free energy. One direct method for validating targets is the use of a luciferase reporter plasmid with a replaceable 3′ UTR. By cloning sequences corresponding to individually predicted target sites into the 3′ UTR of this reporter and co-transfecting it with miRNA precursors, the inhibition of luciferase activity can be measured.

2.11. Role of miRNAs in osteogenesis

The osteogenic differentiation of MSCs to osteoprogenitors, pre-osteoblasts, early osteoblast and mature osteoblasts involves a coordinated action of multiple transcription factors and signaling molecules. The commitment and differentiation of MSCs towards osteogenic lineage is driven by the transcription factor *RUNX-2* and *OSX*. Particularly, many miRNAs participate in the regulation of *RUNX-2* expression, illustrating the high redundancy of miRNA regulation associated with vital signaling pathways. For instance, miR-204 and its homolog miR-211 are highly expressed in murine MSCs and ST2 mesenchymal progenitor cells and their levels are increased during adipogenesis, along with decreased *RUNX-2* level (22). Overexpression of miR-204 leads to suppressed osteoblastogenesis and increase adipogenesis. An inverse outcome results from miR-204 inhibition, suggested that miR-204/211 directs mesenchymal progenitor cells towards adipogenic lineage at the expense of osteogenesis.

Another *RUNX-2* targeting miRNA, miR-335, is abundant in undifferentiated hMSCs whereas its expression is downregulated during osteogenesis and adipogenesis (159). In contrast to miR-204, overexpression of miR-335 inhibits both osteogenic and adipogenic differentiation of hMSCs. Taking into account that miR-335 also suppresses the proliferative and migratory capacities of hMSCs, it may be

associated with a common regulatory pathway controlling MSC proliferation, differentiation, and migration. A more comprehensive view of the miRNA-mediated regulation of *RUNX-2* signaling was obtained recently when a group of 11 miRNAs was shown to attenuate *RUNX-2* expression during osteoblast and chondrocyte differentiation (160). Those miRNAs include miR-23a, miR-30c, miR-34c, miR-133a, miR-135a, miR-137, miR-204, miR-205, miR-207, miR-218 and miR-338.

Besides being a direct target for several miRNAs, *RUNX-2* contributes to miRNA-mediated regulation of osteoblast-related miRNAs. During osteoblast differentiation, induction of *RUNX-2* suppresses the expression of three miRNAs in a cluster, miR-23a-27a–24-2 via direct binding to *RUNX-2* binding element found in the promoter region of the cluster (161).

Additionally, miR-31, miR-106a, and miR-148a are underexpressd in osteo-differentiated MSCs. Those miRNAs target to *RUNX-2* but their target verification and function analysis are needed to provide more conclusive evidence to explain the miRNA regulatory mechanisms (21). Furthermore, miR-31 was observed to be reduced during osteoinductive differentiation of adipose derived stem cells and the usage of Lenti-as-miR-31 significantly promoted osteogenesis with enhanced SATB2 levels in vitro. The anti-miR-31-modified adipose tissue-derived mesenchymal stem cells (ADSCs) via lentiviral vector were applied to repair critical-sized defects (CSDs) in rats combined with the β-tricalcium phosphate (β-TCP) scaffolds (162). Moreover, the miR-31 genetically modified BM-MSCs were also succeeded in repairing rat medial orbital wall defects (163). Li and colleagues found that miR-106a was down-regulated during differentiation of human ADSCs (hADSCs) toward osteogenic lineage, but up-regulated during adipogenesis. Enhanced level of miR-106a promoted adipogenesis of hADSCs, and inhibited osteogenic differentiation, whereas knockdown that miRNA had opposite effects (164). In addition, overexpression of miR-148a promotesd osteoclastogenesis, whereas inhibition of miR-148a attenuated osteoclastogenesis. Antagomir-148a was injected into a tail vein to demonstrate mice lacking miR-148a. The results showed antagomir-148a treatment led a significant increase bone mass (165).

The BMP signaling pathway plays a prominent role in promoting osteoblast differentiation and bone formation (166). Several studies have focused on miRNAs modulated by BMP signaling as a means to understand the role of miRNAs in

osteoblasts. From these studies, it is clear that a panel of BMP-regulated miRNAs is important for the regulation of osteoblast differentiation. Since some miRNAs can be co-expressed and/or co-regulated, it is possible that families of miRNAs may promote one phenotype at the expense of another. These appears to be the case for miR-133 and miR-135, are down-regulated during BMP-2-induced osteoblastic differentiation of C2C12 premyogenic cells, but are up-regulated in these cells during myoblastic differentiation (167). Over-expression of miR-133 or miR-135 blocked the BMP-mediated induction of osteoblastic markers, such as *ALP*, *OCN,* and HOXA10. Further studies demonstrated that *RUNX-2* is a target for miR-133, and Smad5 is a target for miR-135. *RUNX-2* is a transcription factor essential for osteoblast differentiation, whereas Smad5 is an intracellular *RUNX-2* co-receptor (168). The concomitant down-regulation of these two miRNAs by BMP-2 likely plays an important role in the up-regulation of *RUNX-2* and Smad5 during osteogenic differentiation. Similarly, miR-206 is decreased in response to BMP-2 in C2C12 cells and during differentiation of primary murine osteoblasts (169). Over-expression of miR-206 inhibits ALP activity, and Connexin 43 (Cx43) was shown to be a target of miR-206. Cx43 is a gap junction protein necessary for osteoblast differentiation and function (170). *In vivo*, miR-206 is highly expressed in muscle and perichondrial osteoblasts at E14.5, is moderately expressed in bone collar cells at E16.5, and is undetectable in bone at E18.5. Transgenic mice expressing miR-206 in mature osteoblasts display a low bone mass phenotype, particularly evident in the trabecular compartment. Bone formation rate was decreased in the transgenic mice, suggesting a defect in osteoblast function, whereas the osteoclast surface was unchanged. These data confirm miR-206 as a negative regulator of osteoblast function.

Taken together, it is clear that miRNAs play an important role in osteoblast function and differentiation. Thus, defining the function of particular miRNAs in osteoblast commitment and differentiation, could allow for the assembly of a panel of miRNAs that could be used as differentiation markers, similar to the panel of markers presently used to annotate the progression of differentiation, such as *RUNX-2*, *ALP*, *OCN*, and *OSX* (29).

2.12. Clinical application of miRNAs

Clinical applications aberrant miRNA expression, and thereby dysregulation of their target genes, has been implicated in human malignancies and a variety of other pathologies. As with protein-coding genes, the deregulation of miRNAs may result from deletion, amplification, mutation, or dysregulation of transcription factors controlling specific miRNAs. In addition, miRNAs may be influenced by epigenetic mechanisms such as DNA methylation and histone modifications. The pioneer work by Calin et al. showed that miR-15a/miR-16-1 cluster is downregulated or deleted in more than 60% of chronic lymphocytic leukemia patients (72). The same group also demonstrated that a significant percentage of miRNA genes are located in cancer-related or fragile genomic sites, further supporting the association between miRNA expression and disease. In subsequent studies over the past decade, an altered miRNA expression pattern has been described in almost all types of cancer and a large number of other human disorders, including cardiovascular disease, neurological disorders, autoimmune disease, and skeletal disease (71).

2.12.1. MiRNAs as molecular biomarkers

Recent studies have shown significant levels of miRNAs in serum and other body fluids, raising the possibility that miRNA expression profiling could provide a noninvasive method for disease diagnosis and prognosis as well as for prediction of therapeutic responses. Indeed, extracellular miRNAs exhibit several features that support their utility as clinical biomarkers: high stability, conservation among species, tissue and disease-specific expression pattern, and easy assessment by various methods, such as microarrays and real-time polymerase chain reaction (RT-PCR) (171, 172). While the mechanisms by which miRNAs are exported remain unclear, the cause of unusual stability of secreted miRNAs has started to be revealed. Extracellular miRNAs are secreted in microparticles (exosomes, microvesicles, and apoptotic bodies) (173, 174) or associate with Ago2 proteins (175, 176) or lipoprotein complexes (177) and are thereby protected from degrading ribonucleases. Although the biological function of secreted miRNAs remains inconclusive, their utility as diagnostic or prognostic biomarkers has been demonstrated in multiple diseases, including different types of cancers and cardiovascular diseases (172).

2.12.2. MiRNAs as therapeutics

MiRNA gain- and loss-of-function studies in normal tissues often result in minor, if any, phenotype suggesting that other miRNAs are able to compensate for the loss of a specific miRNA. However, under pathologic conditions such as cancer, delivery of synthetic anti-miRNAs selectively affects tumor cell growth and survival without any effect on normal cells, suggesting an increased sensitivity to miRNA regulation under stress. Therefore, inhibition or delivery of miRNAs may provide novel mechanisms to modulate disease processes while avoiding toxic effects in normal tissues. This potential has prompted significant efforts to develop miRNA-targeted therapeutics. The most widely used approach to alter miRNA regulation is the anti-sense strategy, which exploits chemically modified oligonucleotides containing antisense sequences against mature miRNAs. A variety of chemical modifications, such as 2'-0-methyl and locked nucleic acid (LNA) modifications, are described to enhance their stability, cellular uptake and efficacy (178). The most promising results this far have been obtained with LNA-modified anti-miR Miravirsen (Santaris Pharma) directed against miR-122 as a treatment for hepatitis C virus (HCV) infection. Binding of miR-122 to viral 5' non- coding region is essential for HCV replication, and inhibition of this miRNA with anti-miRs suppresses viral replication in rodents and primates (179). The Phase II trial with human patients shows dose- dependent and long-lasting suppression of HCV, without evidence of toxicity (180). Another promising method of miRNA inhibition comprises the use of "microRNA sponges" (26). These inhibitors contain multiple tandem binding sites for a specific miRNA and when introduced to cells, they sequester endogenous miRNAs thereby preventing their interaction with targets. Compared to miRNA inhibitors, the development of miRNA mimics appears to be more problematic. The main challenge is to generate and effectively deliver a double-stranded RNA molecule in which one strand, the "guide", is identical to the mature miRNA while the complementary strand, or "passenger", accounts for the stability and cellular uptake. Further complications arise from the tendency of passenger strand to function as an anti-miR. However, special delivery methods, such as lipid complexes, nanoparticles and viral vectors, appear to provide potent means for miRNA mimicry in diseases associated with decreased miRNA expression (181).

Overall, it is clear that miRNAs play an important role in osteoblast function and differentiation. Future work, defining the function of particular miRNAs in osteoblast commitment and differentiation, could allow for the assembly of a panel of miRNAs that could be used as differentiation markers, similar to the panel of markers presently used to annotate the progression of differentiation, such as *RUNX-2*, *ALP*, *OCN*, and *OSX* (29).

CHAPTER 3

METHODOLOGY

3.1 Collection of human specimen

The collection of human specimen was approved by the Human Ethics Committee of Thammasat University (MTU-EC-DS-1-061-57). All subjects participated in the study after giving written informed consents.

Human bone marrow aspirates were obtained from sternum or iliac crest of normal healthy volunteers. The samples of amnion, chorion, placenta and umbilical cord were obtained from pregnant women after normal deliveries at Thammasat Chalermprakiat Hospital. Subjects who had any clinical history of malignancy, metabolic disorder, or infectious disease were excluded from the study.

3.2 Isolation and culture of MSCs from bone marrow

Bone marrow aspirated (20 ml) from sternum or iliac crest of normal healthy volunteer were placed in 50 ml sterile tube (Costar, corning, USA) containing 500 µl of heparin (LEO 5,000 i.u./u.i./ml). The aspirate of bone marrow was diluted with equal volume of phosphate-buffered saline (PBS) and was carefully layered over Ficoll-Paque PLUS solution (GE Healthcare, Bio-science AB, Sweden). After density gradient centrifugation at 100xg (Hettich, Universal 320K, USA) for 30 min at 20°C, mononuclear cells (MNCs) were removed from the interphase layer, washed twice with 15 ml washing buffer [PBS containing 100 U/ml penicillin and 100 µg/ml streptomycin (GibcoBRL, USA)] and centrifuged at 380xg for 5 min at room temperature. Cell numbers were enumerated using hemocytometer. Bone marrow-derived MNCs were cultured in complete medium [Dulbecco's Modified Eagle's Medium (DMEM; GibcoBRL, USA) containing 10% fetal bovine serum (FBS; Invitrogen, USA), 2 mM L-glutamine (GibcoBRL, USA), 100 U/ml penicillin and 100 µg/ml streptomycin] at density of $1x10^5$ cells/cm^2 in 25-cm^2 tissue culture flasks (Costar, corning, USA). The cells were cultured at 37°C in a humidified tissue culture incubator with 5% CO_2. After 72 h, non-adherent cells were removed and fresh medium was added to the flasks. The cultures were maintained in this condition with

complete change of culture medium every 3 - 4 days. Culture flasks were observed continuously to get hold of developing colonies of fibroblast like cells. After culture for 7 - 12 days, the plastic-adherent cells (about 80 - 90% confluence) were sub-cultured using 0.25% trypsin-EDTA (GibcoBRL, USA) and replaced at density of $1x10^4$cells/cm^2 for further expansion. Some batches of continuously sub-culture cells were cryopreserved in freezing medium (90% FBS and 10% DMSO) and stored in liquid nitrogen for future use.

3.3 Isolation and culture of MSCs from postnatal tissues

Postnatal tissue obtained from pregnant women after normal delivery including amniotic tissue (diameter ~5 cm), chorionic tissue (diameter ~5 cm), placental tissue (size ~3x3x1 cm), and umbilical cords (length ~2 - 4 cm) was dissected under aseptic condition. The tissue was washed with washing buffer and minced into small pieces of approximately 1 - 2 mm^2 in size. The tissue was then digested with 1.6 mg/ml collagenase XI (Sigma-Aldrich, USA) and 200 mg/ml deoxyribonuclease I (Sigma-Aldrich, USA) for 4 h at 37°C with shaking. Subsequently, the cells were washed twice with washing buffer and cultured with complete medium in 25cm^2 tissue culture flasks (Costar, corning, USA). The cells were cultured at 37°C in a humidified tissue culture incubator with 5% CO_2. The cultures were maintained at 37°C in a humidified tissue culture incubator with 5% CO_2. The culture medium was changed every 3 - 4 days. Culture flasks were observed continuously to get hold of developing colonies of fibroblast–like cell. The plastic-adherent cells (about 80-90% confluence) were sub-cultured using 0.25% trypsin-EDTA (GibcoBRL, USA). Some batches of continuously sub-culture cells were cryopreserved in freezing medium (90% FBS and 10% DMSO) and stored in liquid nitrogen for future use.

3.4 Generation of growth curve

For evaluating the growth characteristic of MSCs derived from bone marrow, amnion, chorion, placenta, and umbilical cord , culture-expanded MSCs (passage 2 – 4) were trypsinized using 0.25% trypsin-EDTA and re-plated in 24-well cell culture plate (Costar, corning, USA) containing 1 ml of complete medium at a density of 500 cells/cm^2. The cells were maintained at 37°C in a humidified tissue

culture incubator with 5% CO_2. Subsequently, the cells from each well were harvested at culture day 2, 4, 6, 8, 10, 12, and 14 to determine cell number using hemocytometer. The mean of the triplicate cell counts for each day were calculated and plotted against culture time to generate a growth curve.

3.5 Population doubling assay

To measure the growth kinetics of MSCs derived from bone marrow, amnion, chorion, placenta and umbilical cord, cultured MSCs were trypsinized using 0.25% trypsin-EDTA (the viable cells were enumerated at passage 1 using hemocytometer and trypan blue exclusion assay). For each subsequent passage (passage 2 - 8), 6.0×10^3 cells/cm^2 were seeded on 24-well cell culture plate (Costar, corning, USA) in triplicate. After 48 hours, the cell number after each passaging step was used to calculate the total number of yielded cells and the doubling time was calculated according to the formula:

Population doubling number (PDN) = $\log (N_1 / N_0) \times 3.31$

Population doubling time (PDT) = cell culture time / PDN

(N_1 = cell number at the end of cultivation, N_0 = cell number at culture initiation)

The population doubling time assays were performed in triplicate for each isolated cell population. The mean of the triplicate cell counts for each passage was calculated and plotted against culture time to generate a population doubling time curve.

3.6 Immunophenotypical characterization of MSCs

The cultured MSCs were immunophenotypical characterized using Flow cytometer (FACScalibur^{TM}, Becton Dickinson, USA). Primary cultures from bone marrow, amnion, chorion, placenta and umbilical cord at passage 2 to 5 were detached with 0.25% trypsin-EDTA and washed twice with PBS. In each sample, 4×10^5 cells were resuspended in 50 µl of PBS and incubated with 10 µl of fluorescein isothiocyanate (FITC) or phycoerythrin (PE)-conjugated antibodies against CD34 (BioLegend, USA), CD45 (BioLegend, USA), CD73 (BioLegend, USA), CD90 (BioLegend, USA) or CD105 (BD Bioscience, USA) for 30 min at 4°C in the dark. After washing with PBS, the cells were fixed with 1% paraformaldehyde in PBS. The positive cells were identified by comparison with isotype-match controls [FITC-conjugated mouse immunoglobulin G1 (IgG1) and PE-conjugated mouse

immunoglobulin G2a (IgG2a)]. At least twenty thousand labeled cells were acquired and analyzed using flow cytometer (FACScalibur^{TM}, Becton Dickinson, USA) and CellQuest$^{®}$ software (Becton Dickinson, USA).

3.7 Adipogenic differentiation of MSCs

The adipogenic differentiation potential of MSCs derived from bone marrow, amnion, chorion, placenta, and umbilical cord was examined using passage 3 to 4 of cultured cells. Briefly, 8 x 10^3 cells/cm^2 of MSCs were cultured with MSC complete medium in 35-mm^2 dishes (Costar, corning, USA). The cells were allowed to adhere overnight. Subsequently, the cells were washed with PBS and 2 ml of adipogenic differentiation medium [Dulbecco's Modified Eagle's Medium (DMEM; GibcoBRL, USA) containing 10% fetal bovine serum (FBS; Invitrogen, USA), 2 mM L-glutamine (GibcoBRL, USA), 100 U/ml penicillin, 100 µg/ml streptomycin, 0.5 mM isobutyl-methylxanthine (Sigma-Aldrich, USA), 1 µM dexamethasone (Sigma-Aldrich, USA), 10 µM insulin (Sigma-Aldrich, USA), 100 µM indomethacin (Sigma-Aldrich, USA)] were added. The cells were cultured at 37°C in a humidified tissue culture incubator with 5% CO$_2$. The medium were changed every 3 days. After culture for 3 to 5 weeks, the cells were washed with PBS and fixed with 40% formalin vapor for 10 min at room temperature. Subsequently, the cells were washed twice with distilled water and stained with 0.5% Oil Red O (Sigma-Aldrich, USA) in 60% isopropanol for 20 min with shaking at room temperature. Then, the cells were washed twice with distilled water and observed under inverted microscope (Nikon TS100, Japan). For control group, the cells were maintained in MSCs growth medium, carried out in pararell to the experiments and stained in the same manner.

3.8 Osteogenic differentiation of MSCs

The osteogenic differentiation potential of MSCs derived from bone marrow, amnion, chorion, placenta, and umbilical cord were examined using passage 3 to 4 of the cultured cells. Briefly, 5 x 10^3 cells/cm^2 of MSCs were cultured with MSC complete medium in 35-mm^2 dishes. The cells were allowed to adhere overnight. Subsequently, the cells were washed with PBS and 2 ml of osteogenic differentiation medium [DMEM (GibcoBRL, USA) containing 10% FBS (Invitrogen, USA), 100 U/ml penicillin, 100 µg/ml streptomycin, 0.5 mM isobutyl-methylxanthine (Sigma-Aldrich, USA), 100 nM dexamethasone (Sigma-Aldrich, USA), 10 µM

β-glycerophosphate (Sigma-Aldrich, USA), 50 μg/ml Ascorbic acid (Sigma-Aldrich, USA)] were added. The cells were cultured at 37°C in a humidified tissue culture incubator with 5% CO_2. The medium were changed every 3 days. After every time points of culture, the cells were washed with PBS and fixed with 4% paraformaldehyde at 4°C for 20 minutes. Then, the cells were washed with PBS and stained with Alizarin red S (Sigma-Aldrich, USA) for 30 min at room temperature. Subsequently, the cells were washed twice with distilled water and observed under inverted microscope (Nikon TS100, Japan). For control group, the cells were maintained in MSCs growth medium, carried out in pararell to the experiments and stained in the same manner.

3.9 Bone morphogenetic protein-2 induce osteogenic differentiation

To examine the effect of BMP-2 on osteogenic differentiation of MSCs derived from bone marrow, amnion, chorion, placenta and umbilical cord, 9.5×10^3 cells of MSCs at passage 4 were cultured in 24-well plates (Costar, corning, USA) with MSC complete medium overnight. Subsequently, the cells were washed with PBS and 2 ml of osteogenic differentiation medium with or without 100 ng/ml BMP-2 (R&D systems, USA) was added. Those MSCs cultured with complete medium was used as a control. After induction for 3, 7, 14, 21, and 28 days, the cells were washed with PBS and stained for alkaline phosphatase activity using BCIP®/NBT® Liquid substrate (Sigma-Aldrich, USA). ALP activity was determined by qualitative cytochemical staining and quantitative colorimetric assay.

3.10 Alkaline phosphatase staining

The qualitative alkaline phosphatase assay was determined with the use of *p*-nitrophenyl phosphate (*p*NPP) as a substrate. After 3, 7, 14, 21, and 28 days of culture (according to section 3.9), the cells were washed with PBS and fixed with 4% paraformaldehyde at 4°C for 20 min. Then, the cells were washed with PBS and stained for alkaline phosphatase activity using BCIP®/NBT® Liquid substrate (Sigma-Aldrich, USA) for 30 min at room temperature. Subsequently, the cells were washed twice with distilled water and observed under inverted microscope (Nikon TS100, Japan). For control group, the cells were maintained in MSC complete medium, carried out in pararell to the experiments and stained in the same manner.

3.11 Alkaline phosphatase (ALP) activity assay

The quantitative alkaline phosphatase activity assay was measured using SensoLyte® pNPP alkaline phosphatase assay kit (AnaSpec, USA). Briefly, MSCs were cultured for 3, 7, 14, 21, and 28 days and washed with 1x assay buffer. Subsequently, 200 µl of 0.002% Triton X–100 in 1x assay buffer was added and the adherent cells were scrape off. The cell suspension was incubated at 4°C for 10 min with agitation. Then, the cell suspension was centrifuged at 2500xg for 10 min at 4°C to collect the supernatant for alkaline phosphatase activity assay. After centrifugation, 50 µl of supernatant was added into each well of 96-well plates (Costar, corning, USA). The serially diluted alkaline phosphatase solution, 0, 0.15, 0.30, 0.60 1.20, 2.50, 5.00 and 10.00 ng/ml in 1x assay buffer, was used as a standard. Then, 50 µl of p-nitrophenyl *phosphate* (pNPP) substrate solution was immediately added into each well, mixed by gently shaking the plate for 30 sec and incubated at room temperature for 60 min. Subsequently, ALP activity was measured by using microplate reader (BioTex, USA) using absorbance at 405 nm. The ALP activity in each sample was calculated by comparing the measure OD values against a standard curve generated from 0 - 10 ng/ml of alkaline phosphatase standard solution. Each assay condition was done in triplicate and normalized with the concentrations of total cellular proteins using Bradford assay (Bio-Rad, USA).

3.12 Evaluation of the expression level of genes involved in osteogenic differentiation

3.12.1 RNA extraction

MSCs derived from bone marrow, amnion, chorion, placenta, and umbilical cord (2.5×10^5 cells) at passage 3 - 4 were cultured in $25 cm^2$ tissue culture flasks (Costar, corning, USA) with complete medium and allowed to adhere to the plate overnight. The medium was removed and osteogenic differentiation medium with or without 100 ng/ml of BMP-2 was added. The cells cultured in MSC complete medium were used as a control.

After 3, 7, 14, 21, and 28 days of incubation, total RNA was extracted from the cultured MSCs using PureLink^{TM} RNA Mini Kit (Invitrogen, USA), following the manufacturer's instruction. Briefly, MSCs from each experiment were

detached using 0.25% trypsin-EDTA and transferred to 1.5 ml RNase-free tube. To lyse the cells, 300 µl of lysis buffer containing 1% of 2-mercaptoethanol was added and the lysate was passed 5-10 times through an RNase-free pipetted tip. Subsequently, one volume of 70% ethanol was added to each volume of cell homogenate and vortexed to mix thoroughly. Then, the samples were transferred to the spin cartridges (with the collection tubes) and centrifuged at 12,000xg for 15 sec at room temperature. After discarding the flow-through and re-insert the spin cartridges into the same collection tubes, 700 µl of wash buffer I was added. The samples were then centrifuged at 12000xg for 15 sec at room temperature, the flow-through and the collection tubes were discarded and the spin cartridges were placed into the new collection tube. Subsequently, 500µl of wash buffer II with ethanol was added to the spin cartridges. The spin cartridges will then be centrifuged at 12,000xg for 15 sec at room temperature and the flow-through was discarded. The spin cartridges were re-inserted into the same collection tubes and centrifuged at 12,000xg for 2 min to dry the membranes (with attached RNA). The collection tubes were then discarded and the spin cartridges were inserted into a recovery tubes. To elude the RNA from the membrane into the recovery tube, 10 – 20 µl of Rnase-free water was added to the center of the spin cartridges. After incubating at room temperature for a minute, the spin cartridges were centrifuged at 12,000xg for 2 min at room temperature. The purified RNA was collected and stored at -80°C for further processes.

3.12.2 cDNA synthesis

Messenger RNAs from section 13.1 were reverse transcribed to cDNA using SuperScript$^{®}$ III First Strand Synthesis Kit (Invitrogen, USA) following the manufacturer's instruction. Briefly, the RNA/primer mixture containing 1 µg of total RNA, 1 µl of 50 µM oligo (dT), 1 µl of 10 mM dNTP mix and DEPC-treated water to 10 µl was prepared. The mixture was then incubated on MyCycler^{TM} Thermal cycler PCR (Bio-Rad, USA) at 65°C for 5 min and placed on ice for at least 1 min to stop the reaction. Subsequently, cDNA synthesis mixture containing 2 µl of 10X RT buffer, 4 µl of 25 mM MgCl$_2$, 2 µl of 0.1 M DTT, 1 µl of RNaseOUT^{TM} (40 U/µl) and 1 µl of SuperScript^{TM} III RT (200 U/µl) was added to RNA/primer mixture and incubated on MyCycler^{TM} Thermal cycler (Bio-Rad , USA) at 50°C for 50 min.

After terminating the reactions at 85°C for 5 min, the reactions were incubated at 4°C for 1 min. The cDNA was stored at -20°C or used for qRT-PCR immediately.

3.12.3 Quantitative real-time polymerase chain reaction (qRT-PCR)

The expression levels of *RUNX-2, OSX* and *OCN* were analyzed by quantitative real-time polymerase chain reaction (qRT-PCR). Primer sequences are shown in Table 3.1.

Quantitative real-time PCR samples were prepared using the SYBR® Green PCR Master Mix (Applied Biosystems, USA). The amplification was performed on the StepOne plus™ Real-Time PCR system (Applied Biosystems; ABI USA) using 40 cycles of amplification (denaturation at 95°C for 10 sec, annealing at 60°C for 10 sec and extension at 72°C for 20 sec) after an initial activation at 95°C for 10 min. Melting curves were assessed to ensure single product was quantified. Each sample was examined in duplicate and mean value was calculated. The quantitation was based on normalizing the gene of interest to the invariant control gene (*GAPDH*). The data was analyzed by comparative threshold cycle value (ΔΔCT) method using StepOne™ Software version 2.2 (Applied Biosystems; ABI, USA.) and presented as the relative mRNA expression level.

Table 3.1: The primers and the product size.

Gene	Forward primer	Reverse primer	Product size (bp)
RUNX-2	5'-GACAGCCCCAACTTCCTGT-3'	5'-CCGGAGCTCAGCAGAATAAT-3'	159
Osterix	5'-TGCTTGAGGAGGAAGTTCAC-3'	5'-CTGCTTTGCCCAGAGTTGTT-3'	114
Osteocalcin	5'-CTCACACTCCTCGCCCTATT-3'	5'-TCAGCCAACTCGTCACAGTC-3'	245
GAPDH	5'-CAATGACCCCTTCATTGACC-3'	5'-TTGATTTTGGAGGGATCTCG-3'	159

3.13 Determination of the expression levels of microRNAs involved in osteogenic differentiation

3.13.1 Total RNA extraction

MSCs derived from bone marrow, amnion, chorion, placenta and umbilical cord (2×10^5 cells) at passage 3 – 4 were cultured in 25cm² tissue culture flasks

(Costar, corning, USA) with MSC complete medium and allowed to adhere to the plate overnight. The medium was removed and osteogenic differentiation medium with or without 100ng/ml BMP-2 was added. MSCs cultured in MSC complete medium was used as a control.

After 3, 7, 14, 21, and 28 days of incubation, total RNA was extracted from the cultured MSCs using Trizol® reagent (Invitrogen, USA). Briefly, MSCs from each experiment were lysed using 1 ml of Trizol® reagent and then the homogenized sample was collected to collection tube. To allow complete dissociation of the nucleoprotein complex, the homogenized sample was incubated for 5 min at room temperature. Subsequently, 200 µl of chloroform was added and incubated 2 – 3 min at room temperature. To separate the mixture, the samples were centrifuged at 12000xg for 15 min at 4°C and then the aqueous phase was transferred to a new collection tube. To precipitate RNA, 0.5 mL of 100% isopropanol was added to the aqueous phase and incubated at room temperature for 10 min. The sample was then centrifuged at 12000xg for 10 min at 4°C. Subsequently, the supernatant was removed; leaving only the RNA pellet and 1 ml of 75% ethanol was added to wash the pellet. The sample was centrifuged at 7500×g for 5 min at 4°C. The supernatant was discarded and the RNA pellet was dry for 5 – 10 min and resuspened in 10 – 20 µl of RNAse-free water. Finally, the sample was incubated in a heat block set at 55 – 60°C for 10 – 15 min. The purified total RNA was collected and stored at -80°C for further process.

3.13.2 Reverse transcription of miRNA

MiRNA was reverse transcription into cDNA using TaqMan® MicroRNA Reverse Transcription Kit (Applied Biosystems, USA). Briefly, the 5X miRNA-specific RT primers (hsa-miR-31-5p, hsa-miR-106a-5p, hsa-miR-148a-5p, and U6) and RNA templates were thawed on ice. For each RNA sample, RT master mix and total RNA was mixed in a ratio of 7:5. Then, 3 µL of RT primer was added to 12 µL of RT master mix containing total RNA. The reverse transcription was carried in a MyCycler™ Thermal cycler PCR (Bio-Rad, USA). The reaction mixtures was incubated at 16 °C for 30 min, then at 42 °C for 30 min, and then inactivated at 85°C for 5 min. The product was stored at -20°C or used for qRT-PCR immediately.

3.13.3 Quantitative real-time polymerase chain reaction (qRT-PCR)

The expression levels of hsa-miR-31-5p, hsa-miR-106a-5p, hsa-miR-148a-5p, and U6 were analyzed by quantitative real-time polymerase chain reaction (qRT-PCR). The mature miRNA sequences are shown in Table 3.2.

The qRT-PCR sample was prepared using TaqMan® Universal PCR Master Mix II (2X) (Applied Biosystems, USA). The miRNA-specific primers were included in TaqMan® MicroRNA Inventoried Assays (Applied Biosystems, USA). The assays used in the study included: 002279 (for miR-31-5p), 002169 (miR-106a-5p), and 002134 (miR-148a-5p).

For quantitative calibration and normalization, the expression of U6 (001973) was used as an endogenous control. At the beginning, 1.33 µL of RT reaction product, 1µL of specific primers from MicroRNA assays, 10 µL of TaqMan® master mix, and 7.67 of µL nuclease-free water were mixed together and loaded into microAmp Fast Optical 96-well reaction plate (Applied Biosystems, USA) in triplicated. The mixtures were first incubated at 95°C for 10 min to activate the enzyme, and then they entered a cycle of qRT-PCR (first denatured at 95 °C for 15 sec, and then annealed/extended at 60 °C for 60 sec). The cycle was run for 45 times. The baseline and threshold values were set and the comparative threshold cycle value ($\Delta\Delta$CT) method was applied to quantity the miRNA expression level using StepOne^{TM} Software version 2.2 (Applied Biosystems; ABI, USA.) and presented as the relative miRNA expression level.

Table 3.2: The mature miRNA sequence.

miRNA	mature miRNA sequence
hsa-miR-31-5p	AGGCAAGAUGCUGGCAUAGCU
hsa-miR-106a-5p	AAAAGUGCUUACAGUGCAGGUAG
hsa-miR-148a-5p	AAAGUUCUGAGACACUCCGACU
U6	GTGCTCGCTTCGGCAGCACATATACTAAA ATTGGAACGATACAGAGAAGATTAGCAT GGCCCCTGCGCAAGGATGACACGCAAAT TCGTGAAGCGTTCCATATTTT

3.14 Transient transfections with miRNA inhibitors

The transfection efficiency was monitored by qRT-PCR and a transfection with FAM-labeled miRNA negative control #1. To explore the effect of miRNAs on osteogenic differentiation potential of MSCs, MSCs derived from bone marrow, amnion, chorion, placenta and umbilical cord (3×10^4 cells) at passage $3 - 4$ were cultured in 6-well plate (Costar, corning, USA) with MSC complete medium and allowed to adhere to the plate overnight. The medium was removed and osteogenic differentiation medium was added. MSCs cultured in MSC complete medium was used as a control. For miRNA transfection, 10nM of each miRNA inhibitors diluted in osteogenic differentiation medium were mixed with Lipofectamine 3000 transfection reagent (Invitrogen, USA) and incubated for 10 min at room temperature. Then, the transfection complexes were added into the cell cultures. MSCs transfected with 10nM FAM-labeled miRNA negative control #1 were use as negative control. After 3, 7, 14, and 21 days of incubation, total RNA was extracted and miRNAs expression levels were determined using qRT-PCR as mention in section 3.13. The alkaline phosphatase activity assay was performed according to section 3.10.

3.15 Statistical analysis

The data were presented as mean ± standard error of mean (SEM). Statistical comparisons were performed using the unpaired T-test. P-value of less than 0.05 was considered to be statistically significant.

CHAPTER 4

FINDINGS AND RESULTS

4.1 The morphology of mesenchymal stem cells

Human mesenchymal stem cells (hMSCs) were generated from bone marrow, amnion, chorion, placenta and umbilical cord. The morphology of these MSCs was observed by using inverted microscope.

4.1.1 Morphology of mesenchymal stem cells derived from bone marrow

The mononuclear cells (MNCs) isolated from human bone marrow were cultured in DMEM supplement with 10% FBS a density of 1 x 10^5 cells/cm^2. After cultured for 1 and 3 days, non-adherent cells were removed and fresh medium was added. The MNCs attached to the plastic culture flask and formed small clusters of spindle shape cells. The adherent cell had a heterogeneous morphology. They were many rounds, monocyte-like cells as well as a number of flattened cells mixed with spindle shape cells (Fig. 4.1 A and 4.1 B respectively). After cultured for a week, the adherent cells exhibited fibroblast like morphology and had increase nuclei-cytoplasm ratio (Fig. 4.1 C). The cells were grown until reach 80% confluence and then passaged using 0.25% trypsin-EDTA. The homogeneous population of fibroblast-like cells was maintained at 37°C in a humidified atmosphere containing 5% CO_2. After passage 3, those cells were rapidly proliferated (Fig. 4.1 D).
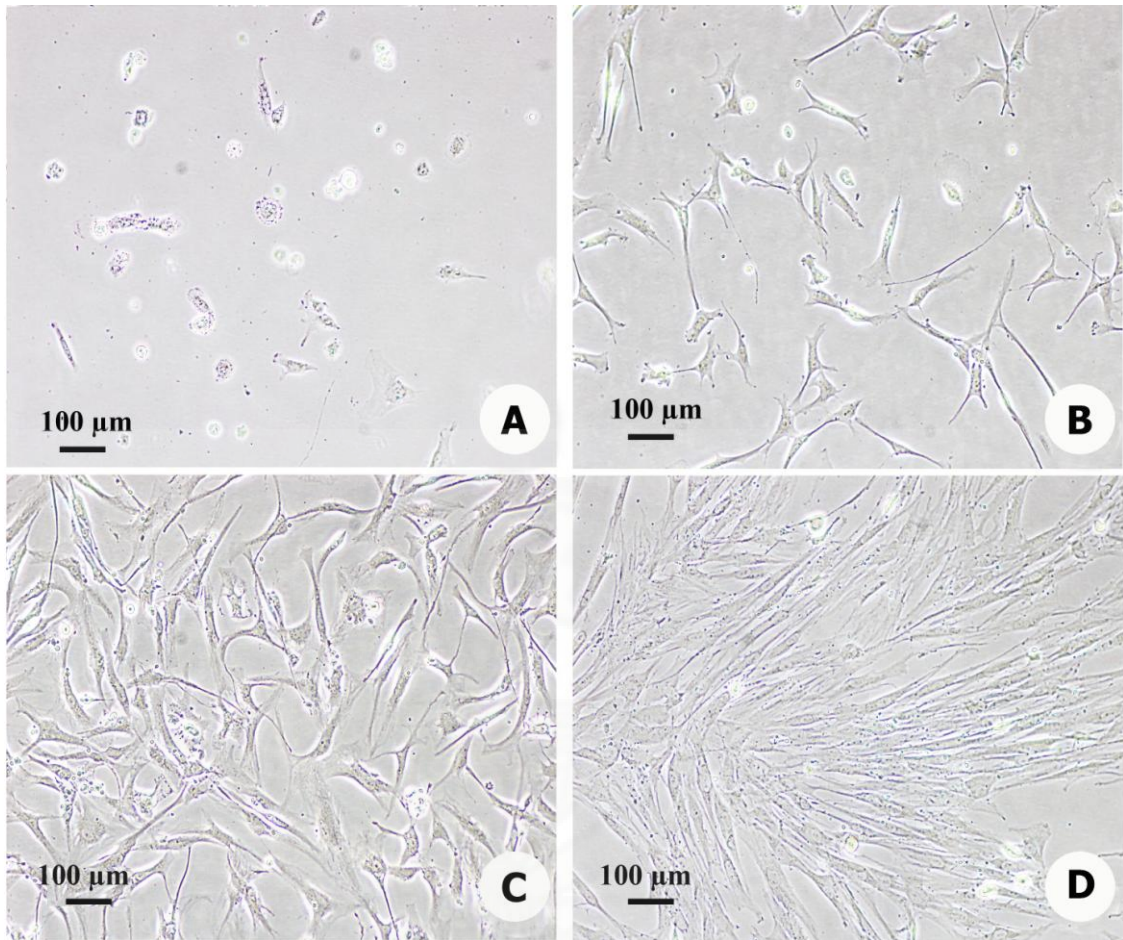
Figure 4.1: Morphology of mesenchymal stem cells derived from bone marrow (BM-MSCs). A: Round-shaped cells at day 1 after the initial seeding; B: Adherent cells at day 3; C: Spindle-shaped cells at day 7; D: 80% confluence of BM-MSCs at passage 3.

.

4.1.2 Morphology of mesenchymal stem cells derived from amnion

To isolate MSCs from amnion, amniotic membranes were digested with enzyme and cultured in DMEM supplemented with 10% FBS. A day after initial plating, some cells from amnion tissue could adhere to the culture flask and exhibited fibroblast-like morphology (Fig. 4.2 A). Three days after culture, non-adherent cells were removed and fresh medium was added (Fig 4.2 B). The cells were grown until reached 80% confluence within 10 – 12 days (Fig. 4.2 C) and then passaged using 0.25% trypsin-EDTA. The homogeneous population of fibroblast-like cells was maintained at 37°C in a humidified atmosphere containing 5% CO_2. After passage 3, the cells were rapidly proliferated. AM-MSCs at passage 3 reached 80% confluence after approximately 3 days of culture (Fig. 4.2 D).
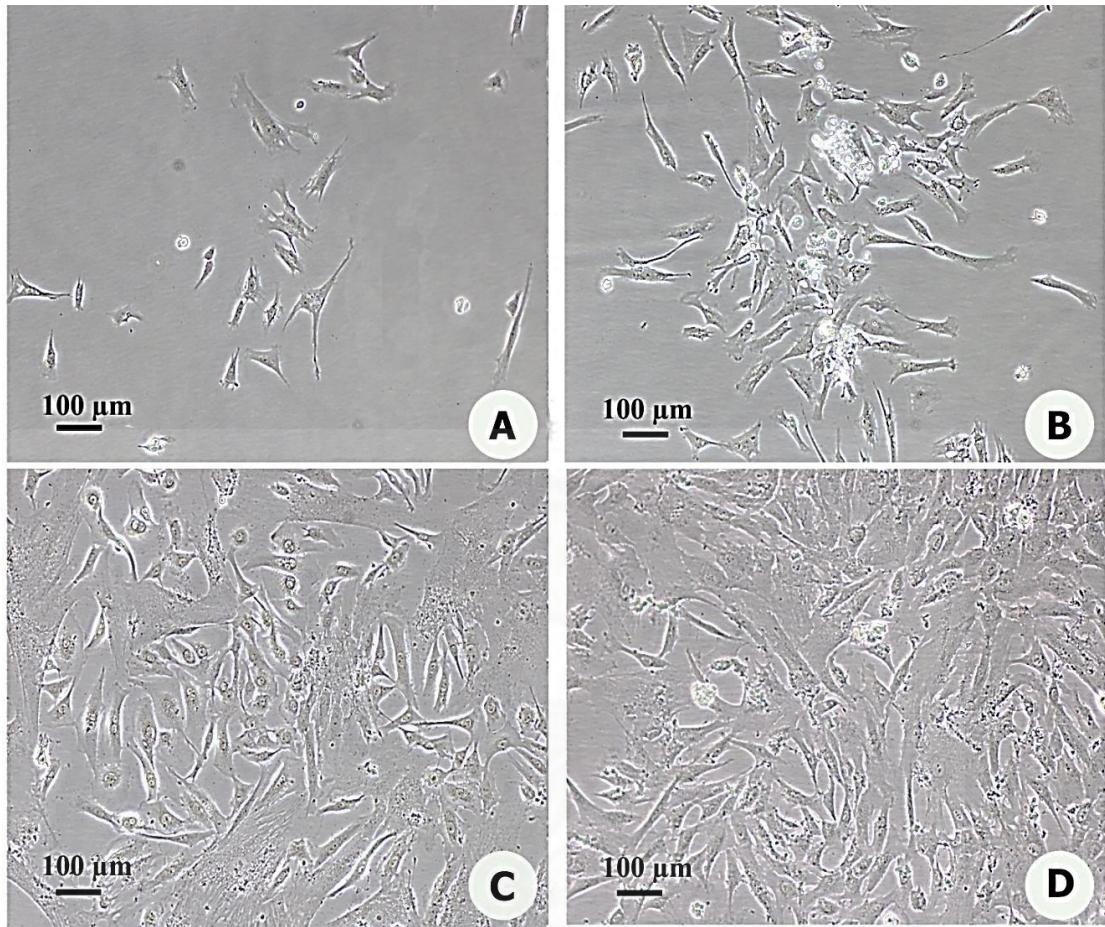
Figure 4.2: Morphology of mesenchymal stem cells derived from amnion (AM-MSCs). A: Some cells from amnion tissue could adhere to the culture flask at day 1 after the initial seeding; B: Adherent cells at day 3; C: Spindle-shaped cells at day 7; D: 80% confluence of AM-MSCs at passage 3.

4.1.3 Morphology of mesenchymal stem cells derived from chorion

To isolate MSCs from chorion, chorion tissue were also cultured in the same condition as the cell isolated from amnion tissue. A day after initial plating, some cells could adhere to the culture flask and exhibited fibroblast-like morphology (Fig. 4.3 A). Three days after culture, non-adherent cell were removed and fresh medium was added (Fig. 4.3 B). The cells were grown until reached 80% confluence within 10 days (Fig. 4.3 C) and then passaged using 0.25% trypsin-EDTA. The homogeneous population of fibroblast-like cells was maintained at 37°C in a humidified atmosphere containing 5% CO_2. After passage 3, the cells were rapidly proliferated. CH-MSCs at passage 3 reached 100% confluence after approximately 3 days of culture (Fig. 4.3 D).
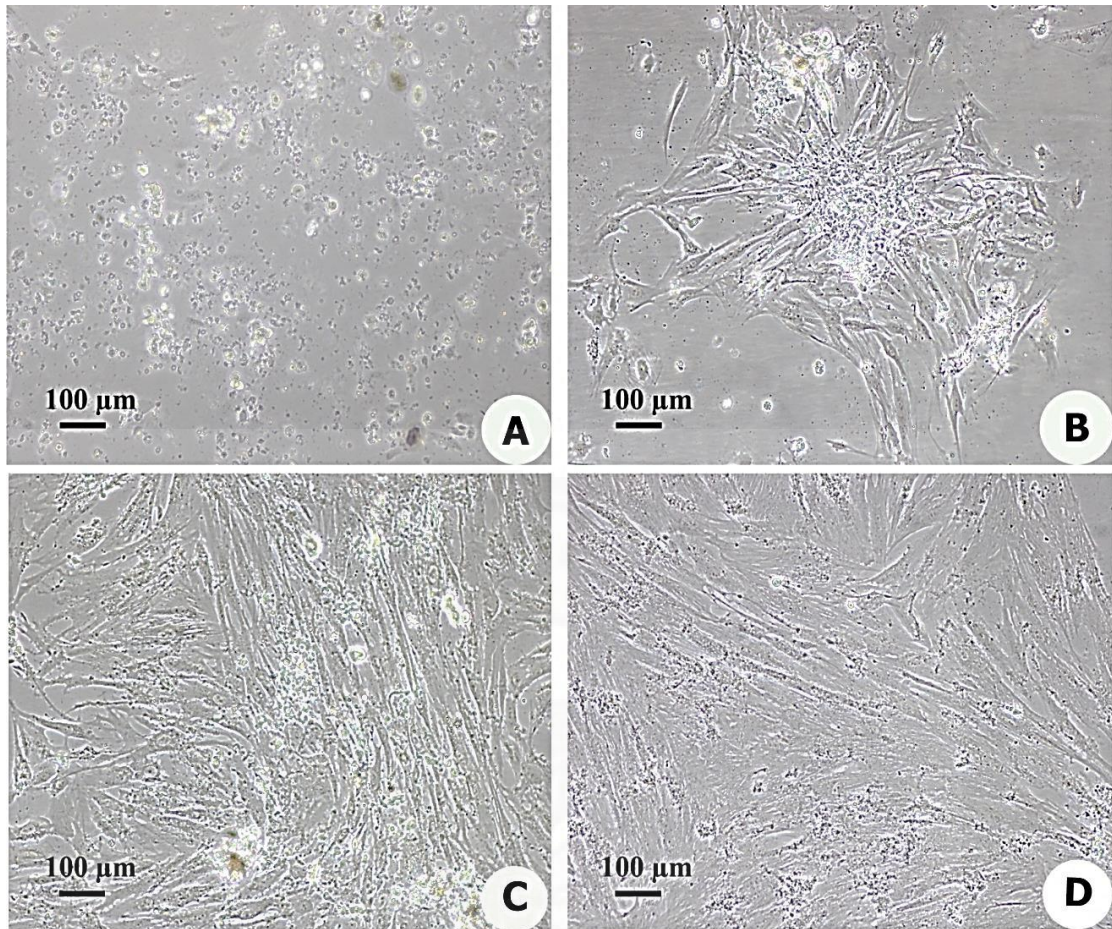
Figure 4.3: Morphology of mesenchymal stem cells derived from chorion (CH-MSCs). A: Spherical-shaped cells at day 1 after the initial seeding; B: Adherent cells at day 3; C: Spindle-shaped cells at day 7; D: 90% confluence of CH-MSCs at passage 3.

4.1.4 Morphology of mesenchymal stem cells derived from placenta

To isolate MSCs from placenta, placental tissues were also cultured in the same condition as the cell isolated from amniotic tissues. A day after initial plating, some cells could adhere to the culture flask and exhibited fibroblast-like morphology (Fig. 4.4 A). Three days after culture, non-adherent cell were removed and fresh medium was added (Fig 4.4 B). The cells were grown until reached 80% confluence within 10 days (Fig. 4.4 C) and then passaged using 0.25% trypsin-EDTA. The homogeneous population of fibroblast-like cells was maintained at 37°C in a humidified atmosphere containing 5% CO_2. After passage 3, the cells were rapidly proliferated. PL-MSCs at passage 3 reached 90% confluence after approximately 3 days of culture (Fig. 4.4 D).
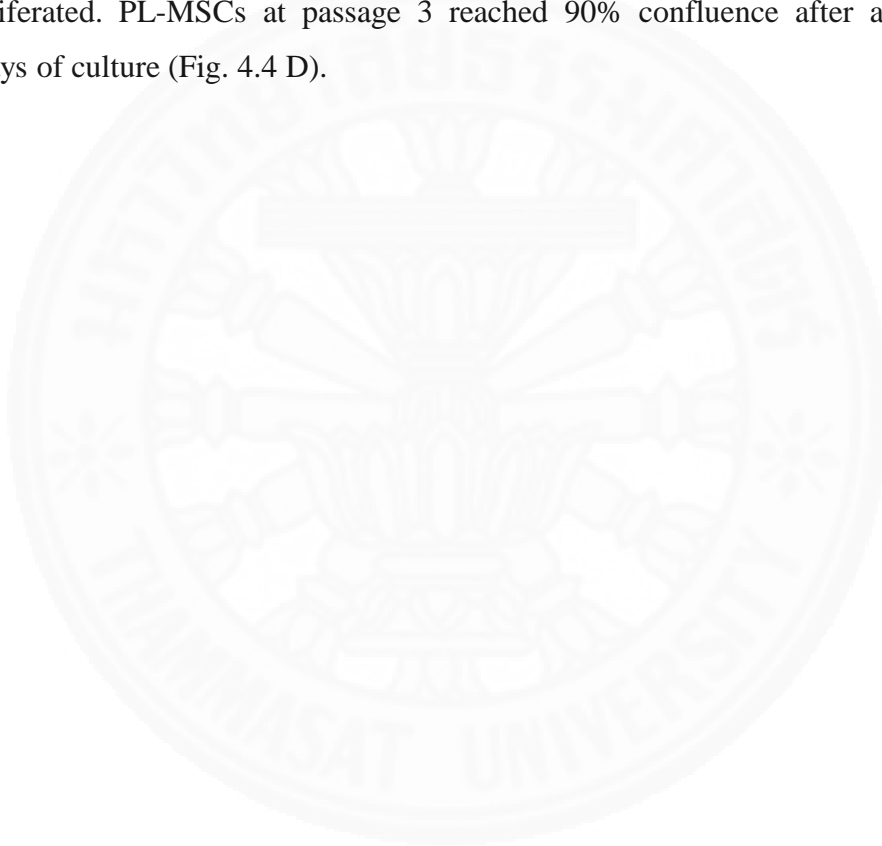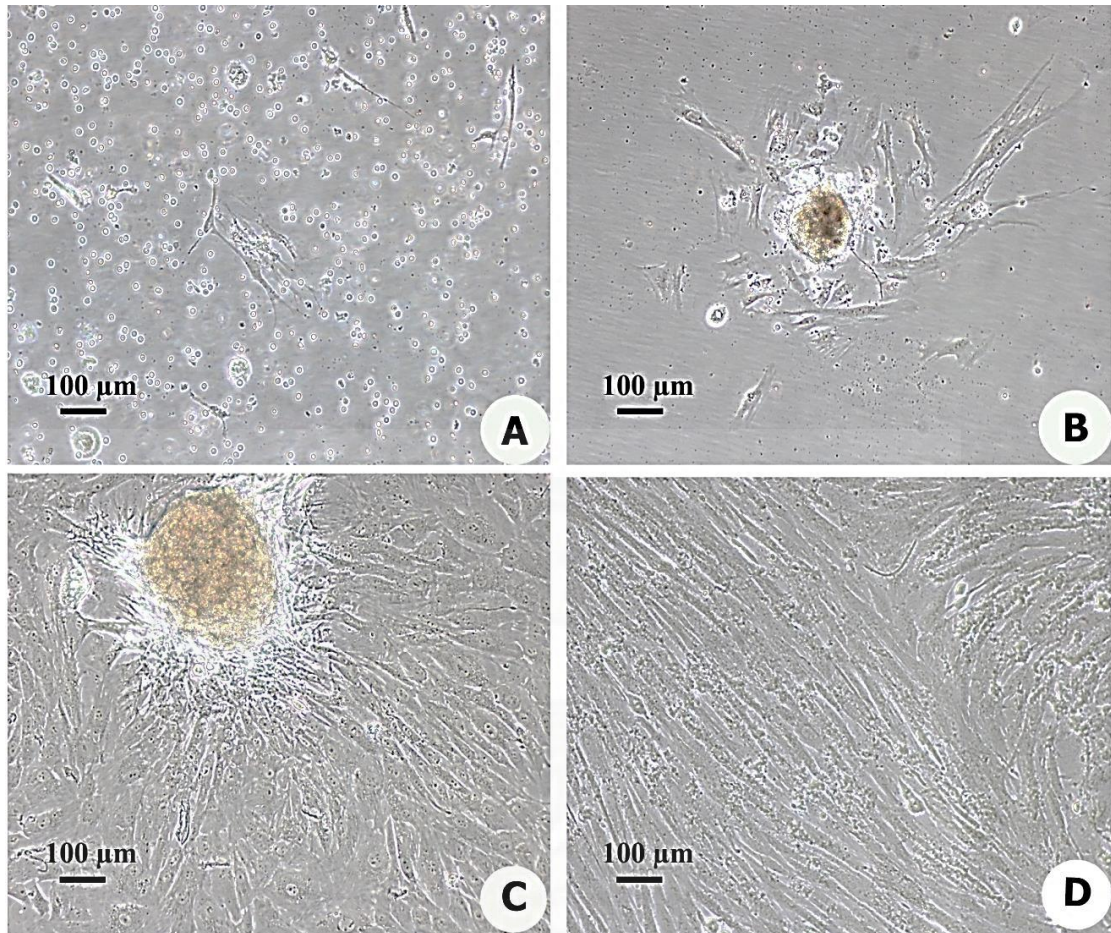
Figure 4.4: Morphology of mesenchymal stem cells derived from placenta (PL-MSCs). A: Spherical-shaped cells at day 1 after the initial seeding; B: Adherent cells at day 3; C: Spindle-shaped cells at day 7; D: 90% confluence of PL-MSCs at passage 3.

4.1.5 Morphology of mesenchymal stem cells derived from umbilical cord

To isolate MSCs from umbilical cord, umbilical cords were also cultured in the same condition as the cell isolated from amniotic tissue. A day after initial plating, some cells could adhere to the culture flask and exhibited fibroblast-like morphology (Fig. 4.5 A). Three days after culture, non-adherent cell were removed and fresh medium was added (Fig 4.5 B). The cells were grown until reached 80% confluence within 10 days (Fig. 4.5 C) and then passaged using 0.25% trypsin-EDTA. The homogeneous population of fibroblast-like cells was maintained at 37°C in a humidified atmosphere containing 5% CO_2. After passage 3, the cells were rapidly proliferated. UC-MSCs at passage 3 reached 100% confluence after approximately 3 days of culture (Fig. 4.5 D).
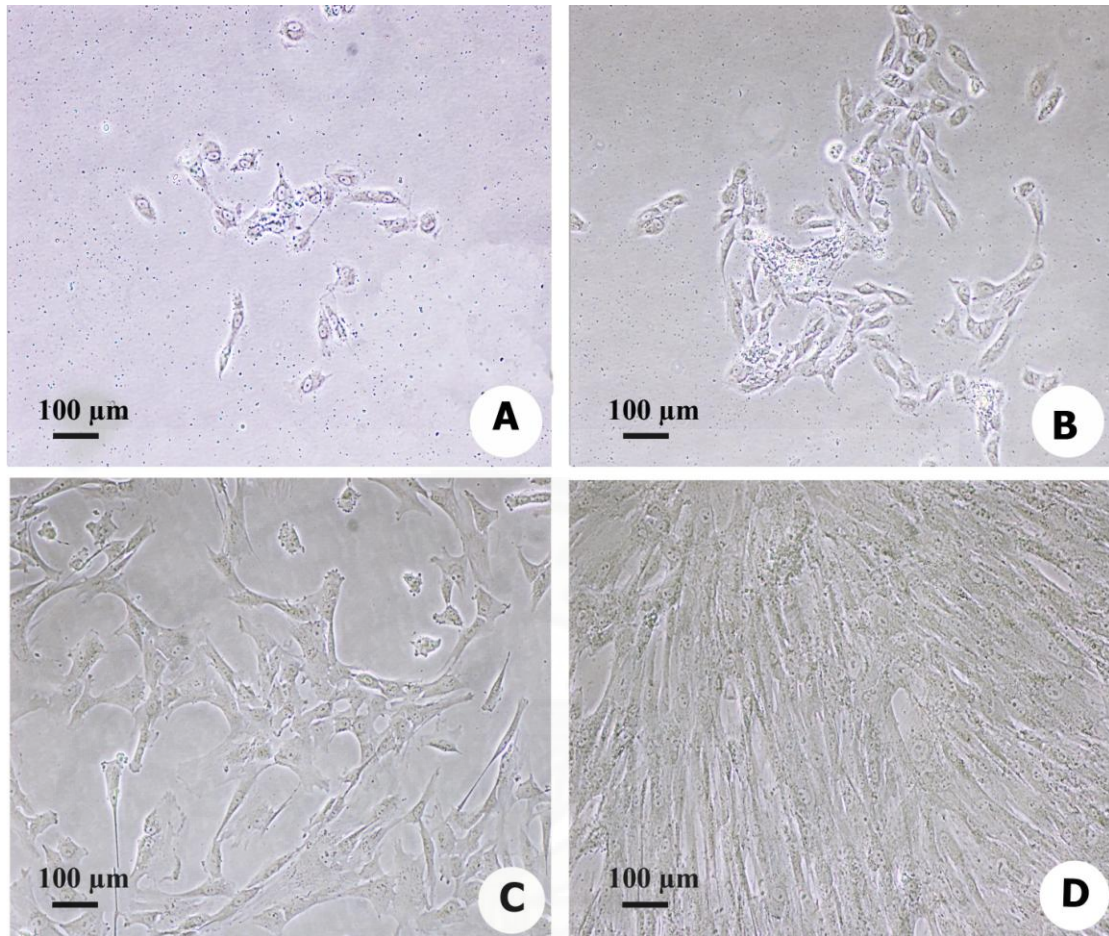
Figure 4.5: Morphology of mesenchymal stem cells derived from umbilical cord (UC-MSCs). A: Spherical-shaped cells at day 1 after the initial seeding; B: Adherent cells at day 3; C: Spindle-shaped cells at day 7; D: 100% confluence of UC-MSCs at passage 3.

4.2 Growth characteristics of MSCs derived from amnion, chorion, placenta, and umbilical cord in comparison to bone marrow derived MSCs

The growth characteristics of MSCs derived from different sources (n = 3) were compared during 14 days. Total numbers of MSCs were evaluated at 0, 2, 4, 6, 8, 10, 12, and 14 days in culture. The results showed that BM-MSCs had a higher proliferative capacity than AM-MSCs, CH-MSCs, PL-MSCs and UC-MSCs. The proliferative capacity of CH-MSCs, and PL-MSCs during early period (passage 3 – 5) were similar to that of UC-MSCs (Fig. 4.6 A, B and C). There was no significant different in cell number and growth kinetic during the 6 days of culture. Between day 6 and 8, the number of AM-MSCs was significantly lower compared to those of BM-MSCs, CH-MSCs, PL-MSCs and UC-MSCs ($p<0.05$). After 8 days, the number of BM-MSCs was significantly higher ($p<0.05$) compared with the amount of cells derived from chorion, placental tissue and umbilical cord. The growth velocity and cell number of MSCs derived from amnion tissue was significantly lower ($p<0.05$) than that of MSCs derived from bone marrow, chorion, placental tissue, and umbilical cord in all of passages examined (Fig. 4.6 A, B and C). It might be important to note that BM-MSCs shown to have the most proliferation capacity, whereas AM-MSCs shown to have the lowest proliferation capacity. Starting from 1 x 10^3 cells at day 0, BM-MSCs were expanded for 20–30 folds within 14 days. On the other hand, CH-MSCs, PL-MSCs and UC-MSCs were expanded for 20 folds and AM-MSCs were expanded for 15 – 18 folds within 14 days (Table. 4.1, 4.2, 4.3 and Fig. 4.6).

Table 4.1: The number of mesenchymal stem cells at passage 3.

Culture	The number of MSCs (x 10^3 cells)				
day	BM-MSCs	AM-MSCs	CH-MSCs	PL-MSCs	UC-MSCs
0	1.00 ± 0.00	1.00 ± 0.00	1.00 ± 0.00	1.00 ± 0.00	1.00 ± 0.00
2	1.72 ± 0.07	1.38 ± 0.05	1.50 ± 0.03	1.62 ± 0.08	1.53 ± 0.06
4	2.96 ± 0.74	2.11 ± 0.07	2.81 ± 0.20	3.12 ± 0.30	2.83 ± 0.06
6	4.36 ± 1.19	3.56 ± 0.20	4.39 ± 0.31	4.57 ± 0.38	4.47 ± 0.06
8	13.44 ± 1.84	8.26 ± 0.27	11.67 ± 1.20	12.67 ± 1.33	12.67 ± 0.58
10	20.22 ± 0.19	13.22 ± 0.96	17.56 ± 0.84	17.44 ± 1.39	16.67 ± 0.58
12	25.56 ± 1.26	16.11 ± 0.69	20.33 ± 0.58	20.33 ± 1.00	19.67 ± 0.58
14	28.33 ± 1.76	17.56 ± 0.84	21.78 ± 0.96	21.67 ± 1.20	21.33 ± 0.58

Values are presented as mean ± SEM.

Table 4.2: The number of mesenchymal stem cells at passage 4.

Culture	The number of MSCs (x 10^3 cells)				
day	BM-MSCs	AM-MSCs	BM-MSCs	PL-MSCs	BM-MSCs
0	1.00 ± 0.00	1.00 ± 0.00	1.00 ± 0.00	1.00 ± 0.00	1.00 ± 0.00
2	1.62 ± 0.07	1.23 ± 0.03	1.23 ± 0.06	1.44 ± 0.19	1.46 ± 0.58
4	2.26 ± 0.37	1.97 ± 0.07	2.40 ± 0.00	2.60 ± 0.20	2.37 ± 0.58
6	4.07 ± 1.01	3.26 ± 0.18	3.82 ± 0.56	4.28 ± 0.40	4.07 ± 0.58
8	12.89 ± 1.07	8.03 ± 0.06	11.22 ± 0.84	11.78 ± 0.51	11.33 ± 0.58
10	19.89 ± 0.51	11.89 ± 0.38	15.67 ± 0.58	17.00 ± 0.58	16.33 ± 0.58
12	24.78 ± 1.95	14.56 ± 0.51	19.78 ± 0.96	20.11 ± 1.07	20.67 ± 0.58
14	26.78 ± 3.15	16.22 ± 0.51	21.00 ± 0.58	21.33 ± 1.00	21.67 ± 0.58

Values are presented as mean ± SEM.

Table 4.3: The number of mesenchymal stem cells at passage 5.

Culture day	The number of MSCs (x 10^3 cells)				
	BM-MSCs	AM-MSCs	CH-MSCs	PL-MSCs	UC-MSCs
0	1.00 ± 0.00	1.00 ± 0.00	1.00 ± 0.00	1.00 ± 0.00	1.00 ± 0.00
2	1.47 ± 0.07	1.16 ± 0.02	1.17 ± 0.06	1.24 ± 0.02	1.30 ± 0.10
4	2.19 ± 0.32	1.73 ± 0.03	2.18 ± 0.05	2.29 ± 0.07	2.20 ± 0.10
6	3.79 ± 1.02	3.14 ± 0.25	3.66 ± 0.56	3.89 ± 0.57	3.33 ± 0.15
8	11.00 ± 0.67	7.93 ± 0.12	10.32 ± 0.35	11.11 ± 0.38	10.67 ± 0.58
10	16.56 ± 1.02	11.22 ± 0.51	15.11 ± 0.38	15.56 ± 0.19	15.67 ± 0.58
12	21.00 ± 1.20	15.89 ± 0.51	18.56 ± 0.51	19.22 ± 0.51	18.67 ± 0.58
14	22.22 ± 1.84	16.56 ± 0.19	19.44 ± 0.19	20.22 ± 0.51	20.67 ± 0.58

Values are presented as mean $\pm$ SEM.
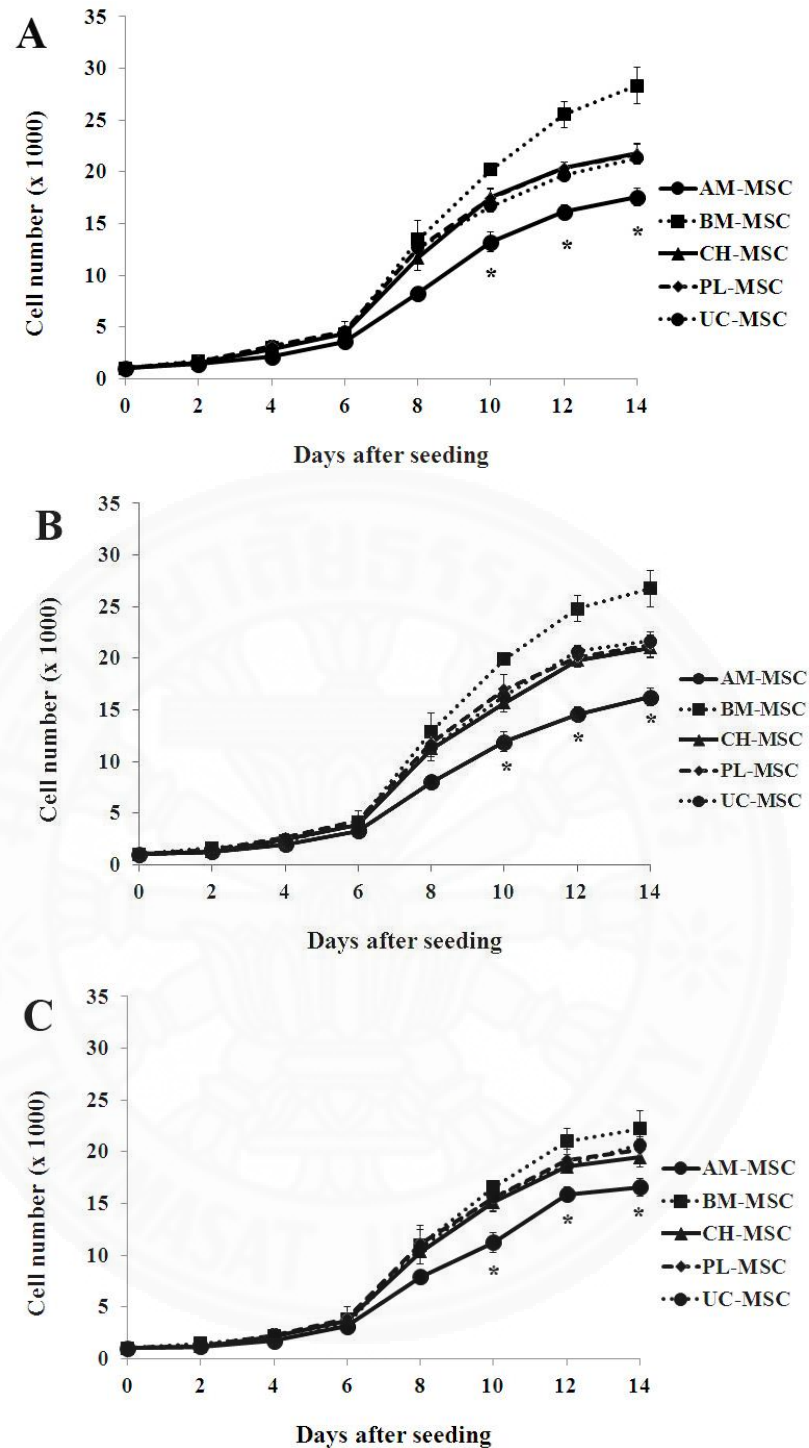
Figure 4.6: Growth curves of MSCs derived from bone marrow, amnion, chorion, placenta and umbilical cord. At t = 0, 1 x 10^3 cells MSCs were seeded in culture plates. Triplicate cultures were harvested at 2, 4, 6, 8, 10, 12 and 14 days, and adherent cells were counted. Results are expressed as mean ± SEM. A: growth curve of MSCs at passage 3, B: growth curve of MSCs at passage 4, C: growth curve of MSCs at passage 5. * $p < 0.05$: significant difference compared with BM-MSCs.

4.3 Population doubling time of MSCs derived from amnion, chorion, placenta, and umbilical cord in comparison to bone marrow-derived MSCs

The population doubling time value for MSCs derived from bone marrow appeared to be significantly lower than those MSCs derived from amnion, chorion, placenta, and umbilical cord indicating the more rapid rate of proliferation of MSCs derived from bone marrow (Table 4.4 and Fig. 4.7). Based on the results, BM-MSCs tended to double their population in the average of 47.79 ± 5.32 hours while those MSCs derived from amnion, chorion, placental tissue and umbilical cord exhibited the doubling time of 54.26 ± 4.13, 52.37 ± 4.08, 51.17 ± 4.97, and 51.30 ± 4.71 hours respectively. The differences were statistically significant ($p<0.05$).

Table 4.4: Population doubling time of mesenchymal stem cells at passage $2 - 8$.

Passage	Population doubling time (hours)				
	BM-MSCs	AM-MSCs	CH-MSCs	PL-MSCs	UC-MSCs
2	42.03 ± 0.00	47.72 ± 0.52	45.64 ± 0.76	43.85 ± 0.39	44.34 ± 1.14
3	43.83 ± 0.42	50.15 ± 1.03	48.55 ± 1.95	45.92 ± 0.43	46.98 ± 0.50
4	48.22 ± 1.57	53.10 ± 0.69	51.98 ± 1.26	49.79 ± 0.55	49.46 ± 0.58
5	51.25 ± 1.84	54.79 ± 1.30	52.76 ± 0.10	51.58 ± 0.61	51.62 ± 0.61
6	52.73 ± 1.33	56.58 ± 0.83	54.79 ± 0.73	54.34 ± 1.23	53.52 ± 1.23
7	54.34 ± 0.73	58.05 ± 0.88	55.71 ± 1.50	55.65 ± 0.77	55.66 ± 0.78
8	56.10 ± 0.00	59.61 ± 0.95	57.12 ± 1.60	57.06 ± 0.83	57.54 ± 0.00

Values are presented as mean $\pm$ SEM.
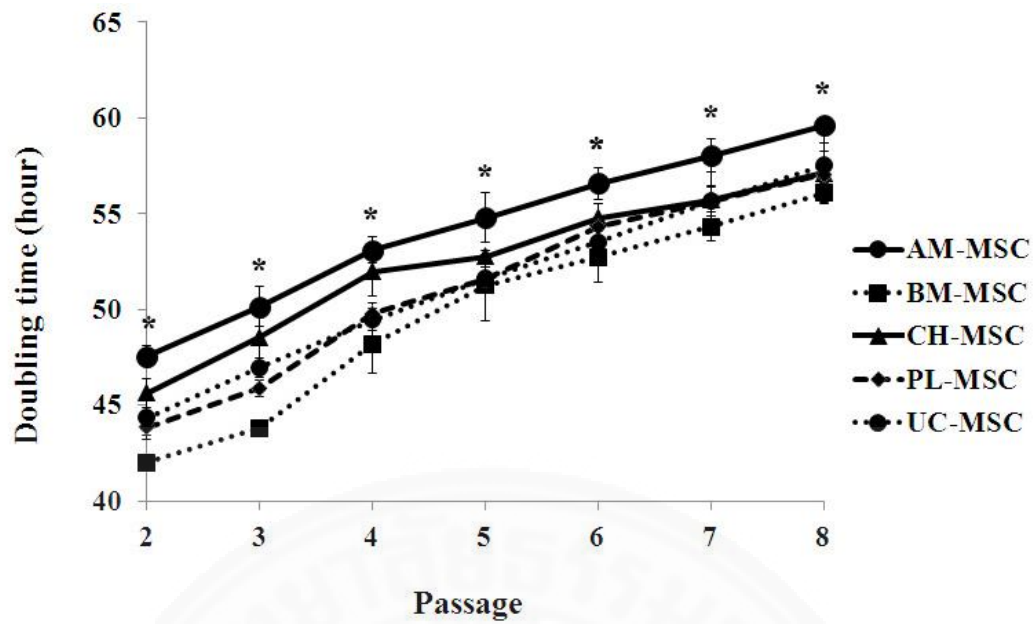
Figure 4.7: Population doubling time of MSCs derived from bone marrow, amnion, chorion, placenta, and umbilical cord. At t = 0, 1.25×10^4 cells MSCs were seeded in culture plates. Triplicate cultures were harvested at passage 2 - 8 and adherent cells were counted every 48 hours. Results are expressed as mean ± SEM. * $p<0.05$: significant difference compared with BM-MSCs.

4.4 Immunophenotype of MSCs derived from amnion, chorion, placenta, and umbilical cord in comparison to bone marrow derived MSCs

Immunophenotype of AM-MSCs, CH-MSCs, PL-MSCs, UC-MSCs, and BM-MSCs (passage 3 − 5) were determined by flow cytometry using phycoerythrin (PE) -conjugated or fluorescein isothiocyanate (FITC) - conjugated antibodies against CD34, CD45, CD73, CD90, and CD105.

AM-MSCs, CH-MSCs, PL-MSCs, and UC-MSCs exhibited the similar immunophenotype as those of BM-MSCs. They expressed high levels of MSCs markers including CD73, CD90, and CD105. In contrast, they did not express hematopoietic markers, CD34 and common leukocyte marker, CD45 (Table 4.5 and Fig. 4.8). Both of these markers were generally used to characterize the presence of contaminating hematopoietic cells in MSC culture. Figure 4.8 summarized the expression profiles of the mesenchymal and hematopoietic cell surface markers of BM-MSCs, AM-MSCs, CH-MSCs, PL-MSCs, and UC-MSCs as determined by flow cytometry.

Table 4.5: The expression of cell-surface markers of MSCs at passage 3 − 5.

MSC sources	Number of the positive cells (%)				
	CD34	CD45	CD73	CD90	CD105
BM-MSCs	1.66 ± 1.33	0.11 ± 0.11	87.75 ± 5.60	87.09 ± 5.74	86.20 ± 5.98
AM-MSCs	1.72 ± 1.01	1.43 ± 0.89	92.66 ± 3.00	84.79 ± 1.18	88.85 ± 3.43
CH-MSCs	1.33 ± 1.17	1.92 ± 0.50	91.98 ± 3.03	81.80 ± 4.87	89.10 ± 3.62
PL-MSCs	0.08 ± 0.48	0.80 ± 0.58	86.32 ± 3.18	81.90 ± 4.83	85.44 ± 3.26
UC-MSCs	2.39 ± 0.65	2.54 ± 1.30	84.24 ± 4.15	86.46 ± 3.98	82.52 ± 1.77

Values are presented as mean ± SEM.
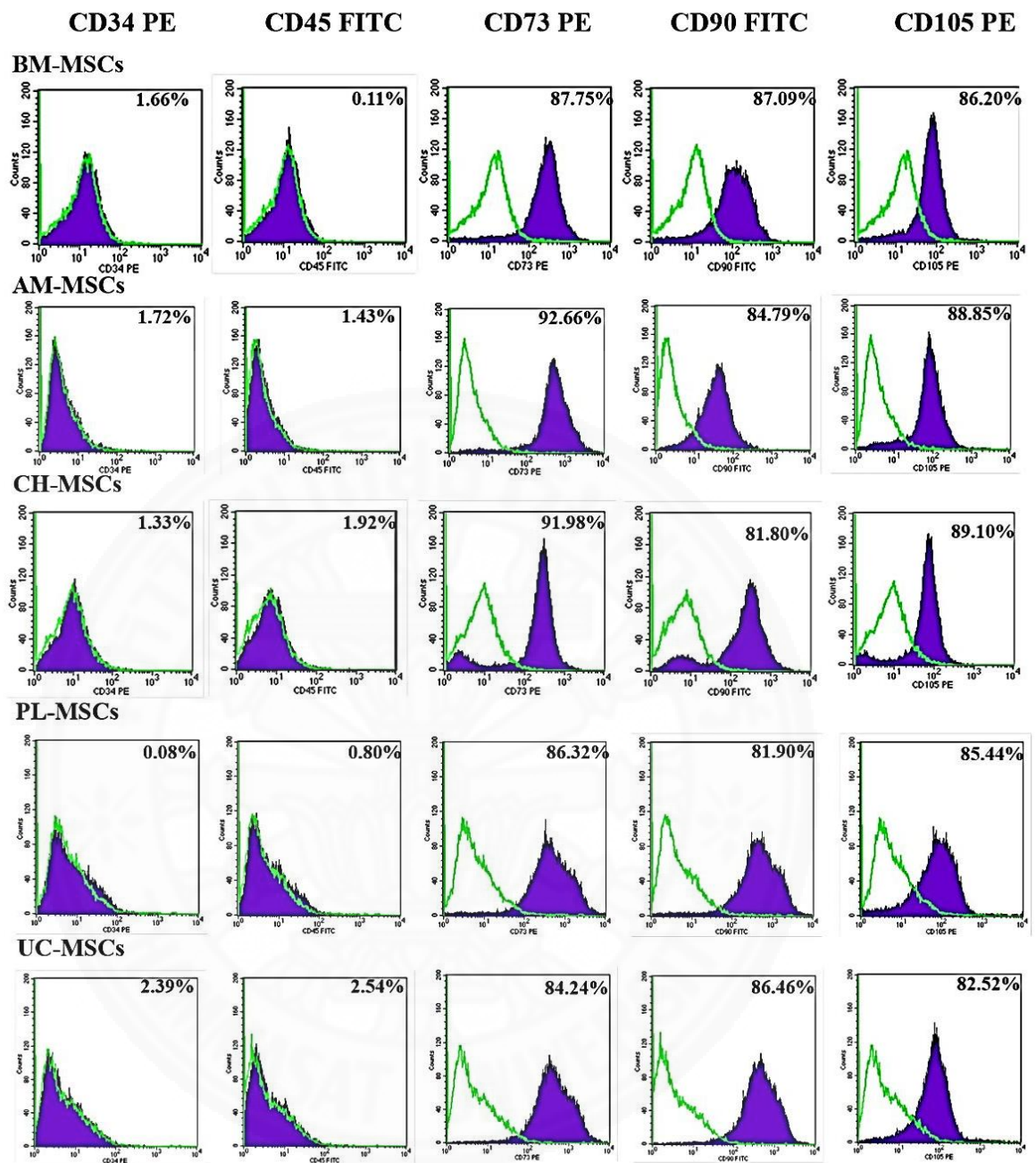
Figure 4.8: Flow cytometric analysis of surface marker expression on AM-MSCs, CH-MSCs, PL-MSCs, UC-MSCs, and BM-MSCs. The green line showed the profile of negative control. The data shown were representative of those obtained in three different experiments.

4.5 Adipogenic differentiation potential of MSCs derived from amnion, chorion, placenta, and umbilical cord in comparison to bone marrow derived MSCs

To assess the adipogenic differentiation potential of AM-MSCs, CH-MSCs, PL-MSCs, and UC-MSCs in comparison to that of BM-MSCs, MSCs at passage 4 were cultured in adipogenic differentiation medium. After 21 days of induction, the differentiating AM-MSCs, CH-MSCs, PL-MSCs, and UC-MSCs became large cells which containing numerous lipid droplets in their cytoplasm similar to that of differentiating BM-MSCs (Fig. 4.9 C, 4.10 C, 4.11 C, 4.12 C, 4.13 C). These lipid droplets were positive for oil red O staining (Fig. 4.9 D, 4.10 D, 4.11 D, 4.12 D, 4.13 D). The controls which cultured in complete medium had no evidence of adipogenic differentiation (Fig. 4.9 A, 4.10 A, 4.11 A, 4.12 A, 4.13 A) and negative for oil red O staining (Fig. 4.9 B, 4.10 B, 4.11 B, 4.12 B, 4.13 B). It might be important to note that AM-MSCs, CH-MSCs, PL-MSCs, and UC-MSCs need a longer period of time (35 − 40 days) to differentiate into adipogenic lineage in comparison to BM-MSCs (21 days).
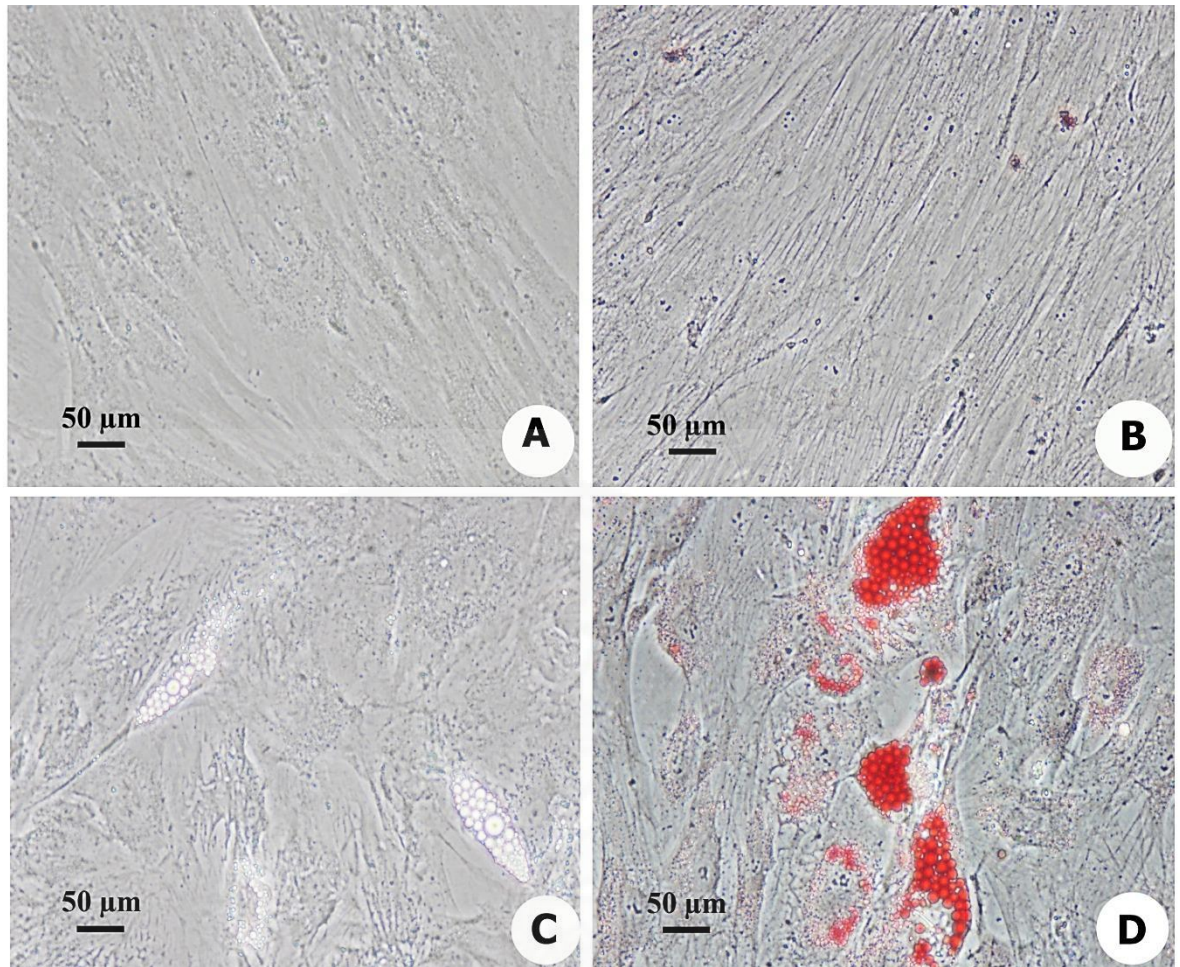
Figure 4.9: Representative photomicrographs of adipogenic differentiation of BM-MSCs. (A) BM-MSCs cultured in DMEM supplemented with 10% FBS for 21 days. (B) Oil red O staining of BM-MSCs cultured in DMEM supplemented with 10% FBS for 21 days. (C) The formation of lipid droplet in cytoplasm of BM-MSCs after adipogenic induction for 21 days (D) The positive for oil red-O staining in BM-MSCs after adipogenic induction for 21 days.
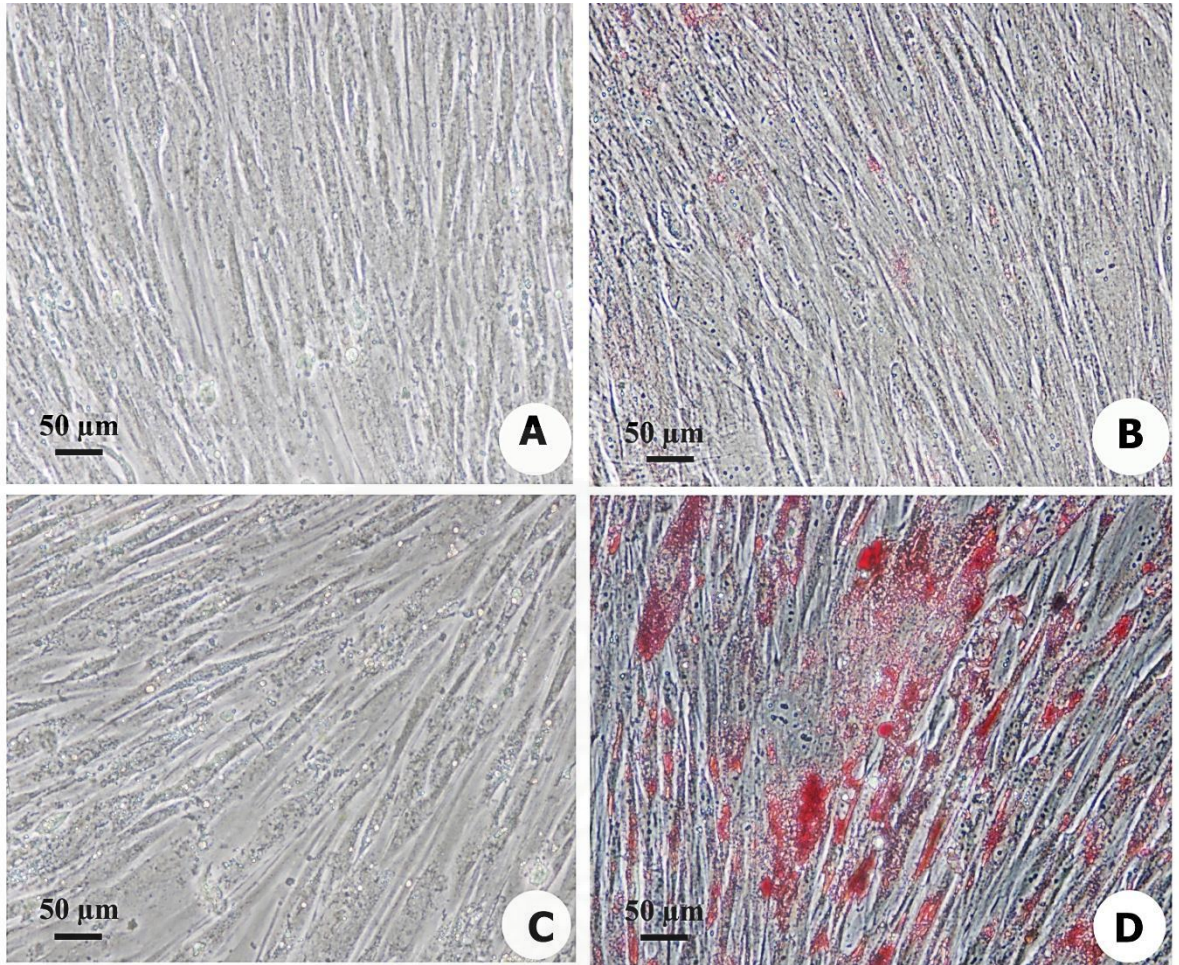
Figure 4.10: Representative photomicrographs of adipogenic differentiation of AM-MSCs. (A) AM-MSCs cultured in DMEM supplemented with 10% FBS for 35 days. (B) Oil red O staining of AM-MSCs cultured in DMEM supplemented with 10% FBS for 35 days. (C) The formation of lipid droplet in cytoplasm of AM-MSCs after adipogenic induction for 35 days (D) The positive for oil red-O staining in AM-MSCs after adipogenic induction for 35 days.
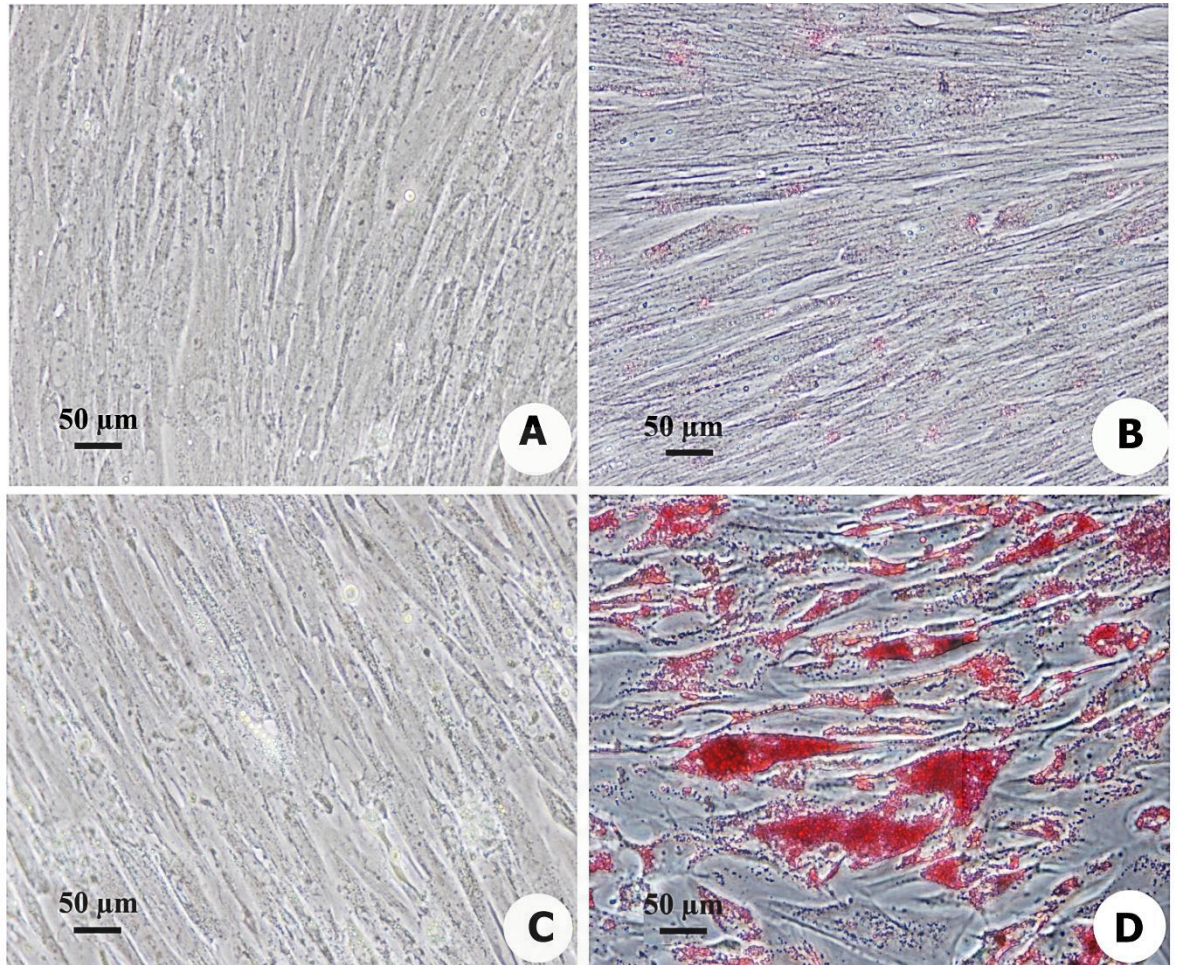
Figure 4.11: Representative photomicrographs of adipogenic differentiation of CH-MSCs. (A) CH-MSCs cultured in DMEM supplemented with 10% FBS for 35 days. (B) Oil red O staining of CH-MSCs cultured in DMEM supplemented with 10% FBS for 35 days. (C) The formation of lipid droplet in cytoplasm of CH-MSCs after adipogenic induction for 35 days (D) The positive for oil red-O staining in CH-MSCs after adipogenic induction for 35 days.
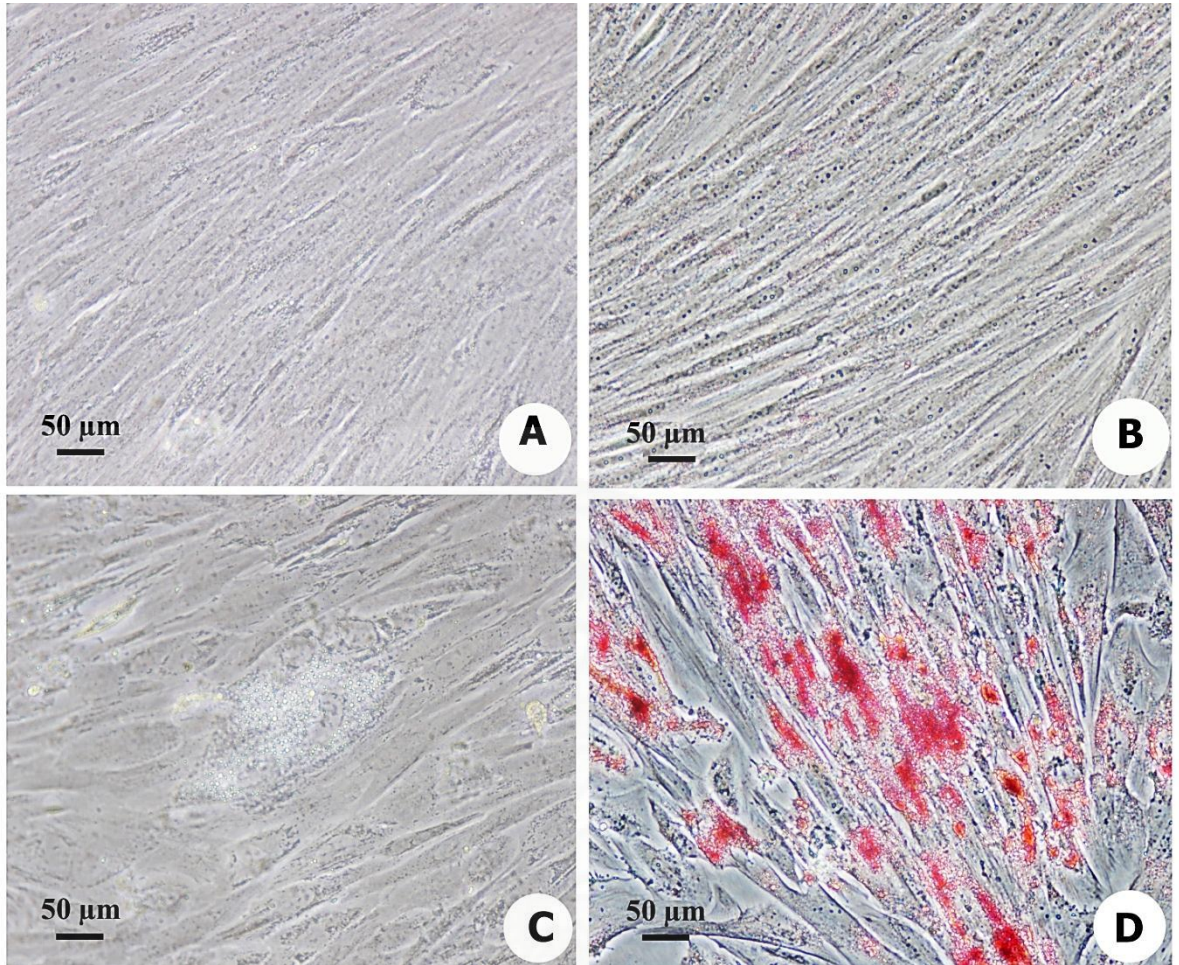
Figure 4.12: Representative photomicrographs of adipogenic differentiation of PL-MSCs. (A) PL-MSCs cultured in DMEM supplemented with 10% FBS for 35 days. (B) Oil red O staining of PL-MSCs cultured in DMEM supplemented with 10% FBS for 35 days. (C) The formation of lipid droplet in cytoplasm of PL-MSCs after adipogenic induction for 35 days (D) The positive for oil red-O staining in PL-MSCs after adipogenic induction for 35 days.
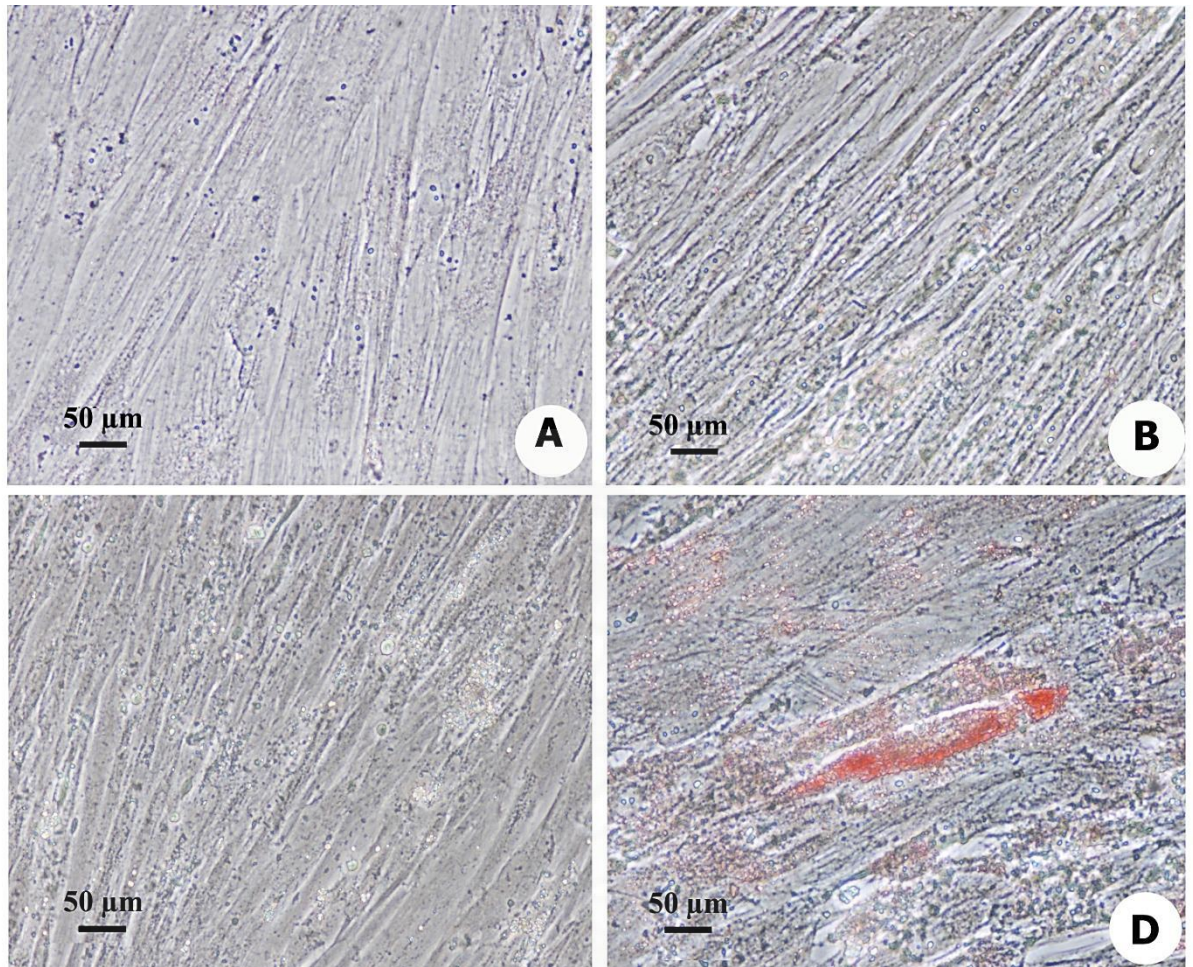
Figure 4.13: Representative photomicrographs of adipogenic differentiation of UC-MSCs. (A) UC-MSCs cultured in DMEM supplemented with 10% FBS for 35 days. (B) Oil red O staining of UC-MSCs cultured in DMEM supplemented with 10% FBS for 35 days. (C) The formation of lipid droplet in cytoplasm of UC-MSCs after adipogenic induction for 35 days (D) The positive for oil red-O staining in UC-MSCs after adipogenic induction for 35 days.

4.6 Osteogenic differentiation potential of MSCs derived from amnion, chorion, placenta, and umbilical cord in comparison to bone marrow derived MSCs

To investigate the osteogenic differentiation potential of AM-MSCs, CH-MSCs, PL-MSCs, and UC-MSCs in comparison to that of BM-MSCs, MSCs at passage 4 were cultured in osteogenic differentiation medium. After 21 days of induction, the spindle shapes of AM-MSCs, CH-MSCs, PL-MSCs, and UC-MSCs were flattened and broadened with increasing time of induction and had the appearance of extracellular calcium deposits in the cells similar to that of BM-MSCs (Fig. 4.14 C, 4.15 C, 4.16 C, 4.17 C, and 4.18 C). The extracellular calcium was positive for alizarin red S staining (Fig. 4.14 D, 4.15 D, 4.16 D, 4.17 D, 4.18 D). The MSCs from untreated control cultures did not have any evidence of extracellular calcium deposit (Fig. 4.14A, 4.15A, 4.16A, 4.17A, 4.18A) and negative for alizarin red S staining (Fig. 4.14B, 4.15B, 4.16B, 4.17B, 4.18B). It is noted that AM-MSCs, CH-MSCs, PL-MSCs, and UC-MSCs need a longer period of time (21 days) to differentiate into osteogenic lineage in comparison to BM-MSCs (14 days).
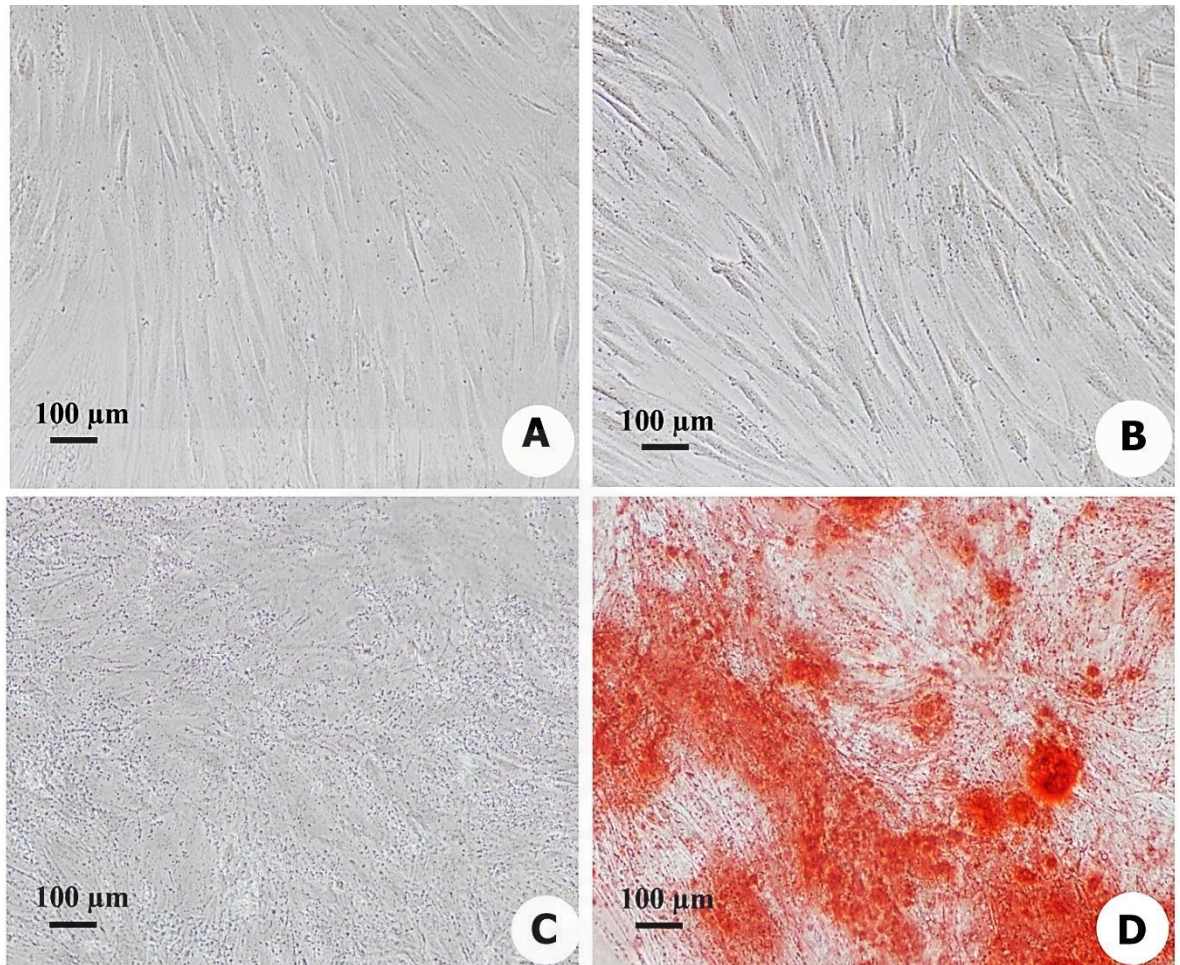
Figure 4.14: Representative photomicrographs of osteogenic differentiation of BM-MSCs. (A) BM-MSCs cultured in DMEM supplemented with 10% FBS for 14 days. (B) Alizarin-red-S staining of BM-MSCs cultured in DMEM supplemented with 10% FBS for 14 days. (C) Osteogenic differentiation evidenced by the extracellular calcium deposits after osteogenic induction for 14 days (D) Alizarin-red-S positive in BM-MSCs cultured in osteogenic differentiation medium for 14 days.
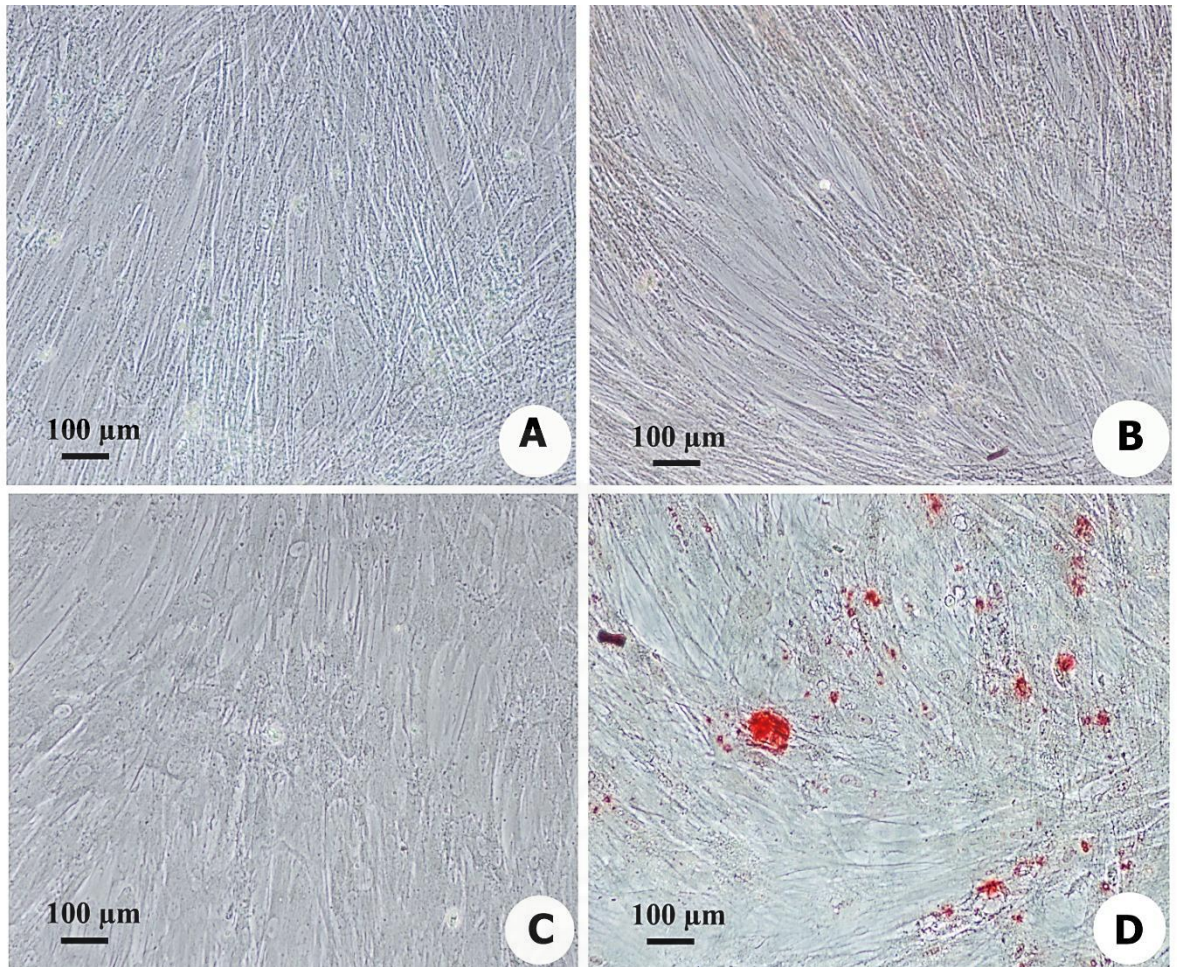
Figure 4.15: Representative photomicrographs of osteogenic differentiation of AM-MSCs. (A) AM-MSCs cultured in DMEM supplemented with 10% FBS for 21 days. (B) Alizarin-red-S staining of AM-MSCs cultured in DMEM supplemented with 10% FBS for 21 days. (C) Osteogenic differentiation evidenced by the extracellular calcium deposits after osteogenic induction for 21 days (D) Alizarin-red-S positive in AM-MSCs cultured in osteogenic differentiation medium for 21 days.
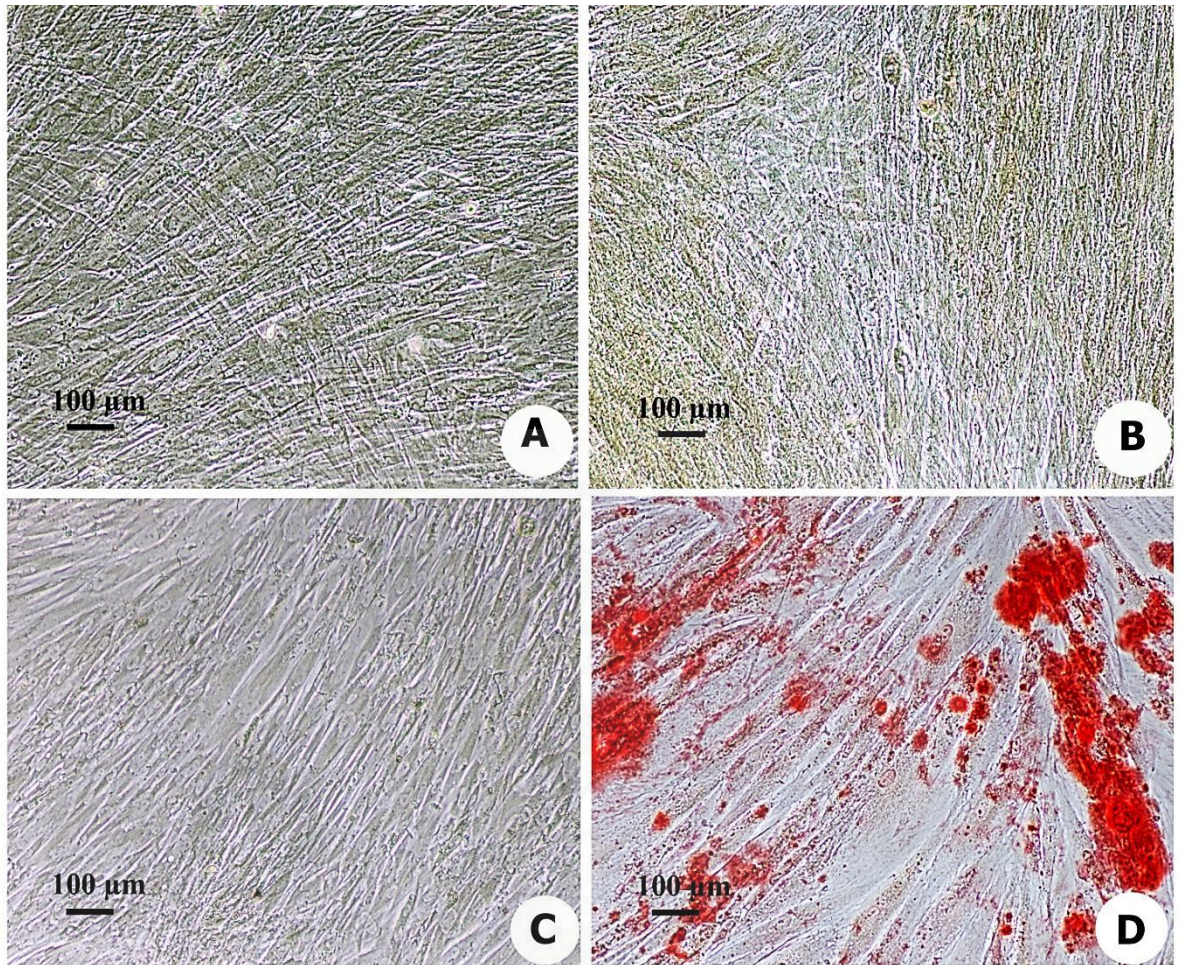
Figure 4.16: Representative photomicrographs of osteogenic differentiation of CH-MSCs. (A) CH-MSCs cultured in DMEM supplemented with 10% FBS for 21 days. (B) Alizarin-red-S staining of CH-MSCs cultured in DMEM supplemented with 10% FBS for 21 days. (C) Osteogenic differentiation evidenced by the extracellular calcium deposits after osteogenic induction for 21 days (D) Alizarin-red-S positive in CH-MSCs cultured in osteogenic differentiation medium for 21 days.
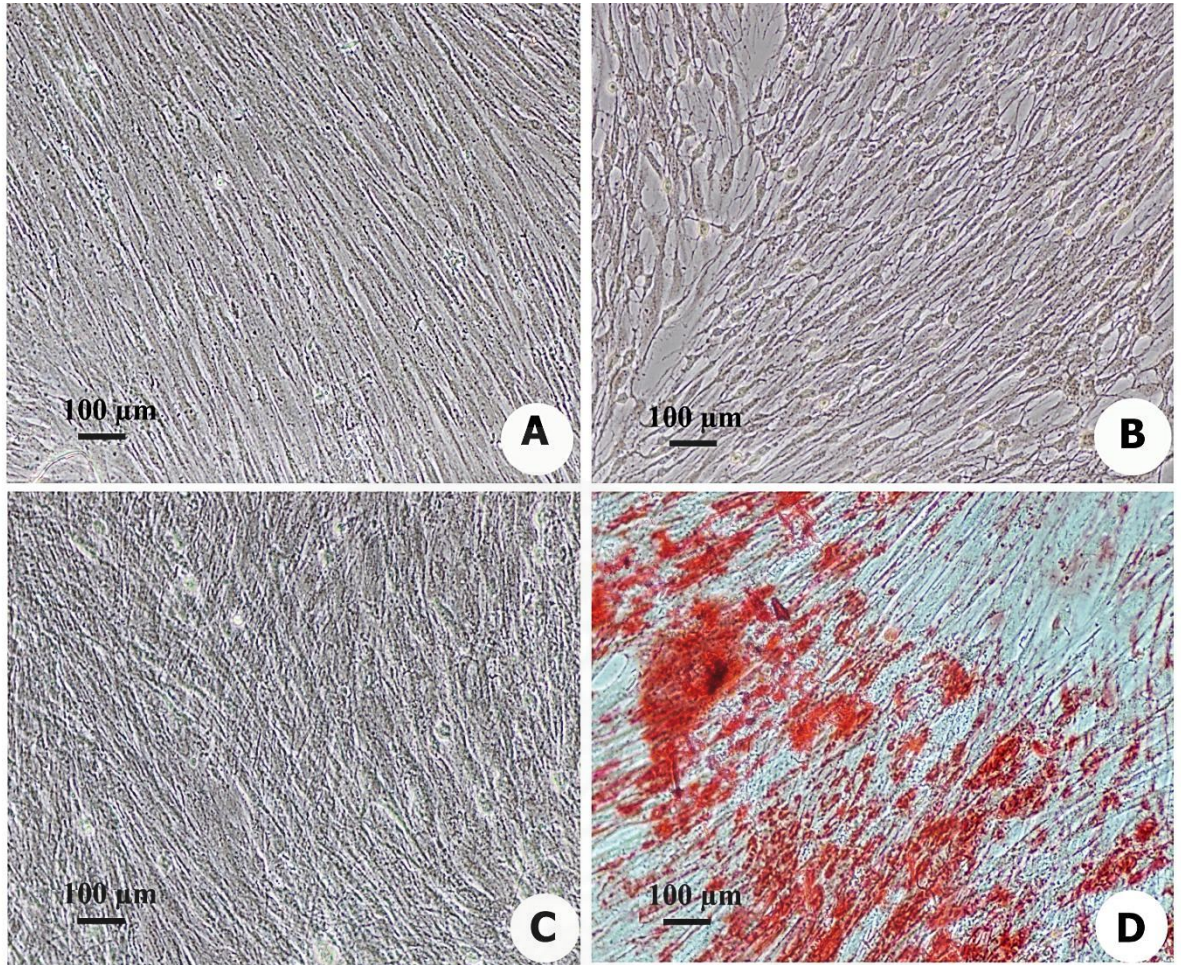
Figure 4.17: Representative photomicrographs of osteogenic differentiation of PL-MSCs. (A) PL-MSCs cultured in DMEM supplemented with 10% FBS for 21 days. (B) Alizarin-red-S staining of PL-MSCs cultured in DMEM supplemented with 10% FBS for 21 days. (C) Osteogenic differentiation evidenced by the extracellular calcium deposits after osteogenic induction for 21 days (D) Alizarin-red-S positive in PL-MSCs cultured in osteogenic differentiation medium for 21 days.
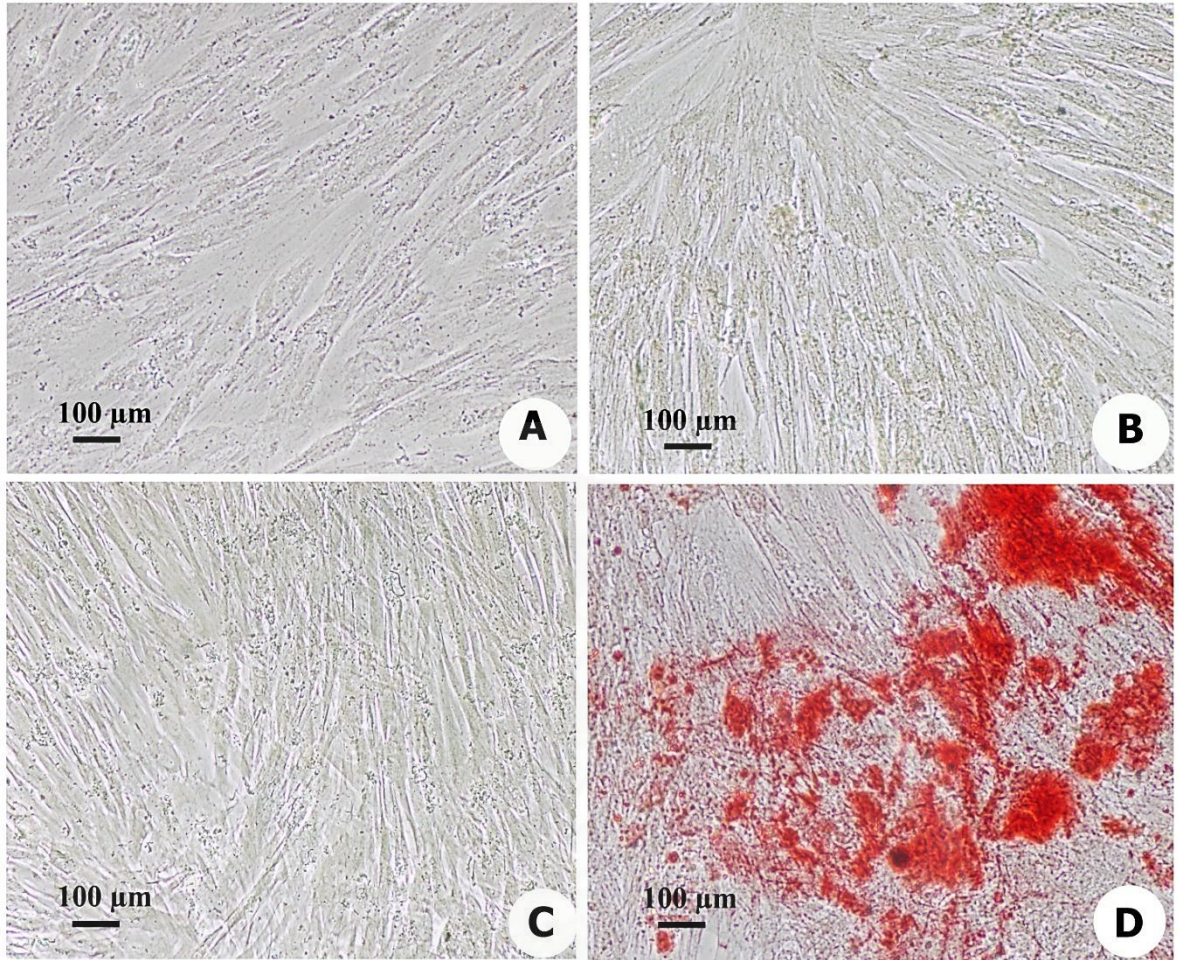
Figure 4.18: Representative photomicrographs of osteogenic differentiation of UC-MSCs. (A) UC-MSCs cultured in DMEM supplemented with 10% FBS for 21 days. (B) Alizarin-red-S staining of UC-MSCs cultured in DMEM supplemented with 10% FBS for 21 days. (C) Osteogenic differentiation evidenced by the extracellular calcium deposits after osteogenic induction for 21 days (D) Alizarin-red-S positive in UC-MSCs cultured in osteogenic differentiation medium for 21 days.

4.7 The expression of alkaline phosphatase after BMP-2 treatment

To determine the effect of BMP-2 on the osteogenic differentiation of AM-MSCs, CH-MSCs, PL-MSCs, and UC-MSCs in comparison to that of BM-MSCs, MSCs were cultured in osteogenic differentiation medium supplemented with BMP-2 for 3, 7, 14, 21, and 28 days. The differentiation potential was compared to those of MSCs cultured in complete medium and osteogenic differentiation medium. After induction for 3 days, few ALP positive cells were observed in BM-MSCs cultured in both osteogenic differentiations medium and osteogenic differentiation medium supplemented with BMP-2 (Fig. 4.19 B, 4.19 C, 4.20 B, and 4.20 C). Interestingly, BM-MSCs cultured in osteogenic differentiation medium supplemented with BMP-2 had higher ALP expression than BM-MSCs cultured in osteogenic differentiation medium without BMP-2 (Fig. 4.19 C, 4.20 C). In contrast to BM-MSCs, the expressions of ALP were not presented in AM-MSCs, CH-MSCs, PL-MSCs, and UC-MSCs which cultured in osteogenic differentiation medium without BMP-2 (Fig. 4.21- 4.28B). Fascinatingly, AM-MSCs, CH-MSCs, PL-MSCs, and UC-MSCs treated with BMP-2 for 3 days exhibited higher alkaline phosphatase expression than that of untreated group (Fig. 4.21 - 4.28 C). Following sequential culture, the expression of ALP was increased over time in all MSCs cultured in osteogenic differentiation medium with or without BMP-2. Remarkably, moderate ALP positive cells were observed in BM-MSCs treated with BMP-2 for 14 days (Fig. 4.19 I, 4.20 I). The intensity of ALP staining was significantly increased in BM-MSCs treated with BMP-2 for 21 and 28 days as compared to BM-MSCs cultured in osteogenic differentiation medium without BMP-2 (Fig. 4.19 K, L, N, O, and 4.20 K, L, N, O). In AM-MSCs, CH-MSCs, PL-MSCs, and UC-MSCs, treatment with BMP-2 could increase the expression of alkaline phosphatase (Fig. 4.21 - 4.28 L, O) as compared to those MSCs cultured in osteogenic differentiation medium without BMP-2 (Fig. 4.21 - 4.28 K, N). However, the intensity of ALP staining was significantly less than that of BM-MSCs at every time point examined (Fig. 4.19 - 4.28 C, F, I, L, O).
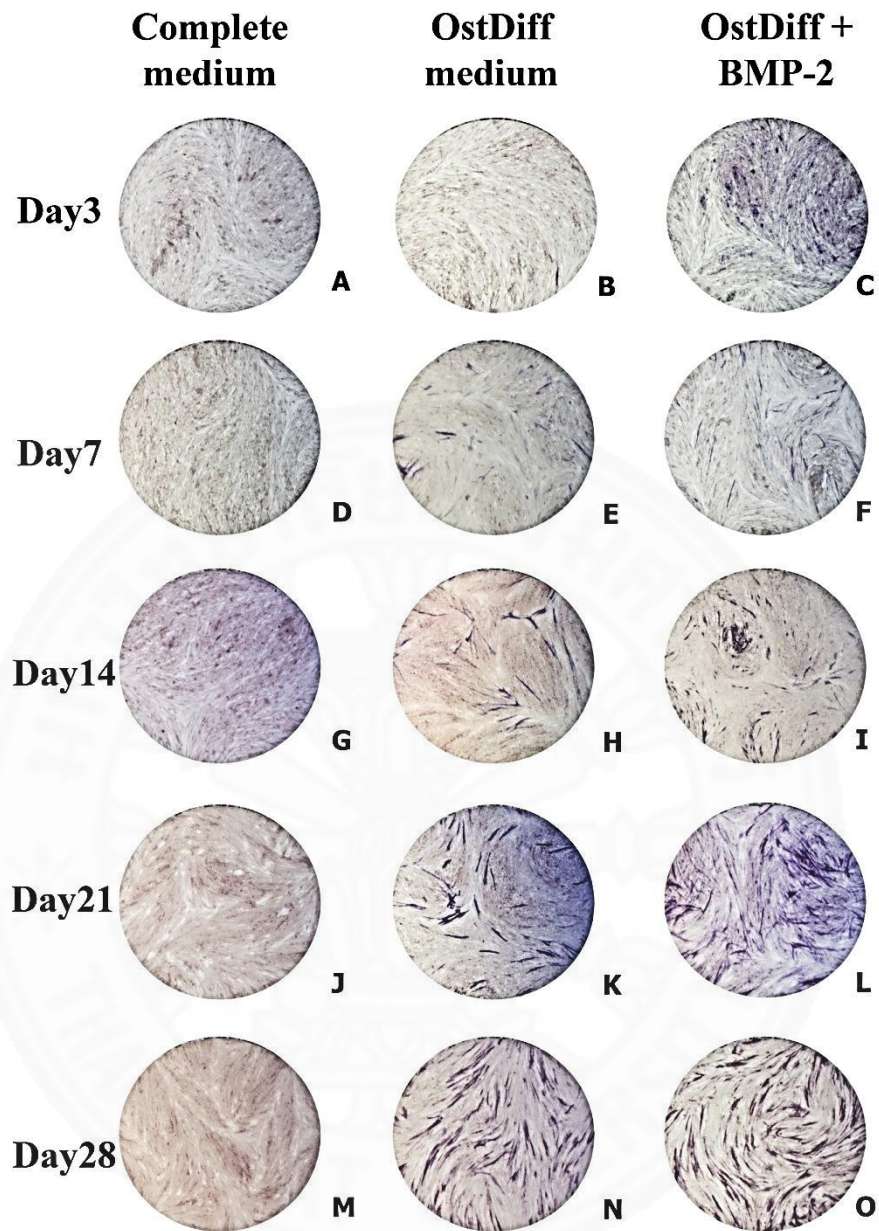
Figure 4.19: The expression of alkaline phosphatase in BM-MSCs cultured in osteogenic differentiation medium supplemented with BMP-2 for 3, 7, 14, 21, and 28 days (C, F, I, L, O, respectively) in comparison to those of MSCs cultured in osteogenic medium without BMP-2 (B, E, H, K, N, respectively). BM-MSCs cultured in DMEM supplemented with 10% FBS served as negative control (A, D, G, J, M, resepectively).
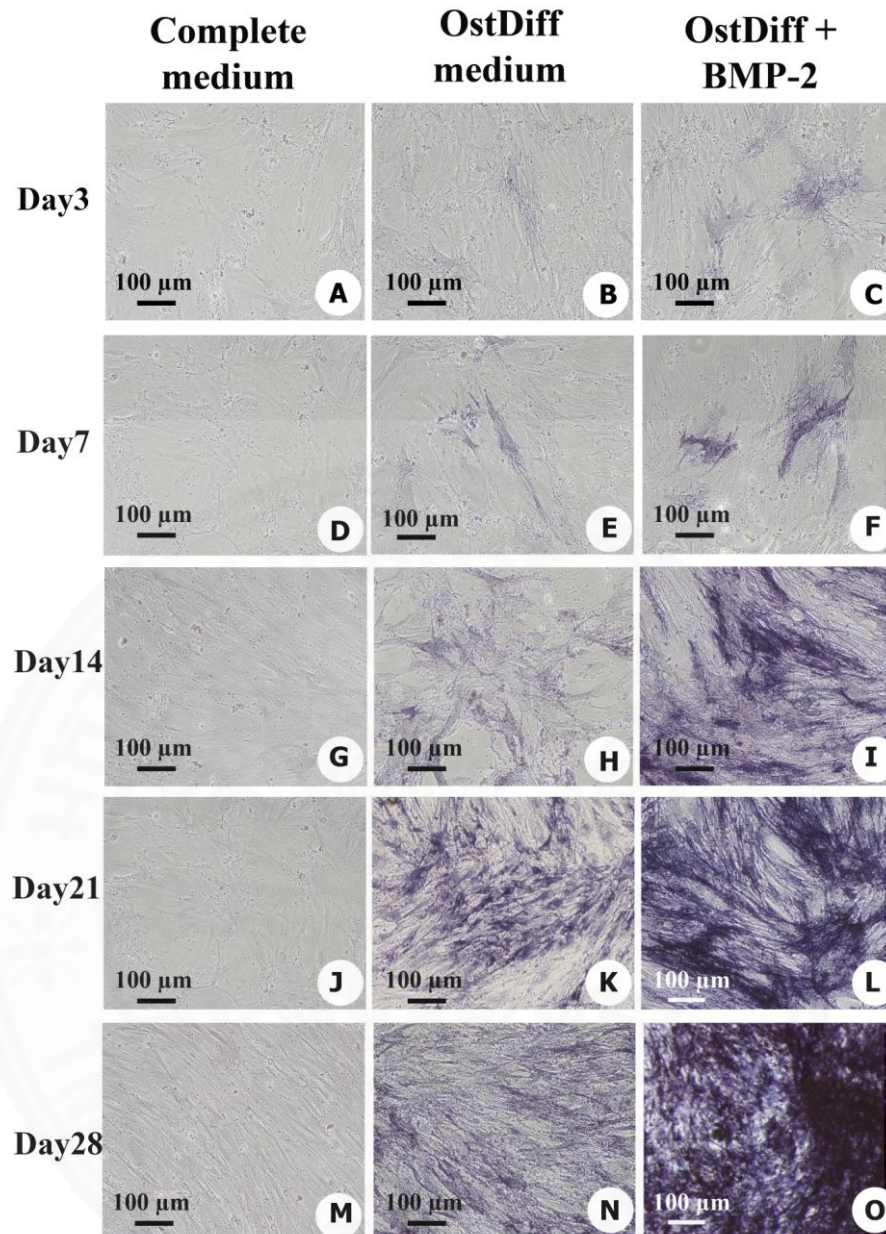
Figure 4.20: Representative photomicrographs of osteogenic differentiation of BM-MSCs. Osteogenic differentiation was evidenced by the formation of alkaline phosphatase-positive aggregate in cytoplasm after induction with osteogenic differentiation medium (B, E, H, K, N) and osteogenic differentiation medium supplemented with BMP-2 (C, F, I, L, O) for 3, 7, 14, 21, and 28 days. No alkaline phosphatase-positive aggregates were found in cytoplasm of BM-MSCs cultured in DMEM supplemented with 10% FBS for 3, 7, 14, 21, and 28 days (A, D, G, J, and M, respectively).
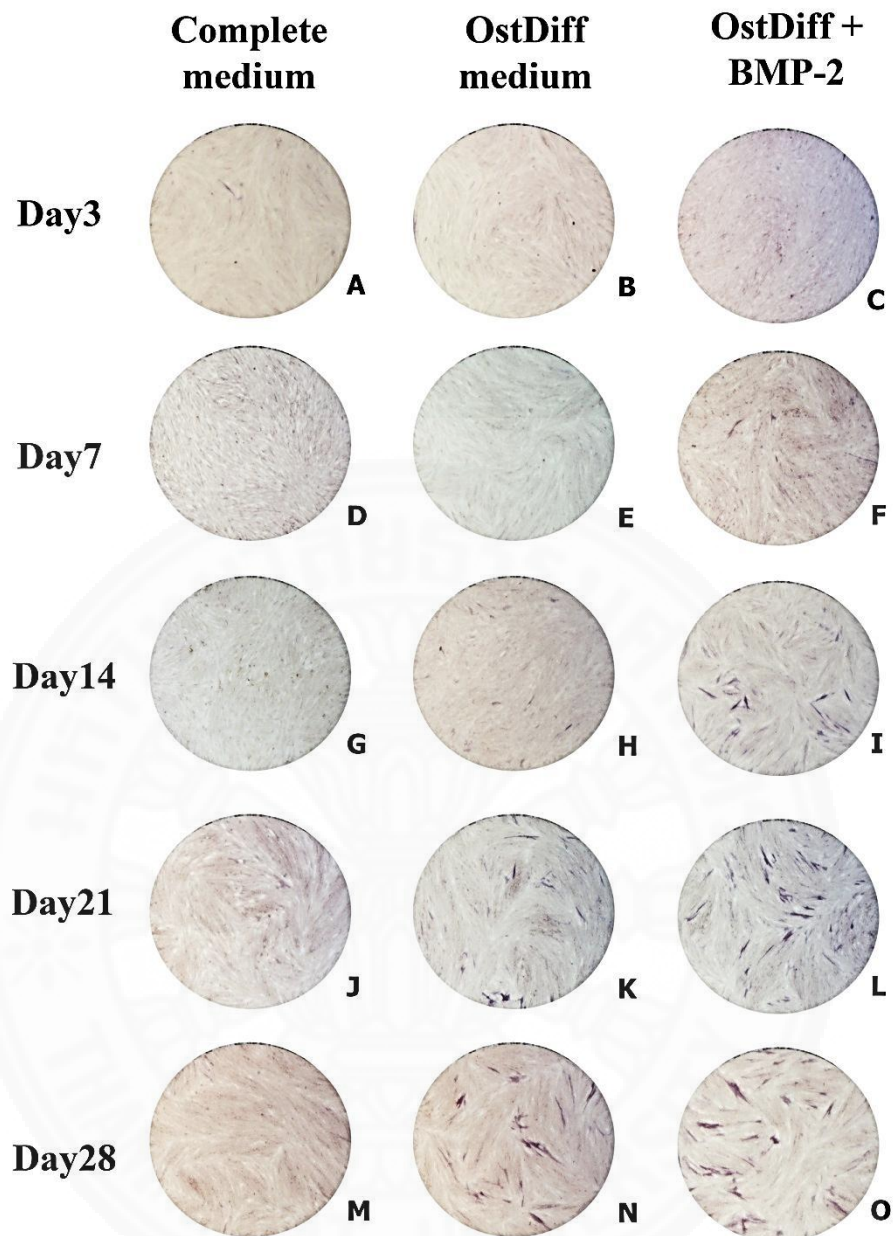
Figure 4.21: The expression of alkaline phosphatase in AM-MSCs cultured in osteogenic differentiation medium supplemented with BMP-2 for 3, 7, 14, 21, and 28 days (C, F, I, L, O, respectively) in comparison to those of MSCs cultured in osteogenic medium without BMP-2 (B, E, H, K, N, respectively). AM-MSCs cultured in DMEM supplemented with 10% FBS served as negative control (A, D, G, J, M, resepectively).
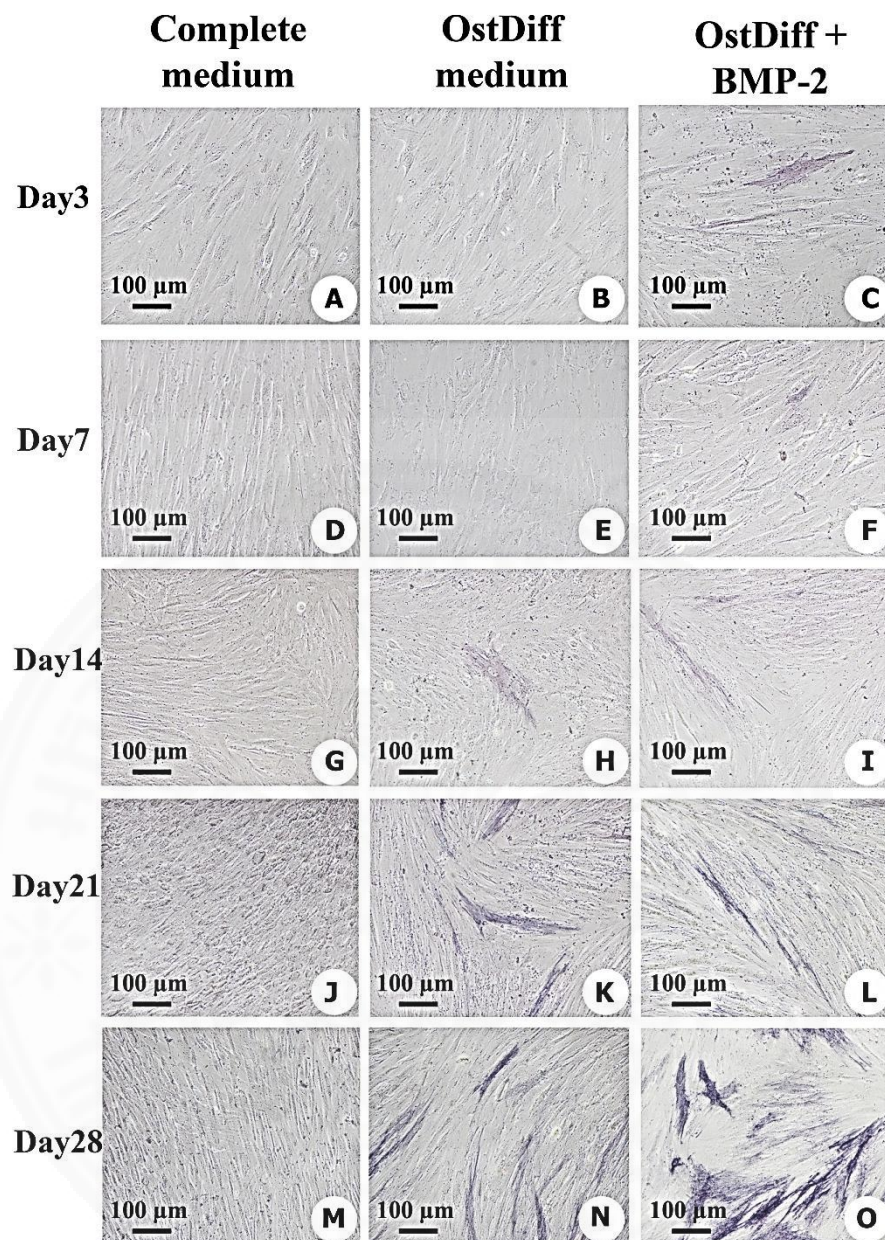
Figure 4.22: Representative photomicrographs of osteogenic differentiation of AM-MSCs. Osteogenic differentiation was evidenced by the formation of alkaline phosphatase-positive aggregate in cytoplasm after induction with osteogenic differentiation medium (B, E, H, K, N) and osteogenic differentiation medium supplemented with BMP-2 (C, F, I, L, O) for 3, 7, 14, 21, and 28 days. No alkaline phosphatase-positive aggregates were found in cytoplasm of AM-MSCs cultured in DMEM supplemented with 10% FBS for 3, 7, 14, 21, and 28 days (A, D, G, J, and M, respectively).
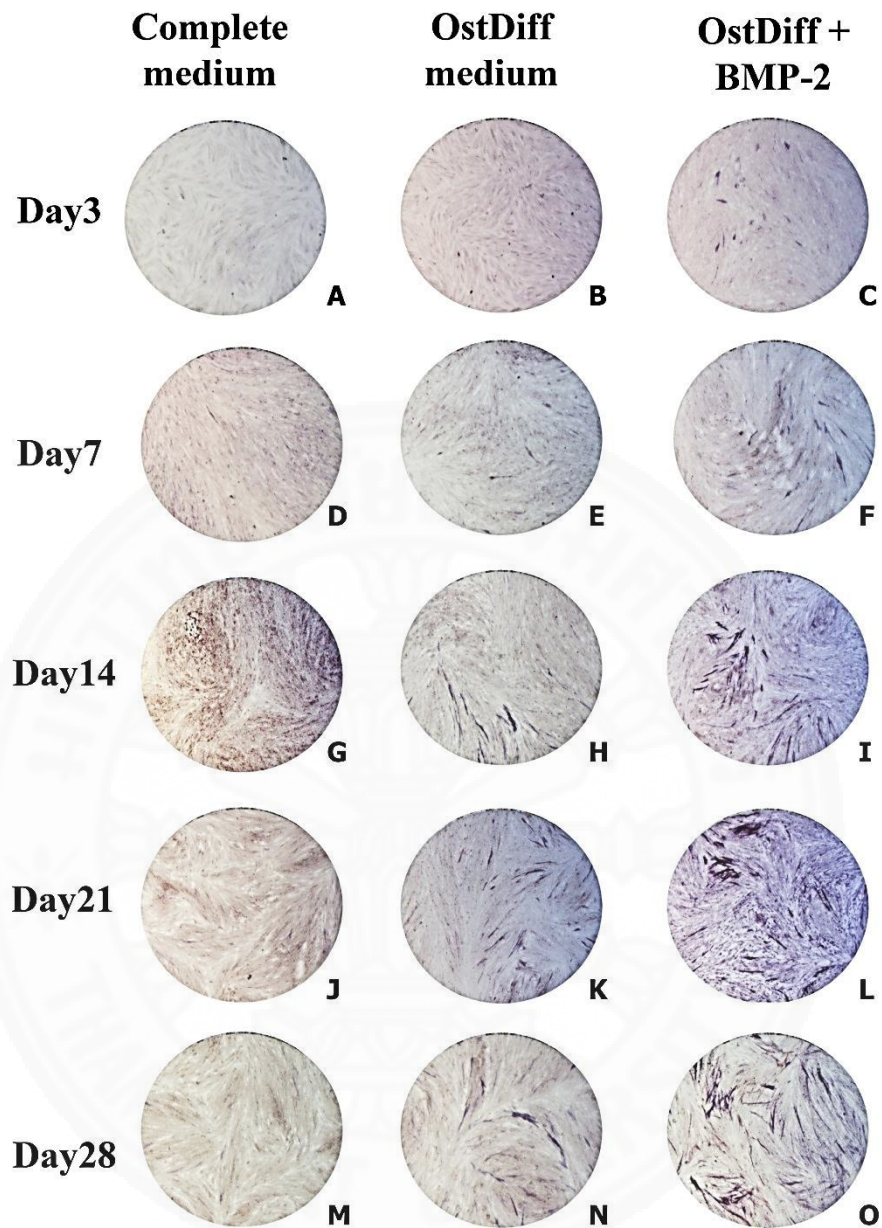
Figure 4.23: The expression of alkaline phosphatase in CH-MSCs cultured in osteogenic differentiation medium supplemented with BMP-2 for 3, 7, 14, 21, and 28 days (C, F, I, L, O, respectively) in comparison to those of MSCs cultured in osteogenic medium without BMP-2 (B, E, H, K, N, respectively). CH-MSCs cultured in DMEM supplemented with 10% FBS served as negative control (A, D, G, J, M, resepectively).
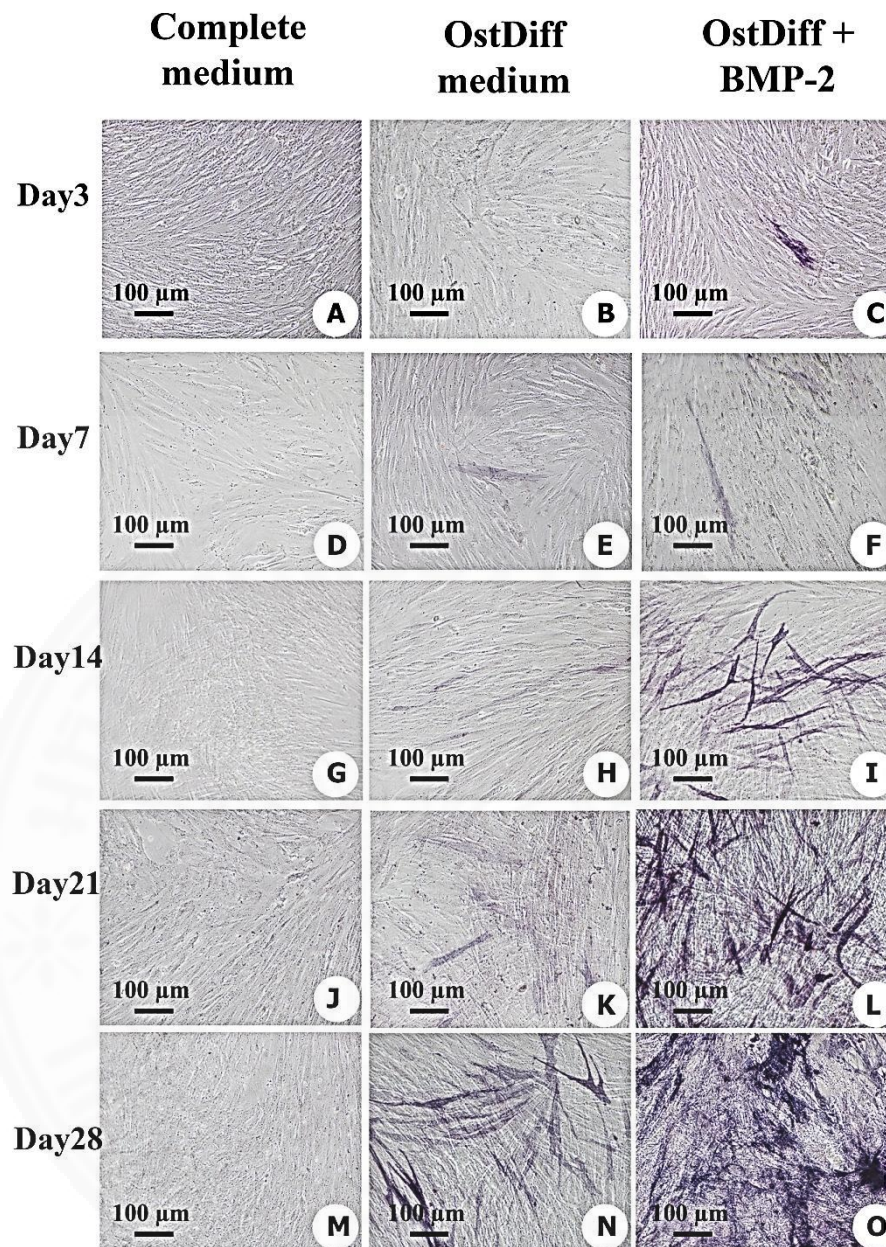
Figure 4.24: Representative photomicrographs of osteogenic differentiation of CH-MSCs. Osteogenic differentiation was evidenced by the formation of alkaline phosphatase-positive aggregate in cytoplasm after induction with osteogenic differentiation medium (B, E, H, K, N) and osteogenic differentiation medium supplemented with BMP-2 (C, F, I, L, O) for 3, 7, 14, 21, and 28 days. No alkaline phosphatase-positive aggregates were found in cytoplasm of CH-MSCs cultured in DMEM supplemented with 10% FBS for 3, 7, 14, 21, and 28 days (A, D, G, J, and M, respectively).

	Complete medium	OstDiff medium	OstDiff + BMP-2
Day3	A	B	C
Day7	D	E	F
Day14	G	H	I
Day21	J	K	L
Day28	M	N	O
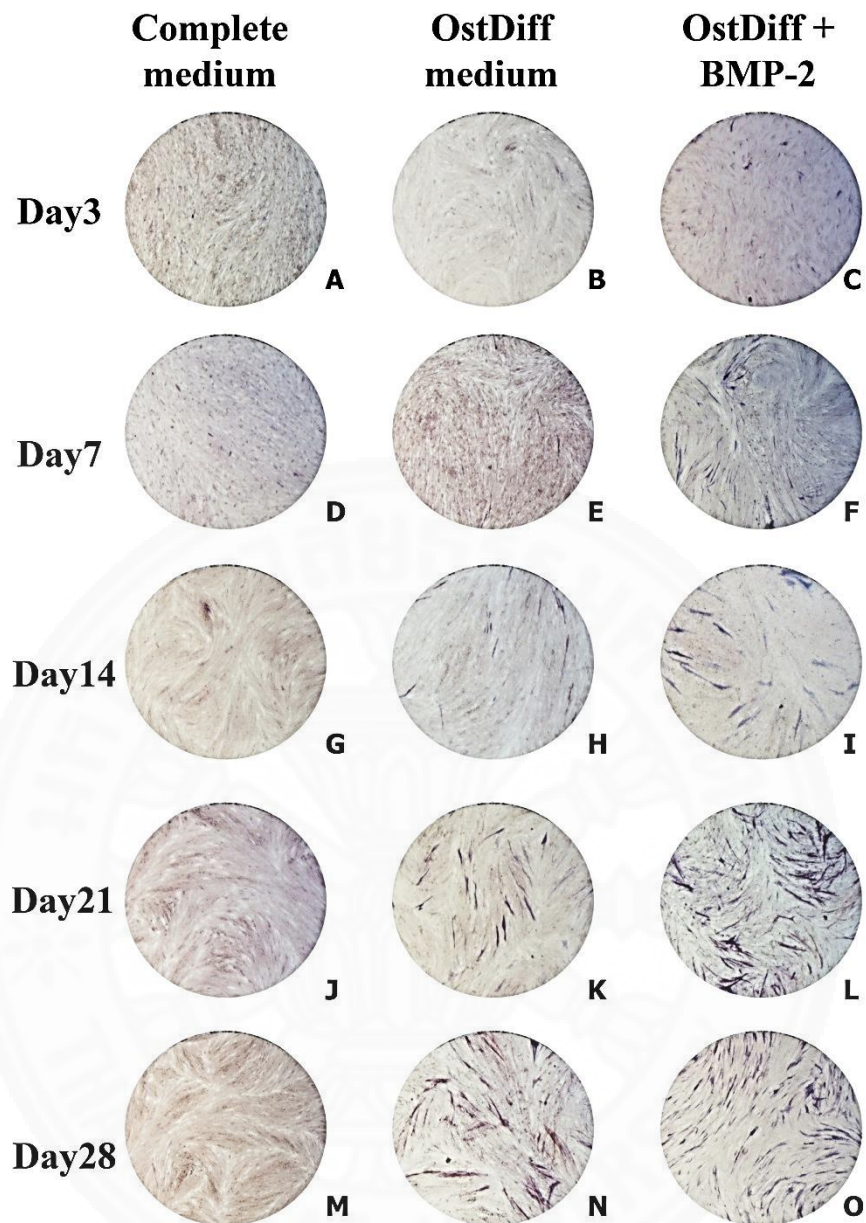
Figure 4.25: The expression of alkaline phosphatase in PL-MSCs cultured in osteogenic differentiation medium supplemented with BMP-2 for 3, 7, 14, 21, and 28 days (C, F, I, L, O, respectively) in comparison to those of MSCs cultured in osteogenic medium without BMP-2 (B, E, H, K, N, respectively). PL-MSCs cultured in DMEM supplemented with 10% FBS served as negative control (A, D, G, J, M, resepectively).

.
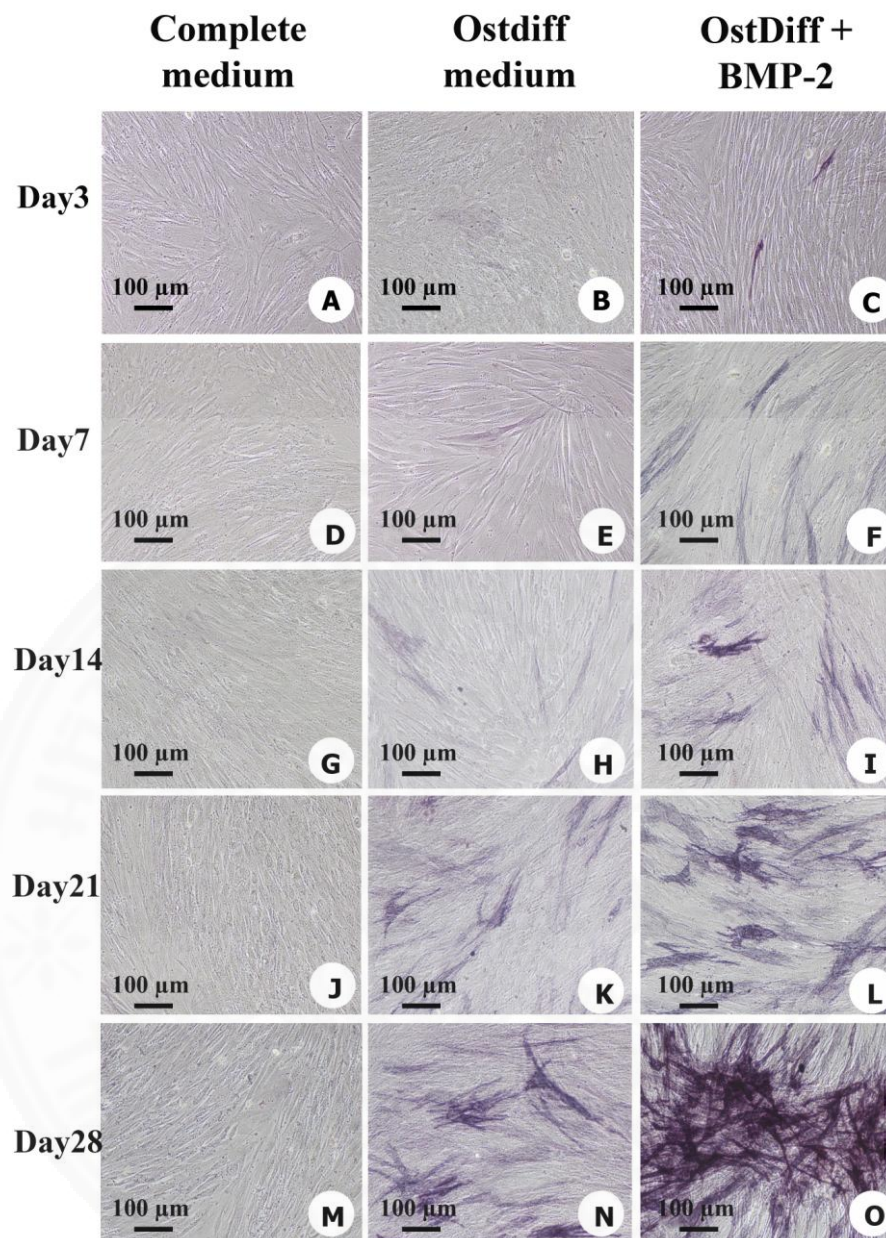
Figure 4.26: Representative photomicrographs of osteogenic differentiation of PL-MSCs. Osteogenic differentiation was evidenced by the formation of alkaline phosphatase-positive aggregate in cytoplasm after induction with osteogenic differentiation medium (B, E, H, K, N) and osteogenic differentiation medium supplemented with BMP-2 (C, F, I, L, O) for 3, 7, 14, 21, and 28 days. No alkaline phosphatase-positive aggregates were found in cytoplasm of PL-MSCs cultured in DMEM supplemented with 10% FBS for 3, 7, 14, 21, and 28 days (A, D, G, J, and M, respectively).
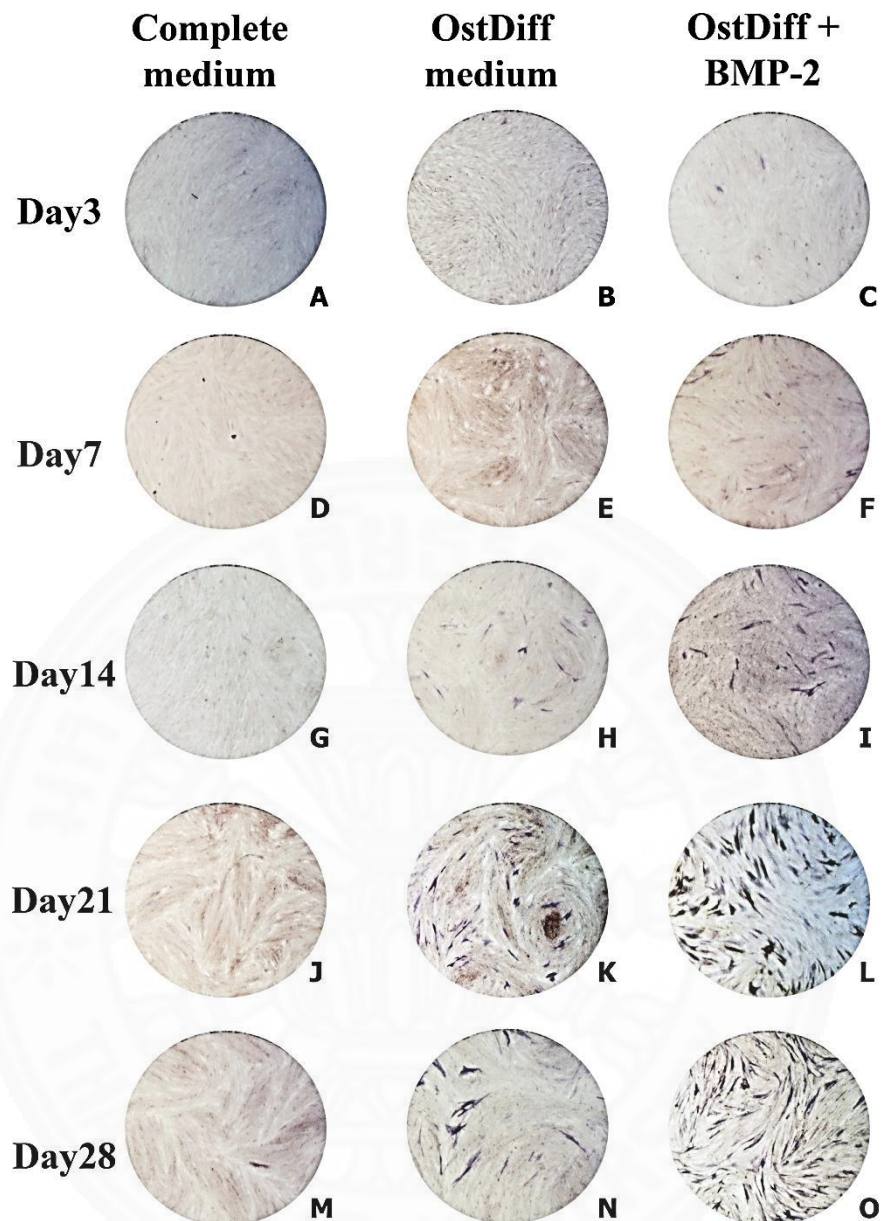
Figure 4.27: The expression of alkaline phosphatase in UC-MSCs cultured in osteogenic differentiation medium supplemented with BMP-2 for 3, 7, 14, 21, and 28 days (C, F, I, L, O, respectively) in comparison to those of MSCs cultured in osteogenic medium without BMP-2 (B, E, H, K, N, respectively). UC-MSCs cultured in DMEM supplemented with 10% FBS served as negative control (A, D, G, J, M, resepectively).

	Complete medium	**OstDiff medium**	**OstDiff + BMP-2**
Day3	100 µm A	100 µm B	100 µm C
Day7	100 µm D	100 µm E	100 µm F
Day14	100 µm G	100 µm H	100 µm I
Day21	100 µm J	100 µm K	100 µm L
Day28	100 µm M	100 µm N	100 µm O
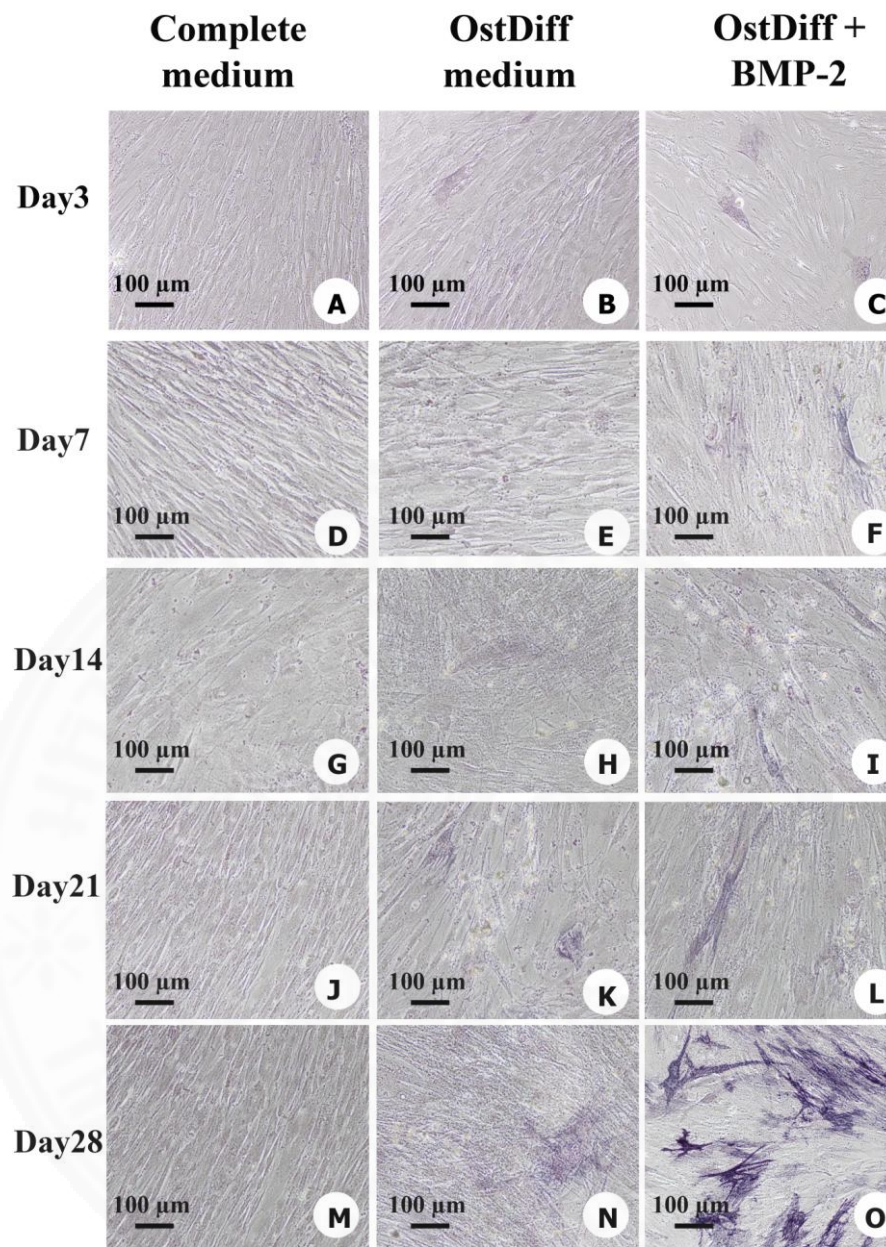
Figure 4.28: Representative photomicrographs of osteogenic differentiation of UC-MSCs. Osteogenic differentiation was evidenced by the formation of alkaline phosphatase-positive aggregate in cytoplasm after induction with osteogenic differentiation medium (B, E, H, K, N) and osteogenic differentiation medium supplemented with BMP-2 (C, F, I, L, O) for 3, 7, 14, 21, and 28 days. No alkaline phosphatase-positive aggregates were found in cytoplasm of UC-MSCs cultured in DMEM supplemented with 10% FBS for 3, 7, 14, 21, and 28 days (A, D, G, J, and M, respectively).

4.8 Alkaline phosphatase activity after BMP-2 treatment

The activity of intracellular ALP in BM-MSCs, AM-MSCs, CH-MSCs, PL-MSCs and UC-MSCs was also quantitative assessed using colorimetric enzymatic assay at day 3, 7, 14, 21, and 28. The results demonstrated that the MSCs cultured in osteogenic differentiation medium supplemented with BMP-2 showed a clear superiority compared to the others (MSCs cultured in complete medium and MSCs cultured in osteogenic differentiation medium) (Fig. 4.29). As early as 14 days after BMP-2 induction, BMP-2 induced BM-MSCs had about a fold increase in alkaline phosphatase activity. In addition, the activity of ALP in the BMP-2 treated groups significantly increased with time. At day 21 and 28, alkaline phosphatase activity in BMP-2 treated groups were significantly increased up to 2 and 2.5-fold, respectively, compared with MSCs cultured in osteogenic differentiation without BMP-2 ($p<0.05$). In contrast, CH-MSCs, PL-MSCs and UC-MSCs at day 14, 21 and 28 after BMP-2 treatment had only a fold increase in alkaline phosphatase activity ($p<0.05$). Remarkably, BMP-2 induced less than a fold increase in alkaline phosphatase activity in AM-MSCs compared with untreated osteogenic differentiation culture ($p<0.05$). Similar to ALP staining, although ALP activity increased over time in BMP-2 treated groups, the ALP activity in AM-MSCs, CH-MSCs, PL-MSCs and UC-MSCs were significantly less than that of BM-MSCs at every time point examined (Fig. 4.29).

Table 4.6: Alkaline phosphatase activity of BMP-2 induced osteogenic differentiation of mesenchymal stem cells derived from bone marrow, amnion, chorion, placenta, and umbilical cord.

MSCs sources	Group	Day (s)				
		3	**7**	**14**	**21**	**28**
BM-MSCs	Complete medium	0.65 ± 0.01	1.07 ± 0.01	1.86 ± 0.01	2.64 ± 0.04	2.88 ± 0.06
	OstDiff	1.20 ± 0.01	7.37 ± 0.01	8.23 ± 0.01	17.99 ± 0.04	18.45 ± 0.05
	OstDiff + BMP-2	3.61 ± 0.04	8.74 ± 0.03	15.40 ± 0.06	36.91 ± 0.00	47.62 ± 0.49
AM-MSCs	Complete medium	0.70 ± 0.01	1.71 ± 0.00	3.18 ± 0.10	3.37 ± 0.12	3.38 ± 0.05
	OstDiff	1.04 ± 0.02	1.97 ± 0.01	3.60 ± 0.04	5.40 ± 0.06	7.54 ± 0.12
	OstDiff + BMP-2	2.03 ± 0.04	2.60 ± 0.14	4.49 ± 0.16	6.27 ± 0.23	13.88 ± 0.07
CH-MSCs	Complete medium	0.66 ± 0.01	1.80 ± 0.01	3.62 ± 0.01	4.17 ± 0.03	5.32 ± 0.02
	OstDiff	1.14 ± 0.01	3.16 ± 0.03	4.59 ± 0.01	10.04 ± 0.02	11.99 ± 0.02
	OstDiff + BMP-2	3.43 ± 0.01	4.32 ± 0.02	8.25 ± 0.04	15.55 ± 0.02	16.43 ± 0.03
PL-MSCs	Complete medium	0.64 ± 0.02	1.75 ± 0.01	3.34 ± 0.04	4.44 ± 0.03	4.62 ± 0.03
	OstDiff	1.06 ± 0.01	2.49 ± 0.01	7.69 ± 0.01	10.12 ± 0.03	11.95 ± 0.04
	OstDiff + BMP-2	3.33 ± 0.03	4.12 ± 0.00	12.53 ± 0.04	16.00 ± 0.16	17.98 ± 0.06
UC-MSCs	Complete medium	0.63 ± 0.02	1.65 ± 0.02	3.16 ± 0.03	3.37 ± 0.12	4.38 ± 0.05
	OstDiff	1.06 ± 0.01	2.68 ± 0.10	4.43 ± 0.22	6.40 ± 0.06	8.54 ± 0.12
	OstDiff + BMP-2	3.33 ± 0.02	3.60 ± 0.14	7.49 ± 0.16	8.44 ± 0.08	14.88 ± 0.07

Values are presented as mean ± SEM.
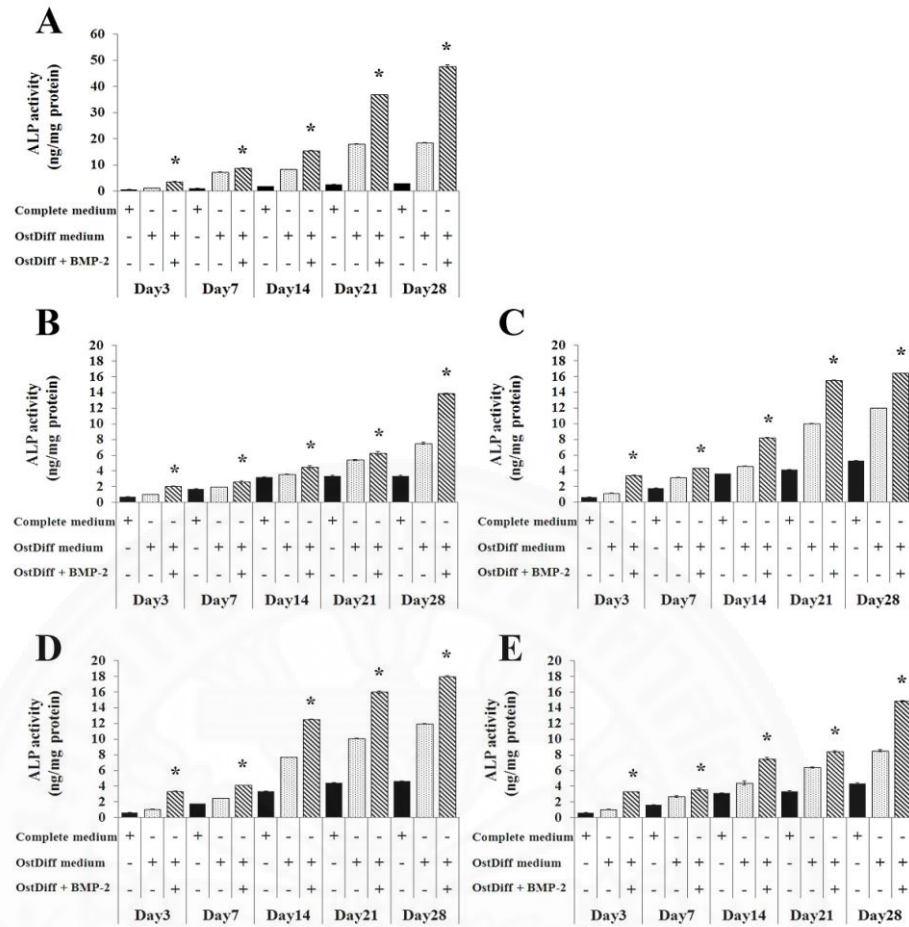
Figure 4.29: Alkaline phosphatase activity of BMP-2 induced osteogenic differentiation of BM-MSCs (A), AM-MSCs (B), CH-MSCs(C), PL-MSCs (D), and UC-MSCs (E). Data are expressed as mean ± SEM. * $p<0.05$: significant difference in comparison to MSCs cultured in osteogenic differentiation medium.

4.9 The expression of osteogenic differentiation genes in MSCs after BMP-2 treatment

The effect of BMP-2 on osteogenic differentiation of BM-MSCs, AM-MSCs, CH-MSCs, PL-MSCs, and UC-MSCs was further investigated through gene expression analysis of osteogenic lineage genes including *RUNX-2*, *OSX*, and *OCN* following 3, 7, 14, 21, and 28 days of culture. The result showed that BMP-2 significantly up-regulated the expression of osteogenic lineage genes, *RUNX-2*, *OSX*, and *OCN* at day 7, 14, 21, and 28 after osteogenic induction while there were no significantly changes in the expression levels of those osteogenic lineage genes during the earlier time points (day 3) (Fig. 4.30 - 4.32). The expression of *RUNX-2* in BM-MSCs was increased over time from day 3 to day 14. The peak of *RUNX-2* expression was found at day 14 in BM-MSCs cultured in osteogenic differentiation with or without BMP-2. Nevertheless, BM-MSCs cultured in osteogenic differentiation with BMP-2 showed significant higher expression of *RUNX-2* than that was cultured in osteogenic differentiation without BMP-2 (Fig. 4.30 A). In contrast to BM-MSCs, *RUNX-2* expression was increased over time from day 3 to day 28 in AM-MSCs, CH-MSCs, PL-MSCs, and UC-MSC cultured in osteogenic differentiation medium with or without BMP-2. Interestingly, AM-MSCs, CH-MSCs, PL-MSCs, and UC-MSCs treated with BMP-2 showed significant higher expression of *RUNX-2* than those of untreated groups (Fig. 4.30B-E). The effect of BMP-2 on the expression levels of other osteogenic lineage genes in AM-MSCs, CH-MSCs, PL-MSCs, and UC-MSCs was also different from BM-MSCs. The expression of *OSX* was increased over time from day 3 to day 28 in BM-MSCs, AM-MSCs, CH-MSCs, PL-MSCs, and UC-MSCs cultured in osteogenic differentiation medium with or without BMP-2 (Fig. 4.31). However, BMP-2 significantly up-regulated *OSX* expression in AM-MSCs, CH-MSCs, PL-MSCs, and UC-MSCs on days 14, 21, and 28 of culture (Fig. 4.31 B, C, D, and E) while the effect of BMP-2 in up-regulating *OSX* expression was observed on day 7, 14, 21, and 28 in cultured BM-MSCs (Fig. 4.31 A). Similar to *OSX,* minimum *OCN* expression was detected in BM-MSCs at day 3 and significantly increased *OCN* levels were observed in BM-MSCs treated with BMP-2 compared with untreated controls at day 7, 14, 21, and 28 (Fig. 4.32 A). The expression of *OCN* was increased to the same extent with time in AM-MSCs, CH-MSCs, PL-MSCs, and UC-MSCs in both BMP-2 treated- and untreated groups (Fig. 4.32 B, C, D, and E).

However, the up-regulating gene expression in AM-MSCs, CH-MSCs, PL-MSCs, and UC-MSCs was significantly observed in BMP-2 treated group at day 14, 21, and 28 (Fig. 4.32 B, C, D, and E).

Table 4.7: The relative *RUNX-2* expression level in MSC derived from bone marrow, amnion, chorion, placenta and umbilical cord.

MSC sources	Group	Day (s)				
		3	7	14	21	28
BM-MSCs	Complete medium	1.00 ± 0.00	1.00 ± 0.00	1.00 ± 0.00	1.00 ± 0.00	1.00 ± 0.00
	OstDiff	2.42 ± 0.10	4.75 ± 0.45	8.45 ± 0.09	6.66 ± 0.43	2.29 ± 0.26
	OstDiff + BMP-2	3.16 ± 0.09	6.86 ± 0.11	15.04 ± 0.16	7.72 ± 0.06	3.86 ± 0.12
AM-MSCs	Complete medium	1.00 ± 0.00	1.00 ± 0.00	1.00 ± 0.00	1.00 ± 0.00	1.00 ± 0.00
	OstDiff	1.12 ± 0.06	1.81 ± 0.13	1.55 ± 0.40	2.45 ± 0.26	2.54 ± 0.26
	OstDiff + BMP-2	1.21 ± 0.02	1.26 ± 0.10	2.66 ± 0.25	3.63 ± 0.33	8.34 ± 0.29
CH-MSCs	Complete medium	1.00 ± 0.00	1.00 ± 0.00	1.00 ± 0.00	1.00 ± 0.00	1.00 ± 0.00
	OstDiff	1.24 ± 0.04	1.33 ± 0.09	4.88 ± 0.43	5.85 ± 0.11	10.10 ± 0.34
	OstDiff + BMP-2	1.29 ± 0.02	1.38 ± 0.16	6.43 ± 0.50	13.47 ± 0.07	14.39 ± 0.15
PL-MSCs	Complete medium	1.00 ± 0.00	1.00 ± 0.00	1.00 ± 0.00	1.00 ± 0.00	1.00 ± 0.00
	OstDiff	1.26 ± 0.04	1.45 ± 0.12	2.43 ± 0.14	6.14 ± 0.10	11.31 ± 0.30
	OstDiff + BMP-2	1.41 ± 0.01	2.54 ± 0.32	3.72 ± 0.11	13.29 ± 0.23	14.73 ± 0.24
UC-MSCs	Complete medium	1.00 ± 0.00	1.00 ± 0.00	1.00 ± 0.00	1.00 ± 0.00	1.00 ± 0.00
	OstDiff	1.22 ± 0.01	1.31 ± 0.08	1.78 ± 0.05	5.36 ± 0.11	9.90 ± 0.31
	OstDiff + BMP-2	1.61 ± 0.02	3.80 ± 0.08	4.36 ± 0.59	13.86 ± 0.74	13.99 ± 0.87

Values are presented as mean ± SEM.

Table 4.8: The relative *OSX* expression level in MSCs derived from bone marrow, amnion, chorion, placenta, and umbilical cord.

MSCs sources	Group	Day (s)				
		3	**7**	**14**	**21**	**28**
BM-MSCs	Complete medium	1.00 ± 0.00	1.00 ± 0.00	1.00 ± 0.00	1.00 ± 0.00	1.00 ± 0.00
	OstDiff	1.17 ± 0.06	1.28 ± 0.09	2.20 ± 0.14	5.40 ± 0.15	6.50 ± 0.49
	OstDiff + BMP-2	1.26 ± 0.03	1.64 ± 0.07	2.78 ± 0.21	7.73 ± 0.23	10.88 ± 0.07
AM-MSCs	Complete medium	1.00 ± 0.00	1.00 ± 0.00	1.00 ± 0.00	1.00 ± 0.00	1.00 ± 0.00
	OstDiff	1.02 ± 0.04	1.14 ± 0.28	1.23 ± 0.16	2.54 ± 0.21	2.55 ± 0.14
	OstDiff + BMP-2	1.08 ± 0.02	1.51 ± 0.34	1.71 ± 0.21	2.87 ± 0.16	3.59 ± 0.24
CH-MSCs	Complete medium	1.00 ± 0.00	1.00 ± 0.00	1.00 ± 0.00	1.00 ± 0.00	1.00 ± 0.00
	OstDiff	1.06 ± 0.05	1.21 ± 0.18	2.60 ± 0.18	4.45 ± 0.18	4.66 ± 0.33
	OstDiff + BMP-2	1.13 ± 0.02	1.60 ± 0.19	3.45 ± 0.30	5.22 ± 0.24	6.36 ± 0.17
PL-MSCs	Complete medium	1.00 ± 0.00	1.00 ± 0.00	1.00 ± 0.00	1.00 ± 0.00	1.00 ± 0.00
	OstDiff	1.08 ± 0.03	1.58 ± 0.04	2.78 ± 0.11	4.19 ± 0.33	4.68 ± 0.20
	OstDiff + BMP-2	1.21 ± 0.03	1.65 ± 0.25	3.09 ± 0.24	5.56 ± 0.09	7.58 ± 0.15
UC-MSCs	Complete medium	1.00 ± 0.00	1.00 ± 0.00	1.00 ± 0.00	1.00 ± 0.00	1.00 ± 0.00
	OstDiff	1.08 ± 0.02	1.28 ± 0.08	2.20 ± 0.13	4.40 ± 0.08	5.50 ± 0.30
	OstDiff + BMP-2	1.20 ± 0.03	1.54 ± 0.13	2.78 ± 0.16	6.73 ± 0.19	7.55 ± 0.23

Values are presented as mean ± SEM.

Table 4.9: The relative *OCN* expression in MSCs derived from bone marrow, amnion, chorion, placenta, and umbilical cord.

MSCs sources	Group	Day (s)				
		3	7	14	21	28
BM-MSCs	Complete medium	1.00 ± 0.00	1.00 ± 0.00	1.00 ± 0.00	1.00 ± 0.00	1.00 ± 0.00
	OstDiff	1.10 ± 0.05	1.15 ± 0.15	2.57 ± 0.09	4.37 ± 0.15	5.95 ± 0.07
	OstDiff + BMP-2	1.36 ± 0.02	1.86 ± 0.07	4.46 ± 0.19	6.42 ± 0.43	8.24 ± 0.06
AM-MSCs	Complete medium	1.00 ± 0.00	1.00 ± 0.00	1.00 ± 0.00	1.00 ± 0.00	1.00 ± 0.00
	OstDiff	1.02 ± 0.04	1.35 ± 0.01	1.37 ± 0.07	1.57 ± 0.06	1.78 ± 0.03
	OstDiff + BMP-2	1.17 ± 0.05	1.44 ± 0.02	1.71 ± 0.05	2.40 ± 0.05	3.58 ± 0.04
CH-MSCs	Complete medium	1.00 ± 0.00	1.00 ± 0.00	1.00 ± 0.00	1.00 ± 0.00	1.00 ± 0.00
	OstDiff	1.04 ± 0.03	1.50 ± 0.10	2.22 ± 0.17	2.81 ± 0.06	3.35 ± 0.08
	OstDiff + BMP-2	1.21 ± 0.03	1.84 ± 0.15	2.49 ± 0.15	5.05 ± 0.13	5.69 ± 0.24
PL-MSCs	Complete medium	1.00 ± 0.00	1.00 ± 0.00	1.00 ± 0.00	1.00 ± 0.00	1.00 ± 0.00
	OstDiff	1.09 ± 0.01	1.41 ± 0.06	1.88 ± 0.21	2.42 ± 0.20	4.37 ± 0.21
	OstDiff + BMP-2	1.28 ± 0.02	1.78 ± 0.12	2.36 ± 0.10	4.61 ± 0.14	7.81 ± 0.37
UC-MSCs	Complete medium	1.00 ± 0.00	1.00 ± 0.00	1.00 ± 0.00	1.00 ± 0.00	1.00 ± 0.00
	OstDiff	1.04 ± 0.01	1.45 ± 0.10	2.30 ± 0.07	3.65 ± 0.20	4.75 ± 0.34
	OstDiff + BMP-2	1.29 ± 0.04	1.71 ± 0.03	2.71 ± 0.09	5.17 ± 0.33	7.46 ± 0.04

Values are presented as mean ± SEM.
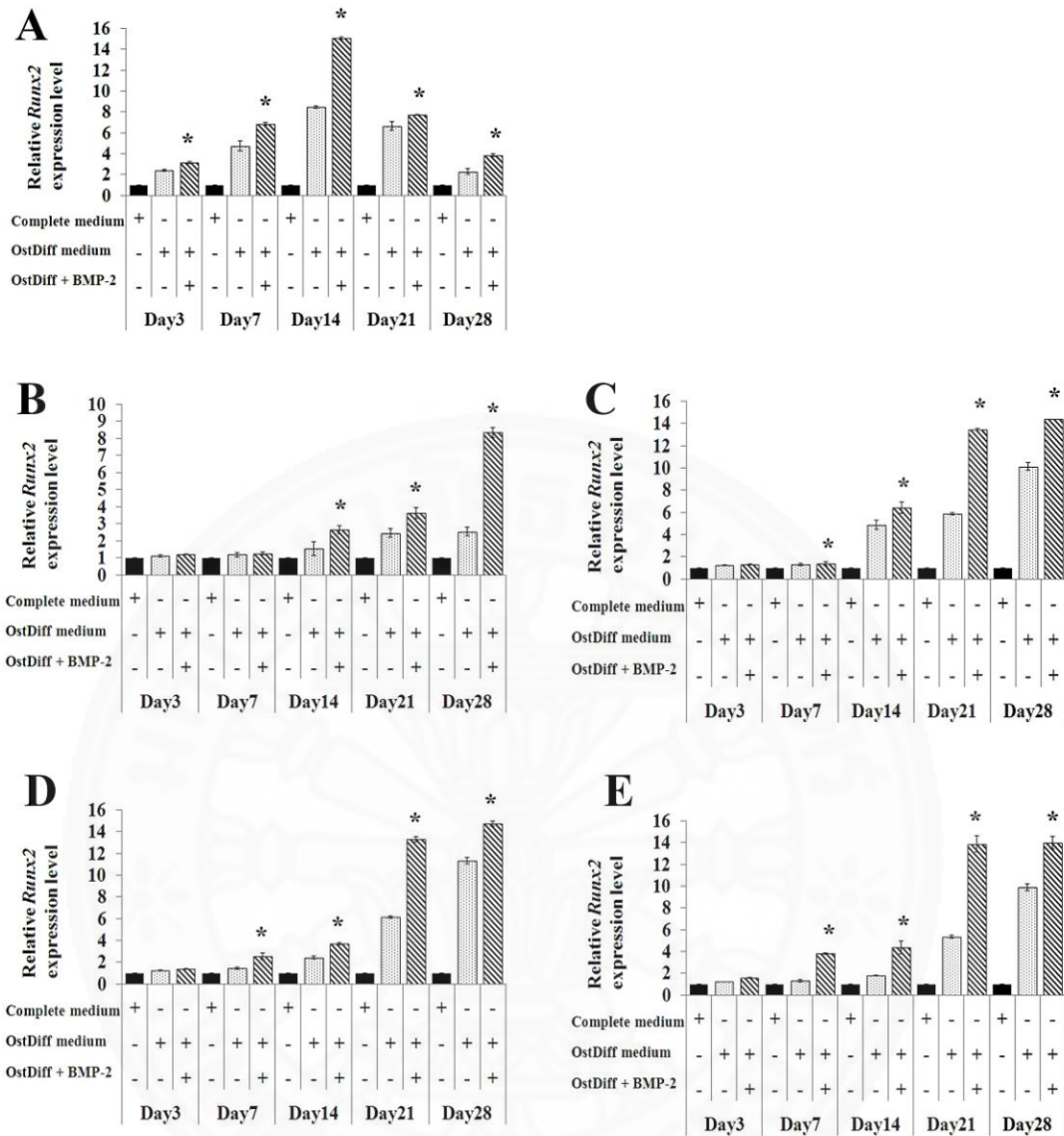
Figure 4.30: The relative *RUNX-2* expression in BMP-2 induced osteogenic differentiation of AM-MSCs (B), CH-MSCs (C), PL-MSCs (D), and UC-MSCs (E) in comparison to BM-MSCs (A). Data are presented as mean ± SEM. * $p<0.05$: significant difference compared to MSCs cultured in osteogenic differentiation medium.
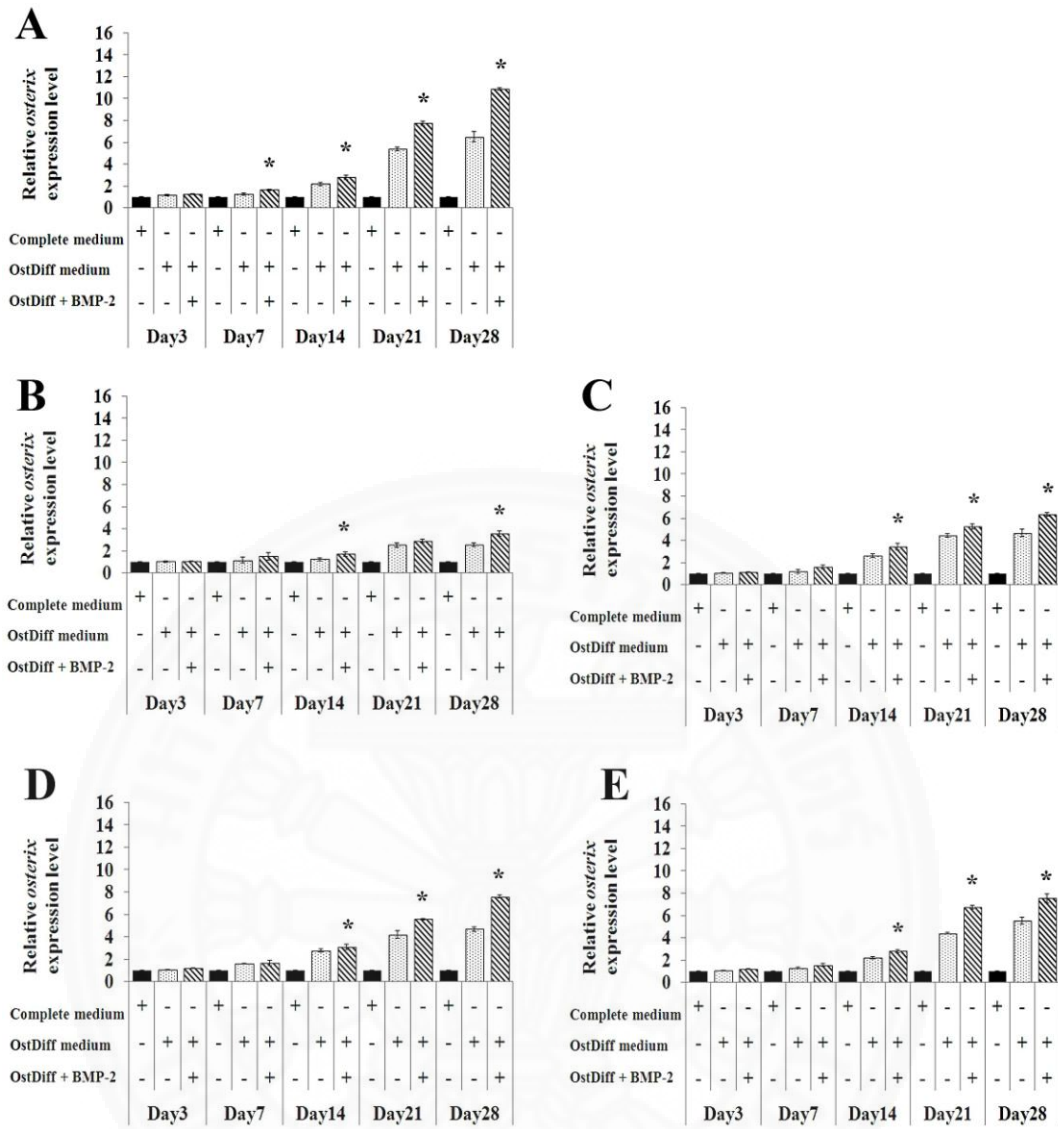
Figure 4.31: The relative *OSX* expression in BMP-2 induced osteogenic differentiation of AM-MSCs (B), CH-MSCs (C), PL-MSCs (D), and UC-MSCs (E) in comparison to BM-MSCs (A). Data are presented as mean ± SEM. * $p<0.05$: significant difference compared to MSCs cultured in osteogenic differentiation medium.
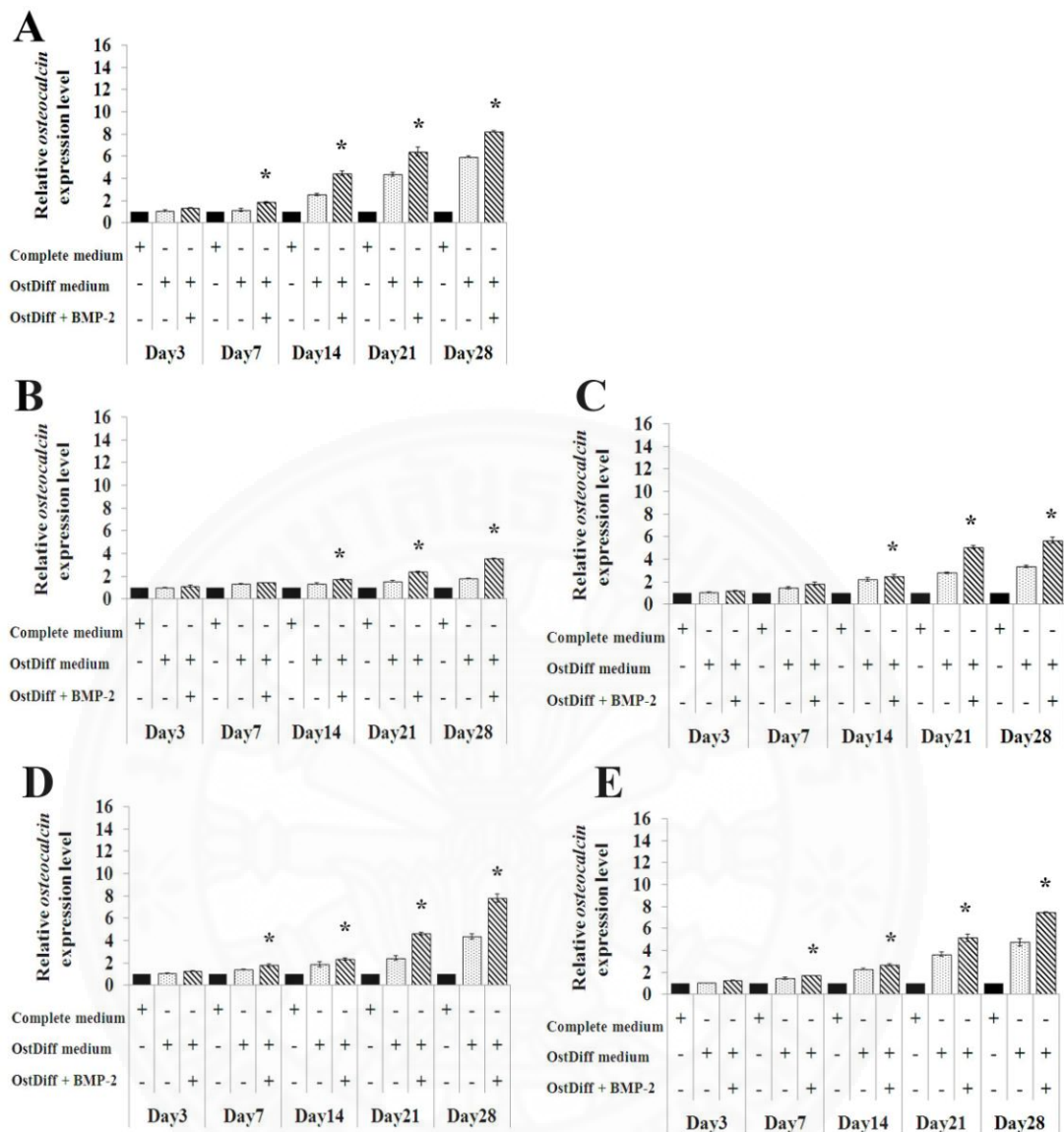
Figure 4.32: The relative *OCN* expression in BMP-2 induced osteogenic differentiation of AM-MSCs (B), CH-MSCs (C), PL-MSCs (D),and UC-MSCs (E) in comparison to BM-MSCs (A). Data are presented as mean ± SEM. * $p<0.05$: significant difference compared to MSCs cultured in osteogenic differentiation medium.

4.10 The expression of miR-31, miR-106a, and miR-148a during osteogenic differentiation

To explore the alteration of miRNAs expression in MSCs during the course of osteogenic differentiation, the expression of miR-31, miR-106a, and miR-148a were quantified at day 3, 7, 14, 21, and 28 using TaqMan MicroRNA Assays and qRT-PCR. The results showed that the expression of miR-31was reduced in a time-dependent manner during the process of osteogenic differentiation of BM-MSCs (Fig. 4.33 A). In addition, the expression of miR-31 in BM-MSCs was significantly decreased after treatment with BMP-2 (Fig. 4.33 A, $p<0.05$). Similar to BM-MSCs, the expression of miR-31 during the process of osteogenic differentiation of AM-MSCs, CH-MSCs, PL-MSCs, and UC-MSCs were also reduced in a time dependent manner (Fig. 4.33 B - E). Interestingly, there was no a dramatically change in the expression of miR-31 in these MSCs during the first week of osteogenic induction when compared to that of BM-MSCs. Nevertheless the expression of miR-31 in these MSCs was intensely decreased after 14 days of osteogenic induction especially in BMP-2 treated MSCs (Fig. 4.33). Although miR-31 expression was down-regulated in AM-MSCs, CH-MSCs, PL-MSCs, and UC-MSCs during osteogenic differentiation in the presence or absence of BMP-2, the expression level still higher than that of BM-MSCs in every time points. Additionally the expressions of miR-106a and miR-148a were found to be robustly down-regulated in BM-MSCs during osteogenic differentiation in the presence or absence of BMP-2 (Fig. 4.34 A, 4.35 A). The expressions of miR-106a and 148a during osteogenic differentiation of AM-MSCs, CH-MSCs, PL-MSCs, and UC-MSCs were also significantly reduced in time dependent manner similar to that of BM-MSCs (Fig.4.34 B - E, 4.35 B - E). However, AM-MSCs, CH-MSCs, PL-MSCs, and UC-MSCs showed less reduction in miR-106a and miR-148a expressions when compared to that of BM-MSCs. It is important to note that AM-MSCs showed the least reduction of miR-106a and 148a expressions. These data indicated that miR-31, miR-106a, and miR-148a were down-regulated during the process of osteogenic differentiation of these MSCs. Fascinatingly, the down-regulated level of these miRNAs were in good agreement with osteogenic differentiation potential of these MSCs.

Table 4.10: The relative miR-31 expression in MSCs derived from bone marrow, amnion, chorion, placenta, and umbilical cord.

MSCs sources	Group	Day (s)				
		3	**7**	**14**	**21**	**28**
BM-MSCs	Complete medium	1.00 ± 0.00	1.00 ± 0.00	1.00 ± 0.00	1.00 ± 0.00	1.00 ± 0.00
	OstDiff	0.78 ± 0.06	0.58 ± 0.05	0.29 ± 0.05	0.20 ± 0.04	0.18 ± 0.03
	OstDiff + BMP-2	0.66 ± 0.02	0.39 ± 0.02	0.26 ± 0.04	0.15 ± 0.04	0.14 ± 0.02
AM-MSCs	Complete medium	1.00 ± 0.00	1.00 ± 0.00	1.00 ± 0.00	1.00 ± 0.00	1.00 ± 0.00
	OstDiff	0.89 ± 0.02	0.83 ± 0.03	0.63 ± 0.04	0.43 ± 0.03	0.39 ± 0.04
	OstDiff + BMP-2	0.85 ± 0.03	0.80 ± 0.02	0.54 ± 0.03	0.36 ± 0.02	0.31 ± 0.03
CH-MSCs	Complete medium	1.00 ± 0.00	1.00 ± 0.00	1.00 ± 0.00	1.00 ± 0.00	1.00 ± 0.00
	OstDiff	0.84 ± 0.04	0.75 ± 0.01	0.46 ± 0.04	0.43 ± 0.03	0.29 ± 0.02
	OstDiff + BMP-2	0.76 ± 0.01	0.72 ± 0.05	0.35 ± 0.03	0.24 ± 0.02	0.22 ± 0.03
PL-MSCs	Complete medium	1.00 ± 0.00	1.00 ± 0.00	1.00 ± 0.00	1.00 ± 0.00	1.00 ± 0.00
	OstDiff	0.85 ± 0.04	0.75 ± 0.01	0.39 ± 0.06	0.28 ± 0.05	0.27 ± 0.02
	OstDiff + BMP-2	0.79 ± 0.03	0.72 ± 0.01	0.33 ± 0.04	0.25 ± 0.06	0.22 ± 0.02
UC-MSCs	Complete medium	1.00 ± 0.00	1.00 ± 0.00	1.00 ± 0.00	1.00 ± 0.00	1.00 ± 0.00
	OstDiff	0.83 ± 0.03	0.75 ± 0.03	0.40 ± 0.01	0.33 ± 0.01	0.29 ± 0.04
	OstDiff + BMP-2	0.80 ± 0.04	0.72 ± 0.01	0.32 ± 0.01	0.24 ± 0.01	0.23 ± 0.03

Values are presented as mean ± SEM.

Table 4.11: The relative miR-106a expression in MSCs derived from bone marrow, amnion, chorion, placenta, and umbilical cord.

MSCs sources	Group	Day (s)				
		3	7	14	21	28
BM-MSCs	Complete medium	1.00 ± 0.00	1.00 ± 0.00	1.00 ± 0.00	1.00 ± 0.00	1.00 ± 0.00
	OstDiff	0.65 ± 0.01	0.65 ± 0.02	0.48 ± 0.05	0.26 ± 0.02	0.22 ± 0.01
	OstDiff + BMP-2	0.59 ± 0.01	0.47 ± 0.02	0.45 ± 0.06	0.23 ± 0.02	0.18 ± 0.03
AM-MSCs	Complete medium	1.00 ± 0.00	1.00 ± 0.00	1.00 ± 0.00	1.00 ± 0.00	1.00 ± 0.00
	OstDiff	0.90 ± 0.01	0.89 ± 0.01	0.73 ± 0.03	0.69 ± 0.02	0.52 ± 0.03
	OstDiff + BMP-2	0.88 ± 0.01	0.79 ± 0.01	0.68 ± 0.01	0.63 ± 0.02	0.41 ± 0.02
CH-MSCs	Complete medium	1.00 ± 0.00	1.00 ± 0.00	1.00 ± 0.00	1.00 ± 0.00	1.00 ± 0.00
	OstDiff	0.88 ± 0.01	0.85 ± 0.01	0.61 ± 0.04	0.53 ± 0.02	0.45 ± 0.02
	OstDiff + BMP-2	0.87 ± 0.01	0.82 ± 0.01	0.58 ± 0.01	0.46 ± 0.02	0.33 ± 0.03
PL-MSCs	Complete medium	1.00 ± 0.00	1.00 ± 0.00	1.00 ± 0.00	1.00 ± 0.00	1.00 ± 0.00
	OstDiff	0.88 ± 0.02	0.85 ± 0.01	0.61 ± 0.00	0.47 ± 0.02	0.41 ± 0.02
	OstDiff + BMP-2	0.87 ± 0.01	0.81 ± 0.02	0.53 ± 0.01	0.40 ± 0.01	0.32 ± 0.01
UC-MSCs	Complete medium	1.00 ± 0.00	1.00 ± 0.00	1.00 ± 0.00	1.00 ± 0.00	1.00 ± 0.00
	OstDiff	0.89 ± 0.01	0.85 ± 0.03	0.62 ± 0.04	0.53 ± 0.01	0.43 ± 0.03
	OstDiff + BMP-2	0.87 ± 0.01	0.82 ± 0.01	0.59 ± 0.04	0.46 ± 0.01	0.34 ± 0.02

Values are presented as mean ± SEM.

Table 4.12: The relative miR-148a expression in MSCs derived from bone marrow, amnion, chorion, placenta, and umbilical cord.

MSCs sources	Group	Day (s)				
		3	**7**	**14**	**21**	**28**
BM-MSCs	Complete medium	1.00 ± 0.00	1.00 ± 0.00	1.00 ± 0.00	1.00 ± 0.00	1.00 ± 0.00
	OstDiff	0.65 ± 0.03	0.60 ± 0.01	0.52 ± 0.03	0.47 ± 0.02	0.43 ± 0.02
	OstDiff + BMP-2	0.60 ± 0.02	0.53 ± 0.03	0.45 ± 0.02	0.36 ± 0.03	0.33 ± 0.01
AM-MSCs	Complete medium	1.00 ± 0.00	1.00 ± 0.00	1.00 ± 0.00	1.00 ± 0.00	1.00 ± 0.00
	OstDiff	0.94 ± 0.03	0.92 ± 0.03	0.86 ± 0.01	0.80 ± 0.01	0.71 ± 0.01
	OstDiff + BMP-2	0.91 ± 0.02	0.90 ± 0.01	0.82 ± 0.01	0.73 ± 0.02	0.65 ± 0.02
CH-MSCs	Complete medium	1.00 ± 0.00	1.00 ± 0.00	1.00 ± 0.00	1.00 ± 0.00	1.00 ± 0.00
	OstDiff	0.91 ± 0.03	0.89 ± 0.02	0.74 ± 0.04	0.69 ± 0.02	0.60 ± 0.01
	OstDiff + BMP-2	0.87 ± 0.01	0.83 ± 0.02	0.72 ± 0.02	0.64 ± 0.02	0.54 ± 0.03
PL-MSCs	Complete medium	1.00 ± 0.00	1.00 ± 0.00	1.00 ± 0.00	1.00 ± 0.00	1.00 ± 0.00
	OstDiff	0.90 ± 0.01	0.88 ± 0.02	0.69 ± 0.02	0.66 ± 0.02	0.59 ± 0.02
	OstDiff + BMP-2	0.86 ± 0.03	0.85 ± 0.01	0.61 ± 0.02	0.56 ± 0.02	0.48 ± 0.02
UC-MSCs	Complete medium	1.00 ± 0.00	1.00 ± 0.00	1.00 ± 0.00	1.00 ± 0.00	1.00 ± 0.00
	OstDiff	0.88 ± 0.04	0.88 ± 0.02	0.66 ± 0.02	0.64 ± 0.01	0.59 ± 0.02
	OstDiff + BMP-2	0.86 ± 0.03	0.85 ± 0.02	0.63 ± 0.03	0.59 ± 0.02	0.51 ± 0.02

Values are presented as mean ± SEM.
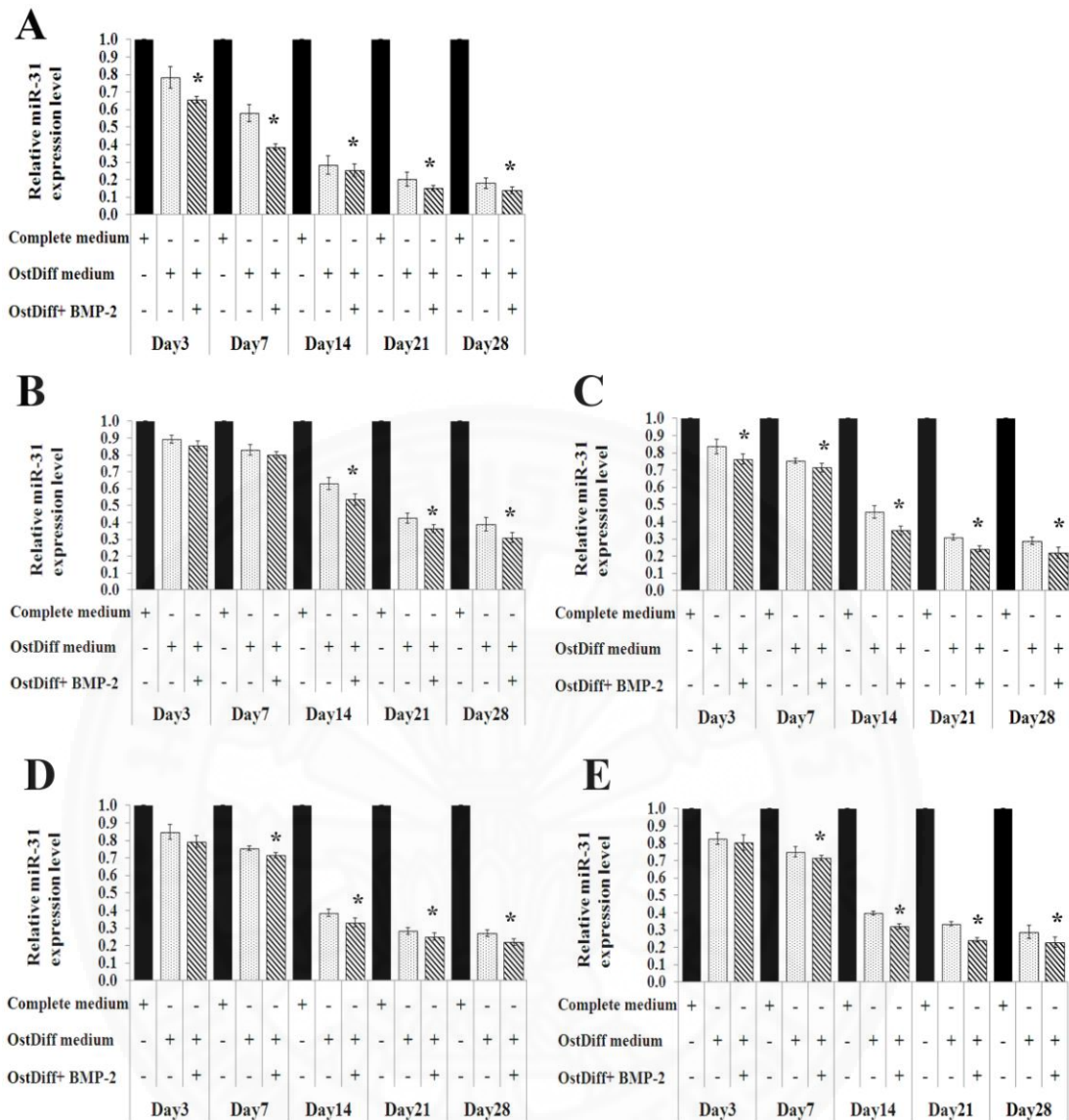
Figure 4.33: The relative miR-31 expression in AM-MSCs (B), CH-MSCs (C), PL-MSCs (D), and UC-MSCs (E) in comparison to that of BM-MSCs (A). Data are presented as mean ± SEM. * $p<0.05$: significant difference compared to MSCs cultured in osteogenic differentiation medium.
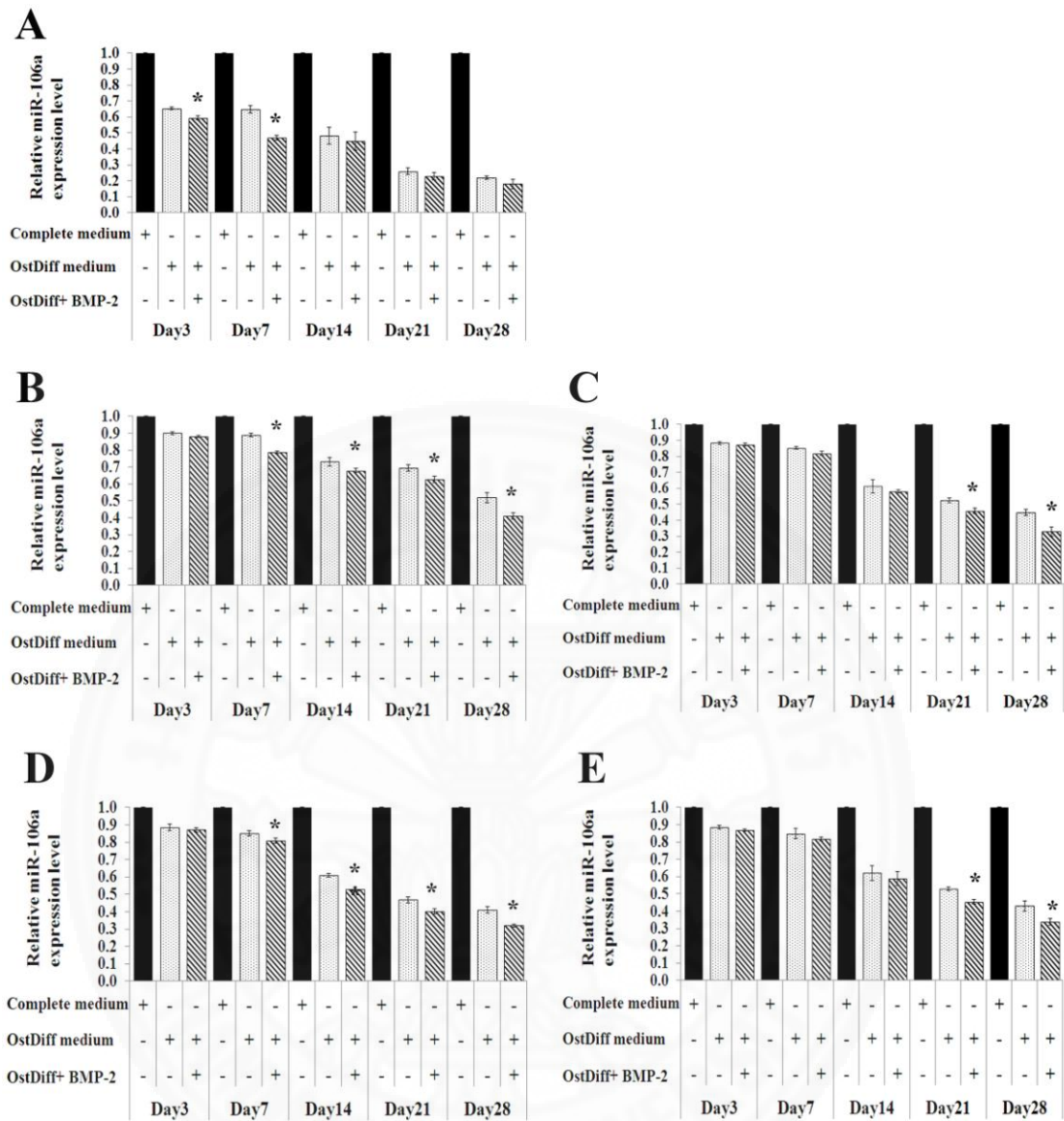
Figure 4.34: The relative miR-106a expression in AM-MSCs (B), CH-MSCs (C), PL-MSCs (D), and UC-MSCs (E) in comparison to that of BM-MSCs (A). Data are presented as mean ± SEM. * $p<0.05$: significant difference compared to MSCs cultured in osteogenic differentiation medium.
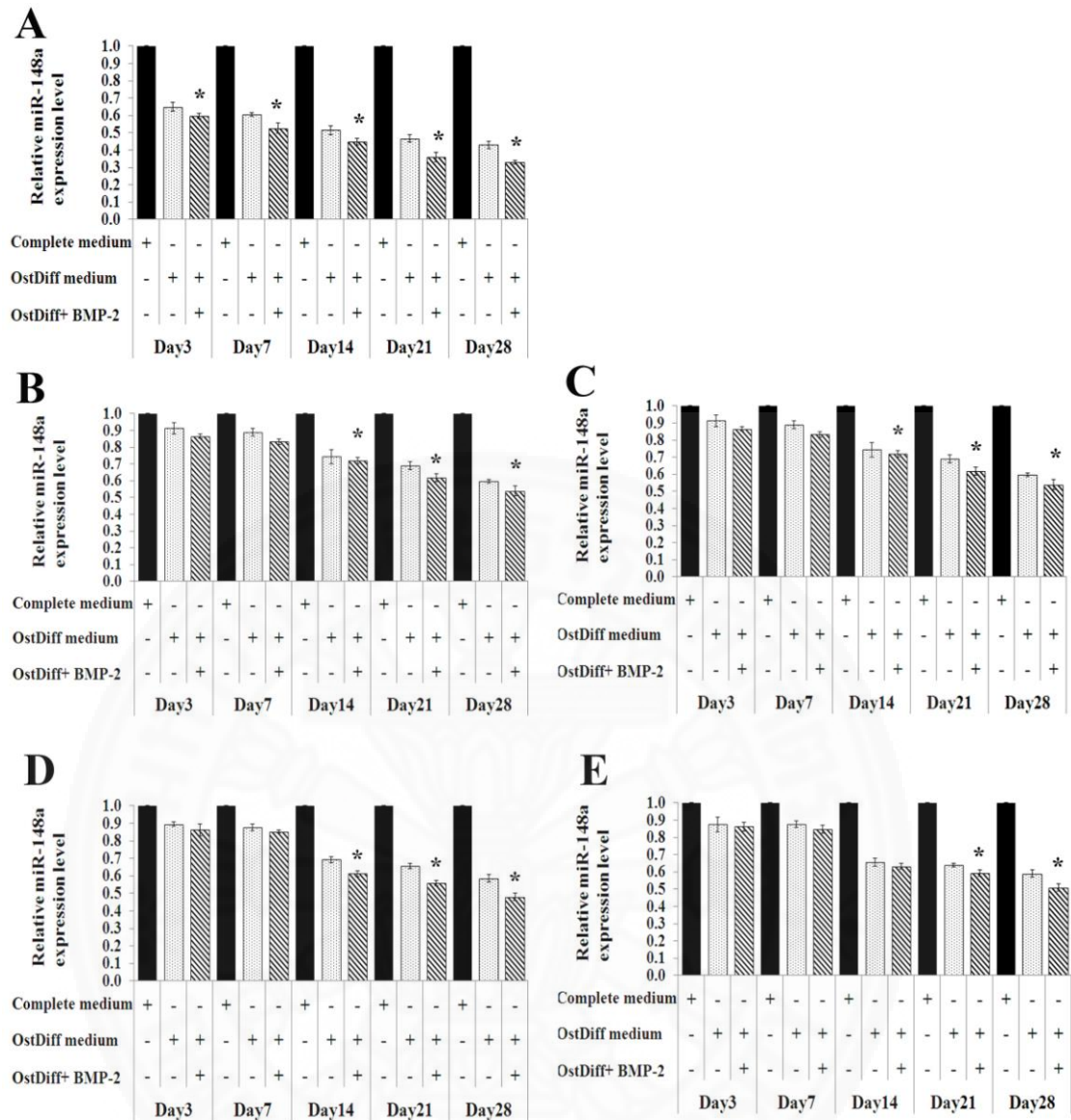
Figure 4.35: The relative miR-148a expression in AM-MSCs (B), CH-MSCs (C), PL-MSCs (D), and UC-MSCs (E) in comparison to that of BM-MSCs (A). Data are presented as mean ± SEM. * $p<0.05$: significant difference compared to MSCs cultured in osteogenic differentiation medium.

4.11 The expression levels of microRNAs after the transient transfection with miRNA inhibitors

To determine the effect of miRNA on osteogenic differentiation capacity of MSCs, BM-MSCs, AM-MSCs, CH-MSCs, PL-MSCs, and UC-MSCs were transfected with anti-miR31, anti-miR106a, and anti-miR148a. After induced differentiation, the expression levels of miR-31, miR-106a and miR-148a were quantified by qRT- PCR at cultured day 3, 7, 14, and 21. The result demonstrated that after transfected with anti-miR31, the expression of miR-31was reduced in a time-dependent manner during the process of osteogenic differentiation of BM-MSCs when compared to those transfected with negative miRNA. Similar to BM-MSCs, the expression of miR-31 during the process of osteogenic differentiation of AM-MSCs, CH-MSCs, PL-MSCs, and UC-MSCs were also reduced in a time dependent manner (Table. 4.13, Fig. 4.36). The expression of miR-31 in these MSCs was intensely decreased after 14 days of osteogenic induction especially in AM-MSCs, CH-MSCs, PL-MSCs, and UC-MSCs (Fig. 4.36). Interestingly, there was a dramatically change in the expression of miR-31 in CH-MSCs and UC-MSCs along the process of osteogenic induction when compared to that of negative control ($p<0.05$) (Fig. 4.36 C and E). Although miR-31 expression was down-regulated in AM-MSCs, CH-MSCs, PL-MSCs, and UC-MSCs during osteogenic differentiation in the presence of anti-miR31, the expression level still higher than that of BM-MSCs in every time points.

Additionally, the expressions of miR-106a and miR-148a were found to be robustly down-regulated in BM-MSCs during osteogenic differentiation in the presence of anti-miR106a and miR-148a (Fig. 4.36 A). The expressions of miR-106a and 148a during osteogenic differentiation of AM-MSCs, CH-MSCs, PL-MSCs, and UC-MSCs were also significantly reduced in time dependent manner similar to that of BM-MSCs (Fig. 4.36). In addition, there was a dramatically change in the expression of miR-106a in AM-MSCs and miR-148a in BM-MSCs and UC-MSCs along the process of osteogenic induction when compared to that of negative control ($p<0.05$) (Fig. 4.36 B, A, and D, respectively). However, AM-MSCs, CH-MSCs, PL-MSCs, and UC-MSCs showed less reduction in miR-106a and miR-148a expressions when compared to that of BM-MSCs. Although miRNAs expression levels decreased over time in 3 anti-miRNAs transfection groups, the miRNA

expression level in AM-MSCs, CH-MSCs, PL-MSCs, and UC-MSCs were significantly less than that of BM-MSCs at every time point examined (Table 4.14, Fig. 4.37).

Table 4.13: The relative expressions of miRNAs - after the transient transfection with anti-miRNAs.

miRNA expression	Day (s)	MSCs sources				
		BM-MSCs	AM-MSCs	CH-MSCs	PL-MSCs	UC-MSCs
miR-31	3	0.75 ± 0.01	0.87 ± 0.01	0.75 ± 0.01	0.80 ± 0.01	0.74 ± 0.02
	7	0.63 ± 0.02	0.78 ± 0.03	0.68 ± 0.01	0.72 ± 0.03	0.65 ± 0.01
	14	0.25 ± 0.02	0.44 ± 0.05	0.33 ± 0.04	0.34 ± 0.03	0.31 ± 0.03
	21	0.19 ± 0.04	0.36 ± 0.04	0.26 ± 0.05	0.21 ± 0.04	0.23 ± 0.04
miR-106a	3	0.51 ± 0.02	0.80 ± 0.01	0.85 ± 0.01	0.87 ± 0.05	0.85 ± 0.01
	7	0.49 ± 0.04	0.73 ± 0.03	0.79 ± 0.02	0.79 ± 0.01	0.79 ± 0.04
	14	0.46 ± 0.05	0.65 ± 0.04	0.57 ± 0.03	0.54 ± 0.03	0.56 ± 0.03
	21	0.23 ± 0.03	0.59 ± 0.03	0.46 ± 0.02	0.39 ± 0.02	0.35 ± 0.03
miR-148a	3	0.50 ± 0.05	0.92 ± 0.01	0.83 ± 0.01	0.80 ± 0.02	0.83 ± 0.06
	7	0.32 ± 0.07	0.82 ± 0.01	0.77 ± 0.04	0.71 ± 0.03	0.77 ± 0.03
	14	0.26 ± 0.02	0.75 ± 0.02	0.69 ± 0.04	0.64 ± 0.05	0.65 ± 0.02
	21	0.14 ± 0.04	0.68 ± 0.03	0.62 ± 0.04	0.58 ± 0.04	0.53 ± 0.02

Values are presented as mean ± SEM
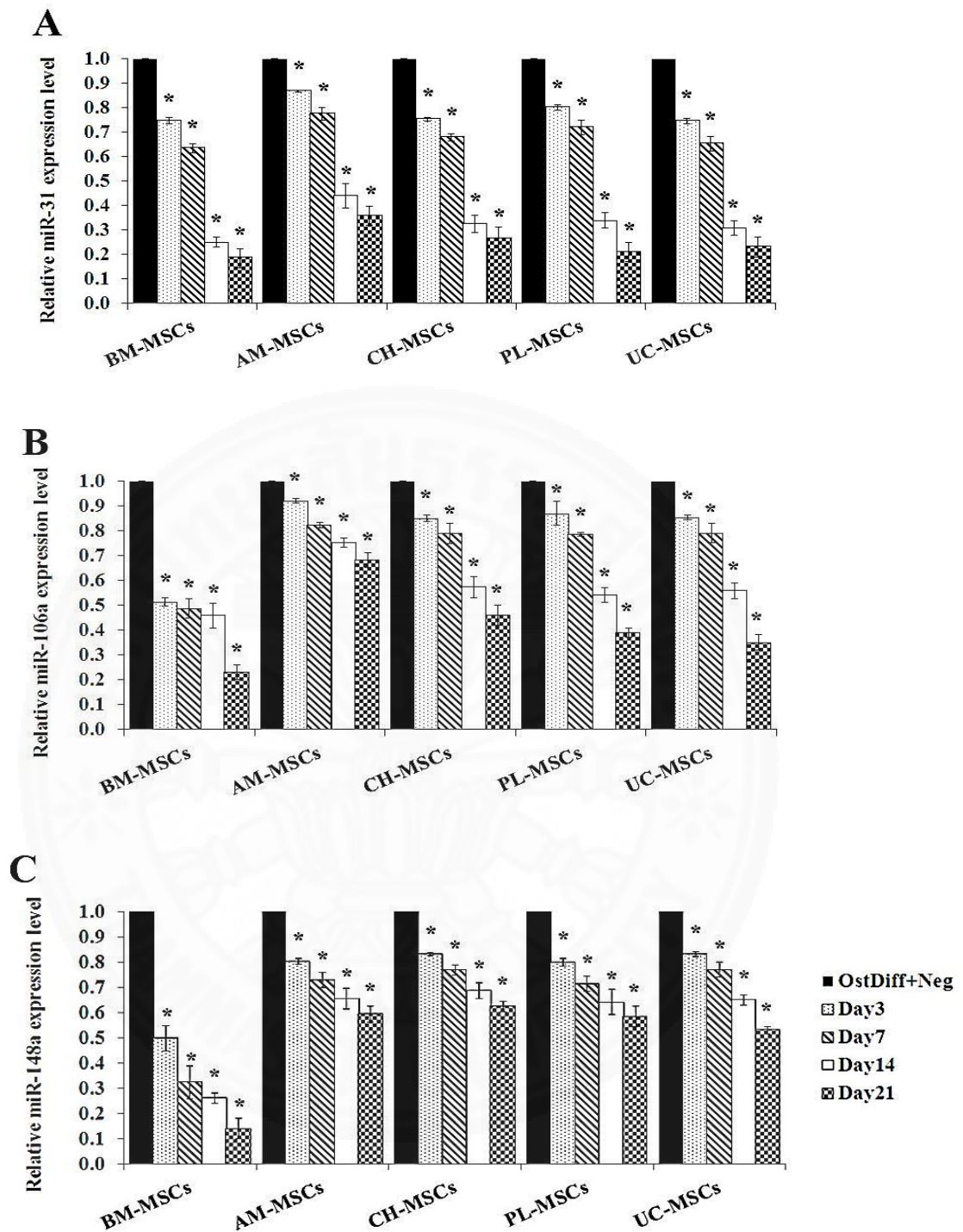
Figure 4.36: Mean value of relative expressions of miR-31 (A), miR-106a (B) and miR-148a (C) during osteogenic differentiation of BM-MSCs, AM-MSCs, CH-MSCs, PL-MSCs, and UC-MSCs after the transient transfection with anti-miR31, anti-miR106a, and anti-miR148a respectively. Data are presented as mean ± SEM. *$p<0.05$: significant difference compared to MSCs cultured in osteogenic differentiation medium + 10nM negative anti-miR in every time point.

Table 4.14: The relative expressions of miR-31, miR-106a, and miR-148a in MSCs derived from bone marrow, amnion, chorion, placenta, and umbilical cord after the transfection with3 anti-miRNAs.

miRNA expression	Day (s)	MSCs sources				
		BM-MSCs	AM-MSCs	CH-MSCs	PL-MSCs	UC-MSCs
miR-31	3	0.81 ± 0.02	0.90 ± 0.05	0.81 ± 0.02	0.84 ± 0.02	0.76 ± 0.01
	7	0.67 ± 0.04	0.82 ± 0.04	0.71 ± 0.03	0.76 ± 0.04	0.68 ± 0.05
	14	0.33 ± 0.02	0.53 ± 0.04	0.41 ± 0.02	0.47 ± 0.04	0.41 ± 0.04
	21	0.25 ± 0.01	0.42 ± 0.02	0.34 ± 0.04	0.36 ± 0.04	0.32 ± 0.03
miR-106a	3	0.55 ± 0.02	0.84 ± 0.03	0.87 ± 0.06	0.92 ± 0.04	0.86 ± 0.03
	7	0.51 ± 0.08	0.79 ± 0.03	0.82 ± 0.04	0.89 ± 0.06	0.80 ± 0.02
	14	0.49 ± 0.07	0.68 ± 0.05	0.64 ± 0.04	0.61 ± 0.03	0.57 ± 0.02
	21	0.31 ± 0.03	0.61 ± 0.03	0.52 ± 0.03	0.42 ± 0.03	0.38 ± 0.02
miR-148a	3	0.51 ± 0.03	0.94 ± 0.02	0.85 ± 0.04	0.82 ± 0.03	0.84 ± 0.05
	7	0.34 ± 0.02	0.89 ± 0.04	0.79 ± 0.05	0.75 ± 0.03	0.78 ± 0.02
	14	0.28 ± 0.04	0.78 ± 0.02	0.73 ± 0.04	0.71 ± 0.02	0.67 ± 0.03
	21	0.18 ± 0.02	0.68 ± 0.04	0.69 ± 0.02	0.62 ± 0.05	0.55 ± 0.04

Values are presented as mean ± SEM
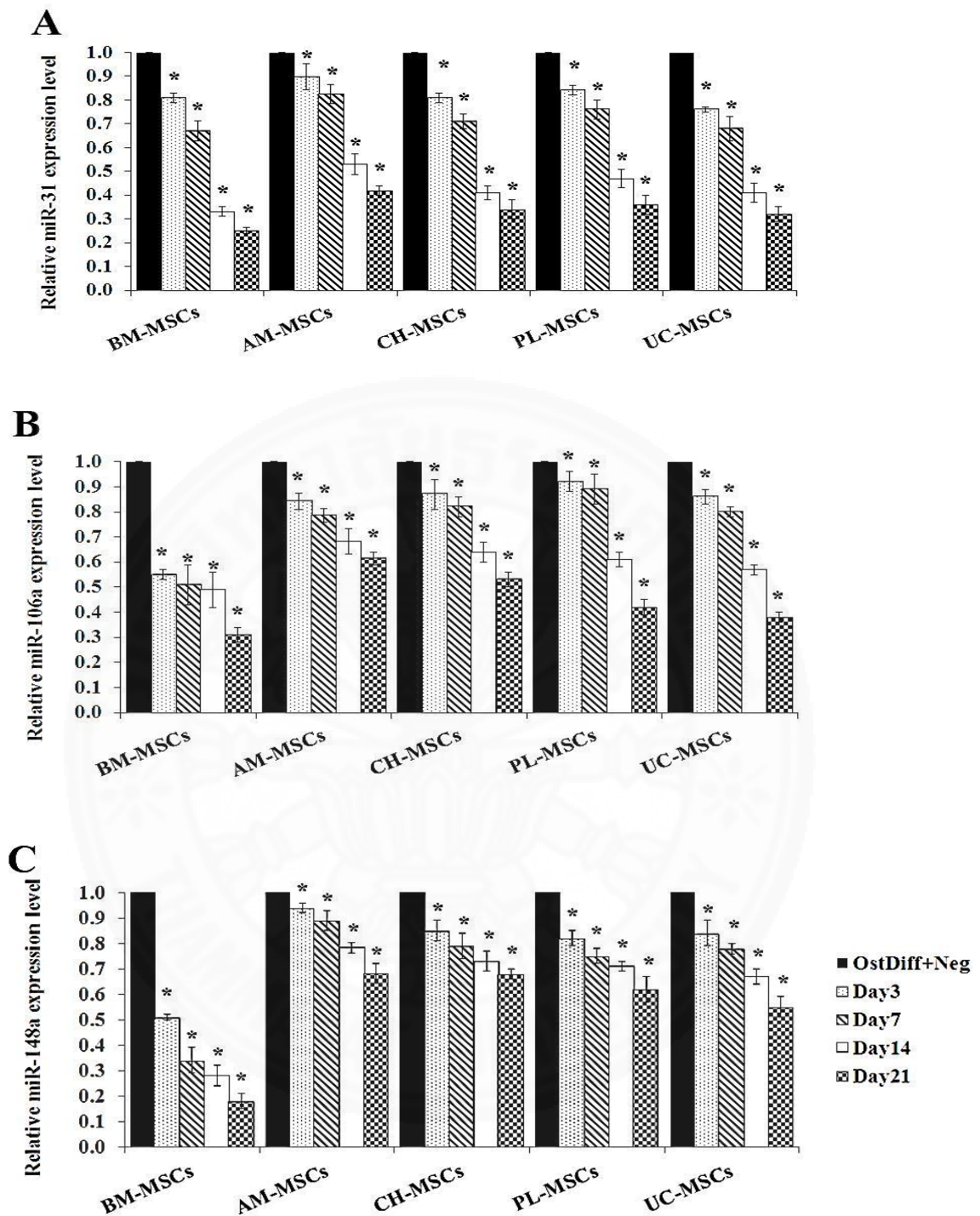
Figure 4.37 Mean value of relative expressions of miR-31 (A), miR-106a (B), and miR-148a (C) during osteogenic differentiation of BM-MSCs, AM-MSCs, CH-MSCs, PL-MSCs, and UC-MSCs after the transient transfection with 3 anti-miRNAs. Data are presented as mean ± SEM. *$p<0.05$: significant difference compared to

MSCs cultured in osteogenic differentiation medium + 10nM negative anti-miR at the same time point.

4.12 The expression of alkaline phosphatase in MSCs after treated with miRNA inhibitors

To investigate the role of miR-31, miR-106a, and miR-148a in osteogenic differentiation of AM-MSCs, CH-MSCs, PL-MSCs, and UC-MSCs in comparison to that of BM-MSCs, the inhibitors of miR-31, miR-106a and miR-148a were employed to alter the expression of miR-31, miR-106a, and miR-148a. The expressions of ALP were examined in MSCs after transfection for 3, 7, 14 and 21 days (Fig. 4.38 - 4.47). The results revealed that the inhibitions of each miRNA, miR-31, miR-106a, miR-148a, and the inhibition using combination of 3 anti-miRNAs enhanced the expression of ALP of BM-MSCs, AM-MSCs, CH-MSCs, PL-MSCs, and UC-MSCs compared to MSCs cultured in osteogenic differentiation medium and MSCs cultured in osteogenic differentiation medium with negative control miRNA (Fig. 4.38 - 4.47). Nevertheless, combination of the 3 anti-miRNAs did not reveal the dramatically change in ALP expression in all MSCs (Fig. 4.38 - 4.47 Ga - Gd). In addition, ALP expressions in AM-MSCs, CH-MSCs, PL-MSCs, and UC-MSCs after treated with miRNA inhibitors were lower than that of BM-MSCs in every time points.
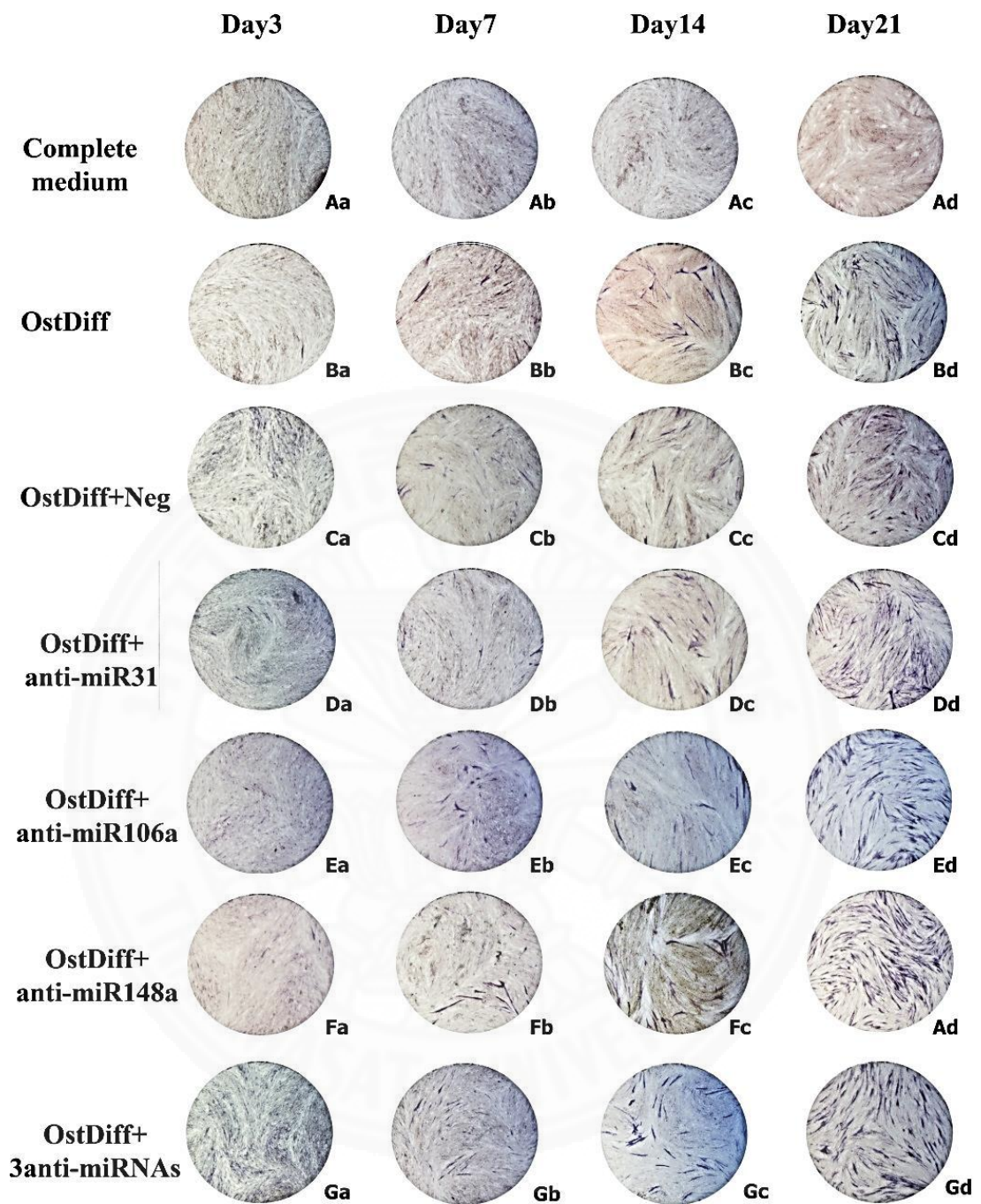
Figure 4.38: The expression of alkaline phosphatase in BM-MSCs after treated with miRNA inhibitors for 3, 7, 14, and 21 days. BM-MSCs cultured in complete medium and osteogenic differentiation medium served as controls.
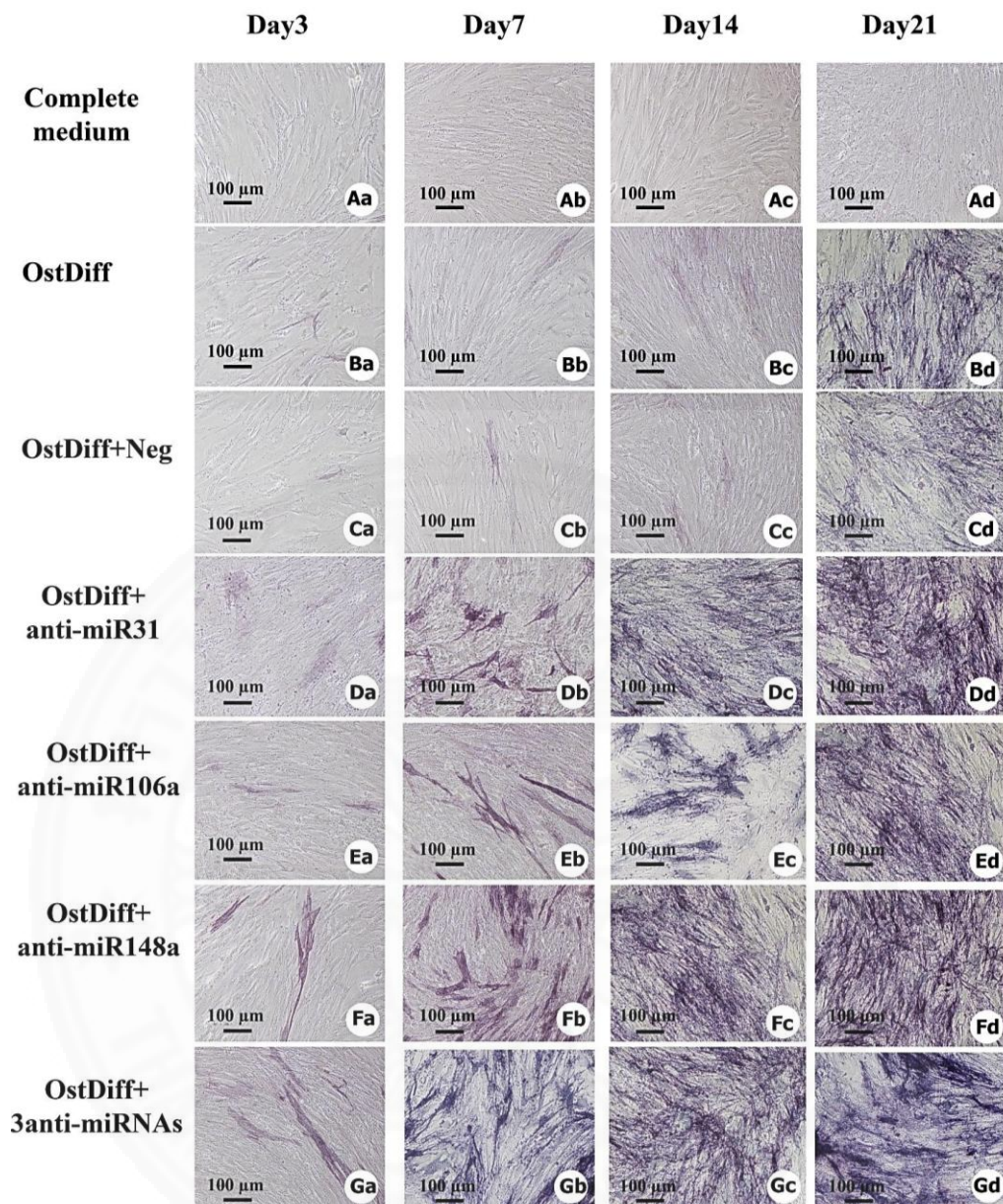
Figure 4.39: Representative photomicrographs of ALP staining in BM-MSCs after treated with anti-miRNAs for 3, 7, 14, and 21 days. Osteogenic differentiation was evidenced by the formation of alkaline phosphatase-positive aggregate in cytoplasm.
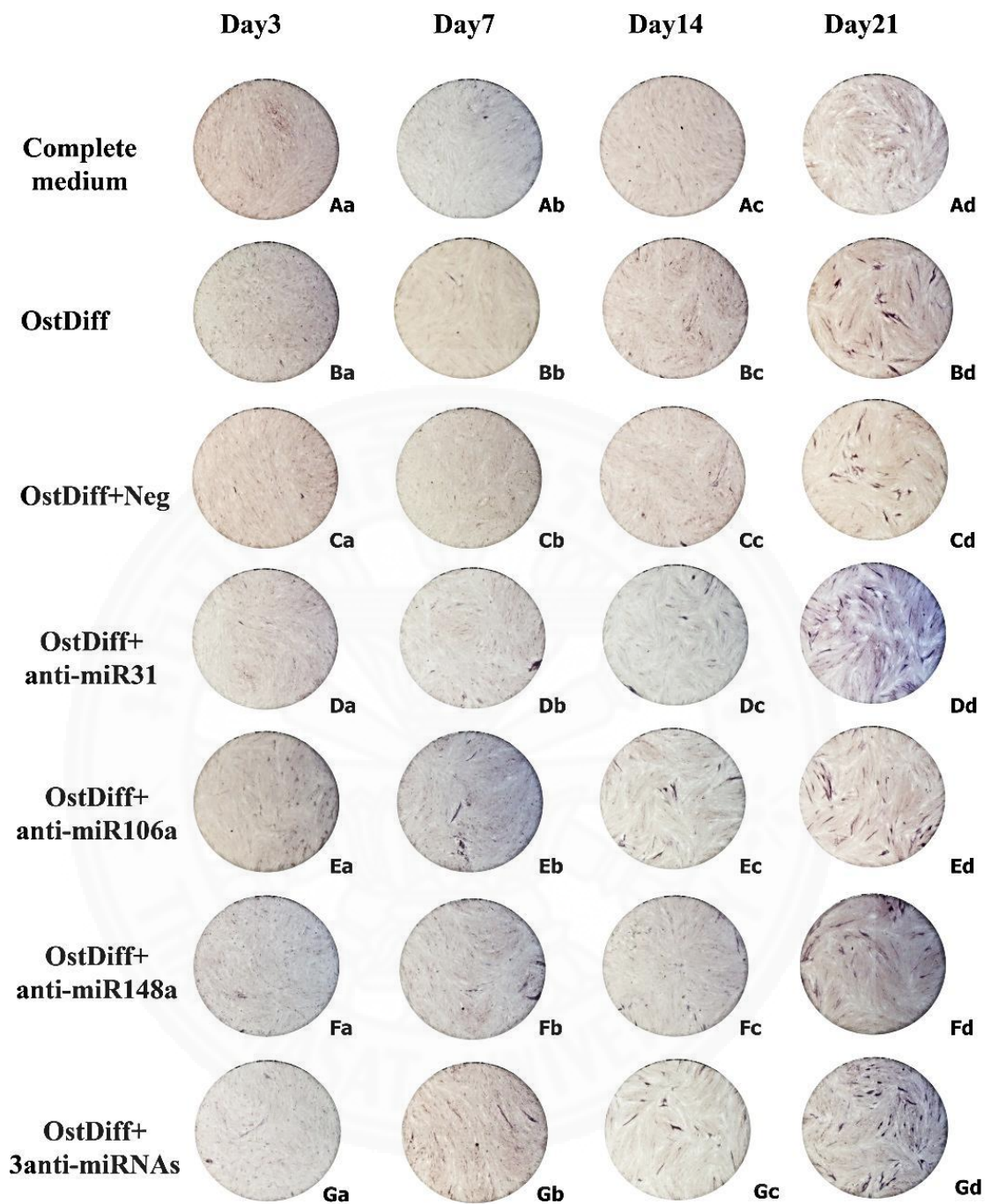
Figure 4.40: The expression of alkaline phosphatase in AM-MSCs after treated with miRNA inhibitors for 3, 7, 14, and 21 days. AM-MSCs cultured in complete medium and osteogenic differentiation medium served as controls.
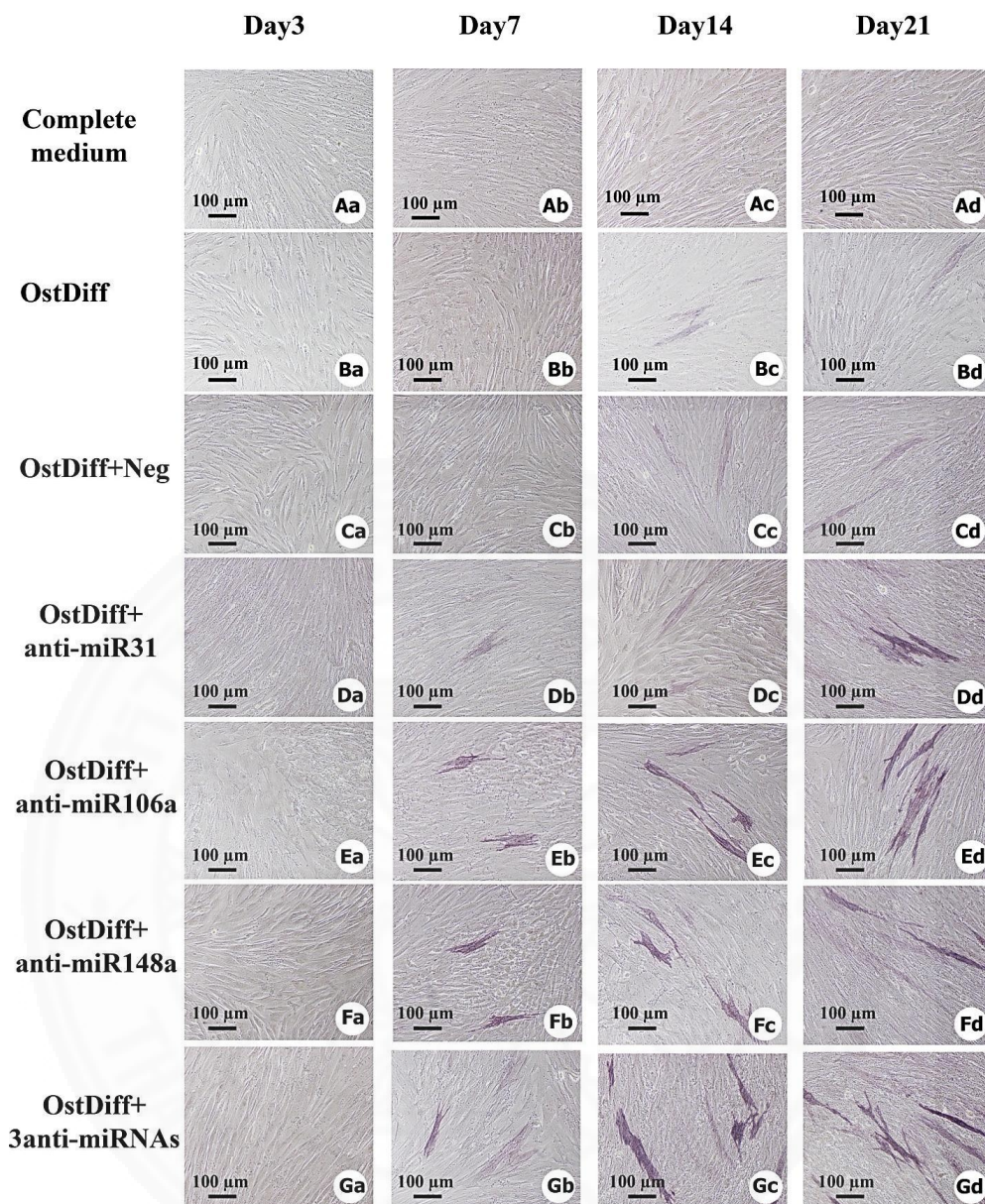
Figure 4.41: Representative photomicrographs of ALP staining in AM-MSCs after treated with anti-miRNAs for 3, 7, 14, and 21 days. Osteogenic differentiation was evidenced by the formation of alkaline phosphatase-positive aggregate in cytoplasm.

	Day3	Day7	Day14	Day21
Complete medium	Aa	Ab	Ac	Ad
OstDiff	Ba	Bb	Bc	Bd
OstDiff+Neg	Ca	Cb	Cc	Cd
OstDiff+ anti-miR31	Da	Db	Dc	Dd
OstDiff+ anti-miR106a	Ea	Eb	Ec	Ed
OstDiff+ anti-miR148a	Fa	Fb	Fc	Fd
OstDiff+ 3anti-miRNAs	Ga	Gb	Gc	Gd
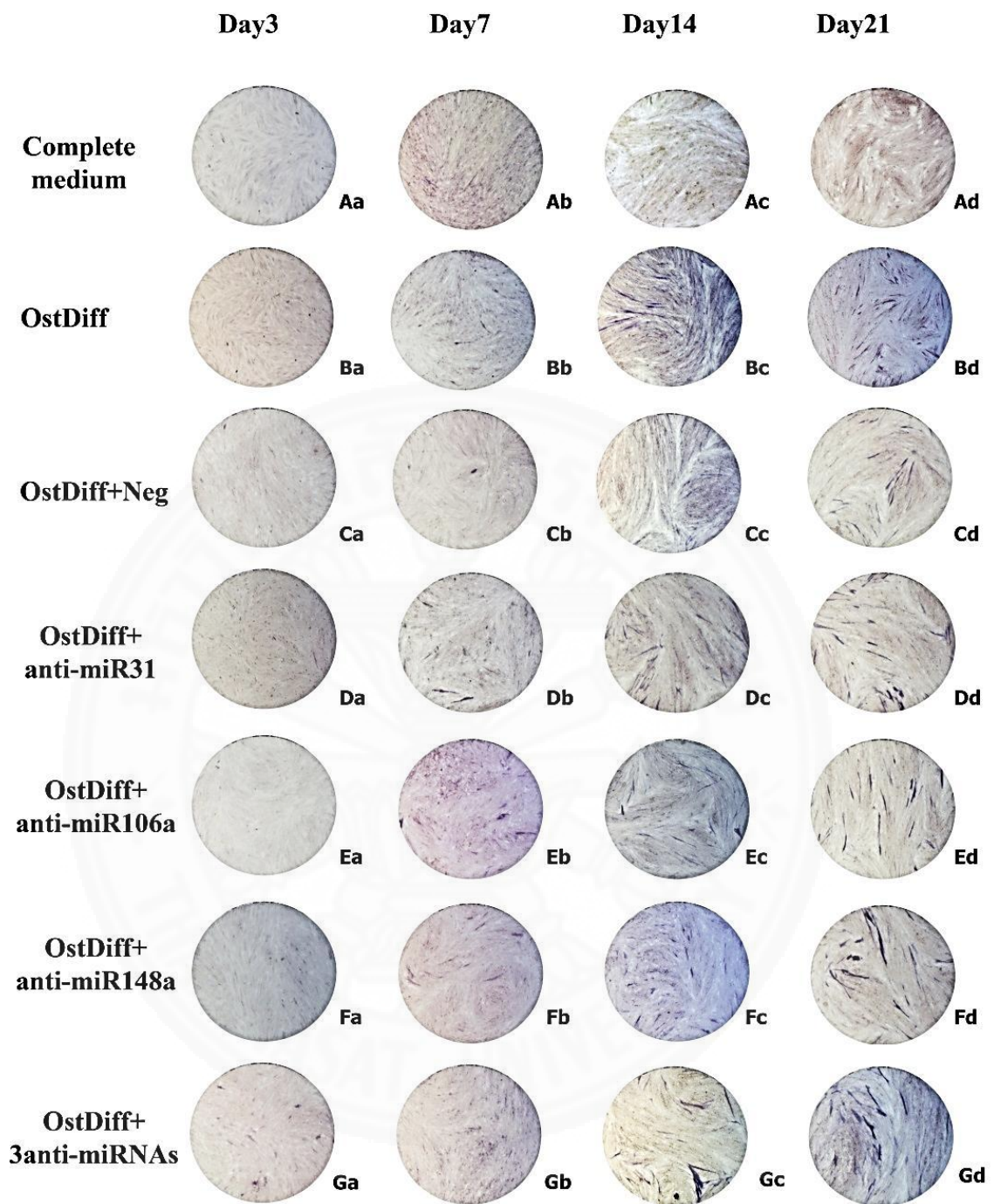
Figure 4.42: The expression of alkaline phosphatase in CH-MSCs after treated with miRNA inhibitors for 3, 7, 14, and 21 days. CHMSCs cultured in complete medium and osteogenic differentiation medium served as controls.

	Day3	Day7	Day14	Day21

Complete medium

OstDiff

OstDiff+Neg

OstDiff+ anti-miR31

OstDiff+ anti-miR106a

OstDiff+ anti-miR148a

OstDiff+ 3anti-miRNAs
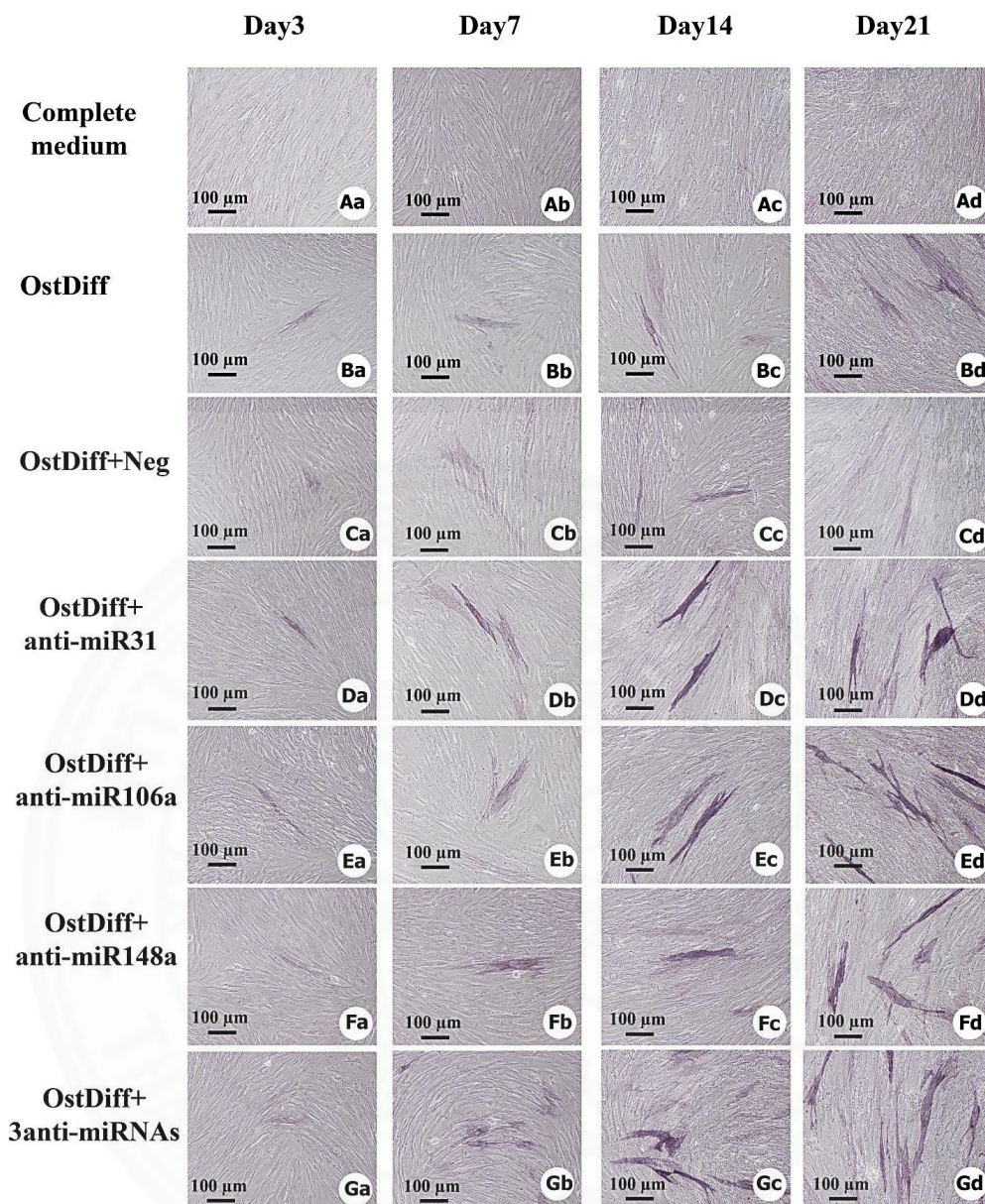
Figure 4.43: Representative photomicrographs of ALP staining in CH-MSCs after treated with anti-miRNAs for 3, 7, 14, and 21 days. Osteogenic differentiation was evidenced by the formation of alkaline phosphatase-positive aggregate in cytoplasm.

	Day3	Day7	Day14	Day21

Complete medium — Aa, Ab, Ac, Ad

OstDiff — Ba, Bb, Bc, Bd

OstDiff+Neg — Ca, Cb, Cc, Cd

OstDiff+ anti-miR31 — Da, Db, Dc, Dd

OstDiff+ anti-miR106a — Ea, Eb, Ec, Ed

OstDiff+ anti-miR148a — Fa, Fb, Fc, Fd

OstDiff+ 3anti-miRNAs — Ga, Gb, Gc, Gd
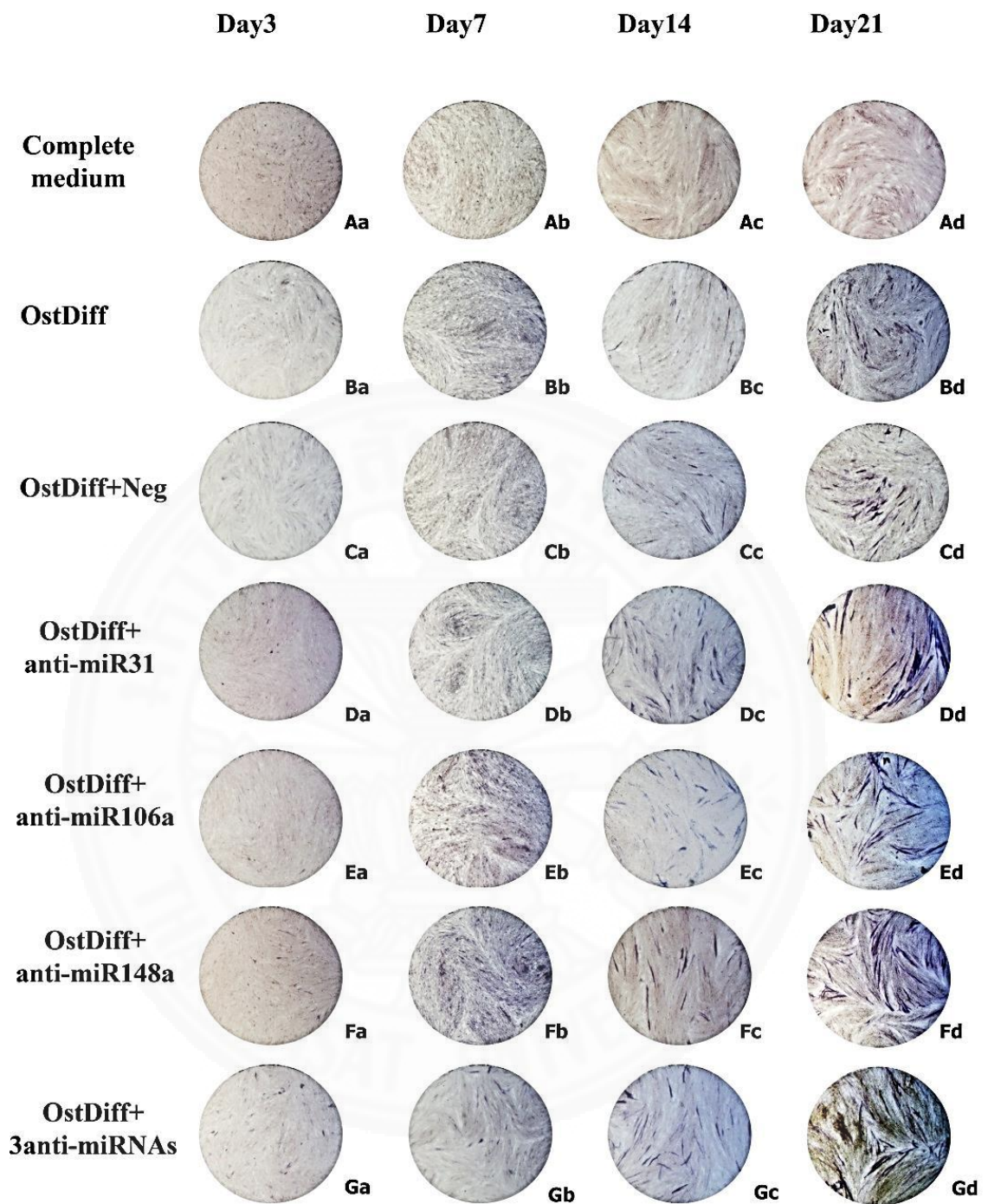
Figure 4.44: The expression of alkaline phosphatase in PL-MSCs after treated with miRNA inhibitors for 3, 7, 14, and 21 days. PL-MSCs cultured in complete medium and osteogenic differentiation medium served as controls.
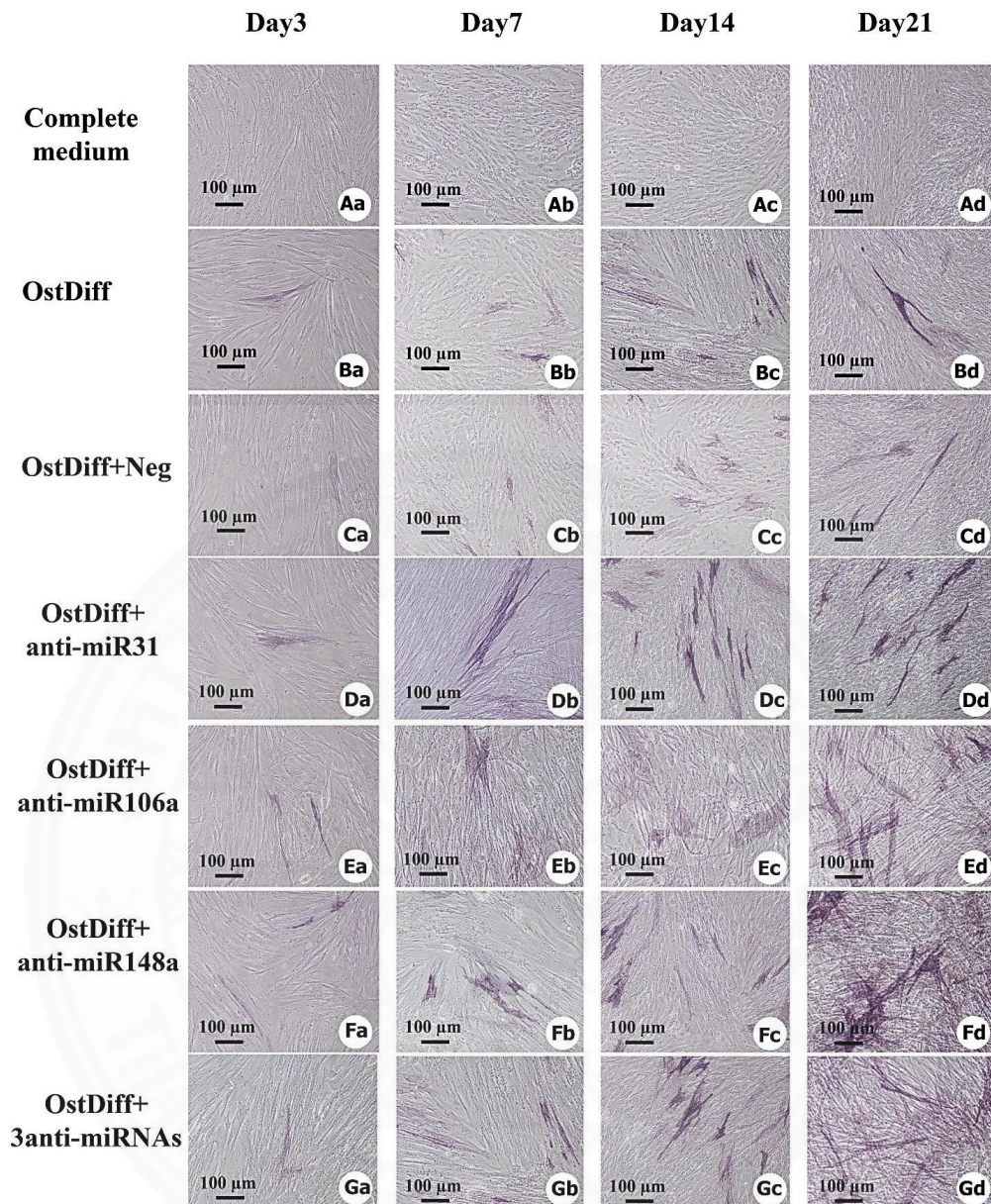
Figure 4.45: Representative photomicrographs of ALP staining in PL-MSCs after treated with anti-miRNAs for 3, 7, 14, and 21 days. Osteogenic differentiation was evidenced by the formation of alkaline phosphatase-positive aggregate in cytoplasm.
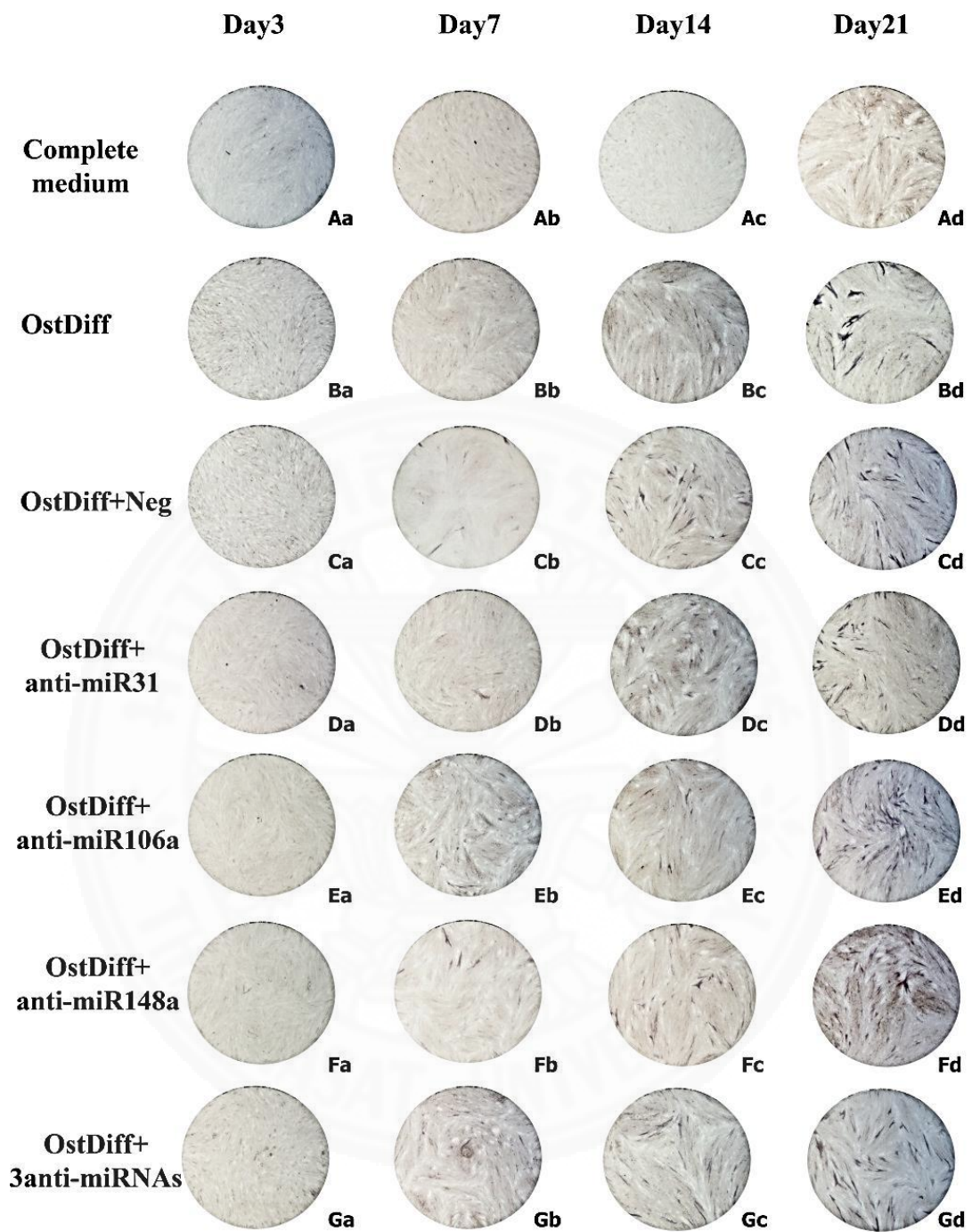
Figure 4.46: The expression of alkaline phosphatase in UC-MSCs after treated with miRNA inhibitors for 3, 7, 14, and 21 days. UC-MSCs cultured in complete medium and osteogenic differentiation medium served as controls.
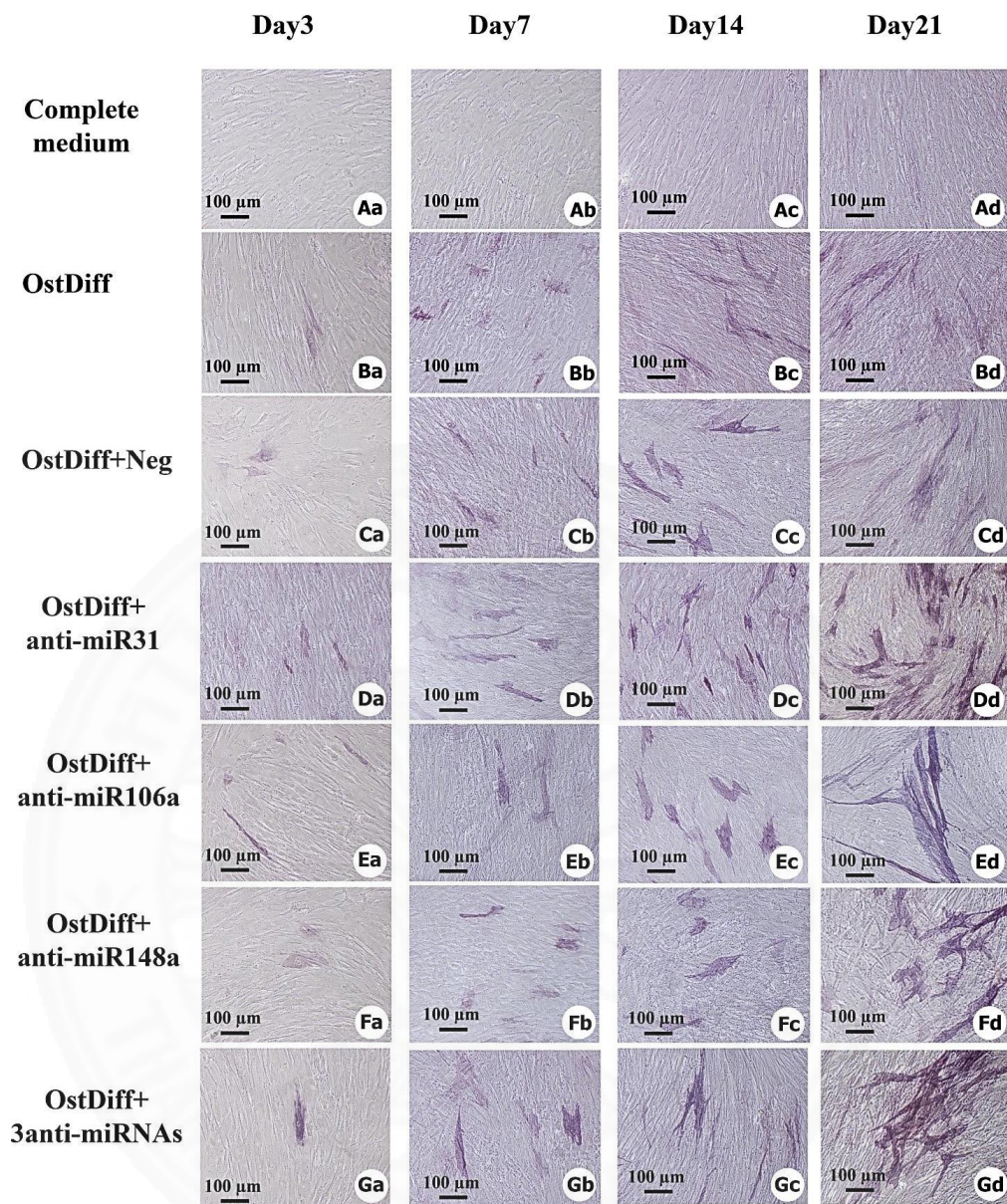
Figure 4.47: Representative photomicrographs of ALP staining in UC-MSCs after treated with anti-miRNAs for 3, 7, 14, and 21 days. Osteogenic differentiation was evidenced by the formation of alkaline phosphatase-positive aggregate in cytoplasm.

4.13 The alkaline phosphatase activity of AM-MSCs, CH-MSCs, PL-MSCs, and UC-MSCs in comparison to BM-MSCs after the transient transfection with miRNA inhibitors

The activities of intracellular ALP in BM-MSCs, AM-MSCs, CH-MSCs, PL-MSCs, and UC-MSCs transfected with anti-miR31, anti-miR106a, anti-miR148a, and the combination of these anti-miRNAs were also quantitative assessed using colorimetric enzymatic assay at day 3, 7, 14, and 21. The results demonstrated that the BM-MSCs cultured in osteogenic differentiation medium with 10nM anti-miR148a showed a clear superiority compared to the others (Table. 14.5, Fig. 4.48).

As early as 7 days after transfection with anti-miR31, anti-miR106a, and anti-miR148a, or the combination of 3 anti-miRNAs, BM-MSCs had about a fold increase in alkaline phosphatase activity. Interestingly, the activity of ALP in the anti-miRNA treated groups significantly increased with time. At day 14 and 21, alkaline phosphatase activities in anti-miRNA transfected groups were significantly increased up to 2 fold, compared with MSCs cultured in osteogenic differentiation medium without anti-miRNA and osteogenic differentiation medium added with negative control of anti-miRNA ($p<0.05$). In contrast, CH-MSCs, PL-MSCs, and UC-MSCs at day 14, and 21 after transfection with anti-miR31, anti-miR106a, anti-miR148a, or the combination of 3 anti-miRNAs had only a fold increase in alkaline phosphatase activity ($p<0.05$). Remarkably, the transfection with anti-miR31, anti-miR106a, anti-miR148a, or the combination of 3 anti-miRNAs induced less than a fold increase in alkaline phosphatase activity in AM-MSCs compared with untreated osteogenic differentiation culture ($p<0.05$). Similar to ALP staining, although ALP activity increased over time in anti-miRNAs transfected groups, the ALP activity in AM-MSCs, CH-MSCs, PL-MSCs, and UC-MSCs were significantly less than that of BM-MSCs at every time point examined.

Table 4.15: ALP activity in MSCs after transient transfection with miRNA inhibitors.

MSCs sources	Group	Day (s)			
		3	**7**	**14**	**21**
BM-MSCs	Complete medium	0.65 ± 0.19	1.09 ± 0.08	1.85 ± 0.05	2.79 ± 0.03
	OstDiff	1.20 ± 0.14	6.82 ± 0.24	8.20 ± 0.05	18.32 ± 0.05
	OstDiff + Neg	1.26 ± 0.08	6.75 ± 0.10	8.24 ± 0.05	18.29 ± 0.02
	OstDiff + anti-miR31	4.49 ± 0.15	7.31 ± 0.05	15.34 ± 0.03	36.79 ± 0.05
	OstDiff + anti-miR106a	4.13 ± 0.01	7.15 ± 0.01	15.25 ± 0.03	35.69 ± 0.03
	OstDiff + anti-miR148a	4.89 ± 0.08	9.72 ± 0.28	18.57 ± 0.02	38.67 ± 0.03
	OstDiff + 3 anti-miR	5.02 ± 0.04	9.65 ± 0.04	18.76 ± 0.02	37.97 ± 0.03
AM-MSCs	Complete medium	0.70 ± 0.18	1.43 ± 0.10	3.03 ± 0.05	3.34 ± 0.03
	OstDiff	1.05 ± 0.04	2.14 ± 0.03	3.63 ± 0.05	5.43 ± 0.04
	OstDiff + Neg	1.03 ± 0.01	2.10 ± 0.06	3.64 ± 0.03	5.46 ± 0.04
	OstDiff + anti-miR31	2.29 ± 0.16	3.23 ± 0.09	3.97 ± 0.06	6.17 ± 0.04
	OstDiff + anti-miR106a	3.11 ± 0.03	3.89 ± 0.04	4.58 ± 0.05	6.44 ± 0.02
	OstDiff + anti-miR148a	2.36 ± 0.14	3.32 ± 0.06	3.87 ± 0.02	6.10 ± 0.03
	OstDiff + 3 anti-miR	4.57 ± 0.03	4.98 ± 0.03	5.37 ± 0.05	8.58 ± 0.02
CH-MSCs	Complete medium	0.66 ± 0.18	1.65 ± 0.05	3.64 ± 0.07	5.25 ± 0.04
	OstDiff	1.10 ± 0.04	3.26 ± 0.18	4.47 ± 0.06	11.59 ± 0.05
	OstDiff + Neg	1.10 ± 0.04	3.32 ± 0.10	4.51 ± 0.03	11.48 ± 0.05
	OstDiff + anti-miR31	4.12 ± 0.05	5.25 ± 0.14	15.57 ± 0.05	17.66 ± 0.03
	OstDiff + anti-miR106a	3.41 ± 0.17	4.27 ± 0.09	12.77 ± 0.02	15.46 ± 0.03
	OstDiff + anti-miR148a	3.66 ± 0.06	4.33 ± 0.06	13.66 ± 0.06	16.46 ± 0.02
PL-MSCs	Complete medium	0.64 ± 0.12	1.64 ± 0.02	3.49 ± 0.04	4.33 ± 0.04
	OstDiff	1.10 ± 0.05	2.45 ± 0.21	7.75 ± 0.02	4.27 ± 0.09
	OstDiff + Neg	1.10 ± 0.02	2.40 ± 0.11	7.73 ± 0.04	4.33 ± 0.06
	OstDiff + anti-miR31	3.69 ± 0.03	4.77 ± 0.09	12.47 ± 0.01	16.77 ± 0.04
	OstDiff + anti-miR106a	3.47 ± 0.12	4.19 ± 0.07	12.15 ± 0.02	16.17 ± 0.03
	OstDiff + anti-miR148a	4.57 ± 0.18	5.70 ± 0.23	13.76 ± 0.02	17.86 ± 0.05
UC-MSCs	Complete medium	0.63 ± 0.03	1.59 ± 0.12	3.25 ± 0.03	3.43 ± 0.02
	OstDiff	1.06 ± 0.03	2.61 ± 0.23	4.54 ± 0.03	6.26 ± 0.03
	OstDiff + Neg	1.07 ± 0.03	2.54 ± 0.12	4.57 ± 0.02	6.25 ± 0.03
	OstDiff + anti-miR31	4.13 ± 0.07	5.29 ± 0.12	14.27 ± 0.04	17.66 ± 0.03
	OstDiff + anti-miR106a	3.35 ± 0.18	4.15 ± 0.03	12.87 ± 0.04	15.56 ± 0.04
	OstDiff + anti-miR148a	3.70 ± 0.06	4.27 ± 0.12	13.06 ± 0.04	15.97 ± 0.04

Values are presented as mean $\pm$ SEM.
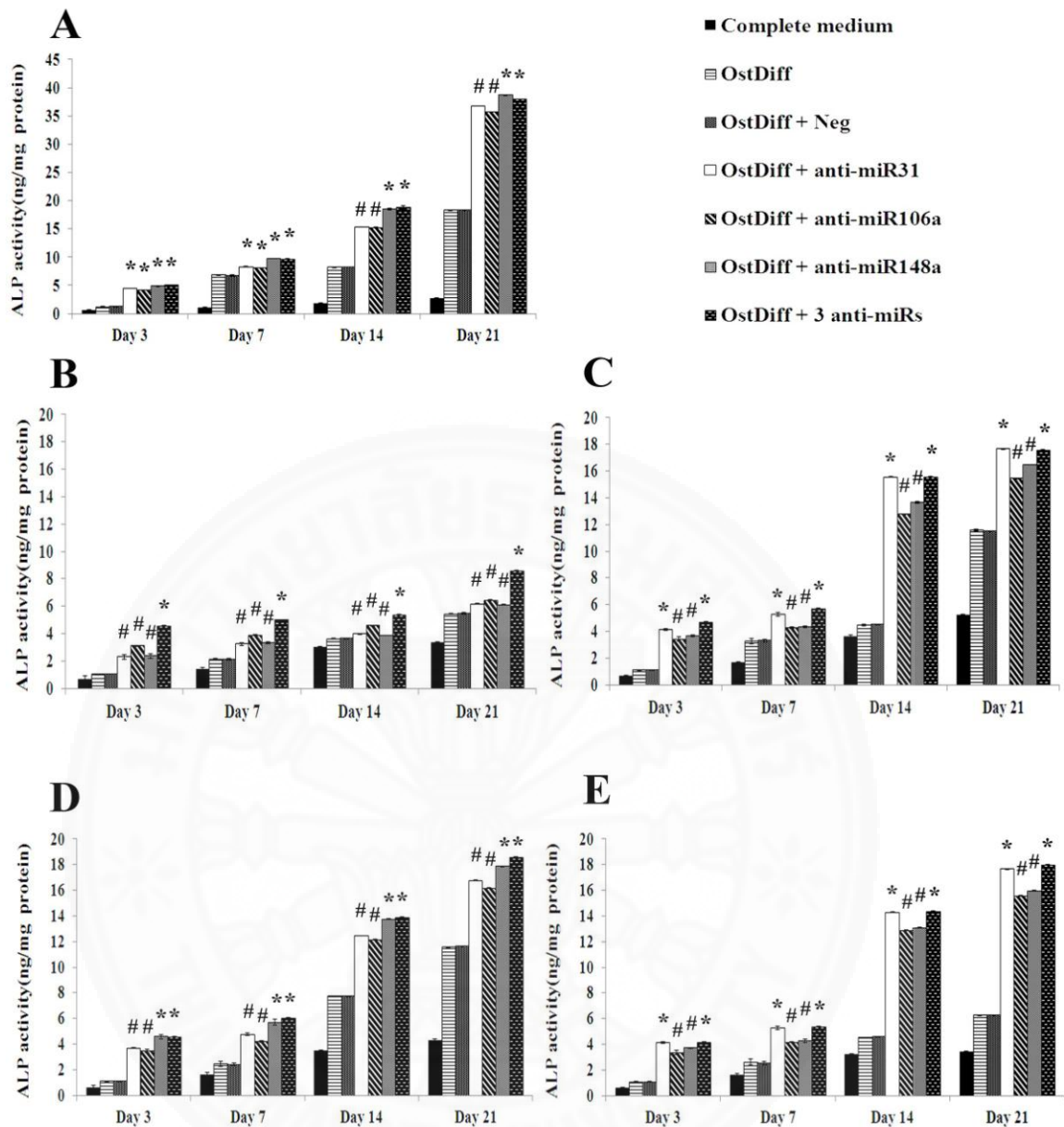
Figure 4.48: Alkaline phosphatase activity of BM-MSCs (A), AM-MSCs (B), CH-MSCs (C), PL-MSCs (D), and UC-MSCs (E) after transient transfection with miRNA inhibitors. Data are presented as mean ± SEM. *$p<0.05$: significant difference compared to MSCs cultured in osteogenic differentiation medium + negative control. #$p<0.05$: significant difference compared to both MSCs cultured in osteogenic differentiation medium + negative control and MSCs cultured in osteogenic differentiation medium + anti-miR31 + anti-miR106a + anti-miR148a.

4.14 The expression of osteogenic lineage genes in MSCs after the transient transfection with miRNA inhibitors.

The effects of miRNA inhibitor on osteogenic differentiation potential of BM-MSCs, AM-MSCs, CH-MSCs, PL-MSCs, and UC-MSCs was further investigated through gene expression analysis including *RUNX-2*, *OSX*, and *OCN* following 3, 7, 14, and 21 days of culture. The results demonstrated that after transfected with anti-miR31, the expressions of *RUNX-2*, *OSX*, and *OCN* were increased in a time-dependent manner during the process of osteogenic differentiation of BM-MSCs when compared to those transfected with negative anti-miRNA (Table. 14.6 - 14.18, Fig. 4.49 - 4.51). The expression of *RUNX-2* in BM-MSCs was increased over time from day 3 to day 14. The peak of *RUNX-2* expression was found during day 14 in BM-MSCs cultured in osteogenic differentiation medium added with anti-miR-148a (Fig. 4.49 A). Nevertheless, BM-MSCs cultured in osteogenic differentiation medium with these anti-miRNAs showed significant higher *RUNX-2* expression than that was cultured in osteogenic differentiation added with negative control of anti-miRNA (Fig. 4.49 A). In contrast to BM-MSCs, *RUNX-2* expression was increased over time from day 3 to day 21 in AM-MSCs, CH-MSCs, PL-MSCs, and UC-MSC cultured in osteogenic differentiation medium added with anti-miR-31, anti-miR-106a, anti-miR148a, and the combination of 3 anti-miRNAs. Interestingly, AM-MSCs, CH-MSCs, PL-MSCs, and UC-MSCs treated with these anti-miRNAs showed higher expression of *RUNX-2* than those of untreated groups (Fig. 4.49 B - E). The effects of miRNA inhibitor on the expression levels of other osteogenic lineage genes in AM-MSCs, CH-MSCs, PL-MSCs, and UC-MSCs were also different from BM-MSCs. The expression of *OSX* was increased over time from day 3 to day 21 in BM-MSCs, AM-MSCs, CH-MSCs, PL-MSCs, and UC-MSCs cultured in osteogenic differentiation medium added with anti-miR-31, anti-miR-106a, anti-miR148a, and the combination of 3 anti-miRNAs (Fig. 4.50). The transfections with anti-miR31, anti-miR106a, anti-miR148a, and the combination of 3 anti-miRNAs significantly up-regulated the *OSX* in AM-MSCs, CH-MSCs, PL-MSCs, and UC-MSCs on days 7, 14, and 21 of culture (Fig. 4.50 B, C, D, and E) while the *OSX* was observed in BM-MSCs every day after transfection (Fig. 4.50A). Similar to *OSX*, minimum *OCN* mRNA expression was detected in BM-MSCs at day 3. The *OCN* expression levels were significantly increased *OCN* in BM-MSCs transfected with

anti-miR-31, anti-miR-106a, anti-miR148a, and the combination of 3 anti-miRNAs at day 3, 7, 14, and 21, compared with negative controls of anti-miRNA (Fig. 4.51 A). The expressions of *OCN* were increased to the same extent with time in AM-MSCs, CH-MSCs, PL-MSCs, and UC-MSCs in anti-miR-31, anti-miR-106a, anti-miR148a, and the combination of 3 anti-miRNAs treated groups (Fig. 4.51 B, C, D, and E). However, the up-regulations of *OCN* in AM-MSCs, CH-MSCs, PL-MSCs, and UC-MSCs were significantly observed in anti-miR-31, anti-miR-106a, anti-miR148a, and the combination of 3 anti-miRNAs transfected groups at day 14 and 21 (Fig. 4.51 B, C, D, and E).

Table 4.16: The relative *RUNX-2* expression level in MSCs derived from bone marrow, amnion, chorion, placenta, and umbilical cord after the transient transfection with anti-miRNAs.

MSCs sources	Group	Day (s)			
		3	7	14	21
BM-MSCs	OstDiff + Neg	1.00 ± 0.00	1.00 ± 0.00	1.00 ± 0.00	1.00 ± 0.00
	OstDiff + anti-miR31	3.00 ± 0.06	6.69 ± 0.08	9.59 ± 0.04	15.79 ± 0.03
	OstDiff + anti-miR106a	3.37 ± 0.08	6.52 ± 0.07	8.95 ± 0.04	13.86 ± 0.05
	OstDiff + anti-miR148a	4.42 ± 0.05	10.62 ± 0.12	14.88 ± 0.04	10.86 ± 0.04
	OstDiff + 3 anti-miRs	4.37 ± 0.04	9.69 ± 0.05	14.57 ± 0.21	15.74 ± 0.16
AM-MSCs	OstDiff + Neg	1.00 ± 0.00	1.00 ± 0.00	1.00 ± 0.00	1.00 ± 0.00
	OstDiff + anti-miR31	1.27 ± 0.02	3.10 ± 0.08	4.23 ± 0.05	7.66 ± 0.06
	OstDiff + anti-miR106a	1.31 ± 0.03	3.16 ± 0.02	4.45 ± 0.07	8.68 ± 0.05
	OstDiff + anti-miR148a	1.25 ± 0.07	2.90 ± 0.06	3.54 ± 0.03	7.97 ± 0.04
	OstDiff + 3 anti-miRs	1.34 ± 0.06	3.08 ± 0.05	4.54 ± 0.04	8.76 ± 0.05
CH-MSCs	OstDiff + Neg	1.00 ± 0.00	1.00 ± 0.00	1.00 ± 0.00	1.00 ± 0.00
	OstDiff + anti-miR31	2.12 ± 0.04	4.43 ± 0.05	9.37 ± 0.08	13.21 ± 0.05
	OstDiff + anti-miR106a	1.64 ± 0.04	3.51 ± 0.01	6.84 ± 0.02	11.43 ± 0.15
	OstDiff + anti-miR148a	1.94 ± 0.02	3.80 ± 0.05	8.31 ± 0.06	13.10 ± 0.03
	OstDiff + 3 anti-miRs	2.14 ± 0.05	4.48 ± 0.05	9.47 ± 0.05	14.05 ± 0.05
PL-MSCs	OstDiff + Neg	1.00 ± 0.00	1.00 ± 0.00	1.00 ± 0.00	1.00 ± 0.00
	OstDiff + anti-miR31	2.67 ± 0.08	3.83 ± 0.08	5.85 ± 0.05	10.75 ± 0.04
	OstDiff + anti-miR106a	1.92 ± 0.01	2.92 ± 0.07	5.12 ± 0.06	9.88 ± 0.02
	OstDiff + anti-miR148a	2.85 ± 0.02	4.38 ± 0.07	6.24 ± 0.03	14.54 ± 0.04
	OstDiff + 3 anti-miRs	2.76 ± 0.04	4.41 ± 0.04	6.32 ± 0.05	14.67 ± 0.04
UC-MSCs	OstDiff + Neg	1.00 ± 0.00	1.00 ± 0.00	1.00 ± 0.00	1.00 ± 0.00
	OstDiff + anti-miR31	2.27 ± 0.08	4.45 ± 0.07	11.21 ± 0.04	13.83 ± 0.05
	OstDiff + anti-miR106a	1.65 ± 0.05	3.59 ± 0.09	6.17 ± 0.03	10.25 ± 0.04
	OstDiff + anti-miR148a	1.93 ± 0.03	3.38 ± 0.02	10.22 ± 0.04	12.45 ± 0.05
	OstDiff + 3 anti-miRs	2.24 ± 0.05	4.38 ± 0.04	10.98 ± 0.01	13.74 ± 0.05

Values are presented as mean ± SEM.
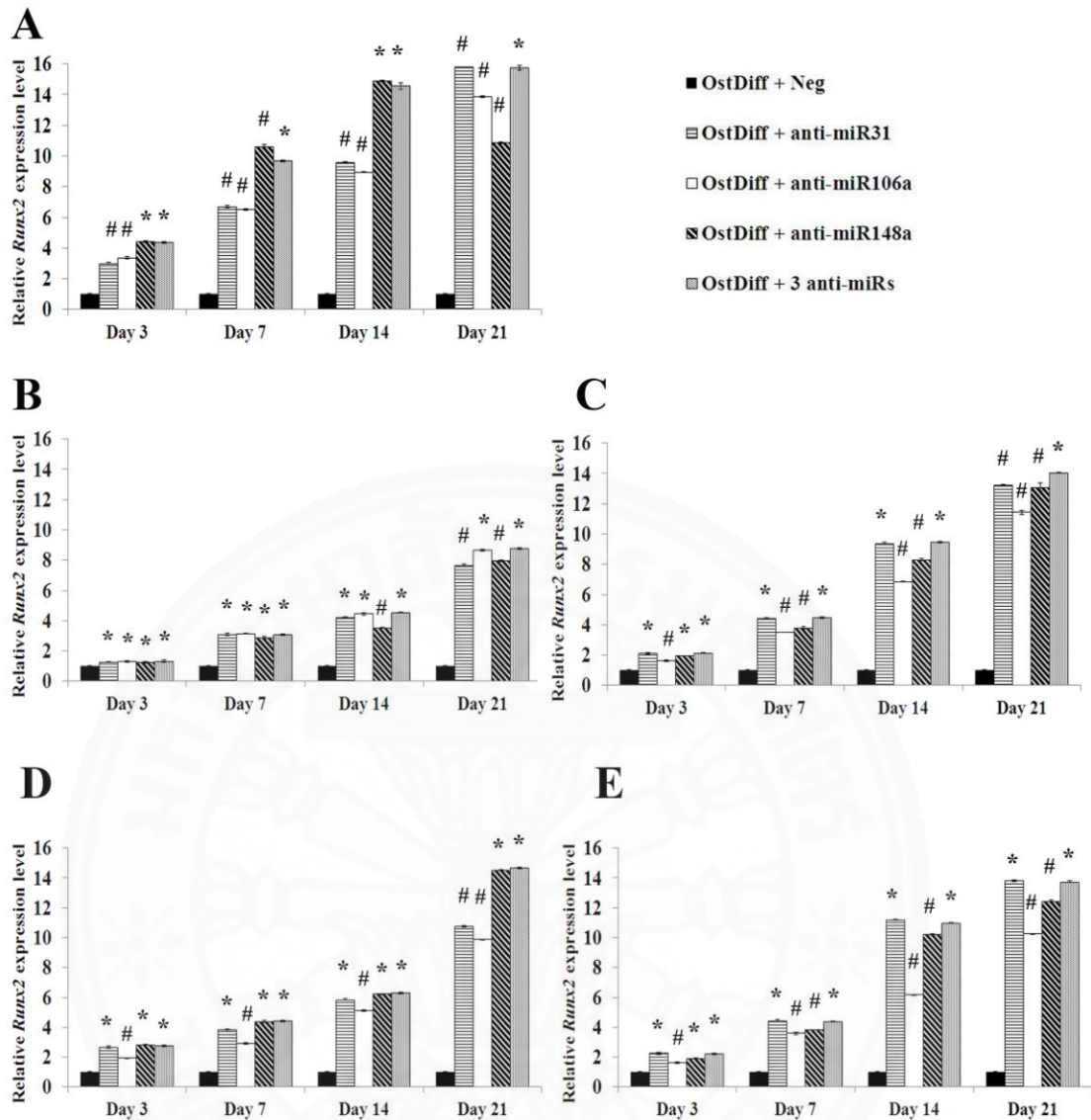
Figure 4.49: The relative *Runx2* expression in BM-MSCs (A), AM-MSCs (B), CH-MSCs (C), PL-MSCs (D), and UC-MSCs (E) after the transient transfection with anti-miR31, anti-miR106a, anti-miR148a, and the combination of 3 anti-miRNAs. Data are presented as mean ± SEM. *$p<0.05$: significantly different compared to MSCs cultured in osteogenic differentiation medium + negative anti-miR. # $p<0.05$: significantly different compared to MSCs cultured in osteogenic differentiation medium + 3 anti-miRNAs.

Table 4.17: The relative *OSX* expression level in MSCs derived from bone marrow, amnion, chorion, placenta, and umbilical cord after the transient transfection with anti-miRNAs.

MSCs sources	Group	Day (s)			
		3	7	14	21
BM-MSCs	OstDiff + Neg	1.00 ± 0.00	1.00 ± 0.00	1.00 ± 0.00	1.00 ± 0.00
	OstDiff + anti-miR31	1.38 ± 0.06	1.95 ± 0.06	2.68 ± 0.03	6.72 ± 0.04
	OstDiff + anti-miR106a	1.28 ± 0.06	1.83 ± 0.06	2.47 ± 0.13	6.56 ± 0.05
	OstDiff + anti-miR148a	2.12 ± 0.05	2.52 ± 0.05	2.98 ± 0.04	7.99 ± 0.14
	OstDiff + 3 anti-miRs	1.95 ± 0.05	2.45 ± 0.05	2.89 ± 0.05	7.87 ± 0.04
AM-MSCs	OstDiff + Neg	1.00 ± 0.00	1.00 ± 0.00	1.00 ± 0.00	1.00 ± 0.00
	OstDiff + anti-miR31	1.31 ± 0.01	1.83 ± 0.03	2.70 ± 0.06	3.73 ± 0.05
	OstDiff + anti-miR106a	1.37 ± 0.01	1.96 ± 0.04	2.87 ± 0.05	3.84 ± 0.04
	OstDiff + anti-miR148a	1.19 ± 0.02	1.76 ± 0.01	2.48 ± 0.07	3.68 ± 0.02
	OstDiff + 3 anti-miRs	1.39 ± 0.05	2.08 ± 0.06	2.78 ± 0.03	3.79 ± 0.04
CH-MSCs	OstDiff + Neg	1.00 ± 0.00	1.00 ± 0.00	1.00 ± 0.00	1.00 ± 0.00
	OstDiff + anti-miR31	1.54 ± 0.01	2.10 ± 0.03	3.51 ± 0.06	5.61 ± 0.05
	OstDiff + anti-miR106a	1.21 ± 0.01	1.65 ± 0.04	2.97 ± 0.05	4.51 ± 0.04
	OstDiff + anti-miR148a	1.40 ± 0.02	1.72 ± 0.01	3.32 ± 0.07	5.18 ± 0.02
	OstDiff + 3 anti-miRs	1.49 ± 0.05	1.94 ± 0.06	3.49 ± 0.03	5.54 ± 0.04
PL-MSCs	OstDiff + Neg	1.00 ± 0.00	1.00 ± 0.00	1.00 ± 0.00	1.00 ± 0.00
	OstDiff + anti-miR31	1.34 ± 0.01	1.35 ± 0.01	4.98 ± 0.04	6.59 ± 0.02
	OstDiff + anti-miR106a	1.14 ± 0.03	1.23 ± 0.03	3.04 ± 0.05	5.15 ± 0.03
	OstDiff + anti-miR148a	1.63 ± 0.09	2.04 ± 0.01	5.21 ± 0.04	7.64 ± 0.05
	OstDiff + 3 anti-miRs	1.61 ± 0.07	2.07 ± 0.06	5.20 ± 0.05	7.81 ± 0.02
UC-MSCs	OstDiff + Neg	1.00 ± 0.00	1.00 ± 0.00	1.00 ± 0.00	1.00 ± 0.00
	OstDiff + anti-miR31	1.58 ± 0.06	2.13 ± 0.06	2.85 ± 0.05	6.61 ± 0.04
	OstDiff + anti-miR106a	1.24 ± 0.05	1.59 ± 0.06	2.45 ± 0.05	4.95 ± 0.04
	OstDiff + anti-miR148a	1.42 ± 0.03	1.73 ± 0.02	2.73 ± 0.06	5.92 ± 0.02
	OstDiff + 3 anti-miRs	1.54 ± 0.02	2.09 ± 0.05	2.81 ± 0.01	6.57 ± 0.03

Values are presented as mean ± SEM.
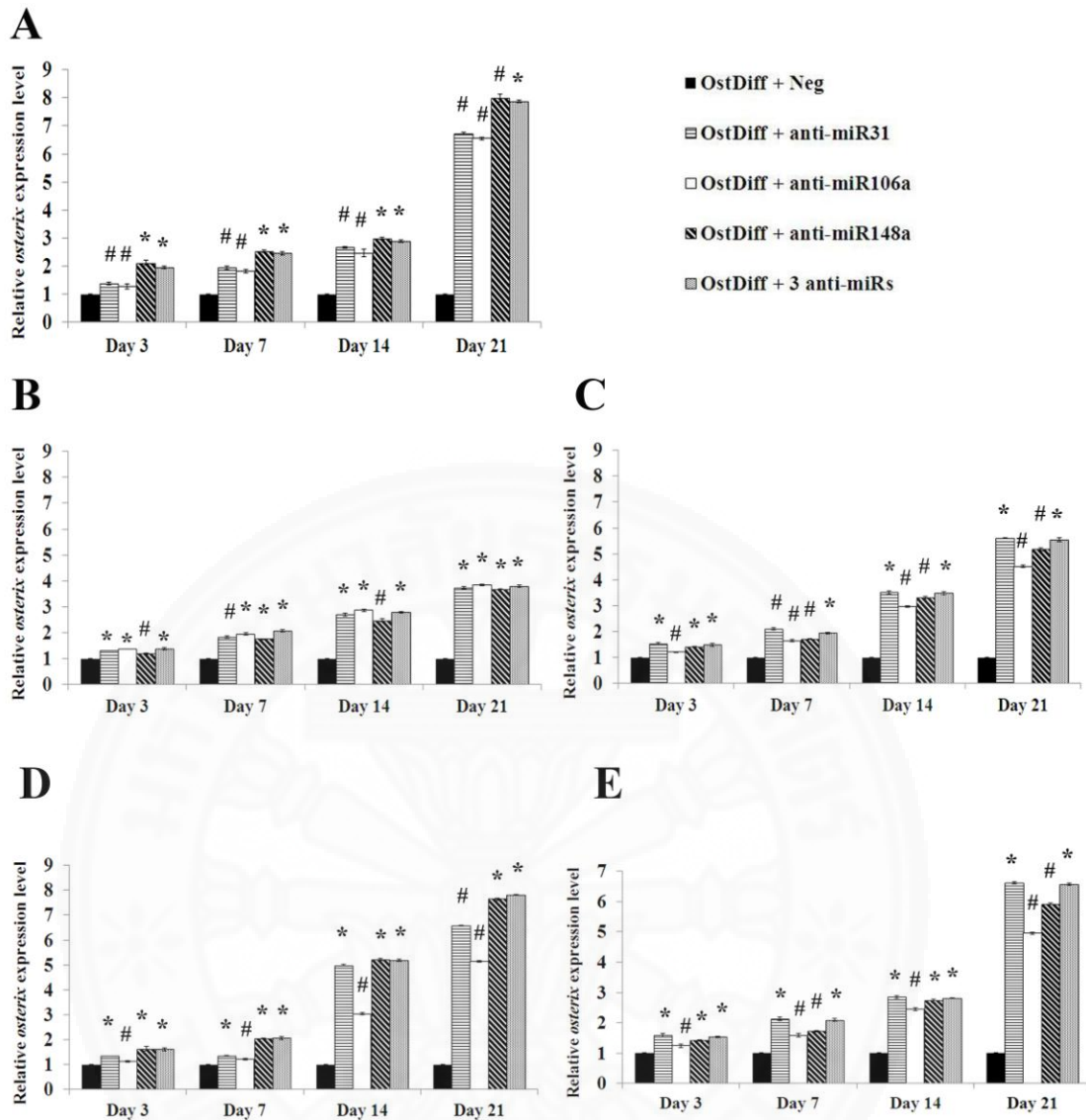
Figure 4.50: The relative *Osterix* expression in BM-MSCs (A), AM-MSCs (B), CH-MSCs (C), PL-MSCs (D), and UC-MSCs (E) after the transient transfection with anti-miR31, anti-miR106a, anti-miR148a, and the combination of 3 anti-miRNAs. Data are presented as mean ± SEM. *$p<0.05$: significantly different compared to MSCs cultured in osteogenic differentiation medium + negative anti-miR. # $p<0.05$: significantly different compared to MSCs cultured in osteogenic differentiation medium + 3 anti-miRNAs.

Table 4.18: The relative *OCN* expression level in MSCs derived from bone marrow, amnion, chorion, placenta, and umbilical cord after the transient transfection with anti-miRNAs.

MSCs sources	Group	Day (s)			
		3	7	14	21
BM-MSCs	OstDiff + Neg	1.00 ± 0.00	1.00 ± 0.00	1.00 ± 0.00	1.00 ± 0.00
	OstDiff + anti-miR31	1.35 ± 0.02	1.93 ± 0.02	3.69 ± 0.05	5.48 ± 0.04
	OstDiff + anti-miR106a	1.23 ± 0.06	1.63 ± 0.04	3.16 ± 0.05	5.07 ± 0.03
	OstDiff + anti-miR148a	1.53 ± 0.08	2.69 ± 0.06	4.58 ± 0.03	7.37 ± 0.03
	OstDiff + 3 anti-miRs	1.50 ± 0.04	2.35 ± 0.07	4.32 ± 0.06	7.83 ± 0.04
AM-MSCs	OstDiff + Neg	1.00 ± 0.00	1.00 ± 0.00	1.00 ± 0.00	1.00 ± 0.00
	OstDiff + anti-miR31	1.24 ± 0.01	1.63 ± 0.03	2.51 ± 0.04	3.61 ± 0.03
	OstDiff + anti-miR106a	1.29 ± 0.05	1.72 ± 0.02	2.58 ± 0.05	3.66 ± 0.05
	OstDiff + anti-miR148a	1.21 ± 0.06	1.70 ± 0.04	2.49 ± 0.02	3.54 ± 0.04
	OstDiff + 3 anti-miRs	1.34 ± 0.04	1.73 ± 0.04	2.57 ± 0.04	3.71 ± 0.03
CH-MSCs	OstDiff + Neg	1.00 ± 0.00	1.00 ± 0.00	1.00 ± 0.00	1.00 ± 0.00
	OstDiff + anti-miR31	1.38 ± 0.01	1.98 ± 0.03	2.87 ± 0.04	4.94 ± 0.03
	OstDiff + anti-miR106a	1.27 ± 0.05	1.90 ± 0.02	2.64 ± 0.05	4.74 ± 0.05
	OstDiff + anti-miR148a	1.34 ± 0.06	1.95 ± 0.04	2.75 ± 0.02	4.81 ± 0.04
	OstDiff + 3 anti-miRs	1.35 ± 0.04	1.92 ± 0.04	2.85 ± 0.04	4.89 ± 0.03
PL-MSCs	OstDiff + Neg	1.00 ± 0.00	1.00 ± 0.00	1.00 ± 0.00	1.00 ± 0.00
	OstDiff + anti-miR31	1.36 ± 0.02	1.74 ± 0.03	3.14 ± 0.05	4.74 ± 0.05
	OstDiff + anti-miR106a	1.30 ± 0.07	1.38 ± 0.02	2.72 ± 0.05	4.42 ± 0.03
	OstDiff + anti-miR148a	1.39 ± 0.03	1.88 ± 0.04	3.35 ± 0.05	4.89 ± 0.03
	OstDiff + 3 anti-miRs	1.39 ± 0.04	1.79 ± 0.03	3.41 ± 0.02	4.94 ± 0.04
UC-MSCs	OstDiff + Neg	1.00 ± 0.00	1.00 ± 0.00	1.00 ± 0.00	1.00 ± 0.00
	OstDiff + anti-miR31	1.39 ± 0.02	1.92 ± 0.06	2.79 ± 0.05	5.24 ± 0.03
	OstDiff + anti-miR106a	1.28 ± 0.01	1.75 ± 0.02	2.22 ± 0.06	3.81 ± 0.05
	OstDiff + anti-miR148a	1.34 ± 0.02	1.83 ± 0.04	2.64 ± 0.02	5.15 ± 0.02
	OstDiff + 3 anti-miRs	1.41 ± 0.04	1.91 ± 0.03	2.76 ± 0.04	5.21 ± 0.04

Values are presented as mean ± SEM.
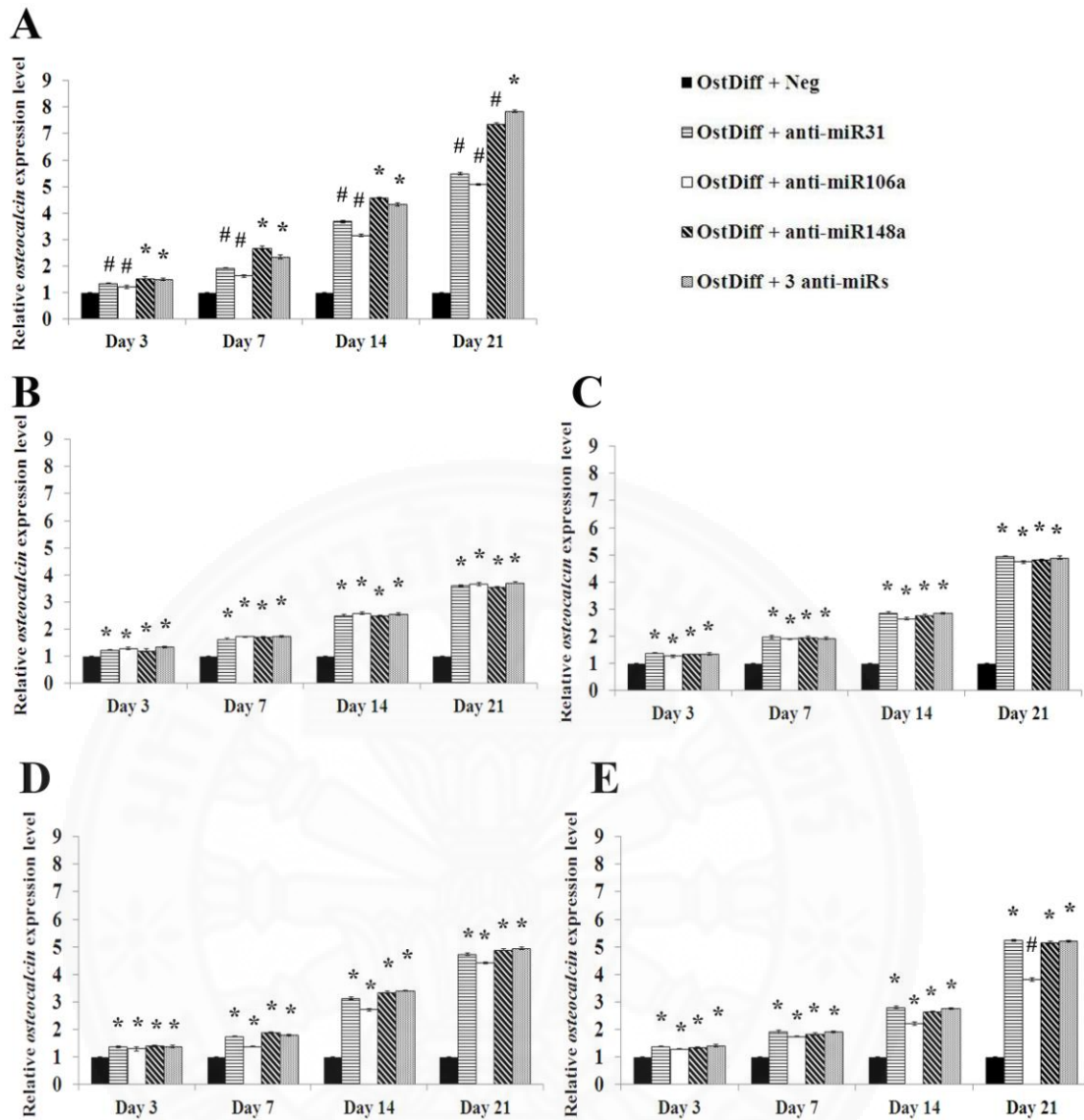
Figure 4.51: The relative *OCN* expression in BM-MSCs (A), AM-MSCs (B), CH-MSCs (C), PL-MSCs (D), and UC-MSCs (E) after the transient transfection with anti-miR31, anti-miR106a, anti-miR148a, and the combination of 3 anti-miRNAs. Data are presented as mean ± SEM. *$p<0.05$: significantly different compared to MSCs cultured in osteogenic differentiation medium + negative anti-miR. # $p<0.05$: significantly different compared to MSCs cultured in osteogenic differentiation medium + 3 anti-miRNAs.

CHAPTER 5

CONCLUSIONS AND RECOMMENDATIONS

MSCs are adherent marrow stromal cells which can self-renew and have the potential to differentiate into osteoblasts, chondrocytes, myoblasts and adipocytes (13). As multipotent progenitors, MSCs have been regarded as one of ideal seed cells for scientific research and bone tissue engineering (182, 183). However, the promotion of MSC differentiation into osteoblasts by osteogenic inducing factors is one of the most crucial issues in bone tissue engineering (182, 184). Bone morphogenetic protein 2 (BMP-2) is one of the most potent BMPs for promoting osteogenic differentiation of BM-MSCs both *in vitro* and *in vivo* (185, 186). Previous study reported that BMP-2 producing cells, via adenoviral gene transfer, produced sufficient protein to heal segmental bone defects in rat model (187). In addition, the acceleration of bone regeneration using rat BM-MSCs transduced with BMP-2 was higher than that of using MSCs alone (188). Several studies in animal models showed the regeneration of bone after implantation of scaffolds seeding with autologous BM-MSCs (189, 190). Although bone marrow is the main source of MSCs for both research and clinical trial, the limited cell number and the invasive procedure for harvesting cell restrict their use in clinical fields. Over the past few years, postnatal tissues, including amnion, chorion, placenta, and umbilical cord, are considered as promising alternative sources of MSCs for using in both research and clinical application. They are easy to isolate and expand *in vitro*. In addition, postnatal tissues can be attained by a less invasive method, without harm to the mother or infant (14, 191). Despite MSCs derived from postnatal tissues share similar characteristics to BM-MSCs, some differences in their differentiation capability and gene expression profile were also reported (192). Evidences supported that MSCs from postnatal tissues took a longer period of time for osteogenic differentiation compared to BM-MSCs (14). Therefore, it is still a challenge to enhance the osteogenic differentiation capability of MSCs from postnatal tissues for using in clinical application. Although many studies have shown the benefits of bone morphogenetic protein 2 (BMP-2) in bone tissue regeneration (52, 193), the BMP-2

induced osteogenic differentiation of MSCs from postnatal tissues are not fully examined.

This study revealed that MSCs could be isolated from postnatal tissues including amnion, chorion, placenta, and umbilical cord through the mechanical and enzymatic digestions. After characterization according to the criteria of International Society for Cellular Therapy (88), the results showed that the plastic-adherent cells from postnatal tissues exhibited fibroblast-like morphology similar to that of BM-MSCs. These cells were typically positive for MSC markers including CD73, CD90, and CD105 and had been shown to be negative for hematopoietic markers including CD34, CD45. The results are in accordance with previous studies (84, 85, 88). Similar to BM-MSCs, MSCs derived from postnatal tissues could differentiate into adipogenic and osteogenic lineages when culture under specific cultured conditions (81, 91). However, MSCs derived from postnatal tissues took a longer period of time than BM-MSCs to differentiate into both adipogenic and osteogenic lineages.

Regarding with the proliferative capacity of MSCs derived from postnatal tissues and bone marrow, the growth curves showed an initial lag phase of 2–6 days in every examined passage. This was followed by a log phase in which the MSCs divided at exponential rates for 6- 8 days. With increasing passage number, the MSC growth rates were slower and the number of cells generated by the end of 14 days in culture was reduced and these results were in accordance with previous studies (194, 195). Among these, BM-MSCs showed the highest proliferative capacity whereas AM-MSCs showed the lowest proliferative capacity. Another index indicating the cell proliferation rate is population doubling time which defines as the time by which the given cell population double their numbers by undergoing proliferation. According to this assay, the population doubling time of BM-MSCs appeared to be much shorter than MSCs derived from postnatal tissues especially during the early passage. Nevertheless, both BM-MSCs and MSCs derived from postnatal tissues gradually lose their ability to proliferate and tend to undergo senescence along with the long culture period. While the rapid *in vitro* proliferation of the MSCs would be of interest; in particular for the cases those required huge number of cells to repair the large tissue defects. Because of the limited number of MSCs in

bone marrow, postnatal tissues which have unlimited supply and their easily accessible without ethical concern seem to be the more appropriate MSC source for using in regenerative medicine.

In this study, the effect of BMP-2 on osteogenic differentiation was investigated to clarify the role of BMP-2 on MSC differentiation. The expression of alkaline phosphatase (ALP) was monitored using ALP staining and ALP activity. Previous study reported that ALP was produced by osteoblasts and was hypothesized to be involved in the degradation of inorganic pyrophosphates to provide sufficient local phosphate or inorganic pyrophosphate for the occurrence of mineralization (196). Therefore, ALP activity was commonly used as a marker of osteogenesis to reflect the degree of osteogenic differentiation. The results revealed that BMP-2 treatment could enhance the efficiency of osteogenic differentiation of both BM-MSCs and MSCs derived from postnatal tissues as evidenced by the increasing level of ALP staining and ALP activity. Correspondingly, the expressions of osteogenic marker genes were also increased in both BM-MSCs and MSCs derived from postnatal tissues after BMP-2 treatment.

Although the molecular mechanisms underlying BMP-2 mediated osteogenesis remains to be fully understood, various studies have demonstrated that BMP-2 play a critical role in osteogenic differentiation of MSCs (15, 182, 186). In addition to the direct application of recombinant BMP-2 proteins, numerous reports have confirmed the ability of adenoviral vector-mediated gene transfer of BMP-2 to induce bone formation both *in vitro* and *in vivo* (16). Previous studies in mouse myoblast cell line, C2C12 demonstrated that BMP-2 inhibited its myogenic differentiation, and instead diverted their differentiation pathway into that of osteoblasts (68). BMP-2 induces *RUNX-2* expression in MSCs in a Smad-dependent fashion and regulates the expression of target genes which are involved in osteoblast differentiation (69).

This study revealed that osteogenic markers, including *RUNX-2, OSX*, and *OCN* were up-regulated in BM-MSCs after BMP-2 treatment. Fascinatingly, the peak expression of *RUNX-2* in BM-MSCs cultured with osteogenic differentiation medium in the presence or absence of BMP-2 was observed at day 14. Remarkably,

the addition of BMP-2 could enhance the expression of *RUNX-2* in BM-MSCs. In contrast to BM-MSCs, the highest expression of *RUNX-2* in MSCs derived from postnatal tissues cultured with osteogenic differentiation medium in the presence or absence of BMP-2 was observed at day 28. Nevertheless, BMP-2 could enhance the expression of *RUNX-2* in MSCs derived from postnatal tissues similar to that of BM-MSCs. *RUNX-2* is a pivotal osteogenic transcription factor. It may be one of the earliest master transcription factors that direct the differentiation of MSCs into osteoblasts (197). Previous study reported that *RUNX-2* was expressed in the *OSX* -/- mouse while *OSX* is not expressed in the *RUNX-2* -/- mouse (198). Base on this finding, *RUNX-2* was proposed to be an upstream regulator of *OSX* expression (15, 64). Previous study suggested that *RUNX-2* plays a role in the commitment step for the common progenitor cells for osteoblasts and chondrocytes, whereas *OSX* plays a role in the final differentiation step in osteogenesis (198). This notion is further supported by evidence that the expression of *OCN*, the final differentiation marker of osteogenesis, is induced by *OSX* over expression but not by *RUNX-2* overexpression (199). This data supported the result of this study. The expression *OSX* at every time point is overlapped with expression of *OCN*. Interestingly, BMP-2 treatment could significantly enhance the expression of *OSX* and *OCN* in both BM-MSCs and MSCs derived from postnatal tissues. Although BMP-2 could enhance the osteogenic differentiation capability of MSCs derived from postnatal tissues, the effect is less pronounced compared to BM-MSCs. This might be due to the endogenous difference in osteogenic differentiation capacity between BM-MSCs and MSCs derived from postnatal tissues as shown by the finding that the endogenous ALP activity of MSCs derived from postnatal tissues was much lower than those of BM-MSCs cultured under the same condition. In addition, the suitable concentration of BMP-2 could still significantly issue for enhancement of the osteogenic capacity of MSCs derived from postnatal tissues. Nevertheless, this study demonstrated that BMP-2 treatment could enhance the osteogenic differentiation capacity of both BM-MSCs and MSCs derived from postnatal tissues as evidence by increased ALP expression and osteogenic gene expression.

Several studies have demonstrated that miRNAs were associated with stem cell self-renewal and differentiation. They play a key role in controlling stem cell

activities (21, 200). To determine the role of miRNA on osteogenic differentiation of MSCs, the expression of miRNA during osteogenic differentiation of MSCs derived from postnatal tissues and BM-MSCs were quantified using qRT-PCR. The results demonstrated that the expression of miR-31, miR-106a, and miR-148a were down-regulated during osteogenic differentiation of these MSCs. In addition, the expressions of these miRNAs were also decreased after BMP-2 treatment in both BM-MSCs and MSCs derived from postnatal tissues. After transfection with anti-miRNAs, alkaline phosphatase activity and the expression of osteogenic markers were increased in MSCs derived from postnatal tissues similar to that of BM-MSCs. Recent study demonstrated that miR-31, miR-106a, and miR-148a were under expressed in BM-MSCs during osteogenic differentiation. These miRNAs target to *RUNX-2* during osteogenic differentiation of BM-MSCs (21).

Although the down regulation of these miRNAs could enhance the osteogenic differentiation capacity of MSCs derived from postnatal tissues, the effect was less pronounced than BM-MSCs. This might be due to the endogenous difference in osteogenic differentiation capacity between BM-MSCs and MSCs derived from postnatal tissues. During osteogenic differentiation, miR-31 showed the highest expression level in CH-MSCs and UC-MSCs, whereas the expression level of miR-148a was much higher than that of BM-MSCs and PL-MSCs. Nevertheless, this study demonstrates that transfection of anti-miRNAs could enhance the osteogenic differentiation capacity of both BM-MSCs and MSCs derived from postnatal tissues as evidence by increased ALP expression and osteogenic gene expressions. Recent study revealed that miR-31, miR-106a, and miR-148a were under-expressed during osteogenic differentiation of human BM-MSCs. The putative targets of these miRNAs, predicted by bioinformatic analysis, include *RUNX-2*, *CBFB*, and BMPs which are involved in bone formation. (21). Previous study reported that miR-31 is a negative regulator of osteogenic differentiation (201). MiR-31 repressed osteogenesis of human MSCs by decreased expression levels of *RUNX-2*, *OCN* and *OSX* (201). In accordance with this study, the anti-miR-31-modified ADSCs via lentiviral vector were applied to repair critical-sized defects (CSDs) in rats combined with the β-tricalcium phosphate (β-TCP) scaffolds. Micro-CT displayed that miR-31 knockout can improve ossification *in vivo* (162). Moreover,

BMP-2 is inhibited by miR-106a which may suppress osteogenesis through the BMP/*RUNX-2* pathway (164).

In conclusion, this study reported the effects of BMP-2 and miRNAs on osteogenic differentiation of postnatal tissues including AM-MSCs, CH-MSCs, PL-MSCs, and UC-MSCs. The results demonstrated that MSCs derived from amnion, chorion, placenta and umbilical cord could be isolated and easily expanded in culture. BMP-2 enhanced osteogenic differentiation of MSCs derived from postnatal tissues similar to BM-MSCs by up-regulating the expression of osteogenic genes including *RUNX-2*, *OSX*, and *OCN*. The ALP activity as well as osteogenic gene expressions was increased during osteogenic differentiation of BM-MSCs and MSCs derived from postnatal tissues. In contrast to expression of osteogenic genes, the expression of miR-31, miR-106a, and miR-148a were decreased during osteogenic differentiation. The transient transfection with anti-miR31, anti-miR106a, and anti-miR148a could increase ALP activity and the expression of osteogenic genes of both BM-MSCs and MSCs derived from postnatal tissues (Fig. 5.1). The knowledge gained from this study will increase understanding on the mechanisms underlying the effects of BMP-2 and miRNAs on osteogenic differentiation of MSCs and might be lead to the progress of bone regeneration using MSCs and provide realistic hope for patient who necessitate receiving stem cell transplantation.
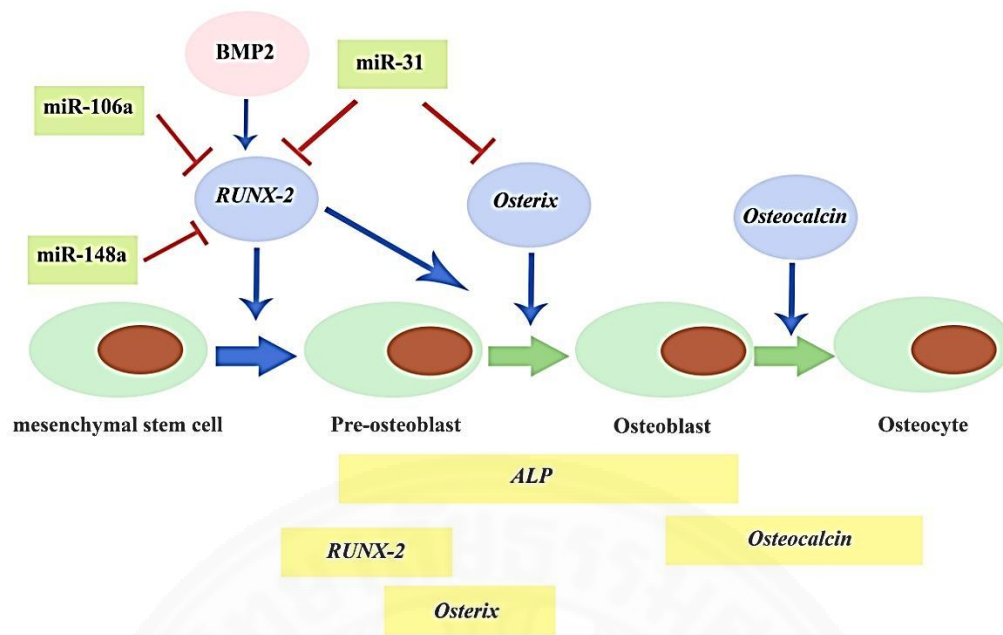
Figure 5.1: Schematic summary of the major activities during osteogenic differentiation of mesenchymal stromal cells. The selected miRNAs (green) correspond to their targets (blue) as well as the osteogenic markers of each differentiated stage are indicated.

REFERENCES

1.   Sanchez-Ramos J, Song S, Cardozo-Pelaez F, Hazzi C, Stedeford T, Willing A, et al. Adult bone marrow stromal cells differentiate into neural cells in vitro. Experimental neurology. 2000;164(2):247-56.

2.   Manochantr S, Tantrawatpan C, Kheolamai P, Y Up, Supokawej A, Issaragrisil S. Isolation, characterization and neural differentiation potential of amnion derived mesenchymal stem cells. Journal of the Medical Association of Thailand = Chotmaihet thangphaet. 2010;93 Suppl 7:S183-91.

3.   Centeno CJ, Faulkner SJ. The use of mesenchymal stem cell in orthopedics. In: Hayat MA, editor. stem cells and cancer stem cells. 12012. p. 173-9.

4.   Barry FP. Biology and clinical applications of mesenchymal stem cells. Birth Defects Res C Embryo Today. 2003;69(3):250-6.

5.   Zhou S, Greenberger JS, Epperly MW, Goff JP, Adler C, Leboff MS, et al. Age-related intrinsic changes in human bone-marrow-derived mesenchymal stem cells and their differentiation to osteoblasts. Aging Cell. 2008;7(3):335-43.

6.   Stenderup K, Justesen J, Clausen C, Kassem M. Aging is associated with decreased maximal life span and accelerated senescence of bone marrow stromal cells. Bone. 2003;33(6):919-26.

7.   Kassem M, Marie PJ. Senescence-associated intrinsic mechanisms of osteoblast dysfunctions. Aging Cell. 2011;10(2):191-7.

8.   Erices A, Conget P, Minguell JJ. Mesenchymal progenitor cells in human umbilical cord blood. Br J Haematol. 2000;109(1):235-42.

9.   Campagnoli C, Roberts IA, Kumar S, Bennett PR, Bellantuono I, Fisk NM. Identification of mesenchymal stem/progenitor cells in human first-trimester fetal blood, liver, and bone marrow. Blood. 2001;98(8):2396-402.

10.   In 't Anker PS, Scherjon SA, Kleijburg-van der Keur C, de Groot-Swings GM, Claas FH, Fibbe WE, et al. Isolation of mesenchymal stem cells of fetal or maternal origin from human placenta. Stem cells. 2004;22(7):1338-45.

11.   Soncini M, Vertua E, Gibelli L, Zorzi F, Denegri M, Albertini A, et al. Isolation and characterization of mesenchymal cells from human fetal membranes. J Tissue Eng Regen Med. 2007;1(4):296-305.

12.   Portmann-Lanz CB, Schoeberlein A, Huber A, Sager R, Malek A, Holzgreve W, et al. Placental mesenchymal stem cells as potential autologous graft for pre- and perinatal neuroregeneration. Am J Obstet Gynecol. 2006;194(3):664-73.

13.   Pittenger MF, Mackay AM, Beck SC, Jaiswal RK, Douglas R, Mosca JD, et al. Multilineage potential of adult human mesenchymal stem cells. Science. 1999;284(5411):143-7.

14.   Manochantr S, Y Up, Kheolamai P, Rojphisan S, Chayosumrit M, Tantrawatpan C, et al. Immunosuppressive properties of mesenchymal stromal cells derived from amnion, placenta, Wharton's jelly and umbilical cord. Intern Med J. 2013;43(4):430-9.

15.   De Biase P, Capanna R. Clinical applications of BMPs. Injury. 2005;36 Suppl 3:S43-6.

16.   Bais MV, Wigner N, Young M, Toholka R, Graves DT, Morgan EF, et al. BMP2 is essential for post natal osteogenesis but not for recruitment of osteogenic stem cells. Bone. 2009;45(2):254-66.

17.   Osyczka AM, Leboy PS. Bone morphogenetic protein regulation of early osteoblast genes in human marrow stromal cells is mediated by extracellular signal-regulated kinase and phosphatidylinositol 3-kinase signaling. Endocrinology. 2005;146(8):3428-37.

18.   Rana TM. Illuminating the silence: understanding the structure and function of small RNAs. Nat Rev Mol Cell Biol. 2007;8(1):23-36.

19.   Bartel DP. MicroRNAs: genomics, biogenesis, mechanism, and function. Cell. 2004;116(2):281-97.

20. Ong SG, Lee WH, Kodo K, Wu JC. MicroRNA-mediated regulation of differentiation and trans-differentiation in stem cells. Adv Drug Deliv Rev. 2015;88:3-15.

21. Gao J, Yang T, Han J, Yan K, Qiu X, Zhou Y, et al. MicroRNA expression during osteogenic differentiation of human multipotent mesenchymal stromal cells from bone marrow. J Cell Biochem. 2011;112(7):1844-56.

22. Huang J, Zhao L, Xing L, Chen D. MicroRNA-204 regulates *RUNX-2*RUNX2 protein expression and mesenchymal progenitor cell differentiation. Stem Cells. 2010;28(2):357-64.

23. Singh V. Skeleton. General Anatomy. 1. India: Elsevier; 2008. p. 75.

24. Egawa S, Miura S, Yokoyama H, Endo T, Tamura K. Growth and differentiation of a long bone in limb development, repair and regeneration. Dev Growth Differ. 2014;56(5):410-24.

25. Clarke B. Normal bone anatomy and physiology. Clin J Am Soc Nephrol. 2008;3 Suppl 3:S131-9.

26. Ebert MS, Sharp PA. MicroRNA sponges: progress and possibilities. RNA. 2010;16(11):2043-50.

27. Kronenberg HM. Developmental regulation of the growth plate. Nature. 2003;423(6937):332-6.

28. Nakashima K, de Crombrugghe B. Transcriptional mechanisms in osteoblast differentiation and bone formation. Trends Genet. 2003;19(8):458-66.

29. Kapinas K, Delany AM. MicroRNA biogenesis and regulation of bone remodeling. Arthritis Res Ther. 2011;13(3):220.

30. Everts V, Delaisse JM, Korper W, Jansen DC, Tigchelaar-Gutter W, Saftig P, et al. The bone lining cell: its role in cleaning Howship's lacunae and initiating bone formation. J Bone Miner Res. 2002;17(1):77-90.

31.   Lakkakorpi P, Tuukkanen J, Hentunen T, Jarvelin K, Vaananen K. Organization of osteoclast microfilaments during the attachment to bone surface in vitro. J Bone Miner Res. 1989;4(6):817-25.

32.   Văananen HK, Laitala-Leinonen T. Osteoclast lineage and function. Arch Biochem Biophys. 2008;473(2):132-8.

33.   Lefebvre V, Bhattaram P. Vertebrate skeletogenesis. Curr Top Dev Biol. 2010;90:291-317.

34.   Komori T, Yagi H, Nomura S, Yamaguchi A, Sasaki K, Deguchi K, et al. Targeted disruption of Cbfa1 results in a complete lack of bone formation owing to maturational arrest of osteoblasts. Cell. 1997;89(5):755-64.

35.   Otto F, Thornell AP, Crompton T, Denzel A, Gilmour KC, Rosewell IR, et al. Cbfa1, a candidate gene for cleidocranial dysplasia syndrome, is essential for osteoblast differentiation and bone development. Cell. 1997;89(5):765-71.

36.   Takeda S, Bonnamy JP, Owen MJ, Ducy P, Karsenty G. Continuous expression of Cbfa1 in nonhypertrophic chondrocytes uncovers its ability to induce hypertrophic chondrocyte differentiation and partially rescues Cbfa1-deficient mice. Genes Dev. 2001;15(4):467-81.

37.   Ducy P, Zhang R, Geoffroy V, Ridall AL, Karsenty G. Osf2/Cbfa1: a transcriptional activator of osteoblast differentiation. Cell. 1997;89(5):747-54.

38.   Bialek P, Kern B, Yang X, Schrock M, Sosic D, Hong N, et al. A twist code determines the onset of osteoblast differentiation. Dev Cell. 2004;6(3):423-35.

39.   Ito Y, Zhang YW. A RUNX2/PEBP2alphaA/CBFA1 mutation in cleidocranial dysplasia revealing the link between the gene and Smad. Journal of bone and mineral metabolism. 2001;19(3):188-94.

40.   Phimphilai M, Zhao Z, Boules H, Roca H, Franceschi RT. BMP signaling is required for RUNX2-dependent induction of the osteoblast phenotype. J Bone Miner Res. 2006;21(4):637-46.

41.   Bruderer M, Richards RG, Alini M, Stoddart MJ. Role and regulation of *RUNX-2* in osteogenesis. Eur Cell Mater. 2014;28:269-86.

42.   Takahashi Y, Yamamoto M, Tabata Y. Osteogenic differentiation of mesenchymal stem cells in biodegradable sponges composed of gelatin and beta-tricalcium phosphate. Biomaterials. 2005;26(17):3587-96.

43.   Nishio Y, Dong Y, Paris M, O'Keefe RJ, Schwarz EM, Drissi H. *RUNX-2-*mediated regulation of the zinc finger Osterix/Sp7 gene. Gene. 2006;372:62-70.

44.   Koga T, Matsui Y, Asagiri M, Kodama T, de Crombrugghe B, Nakashima K, et al. NFAT and Osterix cooperatively regulate bone formation. Nature medicine. 2005;11(8):880-5.

45.   Winslow MM, Pan M, Starbuck M, Gallo EM, Deng L, Karsenty G, et al. Calcineurin/NFAT signaling in osteoblasts regulates bone mass. Dev Cell. 2006;10(6):771-82.

46.   Wang X, Kua HY, Hu Y, Guo K, Zeng Q, Wu Q, et al. p53 functions as a negative regulator of osteoblastogenesis, osteoblast-dependent osteoclastogenesis, and bone remodeling. J Cell Biol. 2006;172(1):115-25.

47.   Kim JH, Liu X, Wang J, Chen X, Zhang H, Kim SH, et al. Wnt signaling in bone formation and its therapeutic potential for bone diseases. Ther Adv Musculoskelet Dis. 2013;5(1):13-31.

48.   Day TF, Guo X, Garrett-Beal L, Yang Y. Wnt/beta-catenin signaling in mesenchymal progenitors controls osteoblast and chondrocyte differentiation during vertebrate skeletogenesis. Dev Cell. 2005;8(5):739-50.

49.   Hill TP, Spater D, Taketo MM, Birchmeier W, Hartmann C. Canonical Wnt/beta-catenin signaling prevents osteoblasts from differentiating into chondrocytes. Dev Cell. 2005;8(5):727-38.

50.   Bennett CN, Longo KA, Wright WS, Suva LJ, Lane TF, Hankenson KD, et al. Regulation of osteoblastogenesis and bone mass by Wnt10b. Proc Natl Acad Sci U S A. 2005;102(9):3324-9.

51.   Kang S, Bennett CN, Gerin I, Rapp LA, Hankenson KD, Macdougald OA. Wnt signaling stimulates osteoblastogenesis of mesenchymal precursors by suppressing CCAAT/enhancer-binding protein alpha and peroxisome proliferator-activated receptor gamma. J Biol Chem. 2007;282(19):14515-24.

52.   Gaur T, Lengner CJ, Hovhannisyan H, Bhat RA, Bodine PV, Komm BS, et al. Canonical WNT signaling promotes osteogenesis by directly stimulating *RUNX-2* gene expression. J Biol Chem. 2005;280(39):33132-40.

53.   Kato M, Patel MS, Levasseur R, Lobov I, Chang BH, Glass DA, 2nd, et al. Cbfa1-independent decrease in osteoblast proliferation, osteopenia, and persistent embryonic eye vascularization in mice deficient in Lrp5, a Wnt coreceptor. J Cell Biol. 2002;157(2):303-14.

54.   Kokubu C, Heinzmann U, Kokubu T, Sakai N, Kubota T, Kawai M, et al. Skeletal defects in ringelschwanz mutant mice reveal that Lrp6 is required for proper somitogenesis and osteogenesis. Development. 2004;131(21):5469-80.

55.   Gong Y, Slee RB, Fukai N, Rawadi G, Roman-Roman S, Reginato AM, et al. LDL receptor-related protein 5 (LRP5) affects bone accrual and eye development. Cell. 2001;107(4):513-23.

56.   Boyden LM, Mao J, Belsky J, Mitzner L, Farhi A, Mitnick MA, et al. High bone density due to a mutation in LDL-receptor-related protein 5. N Engl J Med. 2002;346(20):1513-21.

57.   Little RD, Carulli JP, Del Mastro RG, Dupuis J, Osborne M, Folz C, et al. A mutation in the LDL receptor-related protein 5 gene results in the autosomal dominant high-bone-mass trait. American journal of human genetics. 2002;70(1):11-9.

58.   Babij P, Zhao W, Small C, Kharode Y, Yaworsky PJ, Bouxsein ML, et al. High bone mass in mice expressing a mutant LRP5 gene. J Bone Miner Res. 2003;18(6):960-74.

59.   Morvan F, Boulukos K, Clement-Lacroix P, Roman Roman S, Suc-Royer I, Vayssiere B, et al. Deletion of a single allele of the Dkk1 gene leads to an increase in bone formation and bone mass. J Bone Miner Res. 2006;21(6):934-45.

60.   Li X, Liu P, Liu W, Maye P, Zhang J, Zhang Y, et al. Dkk2 has a role in terminal osteoblast differentiation and mineralized matrix formation. Nat Genet. 2005;37(9):945-52.

61.   Bonewald LF, Johnson ML. Osteocytes, mechanosensing and Wnt signaling. Bone. 2008;42(4):606-15.

62.   Zabka AG, Pluhar GE, Edwards RB, 3rd, Manley PA, Hayashi K, Heiner JP, et al. Histomorphometric description of allograft bone remodeling and union in a canine segmental femoral defect model: a comparison of rhBMP-2, cancellous bone graft, and absorbable collagen sponge. J Orthop Res. 2001;19(2):318-27.

63.   Sellers RS, Peluso D, Morris EA. The effect of recombinant human bone morphogenetic protein-2 (rhBMP-2) on the healing of full-thickness defects of articular cartilage. The Journal of bone and joint surgery American volume. 1997;79(10):1452-63.

64.   Wan M, Cao X. BMP signaling in skeletal development. Biochem Biophys Res Commun. 2005;328(3):651-7.

65.   Urist MR. Bone: formation by autoinduction. Science. 1965;150(3698):893-9.

66.   Katagiri T, Tsukamoto S. The unique activity of bone morphogenetic proteins in bone: a critical role of the Smad signaling pathway. Biol Chem. 2013;394(6):703-14.

67.   Chenard KE, Teven CM, He TC, Reid RR. Bone morphogenetic proteins in craniofacial surgery: current techniques, clinical experiences, and the future of personalized stem cell therapy. J Biomed Biotechnol. 2012;2012:601549.

68.   Katagiri T, Yamaguchi A, Komaki M, Abe E, Takahashi N, Ikeda T, et al. Bone morphogenetic protein-2 converts the differentiation pathway of C2C12 myoblasts into the osteoblast lineage. J Cell Biol. 1994;127(6 Pt 1):1755-66.

69.   Nishimura R, Hata K, Ikeda F, Ichida F, Shimoyama A, Matsubara T, et al. Signal transduction and transcriptional regulation during mesenchymal cell differentiation. J Bone Miner Metab. 2008;26(3):203-12.

70.   Yoshida Y, Tanaka S, Umemori H, Minowa O, Usui M, Ikematsu N, et al. Negative regulation of BMP/Smad signaling by Tob in osteoblasts. Cell. 2000;103(7):1085-97.

71.   Van Rooij E, Purcell AL, Levin AA. Developing microRNA therapeutics. Circulation research. 2012;110(3):496-507.

72.   Cai X, Hagedorn CH, Cullen BR. Human microRNAs are processed from capped, polyadenylated transcripts that can also function as mRNAs. RNA. 2004;10(12):1957-66.

73.   Nerem RM. Tissue engineering: the hope, the hype, and the future. Tissue engineering. 2006;12(5):1143-50.

74.   De Bruyn PP, Kabisch WT. Bone formation by fresh and frozen, autogenous and homogenous transplants of bone, bone marrow and periosteum. The American journal of anatomy. 1955;96(3):375-417.

75.   Zhang ZY, Teoh SH, Chong MS, Schantz JT, Fisk NM, Choolani MA, et al. Superior osteogenic capacity for bone tissue engineering of fetal compared with perinatal and adult mesenchymal stem cells. Stem Cells. 2009;27(1):126-37.

76.   Mieszawska AJ, Fourligas N, Georgakoudi I, Ouhib NM, Belton DJ, Perry CC, et al. Osteoinductive silk-silica composite biomaterials for bone regeneration. Biomaterials. 2010;31(34):8902-10.

77.   Supronowicz P, Gill E, Trujillo A, Thula T, Zhukauskas R, Ramos T, et al. Human adipose-derived side population stem cells cultured on demineralized bone matrix for bone tissue engineering. Tissue Eng Part A. 2011;17(5-6):789-98.

78.   Binderman I, Yaffe A, Zohar R, Benayahu D, Bahar H. Tissue engineering of bone: an ectopic rat model. Frontiers in bioscience. 2011;3:61-8.

79.   Chen Q, Yang Z, Sun S, Huang H, Sun X, Wang Z, et al. Adipose-derived stem cells modified genetically in vivo promote reconstruction of bone defects. Cytotherapy. 2010;12(6):831-40.

80.   Kitoh H, Kitakoji T, Tsuchiya H, Mitsuyama H, Nakamura H, Katoh M, et al. Transplantation of marrow-derived mesenchymal stem cells and platelet-rich plasma during distraction osteogenesis--a preliminary result of three cases. Bone. 2004;35(4):892-8.

81.   Cowan CM, Soo C, Ting K, Wu B. Evolving concepts in bone tissue engineering. Current topics in developmental biology. 2005;66:239-85.

82.   Scotti C, Tonnarelli B, Papadimitropoulos A, Scherberich A, Schaeren S, Schauerte A, et al. Recapitulation of endochondral bone formation using human adult mesenchymal stem cells as a paradigm for developmental engineering. Proc Natl Acad Sci U S A. 2010;107(16):7251-6.

83.   Gawlitta D, Farrell E, Malda J, Creemers LB, Alblas J, Dhert WJ. Modulating endochondral ossification of multipotent stromal cells for bone regeneration. Tissue engineering Part B, Reviews. 2010;16(4):385-95.

84.   Vemuri MC, Chase LG, Rao MS. Mesenchymal stem cell assays and applications. Methods Mol Biol. 2011;698:3-8.

85.   Friedenstein AJ, Chailakhjan RK, Lalykina KS. The development of fibroblast colonies in monolayer cultures of guinea-pig bone marrow and spleen cells. Cell Tissue Kinet. 1970;3(4):393-403.

86.   Dexter TM, Allen TD, Lajtha LG. Conditions controlling the proliferation of haemopoietic stem cells in vitro. J Cell Physiol. 1977;91(3):335-44.

87.   Caplan AI. Mesenchymal stem cells. Journal of orthopaedic research : official publication of the Orthopaedic Research Society. 1991;9(5):641-50.

88.   Dominici M, Le Blanc K, Mueller I, Slaper-Cortenbach I, Marini F, Krause D, et al. Minimal criteria for defining multipotent mesenchymal stromal cells. The International Society for Cellular Therapy position statement. Cytotherapy. 2006;8(4):315-7.

89.   Meirelles Lda S, Nardi NB. Methodology, biology and clinical applications of mesenchymal stem cells. Front Biosci (Landmark Ed). 2009;14:4281-98.

90.   Koo BK, Park IY, Kim J, Kim JH, Kwon A, Kim M, et al. Isolation and characterization of chorionic mesenchymal stromal cells from human full term placenta. J Korean Med Sci. 2012;27(8):857-63.

91.   Horwitz EM, Le Blanc K, Dominici M, Mueller I, Slaper-Cortenbach I, Marini FC, et al. Clarification of the nomenclature for MSC: The International Society for Cellular Therapy position statement. Cytotherapy. 2005;7(5):393-5.

92.   Miki T, Lehmann T, Cai H, Stolz DB, Strom SC. Stem cell characteristics of amniotic epithelial cells. Stem Cells. 2005;23(10):1549-59.

93.   Bilic G, Zeisberger SM, Mallik AS, Zimmermann R, Zisch AH. Comparative characterization of cultured human term amnion epithelial and mesenchymal stromal cells for application in cell therapy. Cell Transplant. 2008;17(8):955-68.

94.   Alviano F, Fossati V, Marchionni C, Arpinati M, Bonsi L, Franchina M, et al. Term Amniotic membrane is a high throughput source for multipotent Mesenchymal Stem Cells with the ability to differentiate into endothelial cells in vitro. BMC Dev Biol. 2007;7:11.

95.   Zhang Y, Adachi Y, Suzuki Y, Minamino K, Iwasaki M, Hisha H, et al. Simultaneous injection of bone marrow cells and stromal cells into bone marrow accelerates hematopoiesis in vivo. Stem Cells. 2004;22(7):1256-62.

96.   Koizumi NJ, Inatomi TJ, Sotozono CJ, Fullwood NJ, Quantock AJ, Kinoshita S. Growth factor mRNA and protein in preserved human amniotic membrane. Curr Eye Res. 2000;20(3):173-7.

97.   Mizokami T, Hisha H, Okazaki S, Takaki T, Wang XL, Song CY, et al. Preferential expansion of human umbilical cord blood-derived CD34-positive cells on major histocompatibility complex-matched amnion-derived mesenchymal stem cells. Haematologica. 2009;94(5):618-28.

98.   Fauza D. Amniotic fluid and placental stem cells. Best Pract Res Clin Obstet Gynaecol. 2004;18(6):877-91.

99.   Zhang Y, Li C, Jiang X, Zhang S, Wu Y, Liu B, et al. Human placenta-derived mesenchymal progenitor cells support culture expansion of long-term culture-initiating cells from cord blood CD34+ cells. Exp Hematol. 2004;32(7):657-64.

100.   Chien CC, Yen BL, Lee FK. In vitro differentiation of human placenta-derived multipotent cells into hepatocyte-like cells. Stem Cells. 2006;24:1759-68.

101.   Li C, Zhang W, Jiang X, Mao N. Human-placenta-derived mesenchymal stem cells inhibit proliferation and function of allogeneic immune cells. Cell Tissue Res. 2007;330(3):437-46.

102.   Weiss ML, Medicetty S, Bledsoe AR, Rachakatla RS, Choi M, Merchav S, et al. Human umbilical cord matrix stem cells: preliminary characterization and effect of transplantation in a rodent model of Parkinson's disease. Stem Cells. 2006;24(3):781-92.

103.   Mitchell KE, Weiss ML, Mitchell BM, Martin P, Davis D, Morales L, et al. Matrix cells from Wharton's jelly form neurons and glia. Stem Cells. 2003;21(1):50-60.

104.   Chen MY, Lie PC, Li ZL, Wei X. Endothelial differentiation of Wharton's jelly-derived mesenchymal stem cells in comparison with bone marrow-derived mesenchymal stem cells. Exp Hematol. 2009;37(5):629-40.

105.   Anzalone R, Lo Iacono M, Corrao S, Magno F, Loria T, Cappello F, et al. New emerging potentials for human Wharton's jelly mesenchymal stem cells: immunological features and hepatocyte-like differentiative capacity. Stem Cells Dev. 2010;19(4):423-38.

106.   Prockop DJ. Repair of tissues by adult stem/progenitor cells (MSCs): controversies, myths, and changing paradigms. Mol Ther. 2009;17(6):939-46.

107.   Kern S, Eichler H, Stoeve J, Kluter H, Bieback K. Comparative analysis of mesenchymal stem cells from bone marrow, umbilical cord blood, or adipose tissue. Stem Cells. 2006;24(5):1294-301.

108. Bieback K, Kern S, Kocaomer A, Ferlik K, Bugert P. Comparing mesenchymal stromal cells from different human tissues: bone marrow, adipose tissue and umbilical cord blood. Biomed Mater Eng. 2008;18(1 Suppl):S71-6.

109. Bernardo ME, Locatelli F, Fibbe WE. Mesenchymal stromal cells. Ann N Y Acad Sci. 2009;1176:101-17.

110. Bianco P, Kuznetsov SA, Riminucci M, Gehron Robey P. Postnatal skeletal stem cells. Methods Enzymol. 2006;419:117-48.

111. Gronthos S, Brahim J, Li W, Fisher LW, Cherman N, Boyde A, et al. Stem cell properties of human dental pulp stem cells. J Dent Res. 2002;81(8):531-5.

112. Augello A, De Bari C. The regulation of differentiation in mesenchymal stem cells. Hum Gene Ther. 2010;21(10):1226-38.

113. Hao M, Meng HX, Li G, Qi PJ, Xu Y, Li CH, et al. [Study of influence of umbilical cord mesenchymal stem cells on CD34+ cells in vivo homing in NOD/SCID]. Zhonghua Xue Ye Xue Za Zhi. 2009;30(2):103-6.

114. Noort WA, Feye D, Van Den Akker F, Stecher D, Chamuleau SA, Sluijter JP, et al. Mesenchymal stromal cells to treat cardiovascular disease: strategies to improve survival and therapeutic results. Panminerva Med. 2010;52(1):27-40.

115. Daar AS, Greenwood HL. A proposed definition of regenerative medicine. J Tissue Eng Regen Med. 2007;1(3):179-84.

116. Branski LK, Gauglitz GG, Herndon DN, Jeschke MG. A review of gene and stem cell therapy in cutaneous wound healing. Burns. 2009;35(2):171-80.

117. Vanecek V, Klima K, Kohout A, Foltan R, Jirousek O, Sedy J, et al. The combination of mesenchymal stem cells and a bone scaffold in the treatment of vertebral body defects. Eur Spine J. 2013;22(12):2777-86.

118. Kawate K, Yajima H, Ohgushi H, Kotobuki N, Sugimoto K, Ohmura T, et al. Tissue-engineered approach for the treatment of steroid-induced osteonecrosis of the femoral head: transplantation of autologous mesenchymal stem cells cultured with

beta-tricalcium phosphate ceramics and free vascularized fibula. Artif Organs. 2006;30(12):960-2.

119. Porter RM, Huckle WR, Goldstein AS. Effect of dexamethasone withdrawal on osteoblastic differentiation of bone marrow stromal cells. J Cell Biochem. 2003;90(1):13-22.

120. Bellows CG, Heersche JN, Aubin JE. Determination of the capacity for proliferation and differentiation of osteoprogenitor cells in the presence and absence of dexamethasone. Dev Biol. 1990;140(1):132-8.

121. Kamalia N, McCulloch CA, Tenebaum HC, Limeback H. Dexamethasone recruitment of self-renewing osteoprogenitor cells in chick bone marrow stromal cell cultures. Blood. 1992;79(2):320-6.

122. Mazziotti G, Angeli A, Bilezikian JP, Canalis E, Giustina A. Glucocorticoid-induced osteoporosis: an update. Trends Endocrinol Metab. 2006;17(4):144-9.

123. Murad S, Grove D, Lindberg KA, Reynolds G, Sivarajah A, Pinnell SR. Regulation of collagen synthesis by ascorbic acid. Proc Natl Acad Sci U S A. 1981;78(5):2879-82.

124. Franceschi RT, Iyer BS, Cui Y. Effects of ascorbic acid on collagen matrix formation and osteoblast differentiation in murine MC3T3-E1 cells. J Bone Miner Res. 1994;9(6):843-54.

125. Chung CH, Golub EE, Forbes E, Tokuoka T, Shapiro IM. Mechanism of action of beta-glycerophosphate on bone cell mineralization. Calcif Tissue Int. 1992;51(4):305-11.

126. Chang YL, Stanford CM, Keller JC. Calcium and phosphate supplementation promotes bone cell mineralization: implications for hydroxyapatite (HA)-enhanced bone formation. J Biomed Mater Res. 2000;52(2):270-8.

127. Fernandes KJ, McKenzie IA, Mill P, Smith KM, Akhavan M, Barnabe-Heider F, et al. A dermal niche for multipotent adult skin-derived precursor cells. Nat Cell Biol. 2004;6(11):1082-93.

128.	Sood R, Zehnder JL, Druzin ML, Brown PO. Gene expression patterns in human placenta. Proc Natl Acad Sci U S A. 2006;103(14):5478-83.

129.	Gupta A, Kedige SD, Jain K. Amnion and Chorion Membranes: Potential Stem Cell Reservoir with Wide Applications in Periodontics. Int J Biomater. 2015;2015:274082.

130.	Gestational Trophoblastic Disease. In: Hui P, editor. Gestational Trophoblastic Disease: Diagnostic and Molecular Genetic Pathology. Current Clinical Pathology. LLC: Humana Press; 2012. p. XIII, 205.

131.	Gude NM, Roberts CT, Kalionis B, King RG. Growth and function of the normal human placenta. Thromb Res. 2004;114(5-6):397-407.

132.	Kobayashi K, Kubota T, Aso T. Study on myofibroblast differentiation in the stromal cells of Wharton's jelly: expression and localization of alpha-smooth muscle actin. Early Hum Dev. 1998;51(3):223-33.

133.	Ambros V. The functions of animal microRNAs. Nature. 2004;431(7006):350-5.

134.	Ambros V, Chen X. The regulation of genes and genomes by small RNAs. Development. 2007;134(9):1635-41.

135.	Bentwich I, Avniel A, Karov Y, Aharonov R, Gilad S, Barad O, et al. Identification of hundreds of conserved and nonconserved human microRNAs. Nat Genet. 2005;37(7):766-70.

136.	Lagos-Quintana M, Rauhut R, Lendeckel W, Tuschl T. Identification of novel genes coding for small expressed RNAs. Science. 2001;294(5543):853-8.

137.	Lee Y, Jeon K, Lee JT, Kim S, Kim VN. MicroRNA maturation: stepwise processing and subcellular localization. EMBO J. 2002;21(17):4663-70.

138.	Rodriguez A, Griffiths-Jones S, Ashurst JL, Bradley A. Identification of mammalian microRNA host genes and transcription units. Genome Res. 2004;14(10A):1902-10.

139.   Carthew RW, Sontheimer EJ. Origins and Mechanisms of miRNAs and siRNAs. Cell. 2009;136(4):642-55.

140.   Bushati N, Cohen SM. microRNA functions. Annu Rev Cell Dev Biol. 2007;23:175-205.

141.   Gregory RI, Yan KP, Amuthan G, Chendrimada T, Doratotaj B, Cooch N, et al. The Microprocessor complex mediates the genesis of microRNAs. Nature. 2004;432(7014):235-40.

142.   Zeng Y, Yi R, Cullen BR. MicroRNAs and small interfering RNAs can inhibit mRNA expression by similar mechanisms. Proc Natl Acad Sci U S A. 2003;100(17):9779-84.

143.   Pillai RS, Bhattacharyya SN, Filipowicz W. Repression of protein synthesis by miRNAs: how many mechanisms? Trends Cell Biol. 2007;17(3):118-26.

144.   Yekta S, Shih IH, Bartel DP. MicroRNA-directed cleavage of HOXB8 mRNA. Science. 2004;304(5670):594-6.

145.   Krutzfeldt J, Poy MN, Stoffel M. Strategies to determine the biological function of microRNAs. Nat Genet. 2006;38 Suppl:S14-9.

146.   Zhao Y, Srivastava D. A developmental view of microRNA function. Trends Biochem Sci. 2007;32(4):189-97.

147.   Aüer H, Newsom DL, Kornacker K. Expression Profiling Using Affymetrix GeneChip Microarrays. Methods Mol Biol. 2009;509:35-46.

148.   Kauppinen S, Vester B, Wengel J. Locked nucleic acid: high-affinity targeting of complementary RNA for RNomics. Handb Exp Pharmacol. 2006(173):405-22.

149.   Lu J, Getz G, Miska EA, Alvarez-Saavedra E, Lamb J, Peck D, et al. MicroRNA expression profiles classify human cancers. Nature. 2005;435(7043): 834-8.

150.   Schmittgen TD, Lee EJ, Jiang J, Sarkar A, Yang L, Elton TS, et al. Real-time PCR quantification of precursor and mature microRNA. Methods. 2008;44(1):31-8.

151.   Chen C, Ridzon DA, Broomer AJ, Zhou Z, Lee DH, Nguyen JT, et al. Real-time quantification of microRNAs by stem-loop RT-PCR. Nucleic Acids Res. 2005;33(20):e179.

152.   Bartel DP. MicroRNAs: target recognition and regulatory functions. Cell. 2009;136(2):215-33.

153.   Yue D, Liu H, Huang Y. Survey of Computational Algorithms for MicroRNA Target Prediction. Curr Genomics. 2009;10(7):478-92.

154.   Lewis BP, Burge CB, Bartel DP. Conserved seed pairing, often flanked by adenosines, indicates that thousands of human genes are microRNA targets. Cell. 2005;120(1):15-20.

155.   Krek A, Grun D, Poy MN, Wolf R, Rosenberg L, Epstein EJ, et al. Combinatorial microRNA target predictions. Nat Genet. 2005;37(5):495-500.

156.   John B, Enright AJ, Aravin A, Tuschl T, Sander C, Marks DS. Human MicroRNA targets. PLoS Biol. 2004;2(11):e363.

157.   Griffiths-Jones S, Grocock RJ, van Dongen S, Bateman A, Enright AJ. miRBase: microRNA sequences, targets and gene nomenclature. Nucleic Acids Res. 2006;34(Database issue):D140-4.

158.   Megraw M, Sethupathy P, Corda B, Hatzigeorgiou AG. miRGen: a database for the study of animal microRNA genomic organization and function. Nucleic Acids Res. 2007;35(Database issue):D149-55.

159.   Tome M, Lopez-Romero P, Albo C, Sepulveda JC, Fernandez-Gutierrez B, Dopazo A, et al. miR-335 orchestrates cell proliferation, migration and differentiation in human mesenchymal stem cells. Cell Death Differ. 2011;18(6):985-95.

160.   Zhang Y, Xie RL, Croce CM, Stein JL, Lian JB, van Wijnen AJ, et al. A program of microRNAs controls osteogenic lineage progression by targeting transcription factor *RUNX-2RUNX-2*. Proc Natl Acad Sci U S A. 2011;108(24):9863-8.

161.   Hassan MQ, Gordon JA, Beloti MM, Croce CM, van Wijnen AJ, Stein JL, et al. A network connecting *RUNX-2*, SATB2, and the miR-23a~27a~24-2 cluster regulates the osteoblast differentiation program. Proc Natl Acad Sci U S A. 2010;107(46):19879-84.

162.   Deng Y, Zhou H, Zou D, Xie Q, Bi X, Gu P, et al. The role of miR-31-modified adipose tissue-derived stem cells in repairing rat critical-sized calvarial defects. Biomaterials. 2013;34(28):6717-28.

163.   Deng Y, Zhou H, Gu P, Fan X. Repair of canine medial orbital bone defects with miR-31-modified bone marrow mesenchymal stem cells. Invest Ophthalmol Vis Sci. 2014;55(9):6016-23.

164.   Li H, Li T, Wang S, Wei J, Fan J, Li J, et al. miR-17-5p and miR-106a are involved in the balance between osteogenic and adipogenic differentiation of adipose-derived mesenchymal stem cells. Stem Cell Res. 2013;10(3):313-24.

165.   Cheng P, Chen C, He HB, Hu R, Zhou HD, Xie H, et al. miR-148a regulates osteoclastogenesis by targeting V-maf musculoaponeurotic fibrosarcoma oncogene homolog B. J Bone Miner Res. 2013;28(5):1180-90.

166.   Leboy PS. Regulating bone growth and development with bone morphogenetic proteins. Ann N Y Acad Sci. 2006;1068:14-8.

167.   Li Z, Hassan MQ, Volinia S, van Wijnen AJ, Stein JL, Croce CM, et al. A microRNA signature for a BMP2-induced osteoblast lineage commitment program. Proc Natl Acad Sci U S A. 2008;105(37):13906-11.

168.   Javed A, Bae JS, Afzal F, Gutierrez S, Pratap J, Zaidi SK, et al. Structural coupling of Smad and *RUNX-2* for execution of the BMP2 osteogenic signal. J Biol Chem. 2008;283(13):8412-22.

169.   Inose H, Ochi H, Kimura A, Fujita K, Xu R, Sato S, et al. A microRNA regulatory mechanism of osteoblast differentiation. Proc Natl Acad Sci U S A. 2009;106(49):20794-9.

170. Lecanda F, Warlow PM, Sheikh S, Furlan F, Steinberg TH, Civitelli R. Connexin43 deficiency causes delayed ossification, craniofacial abnormalities, and osteoblast dysfunction. J Cell Biol. 2000;151(4):931-44.

171. Creemers EE, Tijsen AJ, Pinto YM. Circulating microRNAs: novel biomarkers and extracellular communicators in cardiovascular disease? Circulation research. 2012;110(3):483-95.

172. Etheridge A, Lee I, Hood L, Galas D, Wang K. Extracellular microRNA: a new source of biomarkers. Mutation research. 2011;717(1-2):85-90.

173. Valadi H, Ekstrom K, Bossios A, Sjostrand M, Lee JJ, Lotvall JO. Exosome-mediated transfer of mRNAs and microRNAs is a novel mechanism of genetic exchange between cells. Nat Cell Biol. 2007;9(6):654-9.

174. Zernecke A, Bidzhekov K, Noels H, Shagdarsuren E, Gan L, Denecke B, et al. Delivery of microRNA-126 by apoptotic bodies induces CXCL12-dependent vascular protection. Science signaling. 2009;2(100):ra81.

175. Arroyo JD, Chevillet JR, Kroh EM, Ruf IK, Pritchard CC, Gibson DF, et al. Argonaute2 complexes carry a population of circulating microRNAs independent of vesicles in human plasma. Proc Natl Acad Sci U S A. 2011;108(12):5003-8.

176. Turchinovich A, Weiz L, Langheinz A, Burwinkel B. Characterization of extracellular circulating microRNA. Nucleic Acids Res. 2011;39(16):7223-33.

177. Vickers KC, Palmisano BT, Shoucri BM, Shamburek RD, Remaley AT. MicroRNAs are transported in plasma and delivered to recipient cells by high-density lipoproteins. Nat Cell Biol. 2011;13(4):423-33.

178. Elmen J, Lindow M, Schutz S, Lawrence M, Petri A, Obad S, et al. LNA-mediated microRNA silencing in non-human primates. Nature. 2008;452(7189):896-9.

179. Lanford RE, Hildebrandt-Eriksen ES, Petri A, Persson R, Lindow M, Munk ME, et al. Therapeutic silencing of microRNA-122 in primates with chronic hepatitis C virus infection. Science. 2010;327(5962):198-201.

180.   van der Ree MH, van der Meer AJ, van Nuenen AC, de Bruijne J, Ottosen S, Janssen HL, et al. Miravirsen dosing in chronic hepatitis C patients results in decreased microRNA-122 levels without affecting other microRNAs in plasma. Alimentary pharmacology & therapeutics. 2016;43(1):102-13.

181.   Laitala-Leinonen T. Update on the development of microRNA and siRNA molecules as regulators of cell physiology. Recent Pat DNA Gene Seq. 2010;4(2):113-21.

182.   Petite H, Viateau V, Bensaid W, Meunier A, de Pollak C, Bourguignon M, et al. Tissue-engineered bone regeneration. Nat Biotechnol. 2000;18(9):959-63.

183.   Koc ON, Lazarus HM. Mesenchymal stem cells: heading into the clinic. Bone Marrow Transplant. 2001;27(3):235-9.

184.   Na K, Kim SW, Sun BK, Woo DG, Yang HN, Chung HM, et al. Osteogenic differentiation of rabbit mesenchymal stem cells in thermo-reversible hydrogel constructs containing hydroxyapatite and bone morphogenic protein-2 (BMP-2). Biomaterials. 2007;28(16):2631-7.

185.   Luu HH, Song WX, Luo X, Manning D, Luo J, Deng ZL, et al. Distinct roles of bone morphogenetic proteins in osteogenic differentiation of mesenchymal stem cells. Journal of orthopaedic research : official publication of the Orthopaedic Research Society. 2007;25(5):665-77.

186.   Osyczka AM, Damek-Poprawa M, Wojtowicz A, Akintoye SO. Age and skeletal sites affect BMP-2 responsiveness of human bone marrow stromal cells. Connect Tissue Res. 2009;50(4):270-7.

187.   Lieberman JR, Daluiski A, Stevenson S, Wu L, McAllister P, Lee YP, et al. The effect of regional gene therapy with bone morphogenetic protein-2-producing bone-marrow cells on the repair of segmental femoral defects in rats. J Bone Joint Surg Am. 1999;81(7):905-17.

188.   Lin Z, Wang JS, Lin L, Zhang J, Liu Y, Shuai M, et al. Effects of BMP2 and VEGF165 on the osteogenic differentiation of rat bone marrow-derived mesenchymal stem cells. Exp Ther Med. 2014;7(3):625-9.

189.   Arinzeh TL, Peter SJ, Archambault MP, van den Bos C, Gordon S, Kraus K, et al. Allogeneic mesenchymal stem cells regenerate bone in a critical-sized canine segmental defect. J Bone Joint Surg Am. 2003;85-A(10):1927-35.

190.   Viateau V, Guillemin G, Bousson V, Oudina K, Hannouche D, Sedel L, et al. Long-bone critical-size defects treated with tissue-engineered grafts: a study on sheep. Journal of orthopaedic research : official publication of the Orthopaedic Research Society. 2007;25(6):741-9.

191.   Lu LL, Liu YJ, Yang SG, Zhao QJ, Wang X, Gong W, et al. Isolation and characterization of human umbilical cord mesenchymal stem cells with hematopoiesis-supportive function and other potentials. Haematologica. 2006;91(8):1017-26.

192.   Wagner W, Wein F, Seckinger A, Frankhauser M, Wirkner U, Krause U, et al. Comparative characteristics of mesenchymal stem cells from human bone marrow, adipose tissue, and umbilical cord blood. Exp Hematol. 2005;33(11):1402-16.

193.   Kratchmarova I, Blagoev B, Haack-Sorensen M, Kassem M, Mann M. Mechanism of divergent growth factor effects in mesenchymal stem cell differentiation. Science. 2005;308(5727):1472-7.

194.   Sethe S, Scutt A, Stolzing A. Aging of mesenchymal stem cells. Ageing Res Rev. 2006;5(1):91-116.

195.   Wagner W, Bork S, Horn P, Krunic D, Walenda T, Diehlmann A, et al. Aging and replicative senescence have related effects on human stem and progenitor cells. PloS one. 2009;4(6):e5846.

196.   Wan DC, Siedhoff MT, Kwan MD, Nacamuli RP, Wu BM, Longaker MT. Refining retinoic acid stimulation for osteogenic differentiation of murine adipose-derived adult stromal cells. Tissue engineering. 2007;13(7):1623-31.

197.   Ryoo HM, Lee MH, Kim YJ. Critical molecular switches involved in BMP-2-induced osteogenic differentiation of mesenchymal cells. Gene. 2006;366(1):51-7.

198.   Nakashima K, Zhou X, Kunkel G, Zhang Z, Deng JM, Behringer RR, et al. The novel zinc finger-containing transcription factor osterix is required for osteoblast differentiation and bone formation. Cell. 2002;108(1):17-29.

199.   Lee KS, Kim HJ, Li QL, Chi XZ, Ueta C, Komori T, et al. *RUNX-2* is a common target of transforming growth factor beta1 and bone morphogenetic protein 2, and cooperation between *RUNX-2* and Smad5 induces osteoblast-specific gene expression in the pluripotent mesenchymal precursor cell line C2C12. Molecular and cellular biology. 2000;20(23):8783-92.

200.   Oskowitz AZ, Lu J, Penfornis P, Ylostalo J, McBride J, Flemington EK, et al. Human multipotent stromal cells from bone marrow and microRNA: regulation of differentiation and leukemia inhibitory factor expression. Proc Natl Acad Sci U S A. 2008;105(47):18372-7.

201.   Xie Q, Wang Z, Bi X, Zhou H, Wang Y, Gu P, et al. Effects of miR-31 on the osteogenesis of human mesenchymal stem cells. Biochem Biophys Res Commun. 2014;446(1):98-104.

APPENDIX

APPENDIX A

Reagents and Instrumentations

Reagents

0.25% Trypsin-EDTA	(Cat. No. 25200, GibcoBRL, USA)
2-Propanol	(Cat. No. 109634, Merck, Germany)
BCIP®/NBT Liquid substrate	(Cat. No. B1911, Sigma-Aldrich, USA)
β-glycerophosphate	(Cat. No. G9422, Sigma-Aldrich, USA)
Alizarin Red S	(Cat. No. A3757, Sigma-Aldrich, USA)
Bovine serum albumin (BSA)	(Cat. No. A7888, Sigma-Aldrich, USA)
Bradford reagent	(Cat. No. 5000006, Bio-Rad, USA)
Collagenase from Clostridium	(Cat. No. C2674, Sigma-Aldrich, USA)
D-glucose anhydrous	(Cat. No. 783, Ajax Finechem, Australia)
Deoxyribonuclease I	(Cat. No. D5025, Sigma-Aldrich, USA)
Dexamethasone	(Cat. No. D4902, Sigma-Aldrich, USA)
Dimethyl sulfoxide (DMSO)	(Cat. No. 0231, Sigma-Aldrich, USA)
Dulbecco's Modified Eagle's Medium (DMEM)	(Cat. No. 31600034, GibcoBRL, USA)
Fetal bovine serum	(Cat. No. 26140, GibcoBRL, USA)
FAM™ Dye-Labeled Anti-miR™ Negative Control #1	Cat. No. AM17012, Applied Biosystems, USA)
Ficoll-Paque PLUS solution	(Cat. No. 17-1440-02, GE Healthcare, Bio-Science AB, Sweden)

GlutaMAX^{TM}	(Cat. No. 35050, GibcoBRL, USA)
Indomethacin	(Cat. No. I7378, Sigma-Aldrich, USA)
IsoPrep	(Robbins Scientific Corporation, USA)
Insulin from bovine pancreas	(Cat. No. I6634, Sigma-Aldrich, USA)
Isobutylxanthine	(Cat. No. I7018, Sigma-Aldrich, USA)
L-ascorbic acid	(Cat. No. A4403, Sigma-Aldrich, USA)
Lipofectamine$^®$ RNAiMAX	(Cat. No. IV06 13778, Invitrogen, USA)
Oil red O	(Cat. No. O0625, Sigma-Aldrich, USA)
Penicilin/Streptromycin	(Cat. No. 15140, GibcoBRL, USA)
PureLink^{TM} RNA Mini kit	(Cat. No. 12183018A, Invitrogen, USA)
Recombinant Human BMP-2, CF	(Cat. No. 355-BM-050/CF, R& D Systems Inc., USA)
SensoLyte pNPP Alkaline Phosphatase Assay	(Cat. No. 72146, AnaSpec, USA)
SuperScript$^®$ III First Strand Synthesis Kit	(Cat. No. 18080, Invitrogen, USA)
SYBR$^®$ Green PCR Master Mix	(Cat. No. 11784200, Invitrogen, USA)
Trizol$^®$ reagent	(Cat. No. 15596026, Invitrogen, USA)
TaqMan$^®$ MicroRNA Assays (U6)	(Cat. No. 4427975, Applied Biosystems, USA)
TaqMan$^®$ MicroRNA Assays (hsa-miR-31-5p)	(Cat. No. 4427975, Applied Biosystems, USA)
TaqMan$^®$ MicroRNA Assays (hsa-miR-106a-5p)	(Cat. No. 4427975, Applied Biosystems, USA)
TaqMan$^®$ MicroRNA Assays (hsa-miR-148a-5p)	(Cat. No. 4427975, Applied Biosystems, USA)
TaqMan$^®$ MicroRNA Assays (U6)	(Cat. No. 4427975, Applied Biosystems, USA)
TaqMan Universal Master Mix II, with UNG	(Cat. No. 4440038, Applied Biosystems, USA)
TaqMan$^®$ MicroRNA Reverse Transcription Kit	(Cat. No. 4366596, Applied Biosystems, USA)

Antibodies

FITC anti-human CD45   (Cat. No. 304006, BioLegend, USA)

FITC anti-human CD90   (Cat. No. 328108, BioLegend, USA)

PE anti-human CD34   (Cat. No. 343506, BioLegend, USA)

PE anti-human CD73   (Cat. No. 344004, BioLegend, USA)

PE Mouse anti-human CD105   (Cat. No. 560839, BD Bioscience, USA)

Instrumentations

BD FACScalibur™	(Becton Dickinson, USA)
Class II biological safety cabinets	(LABCONCO, USA)
Centrifugation Machine	(Hettich, Universal 320K, USA)
CO_2 incubator	(NUAIRE TM, USA)
Freezer (-20 °C Templow)	(J.P. SELECTA, Japan)
Freezer (-80°C)	(Sunyo, Japan)
Inverted microscopy (TS100)	(Nikon, Japan)
Microplate reader	(BioTex, USA)
Sunyo Biomedical Freezer	(Sunyo, Japan)
Step one plus™ Real-Time PCR machine	(Applied Biosystems; ABI, USA)
Water bath	(Julabo, USA)

Plasticwares and miscellaneous

0.40 µm Sterile Syringe Filter   (Corning Intercorporated, USA)

6-well plate   (Corning Intercorporated, USA)

24-well plate   (Corning Intercorporated, USA)

96-well plate   (Corning Intercorporated, USA)

35 mm^2 dish   (Corning Intercorporated, USA)

15 ml falcon tube   (Corning Intercorporated, USA)

50 ml falcon tube   (Corning Intercorporated, USA)

Universal fit pipet tips 0.1-10 µl   (Corning Intercorporated, USA)

Universal fit pipet tips 1-200 µl   (Corning Intercorporated, USA)

Universal fit pipet tips 100-1000 µl   (Corning Intercorporated, USA)

Serological pipettes 2 ml   (Corning Intercorporated, USA)

Serological pipettes 5 ml   (Corning Intercorporated, USA)

Serological pipettes 10 ml   (Corning Intercorporated, USA)

Serological pipettes 25 ml   (Corning Intercorporated, USA)

T25 Cell Culture Flask   (Corning Intercorporated, USA)

T75 Cell Culture Flask   (Corning Intercorporated, USA)

APPENDIX B

Reagent Preparation

10X Phosphate buffered saline (PBS)

NaCl	76.5 g
Na_2HPO_4	9.9 g
KH_2PO_4	4.0 g
Distilled water to	1 L

The stock buffer was prepared by dissolving all of above reagents in distilled water, mixed until complete dissolving, adjust pH 7.4, added distilled water to final volume of 1 L and autoclaved. The solution was steriled by autoclaving for 15 min at 121°C, 151b/square inches and store at 4°C.

1X Phosphate buffered saline (PBS)

10X PBS	50 ml
Distilled water	450 ml

The buffer was prepared by mixed 50 ml 10X PBS with 450 ml steriled distilled water. The solution was stored at 4°C.

16% Paraformaldehyde

Paraformaldehyde	80 g
Distilled water	450 ml
10 N NaOH	500 µl

The stock solution was prepared by dissolving all above reagents in distilled water, heat the solution while stirring until the solution was clears, equilibrated to pH 7.4 and added volume to 500 ml. The solution was filtered and stored at 4°C.

4% Paraformaldehyde

16% Paraformaldehyde	2.5 ml
1X PBS	7.5 ml

The solution was prepared by mixed 2.5 ml 16% paraformaldehyde with 7.5 ml 1X PBS and used immediately.

DMEM stock solution

DMEM	1 pack
NaHCO$_3$	3.7 g
Distilled water to	1 L

The stock solution was prepared by dissolving all above reagents in distilled water, stirred until the solution was clear, equilibrated to pH 7.4 and added volume to 1 L. The solution was filtered and stored at 4°C.

DMEM + 10%FBS

DMEM solution	44 ml
FBS	5 ml
1X Penicillin/streptomycin	500 µl
L-glutamine	500 µl

The solution was prepared by mixed all above reagents, stored at 4°C.

2.5 M D-glucose (25 ml)

D-glucose	11.26 g
Distilled water to	25 ml

The solution was prepared by dissolved D-glucose in 25 ml distilled water, filtered with 0.40 µm sterile syringe filter and stored at -20°C

0.5% (w/v) Oil red O in isopropanol

Oil red O	0.5 g
2-Propanol (Isopropanol)	100 ml

The stock solution was prepared by dissolved oil red O in isopropanol and stored at 4°C

Oil red O working solution

0.5% (w/v) Oil red O in isopropanol	6 ml
Distilled water	4 ml

The solution was prepared by dissolving stock Oil red O in distilled water, filtered with Whatman #1 filter paper and used immediately.

Adipogenic differentiation medium

Complete DMEM	48.4 ml
Isobutylxanthine	5.75 mg
20 mM indomethacin	500 µl
2.5 M glucose	500 µl
1 mM Dexamethasone	50 µl
1 mg/ml insulin	50 µl

The solution was prepared by added all above reagents in complete DMEM, filtered with 0.40 µm sterile syringe filter and stored at 4°C.

Osteogenic differentiation medium I

Stock DMEM	44.05 ml
FBS	4.95 ml
1X Penicillin/Streptomycin	500 µl
0.1µM Dexamethasone	500 µl
60 mM Ascorbic acid	500 µl

The solution was prepared by added all reagent above without ascorbic acid in stock DMEM, filtered with 0.40 µm sterile syringe filter and stored at 4°C. Added ascorbic acid freshly before used.

Osteogenic differentiation medium II

Stock DMEM	39.60 ml
FBS	4.45 ml
1X Penicillin/Streptomycin	450 µl
0.1µM Dexamethasone	500 µl
10 mM β-glycerophosphate	5 ml
60 mM Ascorbic acid	500 µl

The solution was prepared by added all above reagents without ascorbic acid in stock DMEM, filtered with 0.40 µm sterile syringe filter and stored at 4°C. Added ascorbic acid freshly before used.

40mM Alizarin Red S

Alizarin Red S	0.274 g
Distilled water	50 ml

The stock solution was prepared by dissolved Alizarin Red S in distilled water, stirred to mix until homogeneous, adjusted pH to 4.1 with 10% (v/v) ammonium hydroxide and stored at room temperature. Keep working ARS dye solution in dark container (cover with foil).

10 µg/ml Recombinant Human BMP-2

Recombinant Human BMP-2	50 µg
Sterile 4 mM HCl	5 ml

The solution was prepared by dissolved Recombinant Human BMP-2 in sterile 4mM HCl and stored at -20°C.

4mM HCl

1 N HCl	1 ml
Distilled water	249 ml

The solution was prepared by adding 1 ml HCl 1N to 249 ml distilled water, filtered with 0.40 µm sterile syringe filter and stored at 4°C.

APPENDIX C

Experiment Procedures

Isolation and culturation of MSCs from bone marrow

Reagents:

DMEM + 10% FBS (v/v) + 2 mM L-glutamine + 100 U/ml penicillin + 100 µg/ml streptomycin

1X Phosphate buffered saline + 100 U/ml penicillin + 100 µg/ml streptomycin

Ficoll-Paque PLUS solution

0.25% trypsin EDTA

5,000 i.u./u.i./ml Heparin

Materials and instruments:

50 ml Falcon tube

Centrifugation machine

Serological pipettes 10 ml

T25 cell culture flask

Procedure

1. Aspirate bone marrow (10 ml) from sternum and place into 50 ml Falcol tube containing 500 µl of heparin (LEO 5,000 i.u./u.i./ml).

2. Dilute at 1:1 ratio with 1X phosphate buffered saline (1XPBS) + 100 U/ml penicillin + 100 µl/ml streptomycin and carefully load onto Ficoll-Paque PLUS solution

3. Centrifuge at 2,000 x g (Hettich, Universal 320K, USA) for 30 min at 20°C.

4. Collect mononuclear cells (MNCs) from the interphase and wash twice with 15 ml of 1X PBS + 100 U/ml penicillin + 100 µl/ml streptomycin.

5. Count cells with hematocytometer.

6. Seed at a density of 1 x 10^5 cells/cm^2 into 25 cm^2 tissue culture flask with DMEM supplement with 2 mM L-glutamine (GibcoBRL, USA) + 10% fetal bovine serum (FBS) + 100 U/ml penicillin + 100 µg/ml streptomycin.

7. Incubate at 37°C, 5% CO_2.

8. Remove non-adherent cells after culture for 3 days

9. Change the medium every 3 - 4 days.

10. Trypsinize the cells using 0.25% trypsin/2 mM EDTA (GibcoBRL, USA) when the cells reach 80% confluence.

11. Re-plate the cells at a density of 1 x 10^4 cells/cm^2.

Isolation and culturation of MSCs from postnatal tissues

Reagents:

DMEM + 10% FBS (v/v) + 2 mM L-glutamine + 100 U/ml penicillin + 100 µg/ml streptomycin

1X Phosphate buffered saline+100 U/ml penicillin+100 µg/ml streptomycin

1.6 mg/ml Collagenase type I-A

200 mg/ml Deoxyribonuclease I

0.25 % Trypsin EDTA

Materials and instruments:

50 ml Falcon tube

Centrifugation machine

Serological pipettes 10 ml

T25 cell culture flask

Procedure

1. Dissect postnatal tissues including amniotic tissue (diameter 5 cm), chorionic tissue (diameter 5 cm), placental tissue (3 x 3 cm^2 in size), umbilical cord (3 - 4 cm^2 in size).

2. Rinse with 1X PBS +100 U/ml penicillin + 100 µg/ml streptomycin and mince into small pieces (1-2 mm^2 in size).

3. Wash the tissues with 1X PBS + 100 U/ml penicillin + 100 µg/ml streptomycin.

4. Centrifuge at 2,000 x g for 5 min

5. Collect the pellets and digested with 5 ml of 1.6 mg/ml collagenase type IX (Sigma-Aldrich, USA.) and 200 mg/ml deoxyribonuclease I (Sigma-Aldrich, USA.) for 4 hours at 37°C with shaking.

6. Wash twice with 1X PBS + 100 U/ml penicillin + 100 µg/ml streptomycin, then centrifuge at 2,000 x g for 5 min.

7. Culture cells and all pellet in DMEM supplemented with 10% FBS + 2 mM L-glutamine + 100 U/ml penicillin + 100 µg/ml streptomycin in 25 cm^2 tissue culture flasks.

8. Maintain the cultures at 37°C in a humidifiled atmosphere containing 5% CO_2

9. Change culture medium every 3 - 4 days.

10. Remove fibroblastoid cells at day 7 (80% confluence) after initiated plating using 0.25% trypsin/ 2 mM EDTA (GibcoBRL, USA). Replate the cells at a density of 1 x 10^4 cells/cm^2.

Immunophenotypical characterization of culture cells

Reagents:

FITC-conjugated anti-human CD45 antibody

FITC-conjugated anti- human CD90 antibody

FITC-conjugated anti- human CD105antibody

PE-conjugated anti- human CD34 antibody

PE-conjugated anti- human CD73 antibody

1X Phosphate buffered saline (1X PBS)

0.25% Trypsin EDTA

1% Paraformaldehyde in 1X PBS

Materials and instruments:

10 ml Serological pipettes

15 ml Falcon tube

Centrifugation machine

Procedure

1. Wash the primary cells (passage 3 - 5) with 1X PBS

2. Add 1 ml of 0.25% trypsin-EDTA into T25-flask and incubate for 3 min at 37°C.

3. Add 1 ml of FBS to stop the reaction.

4. Centrifuge at 2,000 x g for 5 min

5. Collect the cell pellet and wash twice with 1X PBS

3. Stain cells (4×10^5 cells in 50 µl 1X PBS) with 5 µl of fluorescein isothiocyanate (FITC) or phycoerythrin (PE)-conjugated antibodies for 30 min at 4°C in the dark.

4. Wash twice with 1X PBS and fix with 1% paraformadehyde in 1X PBS for 15 min.

5. Acquire and analyze the label cells using flow cytometer (FACS caliber, Becton Dickinson) and Cell Quest software.

Adipogenic differentiation assay of culture cells

Reagents:

0.5% (v/v) Oil Red O

1X Phosphate buffered saline

40% Formalin

Adipogenic differentiation medium

Distilled water

Materials and instruments:

5 ml Serological pipettes

15 ml Falcon tube

35-mm-culture dish

Centrifugation machine

Procedure

1. Seed-e MSCs (7.5×10^4 cells) at passage 4 in 35-mm dish and allow to adhere to the dish overnight.

2. Wash with 1X PBS and change the medium to adipogenic differentiation medium.

3. Culture at 37 °C in humidified atmosphere containing 5% CO_2

4. Replace the adipogenic differentiation medium every 3 days.

5. After 4 weeks of culture, wash the cell with 1X PBS and fix with 40% formalin vapor for 10 min at room temperature.

6. Wash twice with distilled water and stain with 0.10% (v/v) oil Red O in 60% isopropanol for 20 min at room temperature.

7. Wash twice with distilled water.

8. Observe the cells under inverted microscope (Nikon TS100, Japan).

Osteogenic differentiation assay of culture cells

Reagents:

1X Phosphate buffered saline

40 mM Alizarin red S

4% Paraformaldehyde

Distilled water

Osteogenic differentiation medium

Materials and instruments:

5 ml Serological pipettes

15 ml Falcon tube

35-mm culture dish

Centrifugation machine

Procedure

1. Seed MSCs (passage 4) at a density of 4.5 x 10^4 cells in 35-mm dishes and allow to adhere to the dish overnight.

2. Wash with 1X PBS and change the medium to osteogenic differentiation medium.

3. Culture at 37°C in humidified atmosphere containing 5% CO_2.

4. Replace the osteogenic differentiation medium every 3 days.

5. After 4 weeks of culture, wash the cells with 1X PBS and fix with 4% paraformaldehyde for 5 min at 4°C.

6. Stain with Alizarin red S (ARS) for 30 min at room temperature to visualize osteogenic differentiation.

7. Wash twice with distilled water.

8. Observe the cells under inverted microscope (Nikon TS100, Japan).

Proliferation assay

Reagents:

DMEM + 10% (v/v) FBS + 2 mM L-glutamine + 100 U/ml penicillin + 100 µg/ml streptomycin

1X Phosphate buffered saline + 100 U/ml penicillin + 100 µg/ml streptomycin

0.25% Trypsin-EDTA

Materials and instruments:

24-well culture plate

5 ml Serological pipettes

Centrifugation machine

Hemocytometer

Procedure

1. Seed MSCs (1 x 10^3 cells) at passage 2 - 4 into 24-well plate containing 500 µl of complete medium in triplicate.

2. Incubate the cells at 37°C in a humidified tissue culture incubator with 5% CO_2.

3. Harvest the cells using 0.25% trypsin-EDTA and count the total cells using hematocytometer.

4. The mean numbers of cells and plot against culture time to generate a growth curve.

Population doubling time

Reagents:

DMEM + 10% (v/v) FBS + 2 mM L-glutamine + 100 U/ml penicillin + 100 µg/ml streptomycin

1X Phosphate buffered saline + 100 U/ml penicillin + 100 µg/ml streptomycin

0.25% Trypsin-EDTA

Materials and instruments:

24-well culture plate

5 ml Serological pipettes

Centrifugation machine

Hemocytometer

Procedure

1. Seed MSCs (6.0 x 10^3 cells) at passage 1 - 7 into 24-well plate containing 500 µl of complete medium in triplicate.

2. Incubate the cells at 37°C in a humidified tissue culture incubator with 5% CO_2.

3. Harvest the cells using 0.25% trypsin-EDTA at 48 h after seeding and count the total cells using hematocytometer.

4. The doubling time was calculated according to the formula:

Population doubling number (PDN)   =   Log (N_1 / N_0) x 3.31

Population doubling time (PDT)   =   Cell culture time / PDN

(N_1 = Cell number at the end of cultivation, N_0 = Cell number at culture initiation)

Alkaline phosphatase staining

Reagents:

1X Phosphate buffered saline

4% Paraformaldehyde

BCIP®/NBT® Liquid substrate (Sigma-Aldrich, USA)

Recombinant Human BMP-2, CF (R& D Systems Inc., USA)

Complete medium

Distilled water

Osteogenic differentiation medium

Materials and instruments:

5 ml Serological pipettes

24-well plate

Centrifugation machine

Procedure

1. Seed MSCs (passage 4) at a density of 9.5 x 10^3 cells in 24-well plate and allow to adhere to the dish overnight.

2. Wash with 1X PBS and change the medium to osteogenic differentiation medium with or without 100 ng/ml BMP-2.

3. Culture at 37°C in humidified atmosphere containing 5% CO_2.

4. Replace the osteogenic differentiation medium every 3 days.

5. After 3, 7, 14, 21, and 28 days of culture, wash the cells with 1X PBS and fix with 4% paraformaldehyde for 5 min at 4°C.

6. Stain with BCIP®/NBT® Liquid substrate for 30 min at room temperature to visualize.

7. Wash twice with distilled water.

8. Observe the cells under inverted microscope (Nikon TS100, Japan).

Alkaline phosphatase (ALP) activity assay

Reagents:

1X Phosphate buffered saline

4% Paraformaldehyde

Complete medium

Distilled water

Osteogenic differentiation medium

Recombinant Human BMP-2, CF (R& D Systems Inc., USA)

SensoLyte® pNPP alkaline phosphatase assay kit (AnaSpec, USA)

Materials and instruments:

5 ml Serological pipettes

15 ml Falcon tube

24-well plate

Centrifugation machine

Procedure

1. Seed MSCs (passage 4) at a density of 9.5 x 10^3 cells in 24-well plates and allow adhering to the dish overnight.

2. Wash with 1X PBS and change the medium to osteogenic differentiation medium with or without 100 ng/ml BMP-2.

3. Culture at 37°C in humidified atmosphere containing 5% CO_2.

4. Replace the osteogenic differentiation medium every 3 days.

5. After 3, 7, 14, 21, and 28 days of culture, wash the cells with 1X assay buffer.

6. Homogenize tissue in 1X assay buffer, and then centrifuge for 15 min at 10,000 x g at 4°C. Collect the supernatant for the alkaline phosphatase assay.

7. Add 50 µL/well of biological samples containing alkaline phosphatase.

8. Set up alkaline phosphatase standard. Add 50 µL of serially diluted alkaline phosphatase standard solution from 200 to 0 ng/mL to the wells. The final amounts of alkaline phosphatase standard are 10, 5, 2.5, 1.2, 0.6, 0.3, 0.15, and 0 ng/well.

9. Add 50 μL of pNPP substrate solution into each well. Mix the reagents by gently shaking the plate for 30 sec.

10. Immediately start measuring absorbance at 405 nm by using microplate reader (BioTex, USA).

11. The ALP activity in each sample was calculated by comparing the measure OD values against a standard curve generated from 0 - 10 ng/ml of alkaline phosphatase standard solution.

MiRNA transfection

Reagents:

Complete medium

FAM™ Dye-Labeled Anti-miR™ (negative control)

Lipofectamine® RNAiMAX

Osteogenic differentiation medium

TaqMan® MicroRNA Assays (hsa-miR-31-5p, hsa-miR-106a-5p, hsa-miR-148a-5p, U6)

Materials and instruments:

15 ml Falcon tube

5 ml Serological pipettes

24-well plate

Centrifugation machine

Procedure

1. Seed MSCs (passage 4) at a density of 9.5×10^3 cells in 24-well plate and allow adhering to the dish overnight.

2. Dilute Lipofectamine® RNAiMAX reagent and anti-miRNAs in Opti-MEM® medium.

3. Add diluted anti-miRNA to diluted Lipofectamine® RNAiMAX

reagent (1:1 ratio). Incubate for 5 min at room temperature.

4. Wash the cells with 1X PBS and change the medium to osteogenic differentiation medium with 10nM anti-miR31, 10nM anti-miR106a, 10nM anti-miR148a, 10nM of 3 anti-miRs, 10nM negative control anti-miR, or without anti-miR.

5. Culture at 37°C in humidified atmosphere containing 5% CO_2.

6. Replace the osteogenic differentiation medium every 3 days.

7. After 3, 7, 14, and 21 days of culture, determinate the expression levels of miR-31, miR-106a, and miR-148a, and the expression levels of *RUNX-2*, *OSX* and *OCN*.

APPENDIX D

Ethical Approval Document (Thai)

คณะอนุกรรมการจริยธรรมการวิจัยในคน มหาวิทยาลัยธรรมศาสตร์ ชุดที่ 1 (คณะแพทย์ศาสตร์)

....

หนังสือรับรองเลขที่   074/2557

โครงการวิจัยเรื่อง   การเหนี่ยวนำการเจริญพัฒนาเป็นเซลล์กระดูกของเซลล์ต้นกำเนิดมีเซนไคม์จากรก สาย
                          สะดือ และถุงน้ำคร่ำเปรียบเทียบกับเซลล์ต้นกำเนิดมีเซนไคม์จากไขกระดูก
                          (Induction of osteogenic differentiation of mesenchymal stem cells derived from
                          placenta, umbilical cord and amniochorionic membrane in comparison with bone
                          marrow derived mesenchymal stem cells)

รหัสโครงการวิจัย   MTU-EC-DS-1-061-57

ผู้วิจัย   รองศาสตราจารย์ ดร. ศิริกุล มะโนจันทร์
                          ผู้ช่วยศาสตราจารย์ ดร. ชัยรัตน์ ตัณทราวัฒน์พันธ์
                          ผู้ช่วยศาสตราจารย์ ดร. นพ. ภาคภูมิ เขียวละม้าย

หน่วยงานที่รับผิดชอบ   สถานวิทยาศาสตร์พรีคลีนิก
                          คณะแพทยศาสตร์ มหาวิทยาลัยธรรมศาสตร์
                          โทร. 02-9269767, 02-9269757-9, 086-5333969

เอกสารที่รับรอง

1. โครงร่างการวิจัยฉบับปรับปรุงแก้ไขครั้งที่ 1 วันที่ 15 พฤษภาคม 2557

2. เอกสารชี้แจงข้อมูลแก่ผู้เข้าร่วมโครงการวิจัย (Information Sheet) ฉบับปรับปรุงแก้ไขครั้งที่ 1
    วันที่ 15 พฤษภาคม 2557

3. หนังสือแสดงเจตนายินยอมเข้าร่วมการวิจัย (Consent Form) ฉบับปรับปรุงแก้ไขครั้งที่ 1
    วันที่ 15 พฤษภาคม 2557

       คณะอนุกรรมการจริยธรรมการวิจัยในคน มหาวิทยาลัยธรรมศาสตร์ ชุดที่ 1 (คณะแพทยศาสตร์) ได้
พิจารณาอนุมัติด้านจริยธรรมการทำวิจัยในคนให้ดำเนินการวิจัยข้างต้นได้ ตามมติที่ประชุมครั้งที่ 4/2557
วันที่ 30 เมษายน 2557

ระยะเวลาที่อนุมัติ   3   ปี

กำหนดส่งรายงานความก้าวหน้า 1 ปี วันที่ 27 พฤษภาคม 2558

ลงชื่อ...

(รองศาสตราจารย์ นายแพทย์ไวพจน์ จันทร์วิเมลือง)

ประธานคณะอนุกรรมการฯ

ลงชื่อ...

(รองศาสตราจารย์ แพทย์หญิง ทิพาพร ธาระวานิช)

อนุกรรมการและเลขานุการ

อนุมัติ ณ   **วันที่ 28 พฤษภาคม 2557**

หมดอายุ   **วันที่ 27 พฤษภาคม 2560**

BIOGRAPHY

Name	Miss Kulisara Marupanthorn
Date of Birth	September 1, 1982
Educational Attainment	2005: Doctor of Veterinary Medicine
	2009: Master of Science
	(Veterinary Medicine)
Work Position	Instructor
	Faculty of Agricultural Technology and Agro-industry
	Rajamangala University of Technology Suvarnaphumi
Scholarship	2011 – 2013: Rajamangala University of Technology Suvarnaphumi scholarship
Publications	1. Manochantr S, Marupanthorn K, Tantrawatpan C, Kheolamai P. The expression of neurogenic markers after neuronal induction of chorion-derived mesenchymal stromal cells. Neurol Res. 2015;37(6):545-52.
	2. Marupanthorn K, Tantrawatpan C, Tantikanlayaporn D, Kheolamai P, Manochantr S. The Effects of TNF-alpha on Osteogenic Differentiation of Umbilical Cord Derived Mesenchymal Stem Cells. J Med Assoc Thai. 2015;98 Suppl 3:S34-40.
Work Experiences	2009 – present: Instructor
	Faculty of Agricultural Technology and Agro-industry, Rajamangala University of Technology Suvarnaphumi
	2005 – 2009: Instructor
	Faculty of Agriculture and Natural Resources, RajamangalaUniversity of Technology Tawan-Ok